ELECTRICAL RESISTIVITY IMAGING STUDY OF NEAR-SURFACE INFILTRATION

by

ANGELOS LAMPOUSIS

A dissertation submitted to the Graduate Faculty in Earth & Environmental Sciences in partial fulfillment of the requirements for the degree of Doctor of Philosophy, The City University of New York

2009

© 2009

ANGELOS LAMPOUSIS

All Rights Reserved

This manuscript has been read and accepted for the
Graduate Faculty in Earth & Environmental Sciences in satisfaction of the
dissertation requirement for the degree of Doctor of Philosophy.

Dr. Patricia Kenyon

Date	Chair of Examining Committee

Dr. Yehuda Klein

Date	Executive Officer

Dr. Jochen Albrecht

Dr. Amvrossios Bagtzoglou

Dr. Jeff Steiner

Supervision Committee

THE CITY UNIVERSITY OF NEW YORK

Abstract

ELECTRICAL RESISTIVITY IMAGING OF NEAR-SURFACE INFILTRATION

by

Angelos Lampousis

Adviser: Professor Patricia Kenyon

High resolution electrical resistivity images (ERI method) were obtained during vadose zone infiltration experiments on agricultural soils in cooperation with Cornell University's Agricultural Stewardship Program, Cooperative Extension of Suffolk County, Extension Education Center, Riverhead, New York [*as well as Cornell University's Long Island Horticultural Research & Extension Center (LIHREC) in Riverhead, New York*]. One natural soil was also studied. Infiltration was monitored by means of image analysis of two-dimensional array resistivity generated by a Syscal Kid Switch resistivity system (Griffiths et al, 1990). The data was inverted with the computer program RES2DINV (Loke, 2004). The agricultural soils considered were Riverhead sandy loam (RdA), Haven loam (HaA), and Bridgehampton silt loam (BgA). The natural site was located in the Catskill Mountains of New York State. The soils there are classified as Schoharie silty clay loam. The electrical images of the three sites were compared against established soil properties, including particle size distribution, available water capacity, and soluble salts (*from the literature*), as well as against site-specific soil

samples and penetrometer data, which were collected along with the geophysical measurements.

This research evaluates the potential of acquiring high resolution, non-destructive measurements of infiltration in the uppermost 1.5 meter of the vadose zone.
The results demonstrate that resistivity differences can detect infiltration in soils typical of the north-eastern United States. Temporal and spatial variations of soil water content in the upper 1.5 meters (relevant to agriculture) of the subsurface can be monitored successfully and non-destructively with ERI. The sensitivity of the method is higher in subsurface environments that demonstrate high overall apparent resistivity values (e.g. high sand content). Under conditions of increased soil heterogeneity, instead of the formation of a continuous water plume as occurred in the homogeneous agricultural soils, the location of the infiltrated water seems to be highly influenced by the soil heterogeneity, and the water front is scattered into discontinuous layers and travels in additional directions. The geophysical results during infiltration correlate well with soil compaction data. It follows that the ERI method can be used as a proxy for soil compaction and water content variations in agricultural applications. In a natural environment, ERI successfully maps the tree root zone of mature trees. Applications include continuous water content monitoring in high value cash crops, such as viticulture (precision agriculture).

Table of Contents

Table of Contents……..……vi

List of Tables ……..…x

List of Figures……....xi

Acknowledgements……..……...xiii

1. INTRODUCTION…….…….....1

    1.1 Literature review……...5

    1.2 Study area……8

2. SOIL SAMPLING…….……..15

3. SOIL COMPACTION DATA……..……...19

4. EXCAVATION IN MIDDLEBURGH…….……...……....24

5. REMOTE SENSING DATA……...…..……..27

6. THEORY AND METHODS…….…….....31

    6.1 Two-dimensional array resistivity imaging…….…….....31

    6.2 Inversion of results with computer software RES2DINV…….……..34

    6.3 Field methods……...……37

        6.3.1 Geophysical methods……37

        6.3.2 Infiltration experiment…….…….....40

        6.3.3 Lithium tracer (Middleburgh site) ……..……41

        6.3.4 Measurement protocol……...……..……45

7. RESULTS……..……..……..……..49

7.1 First Site: Riverhead, Suffolk County, New York……..…49

7.2 Riverhead baseline measurements……...50

7.3 Riverhead infiltration measurements……..…..52

7.4 Second Site: Mattituck, Suffolk County, New York……..…..…55

7.5 Mattituck baseline measurements…….……...56

7.6 Mattituck infiltration measurements……....57

7.7 Third Site: Southampton, Suffolk County, New York……...60

7.8 Southampton baseline measurements……..……...62

7.9 Southampton infiltration measurements……..…...62

7.10 Fourth Site: Middleburgh, Schoharie County, New York…….……66

7.11 Middleburgh baseline measurements…….....……..67

7.12 Middleburgh infiltration measurements……..……..68

8. DISCUSSION……..…..……...71

8.1 Riverhead infiltration surveys……..……....73

8.2 Mattituck infiltration surveys……..…….……..77

8.3 Southampton infiltration surveys…..…….……..….82

8.4 Middleburgh infiltration surveys…..……..……..…..87

8.5 Baseline measurement analysis – Voronoi maps…..……..……89

8.6 Baseline measurement analysis – Histograms…..……..……..….96

8.7 Baseline measurement analysis, Middleburg, on the effect of tree root…....99

9. CONCLUSIONS…..……...…..…....107

APPENDIX 1 110

1.1 Mattituck, inverted resistivity baseline cross sections (Dipole-Dipole) 111

1.2 Mattituck, inverted resistivity baseline sections (Wenner profiling) 112

1.3 Southampton, inverted resistivity baseline cross sections (Dipole-Dipole).....113

1.4 Southampton, inverted resistivity baseline sections (Wenner profiling) 114

1.5 Middleburgh, line a, inverted resistivity baseline cross sections (Dipole-Dipole)...115

1.6 Middleburgh, line a, inverted resistivity baseline sections (Wenner profiling) 116

1.7 Middleburgh, line b, inverted resistivity baseline cross sections (Dipole-Dipole)...117

1.8 Middleburgh, line b, inverted resistivity baseline sections (Wenner profiling).....117

1.9 Middleburgh, line c, inverted resistivity baseline cross sections (Dipole-Dipole)...118

1.10 Middleburgh, line c, inverted resistivity baseline sections (Wenner profiling).....119

1.11 Middleburgh, line d, inverted resistivity baseline cross sections (Dipole-Dipole).....120

1.12 Middleburgh, line d, inverted resistivity baseline sections (Wenner profiling) 121

APPENDIX 2.....122

2.1 Riverhead, Dipole-Dipole raw resistivity baseline data 124

2.2 Riverhead, Wenner raw resistivity baseline data 129

2.3 Riverhead, Dipole-Dipole raw resistivity infiltration data 131

2.4 Mattituck, Dipole-Dipole raw resistivity baseline data 141

2.5 Mattituck, Wenner raw resistivity baseline data ……..….....146

2.6 Mattituck, Dipole-Dipole raw resistivity infiltration data ……..….....148

2.7 Southampton, Dipole-Dipole raw resistivity baseline data ……..….....153

2.8 Southampton, Wenner raw resistivity baseline data ……..….....158

2.9 Southampton, Dipole-Dipole raw resistivity infiltration data ……..….....160

2.10 Middleburgh, line a, Dipole-Dipole raw resistivity baseline data …….....170

2.11 Middleburgh, line a, Wenner raw resistivity baseline data ……..….....175

2.12 Middleburgh, line b, Dipole-Dipole raw resistivity baseline data …….....177

2.13 Middleburgh, line b, Wenner raw resistivity baseline data ……..….....182

2.14 Middleburgh, line c, Dipole-Dipole raw resistivity baseline data …….....184

2.15 Middleburgh, line c, Wenner raw resistivity baseline data ……..….....189

2.16 Middleburgh, line d, Dipole-Dipole raw resistivity baseline data …….....191

2.17 Middleburgh, line d, Wenner raw resistivity baseline data ……..….....196

2.18 Middleburgh, line d, Dipole-Dipole raw resistivity infiltration data …….....198

BIBLIOGRAPHY ……..……...….....203

List of Tables

Table 1 Previous work in correlating electrical resistivity with hydrological parameters.....6

Table 2 Particle-size distribution for the three soil types at different depths.....10

Table 3 Available water capacity values.....13

Table 4 Cornell Nutrient Analysis Laboratory Soil Analysis Results.....16

Table 5 Soluble Salts Results.....18

Table 6 Penetrometer results Riverhead.....21

Table 7 Penetrometer results Mattituck.....22

Table 8 Penetrometer results Southampton.....23

Table 9 Spectrochemical determination of total recoverable Lithium Chloride....43

Table 10 Summary of Riverhead Infiltration Surveys.....53

Table 11 Summary of Mattituck Infiltration Surveys.....58

Table 12 Summary of Southampton Infiltration Surveys.....63

Table 13 Summary of Middleburg Infiltration Surveys.....66

List of Figures

Figure 1	Map of Long Island, with location of study sites marked	10
Figure 2	Breakabeen Quadrangle	12
Figure 3	Elevation Profiles for Middleburg Location	14
Figure 4	Excavation, Middleburg	25
Figure 5	NDVI results Riverhead	28
Figure 6	NDVI results Mattituck	29
Figure 7	NDVI results Southampton	30
Figure 8	The arrangement of electrodes for a dipole-dipole configuration	32
Figure 9	The arrangement of electrodes for a 2-D electrical survey and the sequence of measurements used to build up a pseudosection (Modified from Griffiths and Barker, 1993)	33
Figure 10	A sample of the RES2DINV output	35
Figure 11	Chargeability Cycle, Modified from Kearey et al (2002)	39
Figure 12	Baseline Geophysical Data – Flowchart	45
Figure 13	Aerial Photograph of Riverhead Site	49
Figure 14	Riverhead Baseline Measurements	50
Figure 15	Infiltration Surveys for the Riverhead Site	53
Figure 16	Aerial Photograph of Mattituck Site	56
Figure 17	Mattituck Baseline Measurements	57
Figure 18	Infiltration Surveys for the Mattituck Site	58
Figure 19	Aerial Photograph of Southampton Site	61

Figure 20 Southampton Baseline Measurements.....62

Figure 21 Infiltration Surveys for the Southampton Site.....63

Figure 22 Middleburg Baseline Measurements.....67

Figure 23 Infiltration Surveys for the Middleburg Site.....69

Figure 24 Riverhead Infiltration Surveys in GIS.....73

Figure 25 Mattituck Infiltration Surveys in GIS.....79

Figure 26 Southampton Infiltration Surveys in GIS.....83

Figure 27 Middleburg Infiltration Surveys in GIS.....87

Figure 28 Voronoi map for the Riverhead Site.....90

Figure 29 Voronoi map for the Mattituck Site.....90

Figure 30 Voronoi map for the Southampton Site.....91

Figure 31 Voronoi map for the Middleburg Site.....91

Figure 32 Histogram for the Riverhead Site.....97

Figure 33 Histogram for the Mattituck Site.....97

Figure 34 Histogram for the Southampton Site.....98

Figure 35 Histogram for the Middleburg Site.....98

Figure 36 Middleburg, Distribution of survey lines and relative position of the trees.....102

Figure 37 Middleburg, Survey Line a – Dipole-Dipole Baseline Measurement.....105

Figure 38 Middleburg, Survey Line b – Dipole-Dipole Baseline Measurement....105

Figure 39 Middleburg, Survey Line c – Dipole-Dipole Baseline Measurement....106

Figure 40 Middleburg, Survey Line d – Dipole-Dipole Baseline Measurement....106

Acknowledgments

I wish to thank my dissertation committee and especially my advisor, Dr. Patricia Kenyon, for guiding me throughout this project. Dr. Jeff Steiner, Dr. Jochen Albrecht, and Dr. Amvrossios Bagtzoglou played a most constructive role in bringing this project to fruition.

I owe my earliest aspirations to pursue graduate studies to my nuclear physicist friends Dr. Giorgos Galios and Dr. Christos Tsabaris. Professor Nenos Georgopoulos further nurtured those aspirations, and introduced me to the rigor and excitement of American scholarship in the context of his philosophy classes in Thessalonica, Greece.

I am indebted to Professor Daniel Habib, one of the founders of the Graduate Center Doctoral Program in Earth and Environmental Sciences, for his complete support during my first most challenging years as an international student in New York City at the Queens College Geology Department. I am similarly indebted to Professor Jeffrey Osleeb, previous Executive Officer of the Doctoral Program in Earth and Environmental Sciences, not only for his crucial support at the beginning of my Ph.D. studies, but also for consistently assessing my status correctly. To paraphrase the renown philosopher, Professor Osleeb "knew myself" perhaps even better than I.

I wish to thank the current Executive Officer of the Doctoral Program in Earth and Environmental Sciences, Dr. Yehuda Klein, for his assistance in initiating my collaboration with Cornell University's Long Island Extension Center as well as for his support with my tuition and other research-related expenses.

Many parts of my dissertation's data collection program were completed with the assistance of a number of exceptional and hard-working professionals. Although in the final version of this dissertation some of those data were not included, I am grateful for the assistance that I received over the last five years from the following individuals: Dr. Frederick Stumm, Research Hydrologist, U.S. Geological Survey, Coram, Long Island, New York; Mr. Ronald Busciolano, U.S. Geological Survey, Mr. William Dorsch, Environmental Services Division, Groundwater Protection Program, Brookhaven National Laboratory, United States Department of Energy; Mr. Richard Tobin, Superintendent of the Massapequa Water District.

My student colleagues Daniel Klinger, Wendy Monterosso, Ylli Kelici, Nick Steiner, and Sal Leggio, have made my adaptation to the American educational system, and for that I am deeply grateful.

Professor Mark Bridgen, Director of Cornell University's Long Island Horticultural Research & Extension Center, Riverhead, New York, provided me with significant logistical support for my experiments in Long Island. I would also like to thank Viticulturist Ms. Alice Wise along with the rest of the exceptional Cornell University staff for their kind assistance.

Mr. Kevin Sanwald, extension educator and agricultural stewardship program technician of the Cornell cooperative extension of Suffolk County, helped me in the most systematic way, both physically during record-high temperatures during the summer of 2007, as well as with his suggestions, which in my humble opinion constitute the earliest contributions in the emerging field of agricultural geophysics.

It is common knowledge that pursuing a Ph.D. is a deeply personal process, one that sometimes requires extremely "personal" support. Although I view my acceptance to the program as a personal achievement,

I could not have completed it without the intellectual and financial support from the following: Adonis Mallios, Constantine Moratos, Christina Lampousis, Peter Lambousis, Dr. Demetrios Kehagias, and Dr. Charles Calomiris.

Finally, rumor has it that married couples get divorced because of a Ph.D. In my case, it seems to have been the opposite, as toward the final stages I received an ultimatum from Dr. Athina Vassilakis that we would not get married if I would not complete my studies. I think that helped too.

CHAPTER 1. INTRODUCTION

Electrical resistivity imaging (ERI) is one of a number of surface geophysical methods that are used for near-surface investigations. Others include seismic refraction, electromagnetics, ground penetrating radar, magnetics, and induced polarization. Surface geophysics' advantages are that they are non-destructive, cost-effective, and provide data at a relatively fast rate. Electrical resistivity is particularly effective in tracing fluid migration in the shallow subsurface, as electrical currents at those depths are carried primarily through the water present in the pore spaces. It differs from ground penetrating radar in that the results depend on resistivity rather than dielectric constant. Certain minerals (e.g. graphite, native metals) conduct electricity through electronic conduction. However, the transmission of electrical currents through most rocks and sediments occurs in an electrolytic rather than an electronic fashion. In the case of electrolytic conduction, current is carried through ions present in groundwater. This phenomenon allows for a non-invasive characterization of the shallow subsurface, which has a wide range of engineering and environmental applications. For instance, electrical monitoring of the migration of many contaminants in the unsaturated zone is possible due to the observed changes in resistivity (Van et al., 1991). Resistivity measurements are also frequently used to estimate aquifer properties, including transmissivity and hydraulic conductivity (Vanderborght et al., 2005). Most recently, the potential of near-surface geophysics in advancing hydrological research on the watershed scale was evaluated (Robinson et al., 2008). This constitutes another important capability of electrical and electromagnetic geophysical methods, which is to infer hydraulic properties on larger scales than the ones

used traditionally in the laboratory (Corwin et al., 2006). In addition to the ability to work on larger scales, the fast data acquisition capability of surface geophysics as compared with drill hole measurements or laboratory experiments makes possible the monitoring of ephemeral geological events, such as the alternating wetting and drying of soils (Amidu and Dunbar, 2007).

A number of researchers in past years have attempted to link geophysical measurements to hydrological properties of sediments. One of the main objectives in this area of research is to overcome the limitations of point measurements, which when done by drilling – as they usually are – are time-consuming, expensive, and potentially destructive, as they have the potential of creating preferential flow paths for pollution. Despite this body of research, which is discussed in the literature review section of this dissertation, only limited attempts have been made that use electrical resistivity to study near-surface infiltration in agricultural fields with high-value crops. In this dissertation, high resolution electrical resistivity images were obtained during vadose zone infiltration experiments on agricultural soils.

Agricultural crops are considered high-value when they provide for higher profit per unit of land than other commonly grown crops. The concept of high-value agricultural crops is linked to the field of economics, as a crop that is considered high-value in one location, may not have the same value at another location, based on its relation to the local, national, and global markets. Generally, fruits, vegetables, ornamentals, and spices are considered among the high-value agricultural crops.

Electrical resistivity methods are pertinent to agriculture, since they can help improve both quality and productivity through their application in precision agriculture

(Allred et al., 2008) and better management of the water supply in dry agricultural regions. Precision agriculture focuses on achieving optimal conditions of growth for the crops in consideration by emphasizing accurate monitoring of soil moisture, and adjusting accordingly the levels of fertilizer and pesticide application. The adoption of precision agriculture by farmers in recent years as a profitable management strategy for their crops, has led to the creation of innovative technologies in many sectors, including agricultural equipment manufacturing and the farm input supplies industry (National Research Council, 1997). Specifically for high-value crops such as vineyards, soil moisture conditions may vary significantly within the same field. Precise monitoring of the soil moisture fluctuations can guide irrigation management in an effort to achieve uniform (i.e., optimal for the vine variety in consideration) application of water.

In this dissertation, the application of two-dimensional electrical resistivity imaging (ERI) is evaluated. Electrical resistivity imaging is a relatively new geophysical method, as opposed to vertical electrical sounding (VES) and constant separation traversing (CST), which are older. Both VES and CST are discussed in the methods section of this dissertation. In the present work, ERI was employed in conjunction with infiltration experiments in agricultural soils of Long Island, New York, hosting high-value crops (i.e. vineyards). An additional non-agricultural site in a forested area in Middleburgh of upstate New York was also studied to further explore the potential of using this method in an undisturbed environment exhibiting different vegetation patterns and subsurface configurations. The agricultural sites are expected to have contrasting soil characteristics as compared with the natural site. For instance, vertical infiltration of the water in agricultural soils is inhibited by a thin layer of compacted soil, which is formed

at the bottom of the near-surface soil horizon, as a result of the effect of the wheels of heavy machinery used in agriculture (e.g., tractors). No such layer exists in natural soils. In addition, this compacted soil inhibits to a certain extent root growth, except for the area directly under the vineyards' rows, where no plowing occurs. Therefore, the root configuration in the agricultural sites due to predetermined geometry of planting, employment of machinery, and the use of a single plant species (i.e., vines) is very different than the natural site where those conditions do not exist. Besides the expected differences in soil drainage rates due to water uptake by the roots, evapotranspiration rates are expected to be different between the agricultural sites and the natural one as well. Under the same weather conditions, evapotranspiration is expected to be less significant in the natural site due to shading from mature trees, and more significant in the agricultural sites where soils between rows are more exposed.

Three main questions served as the core direction of the research as outlined below. The first question is whether the effect of infiltration can be detected in soils typical of the north-eastern United States. Resistivity datasets were inverted to produce a sequence of two-dimensional electrical resistivity images, which monitored near-surface infiltration. Prior to infiltration, a series of baseline surveys in two different electrode configurations were obtained for comparison purposes, including repeatability tests and reciprocal measurements for all sites.

The second question, assuming that the answer to the first research question stated above is positive, is what geophysics demonstrates about the infiltration process in the soils sampled. Further to this question, the potential practical applications of the ERI method in high-value agricultural fields on Long Island are considered.

Finally, the etiology of the observed differences in cross sections between different soils was explored. Baseline geophysical measurements were compared with non-geophysical data to deduct the possible sources of the inferred differences.

1.1 Literature Review

Previous work relevant to this dissertation includes attempts to find correlations between geophysical measurements and hydrological data and applications of surface geophysics to other agricultural sites.

Attempts to find correlations with geophysical measurements have utilized primarily one-dimensional field data, mostly generated by the vertical electrical sounding method (defined in the methods section of this dissertation), and have produced relationships that are specific to the site under investigation (Aristodemou and Thomas-Betts, 2000; Meju, 2000). This one-dimensional approach is particularly common in the unsaturated zone and for the most part limited to well-stratified and homogeneous layers (Kean et al., 1987, Hollenbeck and Jensen, 1998; Rockhold et al., 1997; Simunek and van Genuchten, 1996; Zou et al., 2001). Other -partially successful- attempts to correlate electrical resistivity with hydrological parameters, all essentially one dimensional in nature, are presented in Table 1. Nevertheless, Ezzedine and Rubin (2002) reported that there are no universal methods available for converting geophysical attributes to hydrogeological ones.

Table 1. Previous work in correlating electrical resistivity with hydrological parameters	
Reference	Geophysical-Hydrological Relationship
Niwas and Singhal (1981)	Analytical relationship between transmissivity and transverse resistance.
Mazac et al (1985)	Discussion of the factors influencing relations between electrical and hydraulic properties of aquifers and aquifer materials.
Mazac et al., (1988)	They have concluded that geoelectrical methods may be effectively applied to determine the spatial variation pattern of saturated hydraulic conductivities in the field and to differentiate soil layers according to their properties.
Curtis and Kelly (1990)	Retrieval of resistivity sounding data and hydraulic data from the literature to demonstrate relationships between electrical and recharge characteristics of vadose and soil zones for several sites in Nebraska.
Kalinski, et al., (1993)	Application of direct current surface geoelectrical measurements to estimate vertical advective solute time-of-travel through an unsaturated ground water protective layer.
Frohlich et al., (1994)	Application of geophysical surface methods to estimate hydraulic conductivity and the degree of bedrock fracturing to evaluate the performance of sanitary landfills.
Edet and Okereke (1997)	Combined analysis of lineament length density from radar imagery and surface resistivity data to assess the hydrogeological conditions of a site. Results have shown that the data correlated with the qualitative and quantitative estimation of some aquifer parameters.
Yadav and Abolfazi (1998)	Application of geoelectrical soundings using the Schlumberger configuration in the vicinity of twelve pumping test sites to relate geoelectrical and hydraulic parameters. The normalized aquifer resistivity was correlated with hydraulic conductivity and normalized transverse resistance with aquifer transmissivity.
De Lima and Niwas (2000)	Theoretical and experimental evidence that the electrical resistivity and the induced polarization parameters carry direct information about the volume conductivity of a sandstone matrix.

Quantitative estimates of hydraulic parameters through cross-borehole radar or resistivity surveys have been reported in two papers (Daily et al., 1992, and Binley, et al., 2002), but no such study using surface two-dimensional (2D) resistivity exists. Other methods that have produced interesting links between geophysics and hydrology include the use of seismic data (Rubin et al., 1992), as well as the use of ground-penetrating radar (GPR) in monitoring moisture content in the unsaturated zone (Alumbaugh, 2002; Binley

et al., 2001; Eppstein and Dougherty, 1998; Grote et al., 2003; Kowalsky et al., 2001; van Overmeeren et al., 1997). Kowalsky et al., (2006), developed a joint inversion method for analyzing time-lapse ground-penetrating radar data and hydrologic data to produce more accurate models.

In recent years there has been increasing interest in linking the use of near-surface geophysical methods with agriculture. Allred et al., (2008), predict that this area of research will soon evolve into a distinct discipline within geophysics, which may be called "agrigeophysics." To date, the application of geophysics in agriculture for the most part revolves around soil salinity assessment (e.g., Rhoades and Ingvalson, 1971; Rhoades et al., 1990). With the advent of the precision agriculture trend in agriculture, geophysical methods such as GPR and electromagnetic induction are increasingly being used for mapping soil variability (Doolittle and Collins, 1995; Doolittle et al., 2007). The potential contribution of geophysical applications in achieving sustainable agriculture practices through site-specific management practices, has been largely focused on mapping the apparent soil electrical conductivity (Corwin et al., 2005; Johnson et al., 2005; Lesch et al., 2005).

The application of surface electrical resistivity imaging in agricultural sites was reported in two papers (Michot et al., 2003, and Sénéchal et al., 2005). Michot et al., (2003), attempted to relate electrical resistivity changes during an irrigation event in a single soil type present in a corn field in the Beauce region of France. They developed a site-specific petrophysical relationship, which they applied to their electrical resistivity tomography data obtained at the field. The hydraulic behavior of this particular soil type over the course of a wetting and drying cycle was monitored successfully, but the

requirement of additional field calibration makes this method not practical for routine use. Sénéchal et al., (2005), obtained electrical resistivity tomography data in combination with GPR data to characterize the physical properties of alluvial sediments located at the border of a corn field in the Pyrenees region of France. Their focus was on monitoring the vertical transport of water through the unsaturated zone over a period of twelve months. The authors employed processing techniques, including the common reflection surface method (CRS) and kriging, to improve the resolution of their GPR velocity maps. They attributed the variations in electrical conductivity of water throughout the acquisition year to the residence time of water within the vadose zone, as well as to the effect of agricultural fertilizer application (e.g. nitrate), but they were unable to determine the contribution of each phenomenon.

Finally, recent articles appearing in the literature discuss aspects of resistivity applied to hydrology. Wempe and Mavko (2006) worked on constraining petrophysical interpretations of resistivity data. Ferré et al., (2006), conducted a virtual experiment to evaluate the potential of surface electrical resistivity measurements in constraining the interpretation of hydraulic properties. Mota et al., (2006), used a stochastic method, which combines resistivity and seismic data, to estimate porosity and water saturation.

1.2 Study Area

The study area includes four sites, three agricultural sites on Long Island and another undisturbed one in upstate New York. Most of the soil types found in Long Island have been reviewed by the United States Department of Agriculture (USDA) as part of national comprehensive soil surveys. The three Long Island sites represent

different soil types and were selected after consultation with the personnel of the Cornell University Cooperative Extension of Suffolk County. The selection was made based on fertility and the relative abundance of the soil types within Suffolk County. The soil types selected fall into one of the following soil series: Riverhead, Haven, and Bridgehampton. The Riverhead and Haven series are the most abundant soils within Suffolk County, as the two combined make more than twenty percent of the County. The Bridgehampton series is considered the most fertile in Suffolk County, and was selected for its economic importance.

In terms of physical properties the three soil types differ according to percentages of sand, silt, and clay (See Table 2). Clay content is approximately the same in all three types. Sand is dominant in the Riverhead sandy loam type, varies with depth in the Haven loam, and is subordinate to silt in the Bridgehampton loam.

The first Long Island site (refer to Figure 1) that was considered is located in Cornell University's Horticultural Research and Extension Center in Riverhead, 3059 Sound Avenue, Riverhead, NY 11901 (Coordinates: N 40° 57.618′, W 72° 42.718′). The soil in this case is classified as Riverhead sandy loam (RdA).

The second site is located in a private farm at 41720 Oregon Road, Mattituck, NY 11952 (Coordinates: N 41° 01.229′, W 72° 31.497′), and is classified as Haven loam (HaA). The third site is located in a private farm at 231 Montauk Highway (Route 27), in the hamlet of Water Mill in Southampton, NY 11976 (Coordinates: N 40° 54.238′, W 72° 22.031′), and is classified as Bridgehampton silt loam (BgA).

Table 2. Published particle-size distribution for the three soil types at different depths. Presentation is in order from more sand (RdA) to less sand (BgA). Source: U.S. Department of Agriculture's (USDA) Soil Conservation Service (SCS)

Symbol Name	Depth (cm)	Percent Sand	Percent Clay	Percent Silt
RdA Riverhead sandy loam	0-30	69.4	10	20.6
	30-60	66.9	10	23.1
	60-100	80.8	5.3	13.9
HaA Haven Loam	0-30	47.6	11.7	40.8
	30-60	45	12	43
	60-100	82.3	4.8	12.9
BgA Bridgehampton silt loam	0-30	27.8	12	60.2
	30-60	20.7	12	67.3
	60-100	20.7	12	67.3

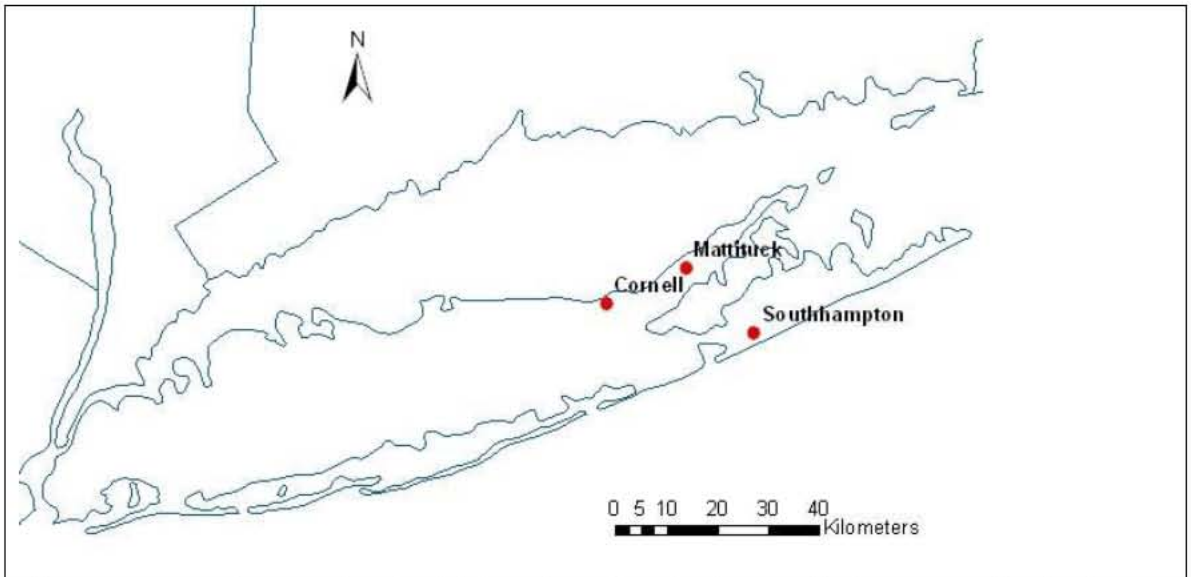

Figure 1. Map of Long Island, with location of study sites marked. New York City is located at the extreme south western corner of this map.

The fourth non-agricultural site is located at Guinea Road, Middleburgh, New York (Coordinates: N 42° 31.088′, W 74° 23.463′), in Schoharie County, in the Catskills of New York State (refer to Figure 2).

The hydrogeological setting of Long Island has been described in comprehensive reports by several authors (McClymonds and Franke, 1972; Smolensky et al, 1989; Buxton et al, 1989; Stumm et al, 2002). Since this is a near-surface resistivity survey it is assumed for the three Long Island sites with regards to geology that they all belong in the upper glacial aquifer. The upper glacial aquifer of Long Island is mainly comprised of till and outwash. Till is poorly sorted and composed of clay, sand, gravel, and boulders. Outwash deposits are well sorted and consist of quartzose sand, fine to very coarse, and gravel, pebble to boulder sized. Outwash in Long Island also contains lacustrine, marine, and reworked deposits (Smolensky at et al, 1989). Till is poorly permeable. Outwash deposits are moderately to highly permeable. Average horizontal hydraulic conductivity in the upper glacial aquifer is approximately 82 ft/d. The ratio of horizontal to vertical hydraulic conductivity is 10:1 (Stumm, 2002).

In addition to the literature data available for the three soil types in Long Island, soil samples and measurements of soil compaction were collected at the same time as the geophysical measurements. This site-specific soil analysis will be discussed in chapter 2.

Another soil physical property that is different among the three soil types is the available water capacity. In standard terms used by the United States Department of Agriculture (USDA) the available water capacity refers to the quantity of water that the soil is capable of storing for use by plants.

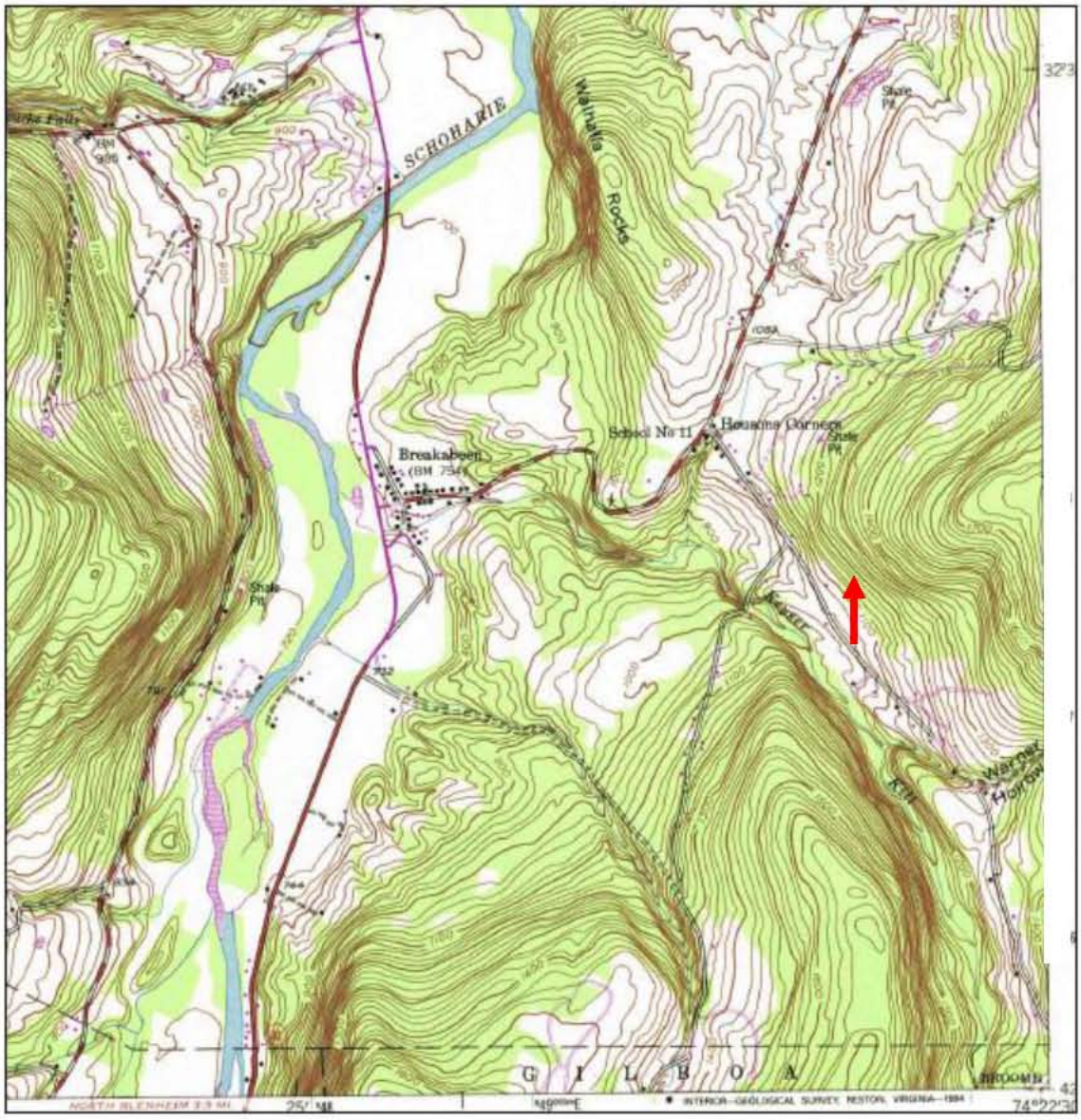

Figure 2
Breakabeen USGS Quadrangle
Map year 1994 (revised from 1943)
Series: 7.5
Scale: 1:24,000

Physical Address: 1248 Guinea Rd
Middleburgh, New York 12122

Coordinates: N 42 31.088
W 74 23.463

Bridgehampton soils are classified as having high available water capacity, as opposed to the Riverhead and Haven soils which are classified as having low available water capacity (See Table 3). Available water capacity data are not available for Middleburgh.

Table 3. Available water capacity values

Soil Type	Available water capacity* (inches)
RdA Riverhead sandy loam	5.1
HaA Haven Loam	4.3
BgA Bridgehampton silt loam	14.9

*The capacity for water storage is given in inches of water per inch of soil for each soil layer. The above numbers assume a 40-inch soil layer. Available water capacity is not an estimate of the quantity of water actually available to plants at any given time.

Source: USDA, Natural Resources Conservation Service, National Cooperative Soil Survey, Suffolk County, New York

The fourth site in Middleburgh is located in the Allegheny Plateau Physiographic Province. The underlying geology consists of the Hamilton group, which is characterized by layers of dark grey shale interbedded with siltstone and sandstone. At our site the main lithology visible in outcrop was shale. Soils are classified as Schoharie silty clay loam. According to the U.S. Department of Agriculture's (USDA) Soil Conservation Service (SCS) the Schoharie series soils are generally found in valleys of former glacial lakes. These soils formed in glaciolacustrine (lake-laid) deposits that consist of clay and silt. The soil sampling and subsequent analysis of soil samples obtained from the Middleburgh site is consistent with the soil classification recorded in USDA literature for the Middleburgh area. Location information (detail from Breakabeen US Topographic Quadrangle map) and elevation information (elevation profiles in North-South and West-East directions) for the Middleburgh site is presented in Figures 2 and 3 respectively.

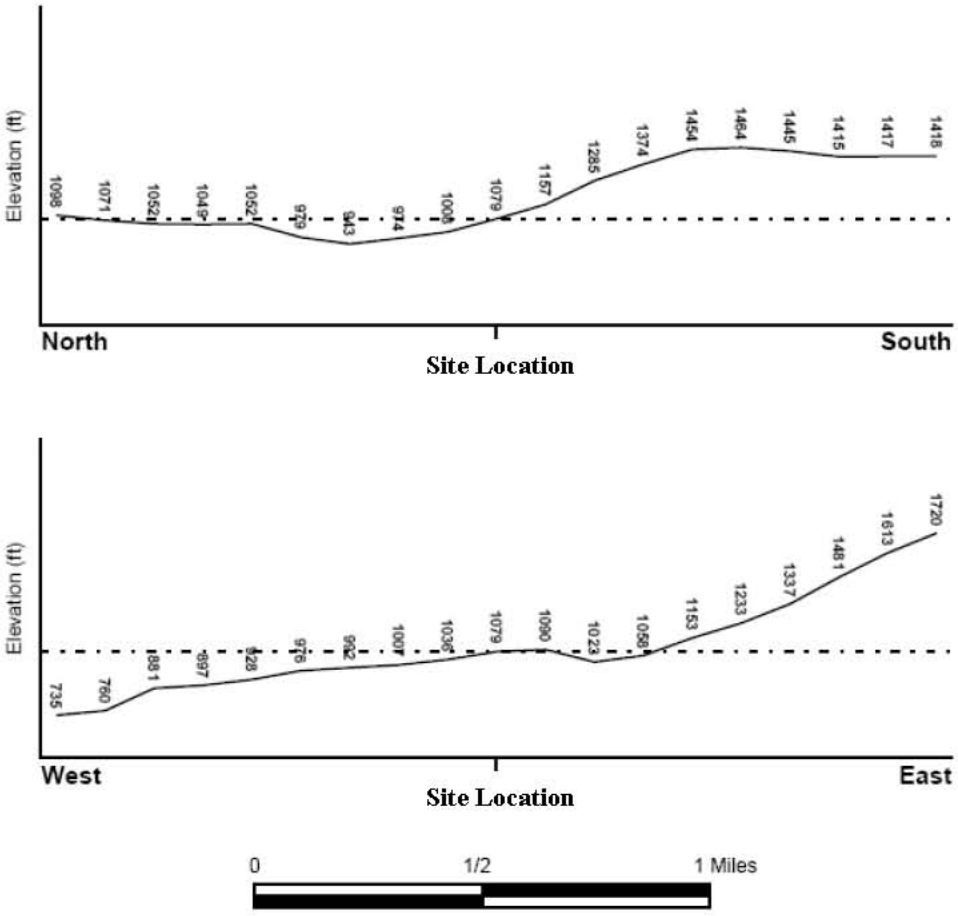

Figure 3. Elevation Profiles for Middleburgh Location

CHAPTER 2. SOIL SAMPLING

Every soil sample from each Long Island site was a composite consisting of soil from cores obtained along the resistivity survey lines. The sampling was conducted in this way in an effort to minimize the effects of any local non-uniformity in the soil. Soil cores one inch in diameter from about 12-14 locations along the resistivity survey line were obtained for each soil sample. The cores reached a depth of twelve inches. The soil cores were mixed well in a paper bag and sent to the laboratory.

Composite soil samples were obtained from the fourth non-agricultural site in Middleburgh as well. The sampling procedure was different in Middleburgh, as at this site the resistivity survey line was excavated after the experiment down to a depth of approximately two meters. In this case composite soil samples were obtained at two different depths from the soil profile exposed on either side of the trench. The soil sample analysis for all samples was conducted at the Cornell Nutrient Analysis Laboratory of the Department of Crop and Soil Sciences of Cornell University in Ithaca, New York.

The results of the particle size distribution analysis are summarized in Table 4. The analysis was performed at the Cornell Nutrient Analysis Laboratory follows the Pipette Method (Alejandro Parra, Cornell Nutrient Analysis Laboratory Supervisor, personal communication). In summary, the method involves the following steps: Soil aggregates are destructed or dispersed into discrete units by chemical, mechanical, or ultrasonic means, and the separation of particles is done according to size limits by means of sieving and sedimentation, as well as other methods (diffraction).

Table 4 - Cornell Nutrient Analysis Laboratory Soil Analysis Results		
Location	USDA Existing Soil Classification	Assigned texture* from soil sampling
Riverhead, Suffolk County, Long Island, New York	RdA, Riverhead sandy loam	Silty loam (SiL)
Mattituck, Suffolk County, Long Island, New York	HaA, Haven Loam	Coarse sandy loam (CoSL) or sandy loam (SL)**
Southampton, Suffolk County, Long Island, New York	BgA, Bridgehampton silt loam	Silty loam (SiL)
1184 Guinea Road, Middleburgh, New York [near-surface layer]	n/a	Silty clay loam (SiCL)
1184 Guinea Road, Middleburgh, New York [deeper layer]	n/a	Silty loam (SiL)

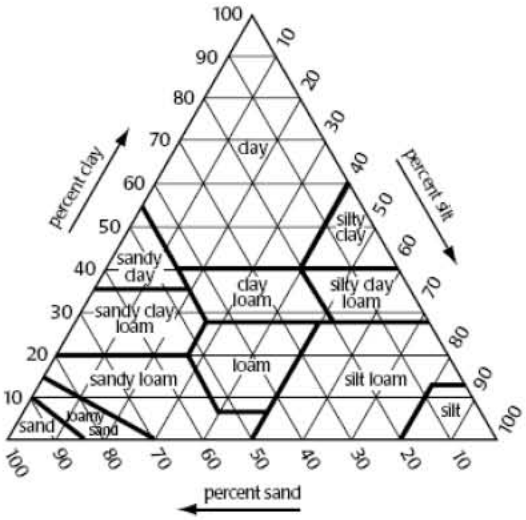

USDA - Textural triangle

*The basis for the assigned value is the textural triangle (above)

** Note: The value "sandy loam" appears as another acceptable result for this sample. According to the Cornell Nutrient Analysis Laboratory this is also a correct result because it has fallen within the experimental error.

Air-dried soil is mechanically shaken overnight in distilled water. The sand fraction is removed from the suspension by wet sieving and then fractioned by dry sieving. The clay and fine silt fractions are determined using the solution remaining from the wet

sieving process. This solution is diluted to 1 L in a sedimentation cylinder, stirred, and 25 mL aliquots are removed with a pipet at calculated, predetermined intervals based on Stokes' Law. The aliquots are dried at 105°C and weighed.

Based on the particle size distribution analysis, the sites in Riverhead and Southampton were assigned a silty loam (SiL) texture, and the site at Mattituck was assigned a coarse sandy loam (CoSL) texture. The two distinct soil horizons that were sampled from the site in Middleburgh, the one near the surface was assigned a texture of silty clay loam (SiCl) and the deeper one a texture of silty loam. There are slight discrepancies between the published data and the measured values.

All soil samples were also analyzed for soluble salts. Excessive amounts of soluble salts in agricultural soils disrupt the osmotic processes of water uptake by the roots and suppress plant growth. Soil samples were evaluated for salinity by determining the electrical conductivity of a 1:2 suspension (by weight) of soil to deionized water, and it is reported in millimhos (See Table 5). The soils in both the Riverhead and Southampton sites appear as strongly saline (conductivity more than 0.9 millimhos), as opposed to the Mattituck and Middleburgh sites, which appear slightly saline.

Grapevines are sensitive to high levels of soluble salts in both soil and irrigation water. Since all of the soil sampling was carried out near the surface (12 inches maximum depth, except for the Middleburgh site where a deeper soil horizon was sampled) it is assumed that high salinity levels in Riverhead and Southampton may be attributed to seasonally higher values during summer. In the absence of rainfall or irrigation, the application of granular fertilizer, which has a high salt content, can be responsible for the elevated salinity. On the other hand, lower salinity levels at the Mattituck site may reflect

the fact that it was the only irrigated site (by means of a drip irrigation system). Therefore, the water applied by the irrigation system may be responsible for washing off the salts present at the top soil. Finally, lower salinity levels for the Middleburgh site are consistent with the fact that this is the only natural and undisturbed site.

Table 5. Cornell Nutrient Analysis Laboratory - Soluble Salts Results

Location	Soluble salts (mmho)
Riverhead, Suffolk County, Long Island, New York	0.16
Mattituck, , Suffolk County, Long Island, New York	0.07
Southampton, , Suffolk County, Long Island, New York	0.17
1184 Guinea Road, Middleburgh, New York [near-surface layer]	0.09
1184 Guinea Road, Middleburgh, New York [deeper layer]	0.07

CHAPTER 3. SOIL COMPACTION DATA

The traffic of agricultural machines in vineyards can cause soil compaction, reducing porosity and inhibiting root growth. More specifically, wheel traffic leads to the formation of a subsoil compaction pan. Periodically farmers need to remove this subsoil pan by deep tillage. It is worth noting that since the presence of a subsoil compaction pan is influenced by agricultural practice, two sites with the same soil type could conceivably exhibit different levels of compaction (e.g. subsoil compaction pan present at different depths or completely absent).

Soil compaction measurements were obtained from ten points at approximately one meter interval along the resistivity lines at the agricultural sites using a Dickey-John soil compaction tester, also known as a cone penetrometer. The penetrometer is marked at three inch intervals at 3, 6, 9, 12, 15, and 18 inches. Cone penetrometer resistance is measured in pounds per square inch (psi). Crop roots are expected to grow well within the range of 0-200 psi, fairly well within 200-300 psi, and poorly from 300 psi and above. By applying even pressure to the handles of the instrument the rod penetrates, and the gauge readings are noted for each one of the intervals.

The penetrometer results are presented on tables 6, 7, and 8. Penetrometer values for the Riverhead (USDA soil classification: Riverhead sandy loam) and the Southampton sites (USDA soil classification: Bridgehampton silt loam) progressively increase with depth. In Riverhead a maximum (i.e. the instrument does not measure precise values above the 300 psi limit) is reached at a depth of fifteen inches. In Southampton the maximum was reached earlier in the process at a depth of twelve

inches. In Mattituck (USDA soil classification: Haven Loam) the maximum was reached extremely near the surface at the first depth interval available at three inches, suggesting a significantly more compacted soil than the other two. Penetrometer data were not obtained at the Middleburgh site due to constraints in equipment use (the instrument is property of Cornell University, and permission to use it could not be obtained, except for the Cornell research center in Riverhead and the private vineyards affiliated with the School).

Table 6. Penetrometer results Riverhead

	Location	1	2	3	4	5	6	7	8	9	10
	Depth	Penetrometer resistance measured in pounds per square inch (psi)*									
	Inches										
Riverhead	3	100	175	150	150	175	175	150	200	200	175
USDA Classification:	6	200	200	200	250	200	200	250	175	200	250
Riverhead sandy loam	9	225	175	200	250	200	225	300	200	250	300
	12	200	150	225	275	275	300+	300	250	275	300
	15	Stone	200	300+	275	300+	300+	300+	300+	300+	300+
	18		300+	300+	300+	300+	300+	Stone	300+	300+	300+
	21		300+	300+	300+	300+	300+		300+	300+	300+
	24		300+	300+	300+	300+	300+		300+	300+	300+

Crop roots are expected to grow well within the range of 0-200 psi, fairly well within 200-300 psi, and poorly from 300 psi and above
The entry "Stone" denotes any incident in which the instrument encountered a rock fragment of unknown size
The entry "MAX" denotes a location in which the instrument reached its absolute maximum value forcing the data collector to stop injecting the needle further, as opposed to the entry 300+, which might be a high value, but allows the needle to continue the penetration.

Table 7. Penetrometer results Mattituck

	Location	1	2	3	4	5	6	7	8	9	10
	Depth	Penetrometer resistance measured in pounds per square inch (psi)*									
Mattituck	Inches										
USDA Classification:	6	275	275	200	300	300+	300+	300+	300+	300+	275
Bridgehampton silt loam	9	300+	300+	250	300+	MAX		300+	MAX	MAX	300+
	12	300+	MAX	300+	300+			MAX			MAX
	15	MAX		300+	MAX						
	18			Stone							
	21										
	24										

Crop roots are expected to grow well within the range of 0-200 psi, fairly well within 200-300 psi, and poorly from 300 psi and above
The entry "Stone" denotes any incident in which the instrument encountered a rock fragment of unknown size
The entry "MAX" denotes a location in which the instrument reached its absolute maximum value forcing the data collector to stop injecting the needle further, as opposed to the entry 300+, which might be a high value, but allows the needle to continue the penetration.

Table 8. Penetrometer results Southampton

	Location	1	2	3	4	5	6	7	8	9	10
	Depth	Penetrometer resistance measured in pounds per square inch (psi)*									
Southampton	Inches										
USDA Classification:	6	175	175	150	200	180	175	100	150	150	150
Haven Loam	9	200	150	175	150	225	175	100	175	175	200
	12	300+	300	300+	200	250	300	250	250	250	275
	15	300+	300+	300+	300+	300+	300+	300+	300+	300	300+
	18	300+	300+		300+	300+	300+	300+	300+	300+	300+
	21	300	300		300	300+	300	300+	300+	300	300+
	24	300	300		275	275	300	300	300+	225	300+

Crop roots are expected to grow well within the range of 0-200 psi, fairly well within 200-300 psi, and poorly from 300 psi and above
The entry "Stone" denotes any incident in which the instrument encountered a rock fragment of unknown size
The entry "MAX" denotes a location in which the instrument reached its absolute maximum value forcing the data collector to stop injecting the needle further, as opposed to the entry 300+, which might be a high value, but allows the needle to continue the penetration.

CHAPTER 4. EXCAVATION IN MIDDLEBURGH

The site in Middleburgh was excavated after the completion of the resistivity survey. The excavation was conducted with a bulldozer. The bulldozer removed the soil adjacent to the final resistivity line of the infiltration experiment down to a depth of two meters on average. Additional soil was removed from the soil profile with hand-tools in an effort to provide a cleaner excavation and approach closer to the location of the resistivity measurement (Figure 4).

The excavation revealed three distinct soil layers. Major tree roots were present near the surface within a depth range of 20 centimeters to 1 meter. Roots were more dominant on either end of the profile, and less prominent around the center of the survey line. The first soil horizon included organic material and was dark-colored. The middle horizon was light-colored and the soil was more friable in certain areas. The third (bottom) horizon consisted of dark-colored soil significantly more compacted than the one found in the other horizons. Bedrock was encountered at a depth of 1.5 meters to 2 meters. From surface to bedrock there were no large size sediment grains found, such as boulders, except for occasional isolated pebbles.

Figure 4 (a) Excavation, Middleburgh: Bulldozer initiates work

Figure 4 (b): Author inside trench for scale

Figure 4 (c): Bulldozer at work

Figure 4 (d): Three distinct soil layers

Figure 4 (e): Soil removal from the soil profile with hand-tools

CHAPTER 5. REMOTE SENSING DATA

Based on satellite data, radiation wavelengths can be linked to the process of photosynthesis to yield normalized difference vegetation index (NDVI) data. Satelite data have been increasingly used in precision agriculture, especially in the evaluation of vineyards (i.e. precision viticulture). For instance, Da Costa et al., (2007), carried out an analysis of high resolution remote sensed images obtained over vineyards of the Bordeaux area in France. Delenne et al., (2008), used remotely sensed data to delineate vineyard boundaries in the Languedoc-Roussillon wine-producing region in France. Hall et al., (2008), used NDVI imagery to evaluate correlations between grapevine leaf area index and other grapevine characteristics (canopy density and canopy area). This study focused at a vineyard of the Cabernet Sauvignon variety located at Charles Sturt University, Wagga, Australia.

Carothers (2000) suggests that NDVI variations may reflect differences in irrigation management practices, root configurations, and plant health. Grote et al., (2003), used NDVI data as a selection factor between study sites (i.e.vineyards).

The NDVI is calculated as follows: NDVI = (NIR – red) / (NIR + red), where

NDVI = Normalized Difference Vegetation Index

NIR = Intensity in the ASTER band in the near infrared (0.807 microns)

RED = Intensity in the ASTER band in the visible red light (0.661 microns)

NDVI data were obtained for the three sites of Long Island that are evaluated in this dissertation. The data were processed using ENVI, which is a remote sensing image analysis software. The Riverhead and Mattituck sites were included in the same image,

which was captured during the month of July 2007 by the ASTER instrument, which is onboard the TERRA satellite. An additional image, which included the Southampton site, was captured by the same instrument during the month of August 2007. The resolution of these images is fifteen meters squared per pixel (i.e., 225 m^2). The images obtained (Figures 5, 6, and 7) show a NDVI varying from 0.4 to 0.6 suggesting similar vegetation conditions.

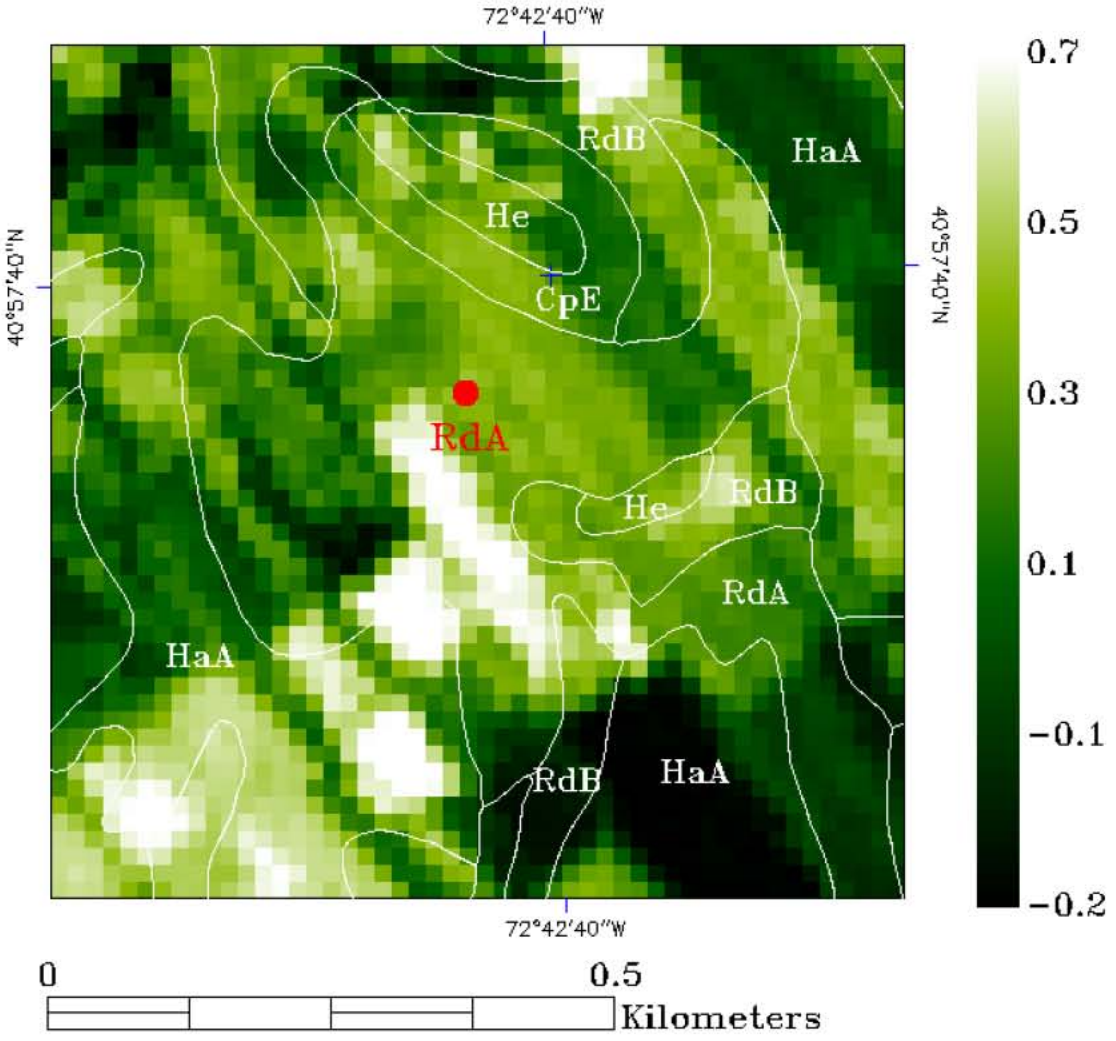

Figure 5. NDVI results Riverhead

Red dot indicates the location of the geophysical survey

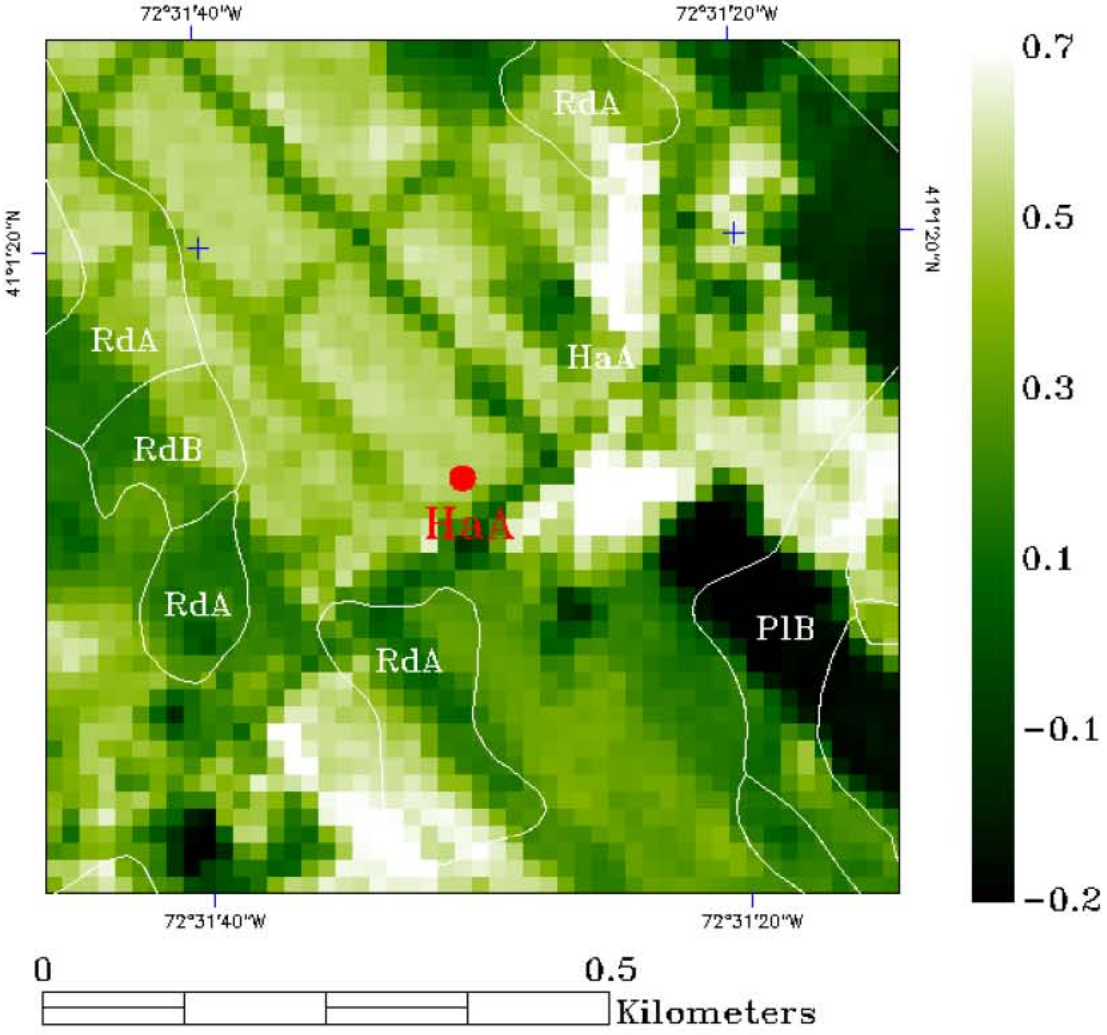

Figure 6. NDVI results Mattituck

Red dot indicates the location of the geophysical survey

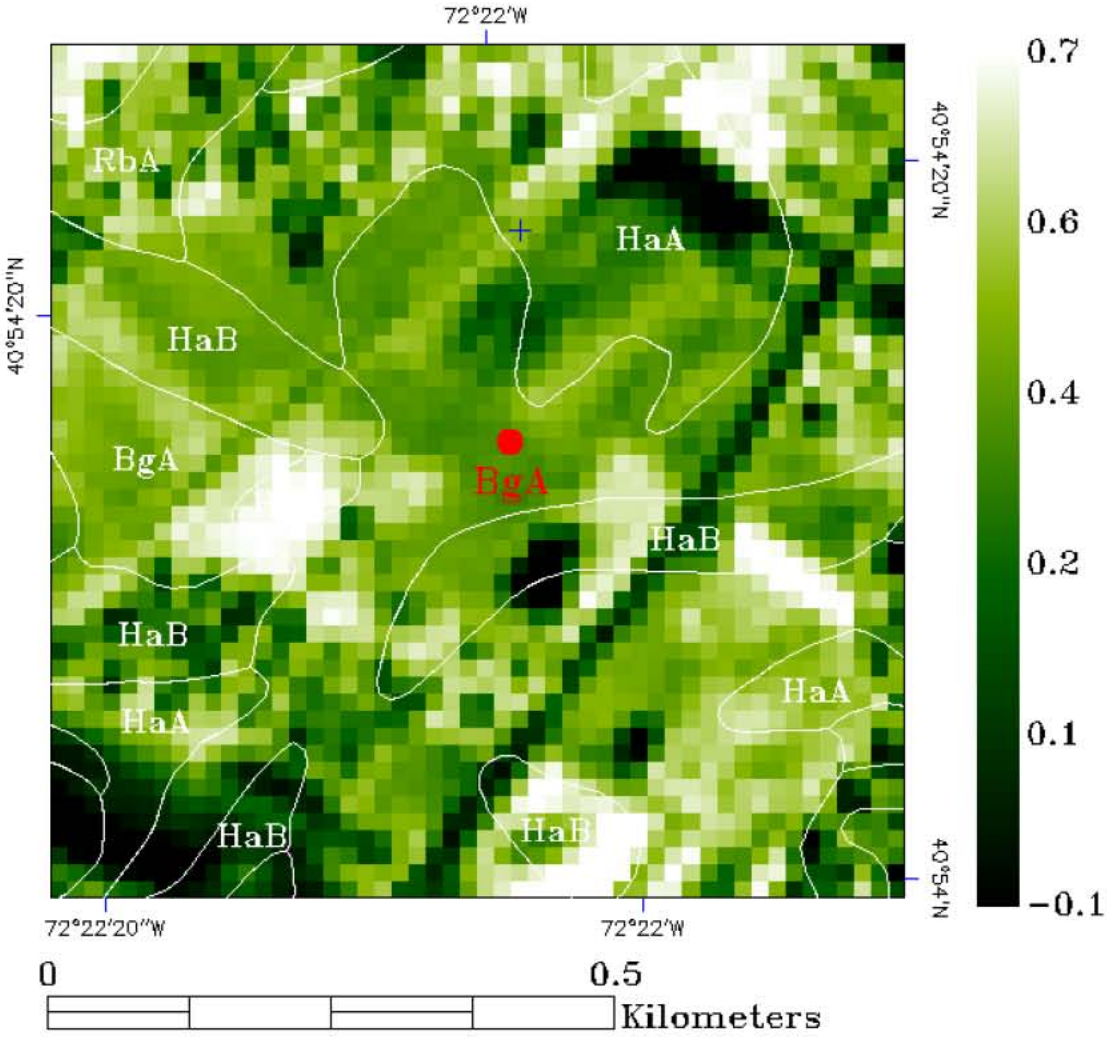

Figure 7. NDVI results Southampton

Red dot indicates the location of the geophysical survey. It should be noted that the color scale is different in this image as compared with Figures 5 and 6.

CHAPTER 6. THEORY AND METHODS

6.1 Two-dimensional array resistivity imaging

Resistivity surveying was developed during the beginning of the 20th century by Conrad Schlumberger. He obtained the first surface electrical measurements in 1912 in Normandy. Subsurface conditions are inferred through measuring the electrical currents that are carried by the movement of the ions available within the pore spaces. Certain minerals may conduct electricity based on electron movement (e.g. graphite), but most geologic materials conduct electricity by the movement of ions through cracks and pores.

In resistivity surveying, current is injected into the ground through two current electrodes. The potential difference is measured between a pair of potential electrodes. Typically, both the current and potential electrodes are arranged along a straight line. During the survey the location of the electrodes is changed. Short distances between electrodes record near surface areas. Larger distances between the electrodes record deeper areas. The arrays used in this dissertation were the dipole-dipole and Wenner. Figure 8 shows a possible sequence of measurements for the dipole-dipole electrode configuration. The spacing between the two current electrodes remains fixed, and it is the same as the distance between the two potential electrodes, which also remains fixed (i.e. symbol "a" in Figure 8). The distance between the two electrode pairs is progressively increased by a separation factor n. By increasing factor n the depth of investigation also increases. Figure 9 shows a possible sequence of measurements for the Wenner electrode configuration and for a system of 24 electrodes. In the Wenner array, four electrodes are

separated by equal distances. The two outer electrodes are the current electrodes and the two inner ones are the potential electrodes. The current electrodes are responsible for transmitting the current into the ground, whereas the potential electrodes measure the potential gradient within the subsurface. The separation is increased from "a" to "2a", "3a", etc.

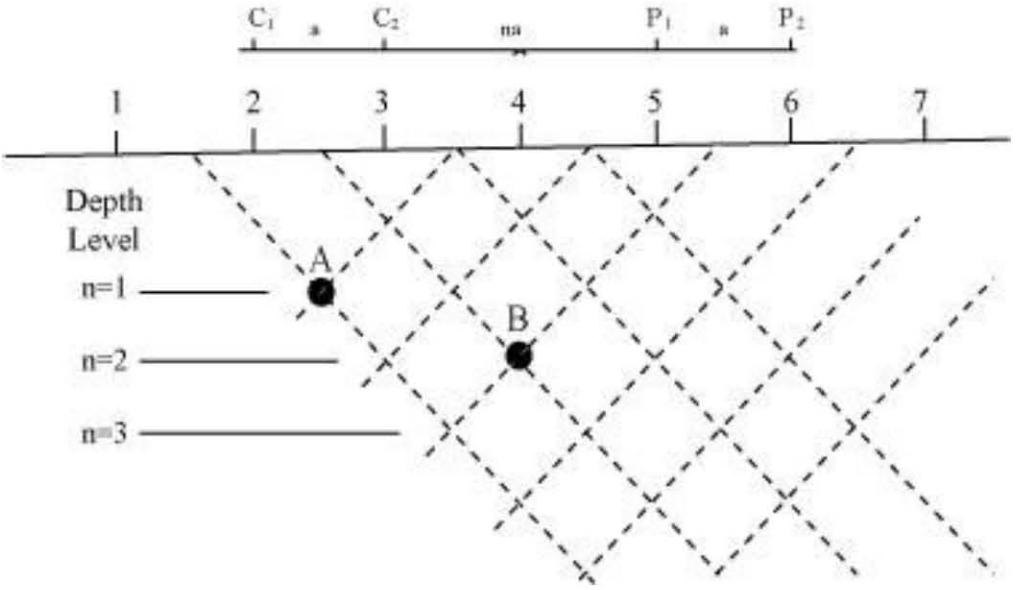

Figure 8. The arrangement of electrodes for a dipole-dipole electrode configuration.

A: Plotting point for dipole 1-2 and dipole 3-4 measurement

B: Plotting point for dipole 2-3 and dipole 5-6 measurement

Before the 1990's, resistivity surveying comprised the one dimensional (1D) techniques of vertical electrical sounding (VES) and constant separation traversing (CST). In VES deeper current penetration is achieved by progressively expanding the electrode spread on either side of an established point. The relative spacing remains the same between the current and potential electrodes. This method estimates vertical

variations in resistivity, thus is effective in the delineation of layer thickness and resistivity when the ground consists of horizontal layers. CST is more effective in the delineation of lateral variations. The electrode spacing remains fixed and the electrode spread is moved altogether along the survey transect.

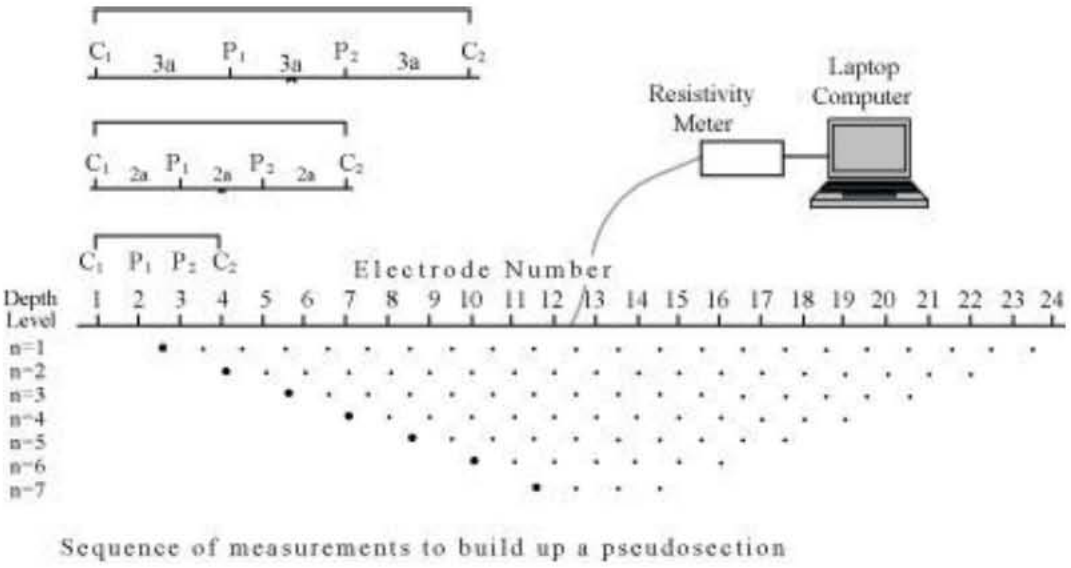

Figure 9. The arrangement of electrodes for a 2-D electrical survey and the sequence of measurements used to build up a pseudosection (Modified from Griffiths and Barker, 1993).

The method of investigation that was employed in this dissertation is two-dimensional array resistivity imaging, as described in the work carried out by the University of Birmingham research group (Griffiths and Turnbull, 1985; Griffiths et al, 1990). These surveys are conducted by using at least 24 electrodes laid out on a straight line with a constant spacing. Four electrodes are activated at a time. The active electrodes are changed automatically by a computer program in a laptop computer or the resistivity meter itself. By increasing the electrode separation the apparent resistivity can be measured at greater depth.

In order to plot the raw data from a two-dimensional imaging survey, the pseudosection method is used (Musset and Khan, 2000). In the dipole-dipole array (Figure 8), the current dipole consists of a pair of adjacent electrodes that is used to inject current into the ground and the potential dipole consists of another pair of electrodes that is used to measure the potential difference. In two-dimensional imaging the measured value of apparent resistivity is plotted at the intersection of 45° lines drawn down from the midpoint of each pair. The apparent resistivity values are then contoured to produce a 2D picture of the subsurface. This represents qualitatively the spatial variation of resistivity in the cross-section. The plot obtained by contouring the apparent resistivity values is called a pseudosection –literally a "lying section" – because the plotting depths are arbitrary and the variation of resistivity within the section is averaged over a large volume.

6.2 Inversion of results with computer software RES2DINV

It is possible to invert the pseudosections into a "true" resistivity section. Inversion techniques have been reviewed and compared by several authors (Clearbout and Muir, 1973; deGroot-Hedlin and Constable, 1990; Edwards, 1977; Loke and Barker, 1996a; Loke and Dahlin, 2002; Sasaki, 1989; Sasaki, 1992; Yeh et al, 2002). All inversion methods essentially try to find a model for the subsurface whose electrical response agrees with the measured data.

For the needs of this study, the computer program RES2DINV was used. This program uses an iterative method that starts from an initial model and tries to find an improved model whose calculated apparent resistivity values are closer to the measured values (Loke and Barker, 1996b).

A sample of the RES2DINV output is presented in Figure 10. The first cross section is a pseudosection contoured from the raw data (measured apparent resisitivity), the second contours the predicted apparent resistivity data based on the inversion (calculated apparent resisitivity). The third cross section is plotted at true vertical scale and represents the inverted data for true resistivity (inverse model resistivity). In the third section, the resistivity values have been modified over the course of several iterations in an effort to minimize the difference between the calculated and measured apparent resistivity values. The root-mean-squared (RMS) error is an indicator of this difference.

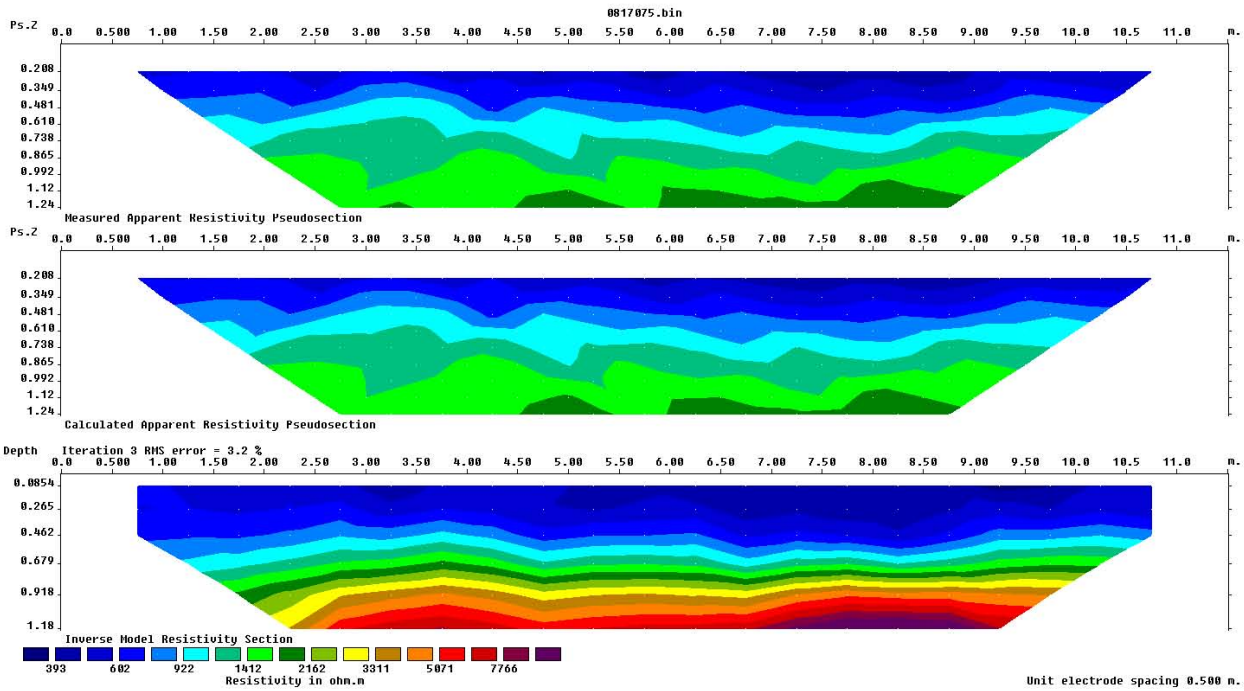

Figure 10. A sample of the RES2DINV output

Contour intervals in the cross sections can be adjusted by means of a logarithmic transformation and by defining a set minimum value. For all measurements within the same site the contour intervals were adjusted to provide uniform contouring for all measurements, thus allowing for comparison between measurements obtained within the same site. Attempts to produce universal contouring for all sites through RES2DINV were unsuccessful due to the large average resistivity variations between the four sites. The large contour intervals that would be required for a universal contouring scheme would provide significantly less detail at the near-surface soil layer, which is the focus of this dissertation. Instead, the different sites were compared through summary statistics produced for each site in the ArcGIS environment. Those processed data are presented in the discussion section of this dissertation.

The Gauss-Newton least-squares inversion method (deGroot-Hedlin and Constable, 1990; Sasaki, 1992) is considered suitable for most data sets (Loke, 2002), therefore it was used as the basic approach for all sites presented in this dissertation. The program proceeds with additional iterations until the RMS error changes by less than 0.5% between successive iterations (Loke, 2004).

The Gauss-Newton least-squares inversion method was used without modification for all the baseline measurements obtained during the pre-infiltration stage. For the measurements obtained during infiltration, the same method was refined on a site-by-site basis in an effort to highlight the effect of infiltration and to reduce the RMS error. The inversion procedure adjustments included a) using a narrower model cell, b) reducing the effect of side blocks, and c) removing bad data points.

The default model cell produced in RES2DINV is equal to the unit electrode spacing, which for this dissertation is 0.5 meters. By reducing the cell width to half the unit electrode spacing better results may be produced in cases where large resistivity variations are observed near the surface. This was done at the Mattituck site, where large resistivity variations near the surface were observed.

The side blocks of the pseudosections produced by RES2DINV carry more weight than the interior blocks due to the additive effect of all the elements associated with it. By reducing the effect of the model blocks located at the bottom and on either side of the pseudosection better results may be obtained for certain data-sets.

Finally, the removal of bad data points was found to reduce significantly the RMS error. Bad data points can be due to a number of causes, including contact problems between specific electrodes and the ground, and the presence of telluric currents. In certain data-sets that were inverted for this dissertation the removal of only one bad datum from the data-set effectively reduced the RMS error. The removal of bad data points in no case exceeded three points.

6.3 Field Methods

6.3.1 Geophysical methods

This dissertation data collection program was conducted using the above-mentioned electrode arrays (i.e. dipole-dipole and Wenner). The factors influencing the electrode array selection included the signal-to-noise ratio, survey speed, depth of

investigation, sensitivity, resolution of geologic units, and others. The Wenner array has higher signal strength than the dipole-dipole array. Therefore, it has a better signal-to-noise ratio. The Wenner array has also a deeper depth of investigation and data are obtained at a faster rate than the dipole-dipole array. However, the dipole-dipole array is more effective in detecting horizontal resistivity variations and it has a better horizontal coverage than the Wenner array.

The resistivity meter that was used (Syscal Kid Switch, Iris Instruments) allows for electrode spacing with a range between half meter and three meters. Its output characteristics are 200 V maximum output voltage, 25 W maximum output power, and 500 mA maximum output current.

The resistivity meter has the ability to perform induced polarization (IP) measurements. IP is a method specifically designed to evaluate the capacitance of the ground (Keller and Frischknecht, 1966). This method is valuable in shallow surveys due to its ability to detect the presence of clay. IP is caused by the membrane polarization and electrode polarization effects. Membrane polarization is the relevant mechanism for the data of this dissertation. Membrane polarization is associated with small size pores typically found in clay-rich environments. As current is passing in the form of electrolytic flow through the ground, negatively charged clay minerals tend to concentrate on the surface of narrow or blocked pores. These, in turn, attract positive ions on the other side. This accumulation of opposite charges on either side of a blocked or narrow pore creates a small current when the external current is switched off.

The measured parameter in the IP surveys is chargeability. Chargeability (M) is measured in in millivolt per volt (mV/V) or in milliseconds. When the current is

switched off the electric field will drop suddenly to a lower value, but there is some additional time required for it to drop to zero (Figure 11). Chargeability is measured between two different times after the initial drop.

$$M = A / \Delta c \qquad \text{(Keary et al, 2002)}$$

Where M: Chargeability

A: Area beneath the decay curve over a certain time interval (t_1-t_2)

Δc: steady-state potential difference

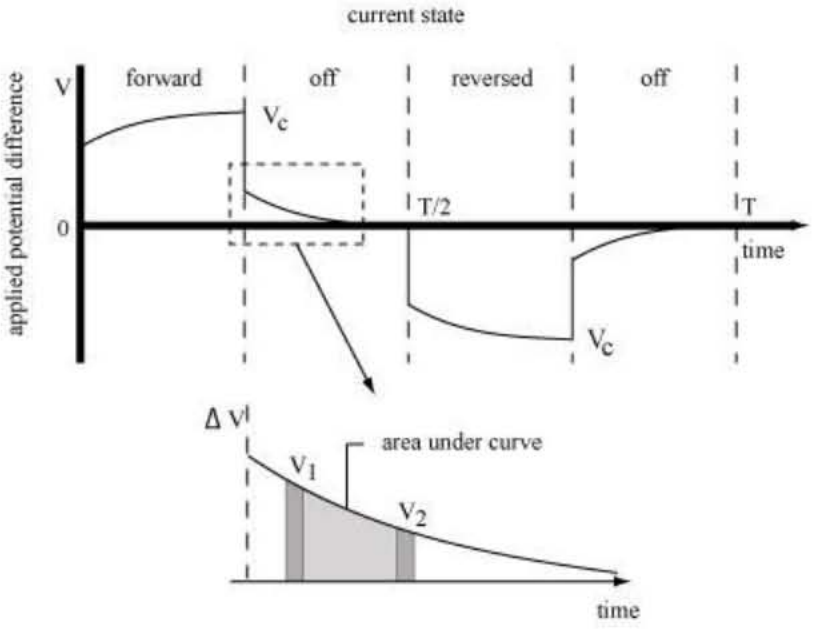

Figure 11. Chargeability Cycle, Modified from Kearey et al (2002)

The resistivity meter allows for combined measurements of resistivity and IP. However, the IP mode requires significantly more time for the measurement to reach completion. When measuring resistivity only there are two options for the current injection time, the short mode, and the standard mode. In terms of the total time required to construct a pseudosection, the IP mode is the lengthier, the short is the shortest, and the standard is in between. Another factor that affects the duration of each measurement is

the choice of electrode array. The Wenner electrode configuration requires less time than dipole-dipole, because it requires fewer measurements to construct a pseudosection. Based on the above-mentioned it can be easily concluded that when following an infiltration experiment there is a tradeoff between accuracy and duration of the measurement.

In an effort to clearly demonstrate the effect of mode and of array type on the results, comparative measurements for the two array types were obtained. Especially when evaluating time-dependent phenomena (e. g. infiltration experiments), IP surveying was conducted only as part of the baseline measurements. This is considered a good compromise between the need to follow as close as possible the progress of an infiltration experiment time and to evaluate the presence and effects of clay lenses on the results at the same time.

6.3.2 Infiltration Experiment

A flooding-type infiltrometer was constructed specifically for this dissertation. This is a 14.5-inch long plastic cylinder of 11.5 inches in diameter (total volume: 5 gallons), which is open at both ends. During the field experiment the cylinder was driven into the ground to a depth of 3 to 5 centimeters. After the infiltration was initiated a reasonably steady rate was achieved. The experiments lasted from 6 to 10 hours depending on soil type. Two infiltrometers were installed at two different locations along the survey line.

6.3.3 Lithium Tracer (Middleburgh Site)

The selection of Lithium Chloride as a tracer for the experiment performed at the Middleburgh site was based on the discussion offered by Flury and Wai (2003) on the ideal water tracer characteristics. Inevitably, the tracer selected by any researcher always deviates from the ideal water tracer, depending upon site-specific characteristics and other environmental factors. Other tracer options were evaluated on-site, including Rhodamine-WT (obtained from Dr. Pengfei Zhang's laboratory, City College of New York Department of Earth and Atmospheric Sciences) and fluorescent dyes in liquid and powder form in various concentrations (obtained from commercial supplier Norlab Inc., 7465 Industrial Parkway, Lorain, Ohio, 44053, product description: fluorescent yellow-green dye, and based on Markus Flury, personal communication, 1/26/07).

Lithium tracer was considered most suitable for this experiment due to environmental and logistical considerations. Lithium Chloride is expected to enhance the effect of infiltration as it is captured with resistivity surveying. It is noted that no tracer was applied to the agricultural sites, because of concerns about contamination of the edible products produced at the site. It is expected that organic matter and fine particles present at the Middleburgh site increase sorption of Lithium. However, Dierberg and DeBusk (2005) found that Lithium at low initial tracer concentrations was less affected by adsorption and microbial processes than was Rhodamine-WT (28–516 mg/L for Lithium and 4.9-64 mg/L for Rhodamine-WT). Lithium is a naturally occurring element, but it is absent in most soils or found in small concentrations, which makes its detection straightforward (Lund and Young, 2005).

Infiltration at the Middleburgh site was carried out for an initial one-hour period to achieve a steady state flow regime. Sixteen gallons of water were infiltrated through either infiltrometer during this time. Then another fifteen gallons of 15 mg/L Lithium Chloride tracer was injected during the experiment.

Table 9. Spectrochemical determination of total recoverable Lithium Chloride.
Middleburgh Study Site
Spectrometer: M Series 650244 v1.23 Analysis Date: 4/9/2008

Soil Sampling ID	Soil Sampling Location between electrodes	LiCl Concentration mg/L
Blank	n/a	0
Standard 1	n/a	0.164
Standard 2	n/a	0.327
Standard 3	n/a	0.486
1	4-5	1.0979
2 (Deeper Sampling 16-32 inches)	5-6	1.0477
3	6-7	1.439
4 (Infliltrometer A)	7-8 (Infliltrometer Location)	2.4735
5	8-9	0.755
6 (Unsuccessful Sampling)	9	n/a
7	9-10	1.339
8	10-11	1.0197
9	11-12	0.8706
10 (Unsuccessful Sampling)	12	n/a
11	12-13	0.9482
12 (Infliltrometer B)	13-14 (Infliltrometer Location)	2.7511
13	14-15	1.1229
14 (Deeper Sampling 16-32 -inches)	15-16	0.5910
15	16-17	0.6843
Tap Water Sample	n/a	0.0595
Bottled Water ("Miscoe Spring Water")	n/a	0

Soil samples were obtained with a hand-operated auger immediately after the termination of the infiltration experiment. The auger that was used consisted of a cylinder (16" length, 3-1/4" diameter). One end of the auger has cutting lips for more effective penetration and the other end is connected to a rod, which in turn is connected to a "cross" handle. By rotation of the handle the auger head advances into the soil. Soil was collected inside the auger and emptied on the surface. The equipment was cleaned after each use to prevent cross contamination. Contamination from rusting of this equipment is not possible, as the soil auger was purchased specifically for this dissertation and this was the first time that it was used. All samples were collected from the top soil layer within a range of 16 inches from the surface, except for two samples, which were collected at a deeper layer within a range of 16 to 32 inches. Soil sampling was unsuccessful in two locations (samples 6 and 10) due to extensive root presence, which prohibited penetration of the hand-auger. The sampling equipment was cleaned before reaching the deeper sampling interval to avoid contamination from penetrating the top layer.

Subsequent analysis at the laboratory of the Department of Earth and Atmospheric Sciences of City College of New York included the spectrochemical determination of total recoverable Lithium Chloride. The laboratory analysis was conducted according to EPA method 200.2 (Martin et al, 1994). Table 9 summarizes the result of this analysis. Highest Lithium concentrations were recorded for the soil samples obtained directly from the infiltration locations (soil samples 4 and 12). The recorded values were 2.4735 mg/L over infiltrometer A and 2.7511 mg/L over infiltrometer B, respectively. The next highest value (1.439 mg/L, soil sample 3) was recorded for the soil sample obtained between electrodes 6 and 7, which was 1 meter from infiltrometer A (i.e.

one of two Lithium tracer application locations). Another high concentration was recorded for the soil sample obtained between electrodes 9 and 10 (1.339 mg/L, soil sample 7). The remaining values range from 0.5910 mg/L (minimum) to 1.1229 mg/L (maximum). A water sample from the local tap water, which was injected prior to the tracer introduction, was analyzed and the Lithium concentration was found to be 0.0595 mg/L. The spectrochemical analysis of a water sample from the bottled water, which was used for the tracer solution (Label: "Miscoe Spring Water"), did not yield any Lithium concentrations.

The results demonstrate that the movement of water during infiltration was almost entirely vertical, except in one case, which suggests localized lateral water movement (sample 3). The remaining values most likely represent background concentrations for Lithium (except for the high concentration recorded for soil sample 7). This is consistent with Claridge et al (1999), who reported that lateral movement of Lithium tracer is more significant in wet soils, as opposed to dry soils. The infiltration area was protected from rainfall for a period of two weeks prior to the experiment, which would account for dryer conditions than normal for the top soil for the particular site. The unusually high concentration recorded for soil sample 7 does not correlate with the inferred water front migration through the geophysical data. On the other hand, the excavation revealed an extensive root system in this location (i.e. approximately at the mid-distance between the two infiltrometers). Thus, it is possible that the recorded high Lithium concentration is the result of the combined effect from infiltration originating from both infiltrometers and flowing preferentially along the root system in small quantities not detected with geophysics.

6.3.4 Measurement Protocol

The data collection program was divided into a pre-infiltration stage and an infiltration stage. Seven data sets were collected for each site in the pre-infiltration stage in order to evaluate the consistency of the ERI imaging method (See flowchart "Baseline Geophysical Data", Figure 12).

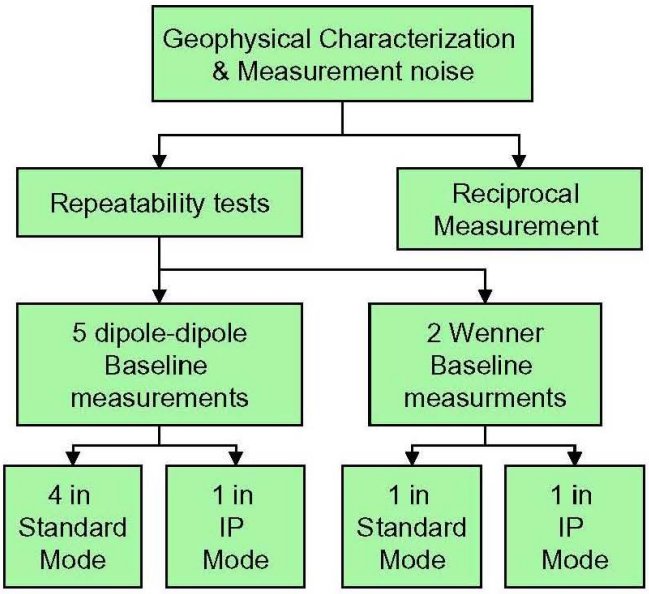

Figure 12. Baseline Geophysical Data – Flowchart

Out of these seven data sets, five were obtained using the dipole-dipole array and two using the Wenner array. There was one measurement from each array type in the induced polarization (IP) mode. The remaining measurements were all conducted in standard mode. One of the five dipole-dipole array measurements was a reciprocal measurement, in which the current and potential electrode pairs are interchanged. Both the repeatability and reciprocal measurements demonstrated that the ERI imaging method provides consistent data between measurements within the same field and under the same

meteorological conditions. Significant temperature changes between measurements of the pre-infiltration stage and the infiltration stage were not encountered. The evaluation of the effect of seasonal variations in soil resistivity within the same site is beyond the scope of this dissertation, therefore it was not considered.

Deviations from the pre-infiltration norm, described above, include the acquisition of additional baseline measurements at the Riverhead and Middleburgh sites. In the Riverhead study site seven additional measurements for a total of fourteen datasets were collected in the pre-infiltration stage to evaluate within-field variations of resistivity. The results were very similar to those obtained along the resistivity line, indicating little within-field variability. A significantly higher number of pre-infiltration measurements were obtained in the forested area in Middleburgh to evaluate the effect of tree roots in the resistivity data. The results of the latter measurements will be discussed in chapter 8.7.

During the infiltration stage, data were collected during different time intervals in an effort to monitor the migration of the water front, as well as other changes in the subsurface resistivity over a period of six to eight hours on average. Only the dipole-dipole array was used during infiltration.

From the three types of sections and pseudosections described in the methods section of this dissertation (measured apparent resisitivity, calculated apparent resisitivity, and inverse model resistivity) only the inverted sections will be presented in the results in chapter 7. The measured apparent resistivity for all lines will be presented in Appendix 2. A comparison of all the inverted sections for the baselines obtained during the pre-infiltration stage, including the four available dipole-dipole measurements, the

one dipole-dipole reciprocal measurement, and the two Wenner measurements will be presented only for the Riverhead study site (Figure 14 (a) through (g)). From the three remaining sites, only one representative dipole-dipole baseline measurement will be presented, as well as one representative Wenner baseline measurement (Figures 17, 20, and 22). Cross sections of inverted resistivity data for the remaining baselines will be presented in Appendix 1.

Resistivity data sets were obtained almost continuously during the period of infiltration.

All the completed inverted sections for the series of data-sets obtained during infiltration will be presented for each site. A barrel symbol superimposed on the inverted sections will mark the location of the two infiltrometers in relation to the electrodes. A table summarizing the infiltration surveys will be presented (Tables 10, 11, 12, and 13), followed by the respective cross sections for every site. Underneath each image, the sequence number of each measurement during infiltration is indicated, along with the time difference from the initiation of infiltration (i.e. symbol "Δt"), and the volume of water added to either infiltrometer (i.e. infiltrometer "A" is located on the top left of each image, and infiltrometer "B" is located on the top right of each image). Each infiltrometer could hold 5 gallons of water. After the initiation of infiltration a reasonable effort was made to maintain a constant head. In Tables 10, 11, 12, and 13 the volume of water noted next to each geophysical survey at different times "Δt" from the initiation of infiltration represents the amount of water that was infiltrated during the respective measurement. The color scheme for the infiltration results was adjusted using the contour interval

options offered by RES2DINV in an effort to highlight small-range resistivity changes near the surface.

It should be noted that these measurements were conducted during the summer of 2007, which was one of the driest on record. Ambient temperatures were within the range of 80 and 100 degrees Fahrenheit. Specifically, the day of the infiltration experiment at the Mattituck site the temperature exceeded 100 degrees Fahrenheit.

CHAPTER 7. RESULTS

7.1 First Site: Riverhead, Suffolk County, New York

The first site is Cornell University's Horticultural Research and Extension Center located at 3059 Sound Avenue, Riverhead, NY 11901 (Coordinates: N 40° 57.618′, W 72° 42.718′). The soil is classified as Riverhead sandy loam (RdA). An aerial photograph of the site, as well as soil classification information is presented in Figure 13.

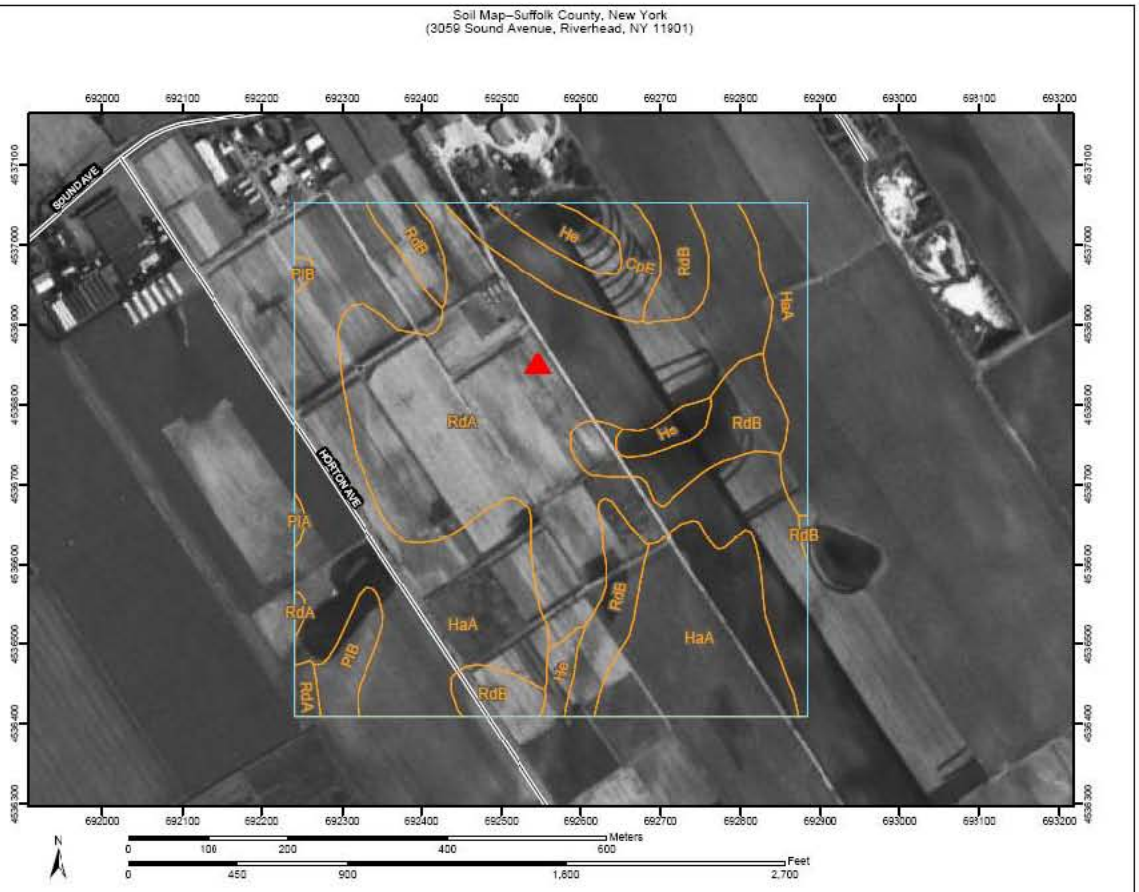

Figure 13. Aerial Photograph - Soil Type: RdA Riverhead sandy loam
Physical Address: Long Island site is Cornell University's Horticultural Research and Extension Center in Riverhead, 3059 Sound Avenue, Riverhead, NY 11901
Coordinates: N 40° 57.618′, W 072° 42.718′
▲ Site Location
Source: USDA, Natural Resources Conservation Service, National Cooperative Soil Survey, Suffolk County, New York

7.2 Riverhead baseline measurements

The baseline measurements for the Riverhead site (Figure 14 [a] through [g]), demonstrate a well stratified subsurface environment. Resistivity values increase with depth. The lowest resistivity values observed near the surface demonstrate the effect of the available background moisture and a lesser compaction, as opposed to deeper layers. The images are consistent with one another, and they satisfactorily meet the repeatability requirements. The reciprocal measurement represented in Figure 14 (d), in which the current and potential electrode pairs are interchanged, is very similar to the rest of the dipole-dipole measurements due to the horizontal continuity of the resistivity ranges with depth. In the absence of horizontal variations the reciprocal measurement does not demonstrate significant differences from the rest of the baseline measurements. The two Wenner baseline measurements, one in induced polarization mode presented in Figure 14 (f) and the other in standard mode presented in Figure 14 (g), provide similar results with the dipole-dipole measurements for resistivity ranges and relative increase with depth. Chargeability (i.e., induced polarization) values ranged from 2.06 to 3.67 mV/V.

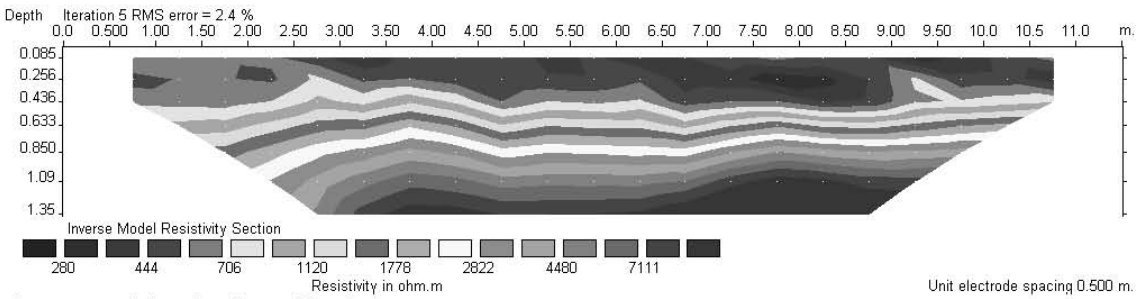

Figure 14 (a) Dipole – dipole 1
Riverhead baseline measurements

****

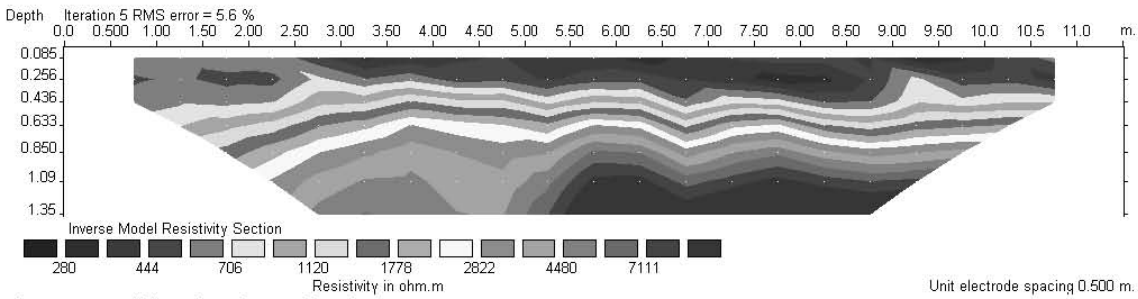

Figure 14 (b) Dipole – dipole 2
Riverhead baseline measurements

****

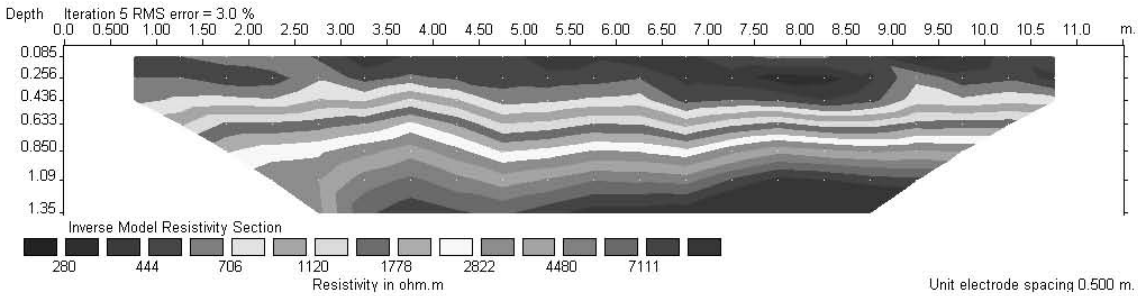

Figure 14 (c) Dipole – dipole 3
Riverhead baseline measurements

****

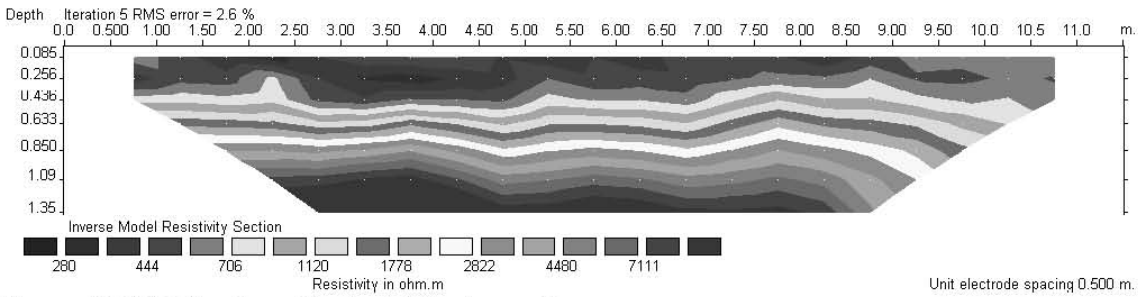

Figure 14 (d) Dipole – dipole 4 (Reciprocal)
Riverhead baseline measurements

****

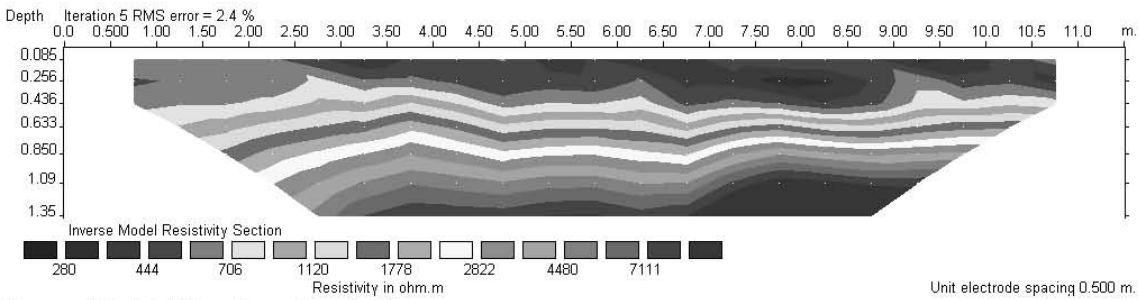

Figure 14 (e) Dipole – dipole 5
Riverhead baseline measurements

****

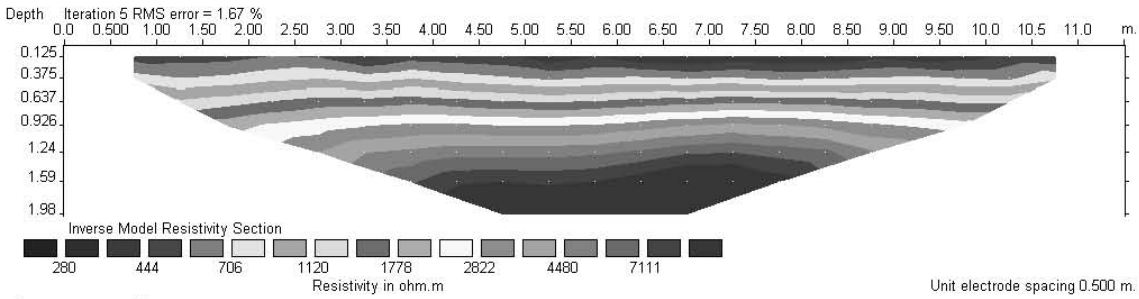

Figure 14 (f) Wenner 1
Riverhead baseline measurements

****

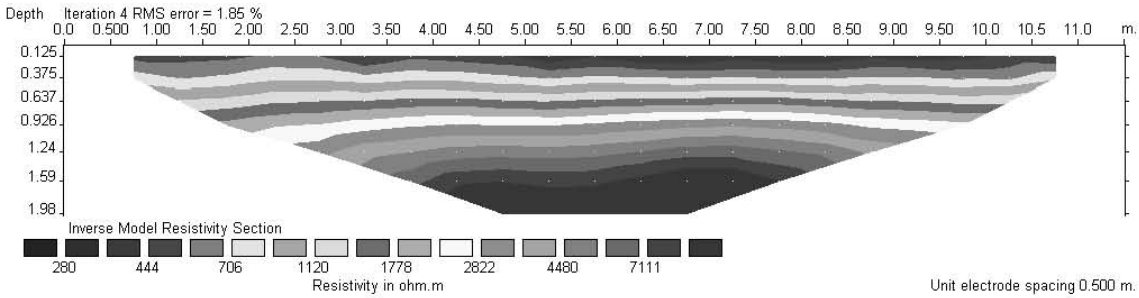

Figure 14 (g) Wenner 2
Riverhead baseline measurements

****

7.3 Riverhead infiltration measurements

A summary of the infiltration surveys conducted at the Riverhead study site is presented in Table 10, followed by the respective cross sections for the same site (Figure 15a through 15h). A total of 24.5 gallons of water was infiltrated through the left infiltrometer, and a total of 36.5 gallons of water was infiltrated through the right infiltrometer during the experiment.

Table 10. Summary of Riverhead Infiltration Surveys			
		Infiltrometer A	Infiltrometer B
Survey #	Δt Hours : minutes	Amt. Water (gallons)	Amt. Water (gallons)
1	00:00 – 00:50	0	0
2	00:51 – 01:35	8	12
3	01:36 – 02:25	4	4
4	2:26 – 3:40	4.5	11.5
5	3:41 – 4:30	4	5
6	4:31 – 5:40	4	4
7	5:41 – 7:35	0	0
8	7:36 – 8:25	0	0
	Total Amt. Water	24.5	36.5

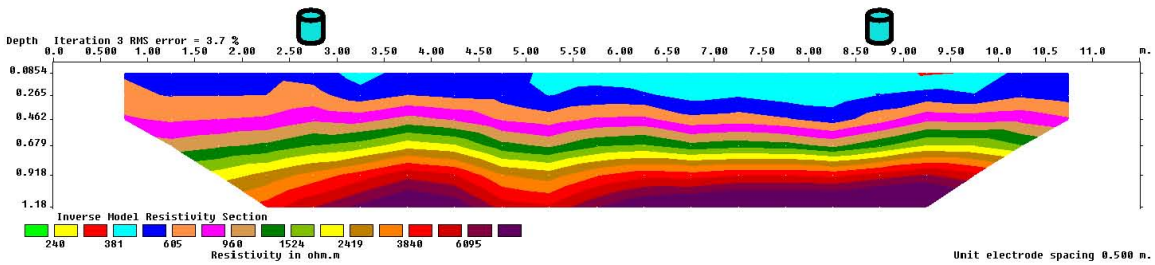

Figure 15 (a) Infiltration Survey 1
Δt = 00:00 – 00:50, Infiltr. A: 0 gal, Infiltr. B: 0 gal
Riverhead infiltration measurements

****

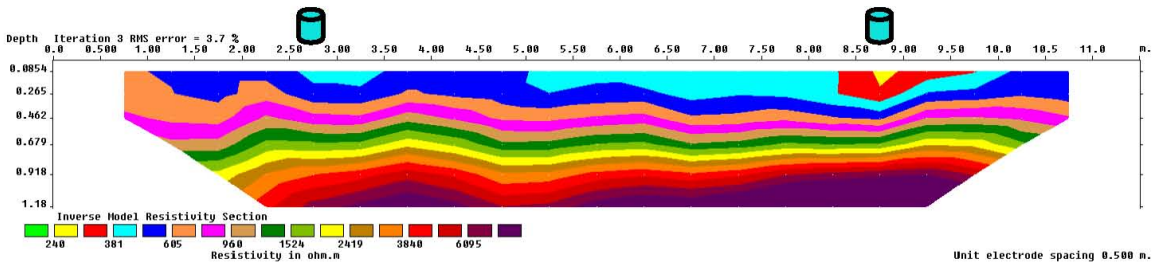

Figure 15 (b) Infiltration Survey 2
Δt = 00:51 – 01:35, Infiltr. A: 8 gal, Infiltr. B: 12 gal
Riverhead infiltration measurements

****

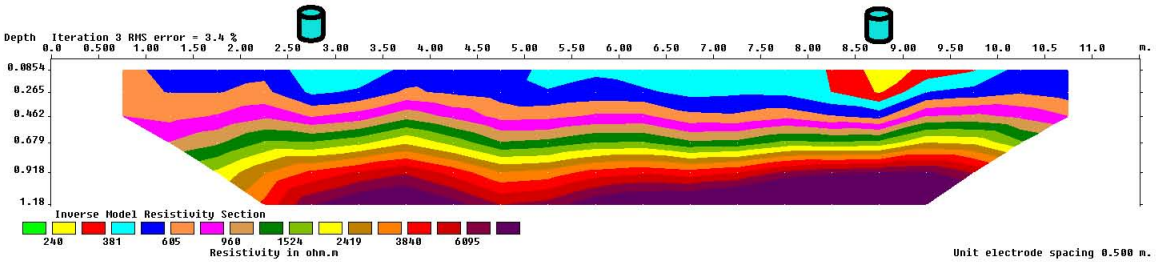

Figure 15 (c) Infiltration Survey 3
Δt = 01:36 – 02:25, Infiltr. A: 4 gal, Infiltr. B: 4 gal
Riverhead infiltration measurements

****

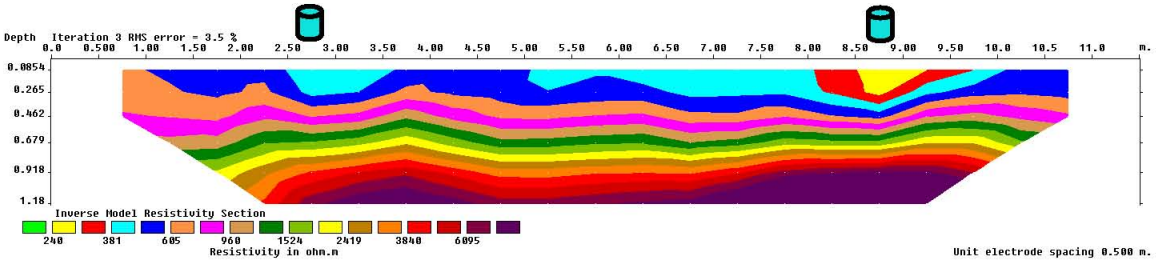

Figure 15 (d) Infiltration Survey 4
Δt = 2:26 – 3:40, Infiltr. A: 4.5 gal, Infiltr. B: 11.5 gal
Riverhead infiltration measurements

****

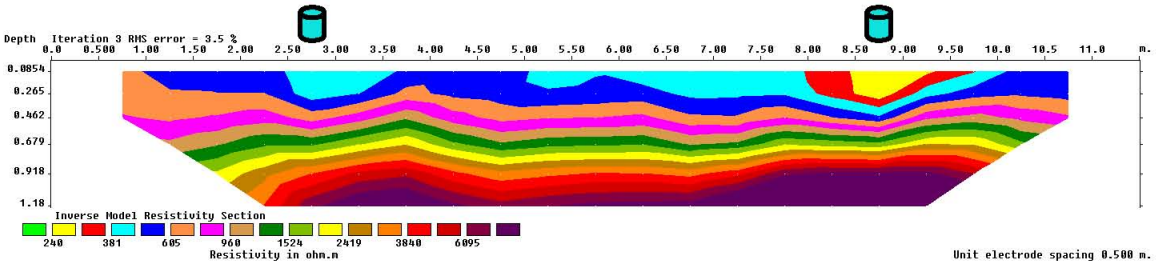

Figure 15 (e) Infiltration Survey 5
Δt = 3:41 – 4:30, Infiltr. A: 4 gal, Infiltr. B: 5 gal
Riverhead infiltration measurements

****

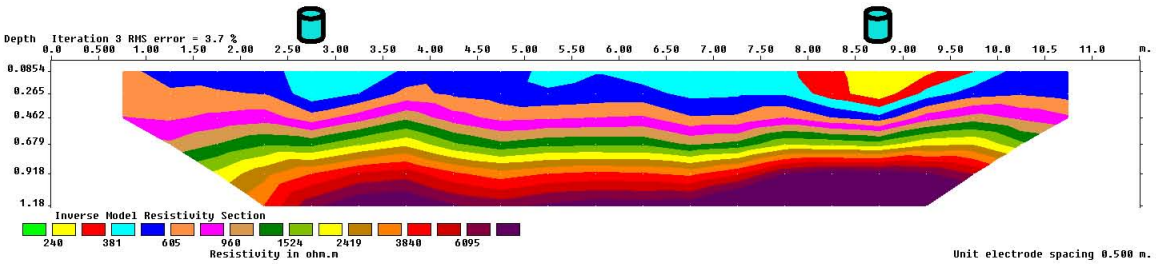

Figure 15 (f) Infiltration Survey 6
Δt = 4:31 – 5:40, Infiltr. A: 4 gal, Infiltr. B: 4 gal
Riverhead infiltration measurements

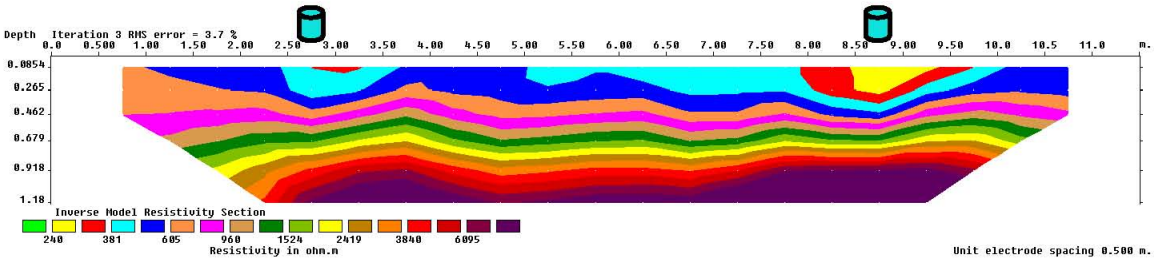

Figure 15 (g) Infiltration Survey 7
Δt = 5:41 – 7:35 Infiltr. A: 0 gal, Infiltr. B: 0 gal
Riverhead infiltration measurements

****

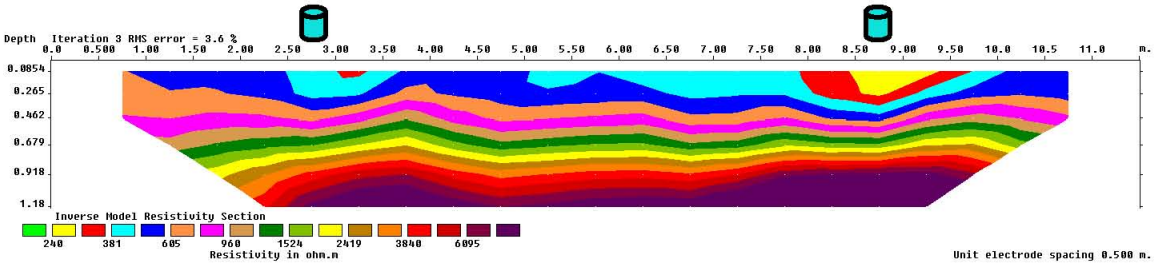

Figure 15 (h) Infiltration Survey 8
Δt = 7:36 – 8:25, Infiltr. A: 0 gal, Infiltr. B: 0 gal
Riverhead infiltration measurements

****

7.4 Second Site: Mattituck, Suffolk County, New York

The second site is located at 41720 Oregon Road, Mattituck, NY 11952 (Coordinates: N 41° 01.229′, W 72° 31.497′). The soil is classified as Haven loam (HaA). An aerial photograph of the site, as well as soil classification information is presented in Figure 16. In Mattituck, a total of 7 gallons of water was infiltrated through each infiltrometer.

Figure 16. Aerial Photograph - Soil Type: HaA, Haven loam
Physical Address: 41720 Oregon Road, Mattituck, NY 11952
Coordinates: N 41° 01.229′, W 072° 31.497′
▲ Site Location
Source: USDA, Natural Resources Conservation Service, National Cooperative Soil Survey, Suffolk County, New York

7.5 Mattituck baseline measurements

One representative dipole-dipole baseline measurement and one representative Wenner baseline measurement is presented in Figure 17. Cross sections of inverted resistivity data for the remaining baselines will be presented in Appendix 1. Chargeability (i.e., induced polarization) values ranged from 0.59 to 3.01 mV/V.

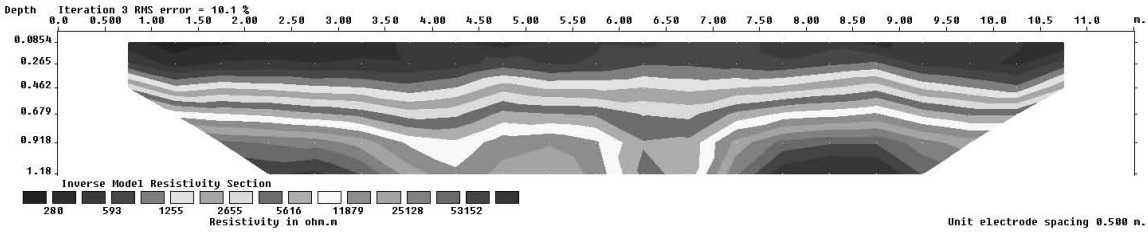

Figure 17 (a) Dipole – dipole
Mattituck baseline measurements

****

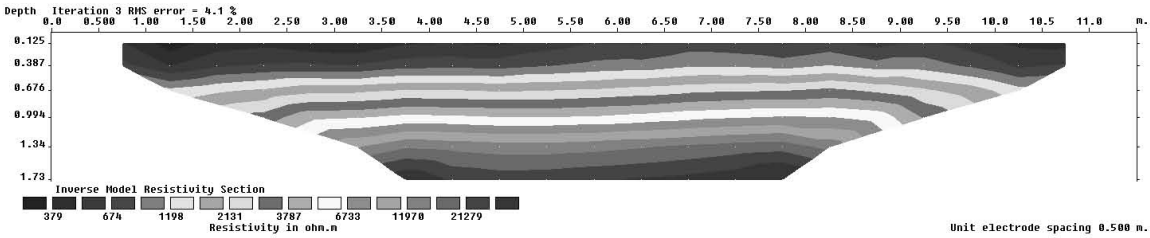

Figure 17 (b) Wenner
Mattituck baseline measurements

****

7.6 Mattituck infiltration measurements

A summary of the infiltration surveys conducted at the Mattituck study site is presented in table 11, followed by the respective resistivity sections for the same site. During the infiltration experiment, water was also applied between the vines from the drip emitters (between Δt 1:35 to 5:55 PM). The drip irrigation system was mounted on wire 24 inches above ground along the entire length of each grape row. 16 inside drip emitters were above the 24 electrodes (inline emitters are placed inside the tubing during the manufacturing process and are equally spaced). A 500 ml graduated cylinder was used to record representative volumes of water released by various emitters per unit of time. The irrigation system provided uniform water application at a rate of 500 ml every 10 minutes or 3,000 ml per hour. The irrigation system contributed approximately 38

gallons of water across the twelve meters of the electrode array (i.e. 16 emitters x 3 litters x 3 hours = 144 litters or 38.041 gallons).

Table 11. Summary of Mattituck Infiltration Surveys			
		Infiltrometer A	Infiltrometer B
Survey #	Δt Hours : minutes	Amt. Water (gallons)	Amt. Water (gallons)
1	0:00 - 1:40	0	0
2	1:41 - 2:30	4	4
3	2:31 - 3:15	2	1
4	3:16 - 4:15	0	0
5	4:16 - 5:00	0	0
6	5:01 - 6:00	3	2
7	6:01 – 7:00	0	0
	Total Amt. Water	7	7

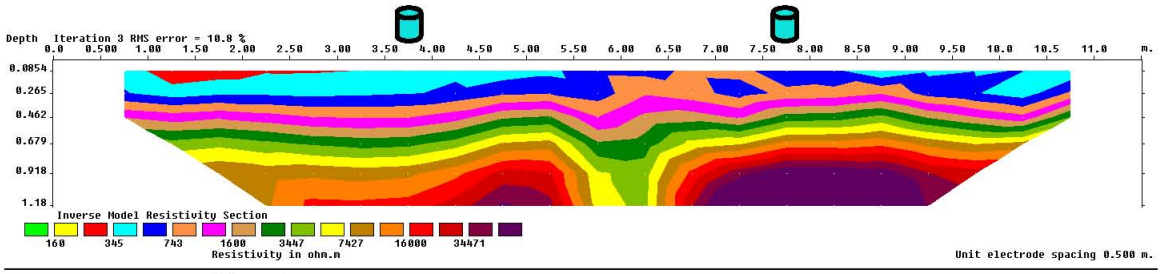

Figure 18 (a) Infiltration Survey 1
Δt = 0:00 - 1:40, Infiltr. A: 0 gal, Infiltr. B: 0 gal
Mattituck infiltration measurements

****

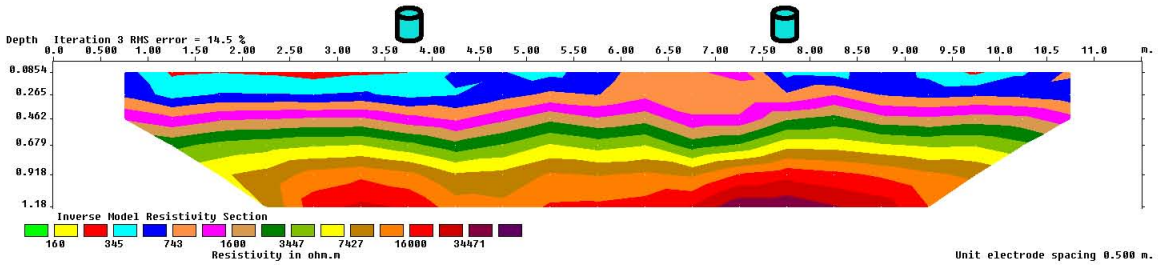

Figure 18 (b) Infiltration Survey 2
Δt = 1:41 - 2:30, Infiltr. A: 4 gal, Infiltr. B: 4 gal
Mattituck infiltration measurements

****

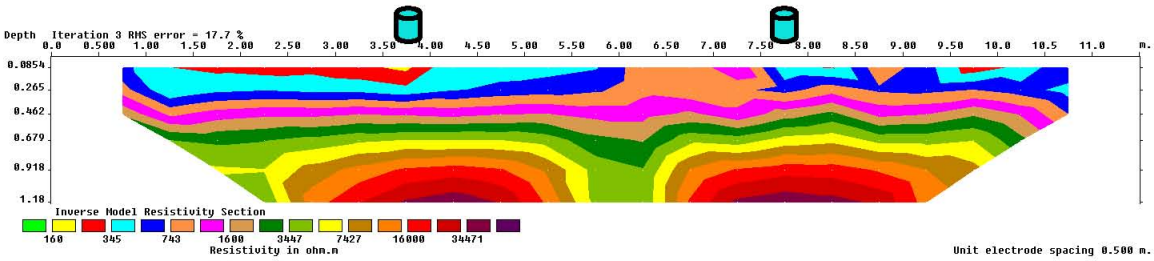

Figure 18 (c) Infiltration Survey 3
Δt = 2:31 - 3:15, Infiltr. A: 2 gal, Infiltr. B: 1 gal
Mattituck infiltration measurements

****

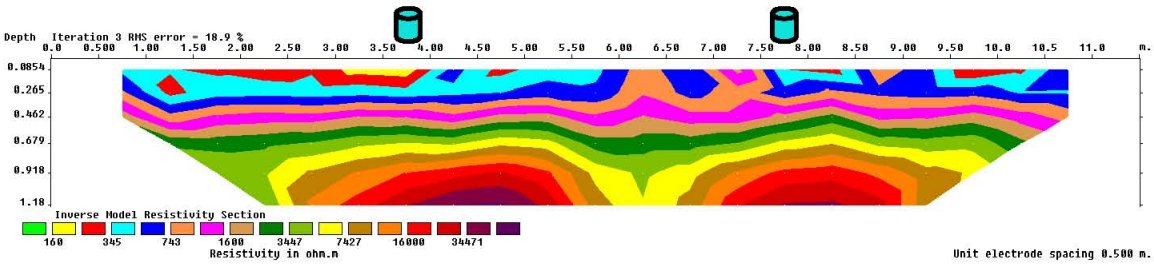

Figure 18 (d) Infiltration Survey 4
Δt = 3:16 - 4:15, Infiltr. A: 0 gal, Infiltr. B: 0 gal
Mattituck infiltration measurements

****

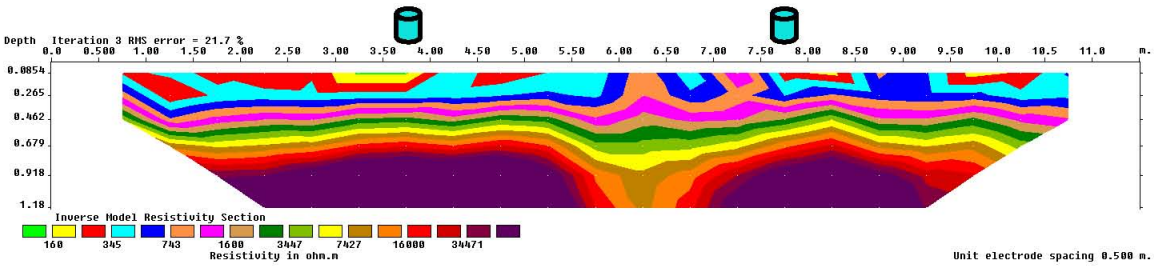

Figure 18 (e) Infiltration Survey 5
Δt = 4:16 - 5:00, Infiltr. A: 0 gal, Infiltr. B: 0 gal
Mattituck infiltration measurements

****

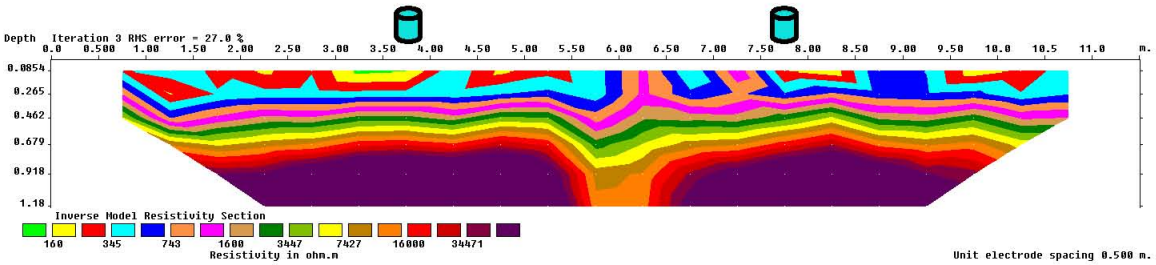

Figure 18 (f) Infiltration Survey 6
Δt = 5:01 - 6:00, Infiltr. A: 3 gal, Infiltr. B: 2 gal
Mattituck infiltration measurements

****

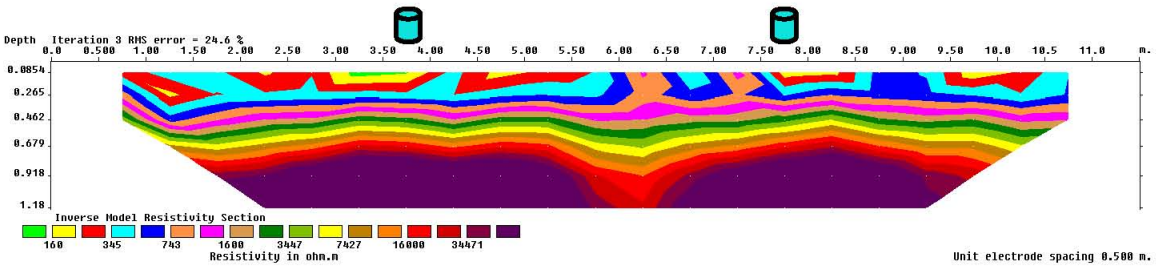

Figure 18 (g) Infiltration Survey 7
Δt = 6:01 – 7:00 Infiltr. A: 0 gal, Infiltr. B: 0 gal
Mattituck infiltration measurements

****

7.7 Third Site: Southampton, Suffolk County, New York

The third site is located at 231 Montauk Highway (Route 27), Water Mill in Southampton, NY 11976 (Coordinates: N 40° 54.238′, W 72° 22.031′). The soil is classified as Bridgehampton silt loam (BgA). An aerial photograph of the site, as well as soil classification information is presented in Figure 19.

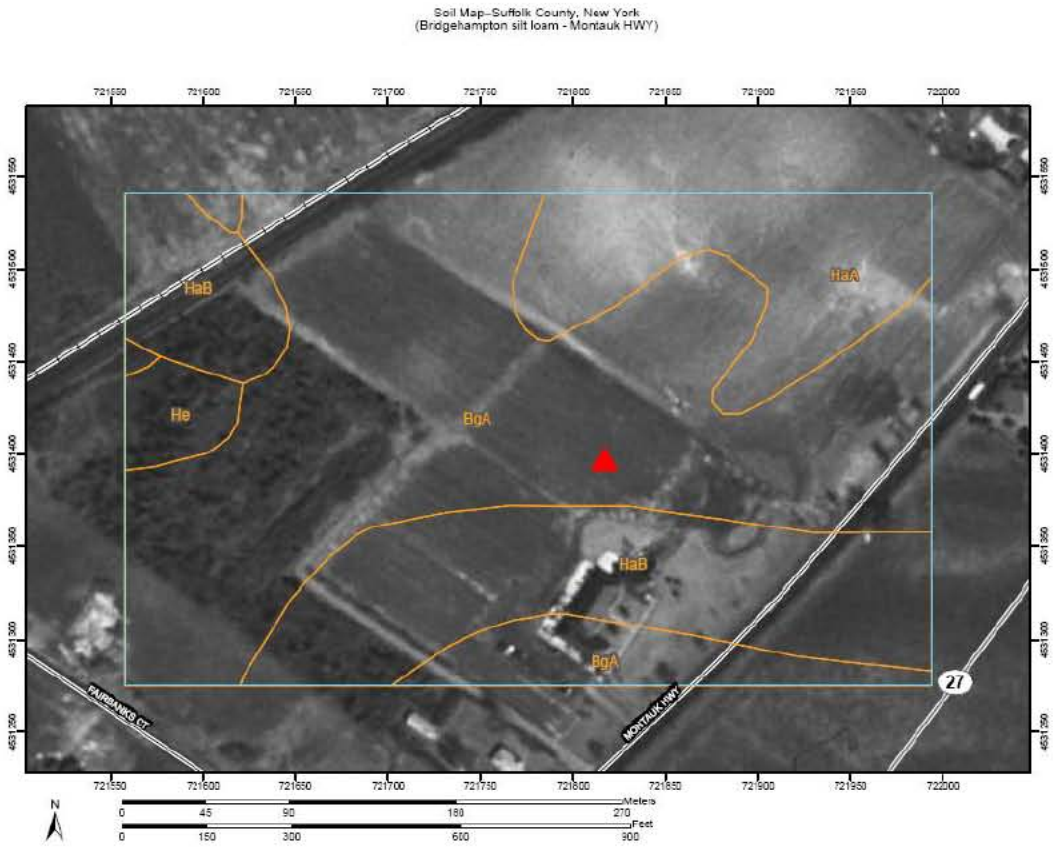

Figure 19. Aerial Photograph - Soil Type: BgA, Bridgehampton silt loam
Physical Address: 231 Montauk Highway (Route 27), Hamlet of Water Mill in Southampton, NY 11976
Coordinates: N 40° 54.238′, W 072° 22.031′
▲ Site Location
Source: USDA, Natural Resources Conservation Service, National Cooperative Soil Survey, Suffolk County, New York

7.8 Southampton baseline measurements

One representative dipole-dipole baseline measurement and one representative Wenner baseline measurement is presented in Figure 20. Cross sections of inverted resistivity data for the remaining baselines will be presented in Appendix 1. Chargeability (i.e., induced polarization) values ranged from 0.79 to 2.88 mV/V.

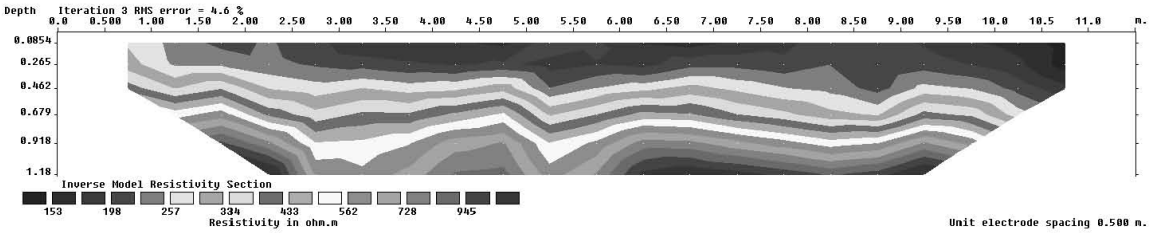

Figure 20 (a) Dipole – dipole
Southampton baseline measurements

****

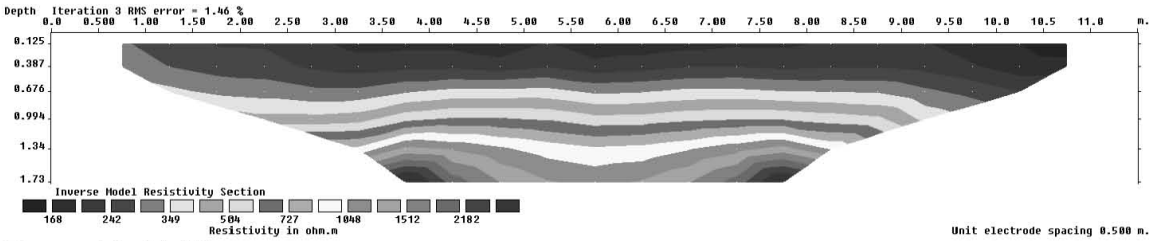

Figure 20 (b) Wenner
Southampton baseline measurements

****

7.9 Southampton infiltration measurements

A summary of the infiltration surveys conducted at the Southampton study site is presented in table 12, followed by the respective resistivity sections for the same site (Figure 21).

Table 12. Summary of Southampton Infiltration Surveys			
		Infiltrometer A	Infiltrometer B
Survey #	Δt Hours : minutes	Amt. Water (gallons)	Amt. Water (gallons)
1	0:00 - 0:55	0	0
2	0:56 - 1:50	4	4
3	1:51 - 2:45	0	0
4	2:46 - 3:35	4	4
5	3:36 - 4:25	4	0
6	4:26 - 5:25	0	4
7	5:26 - 7:25	0	0
8	7:26 - 8:25	3	3
9	8:26 - 9:25	0	0
10	9:26 – 10:25	0	0
	Total Amt. Water	15	15

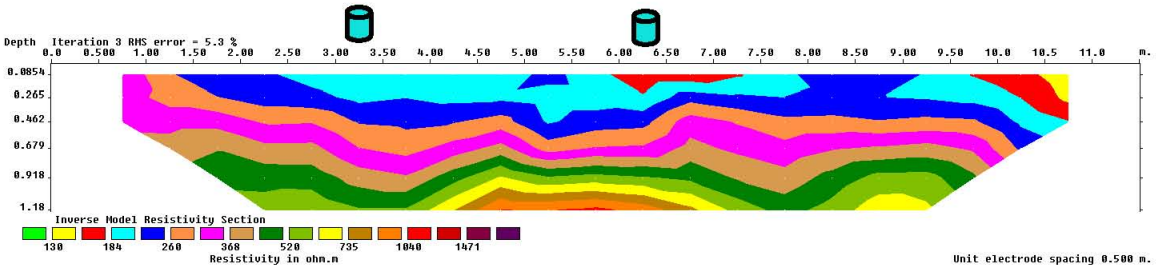

Figure 21 (a) Infiltration Survey 1
Δt = 0:00 - 0:55, Infiltr. A: 0 gal, Infiltr. B: 0 gal
Southampton infiltration measurements

****

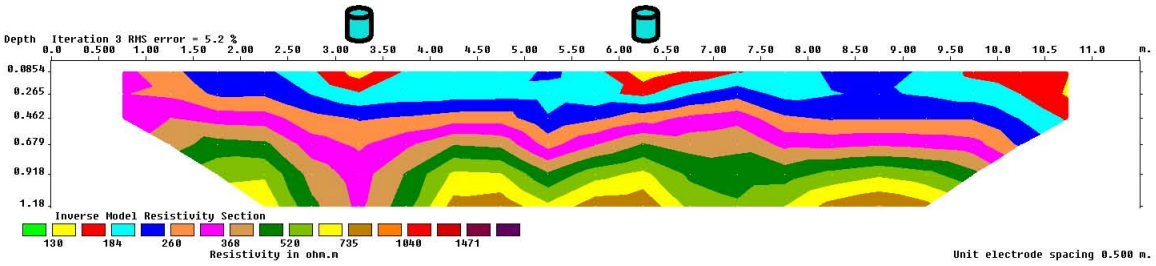

Figure 21 (b) Infiltration Survey 2
Δt = 0:56 - 1:50, Infiltr. A: 4 gal, Infiltr. B: 4 gal
Southampton infiltration measurements

****

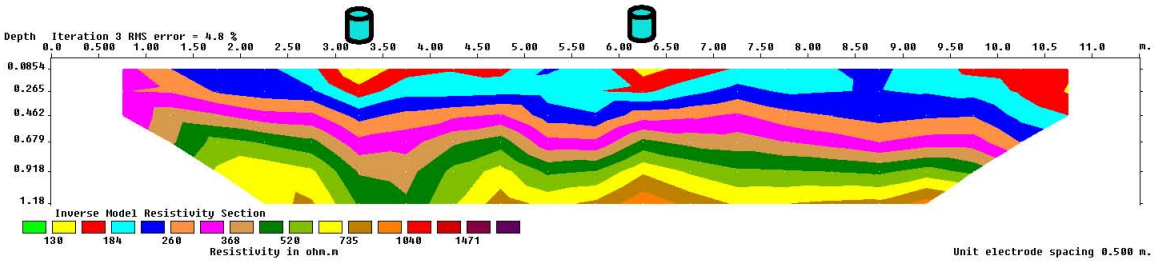

Figure 21 (c) Infiltration Survey 3
Δt = 1:51 - 2:45, Infiltr. A: 0 gal, Infiltr. B: 0 gal
Southampton infiltration measurements

****

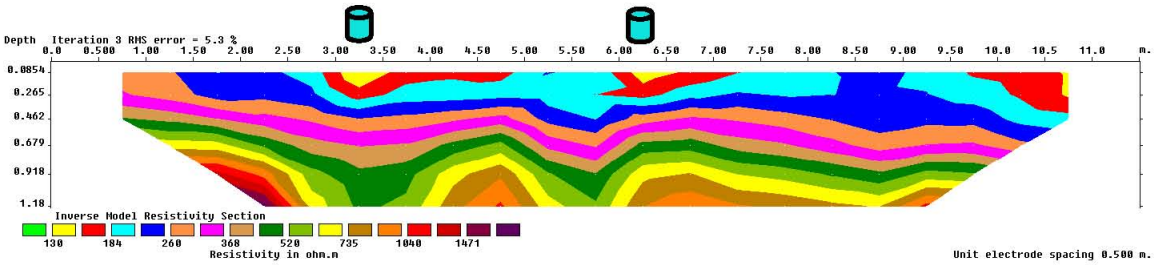

Figure 21 (d) Infiltration Survey 4
Δt = 2:46 - 3:35, Infiltr. A: 4 gal, Infiltr. B: 4 gal
Southampton infiltration measurements

****

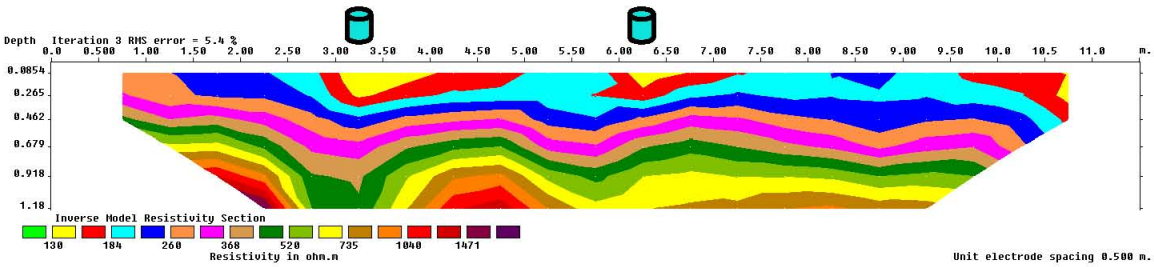

Figure 21 (e) Infiltration Survey 5
Δt = 3:36 - 4:25, Infiltr. A: 5 gal, Infiltr. B: 0 gal
Southampton infiltration measurements

****

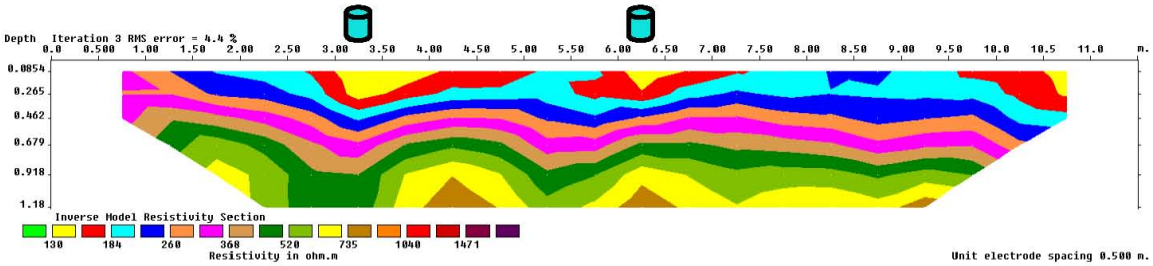

Figure 21 (f) Infiltration Survey 6
Δt = 4:26 - 5:25, Infiltr. A: 0 gal, Infiltr. B: 4 gal
Southampton infiltration measurements

****

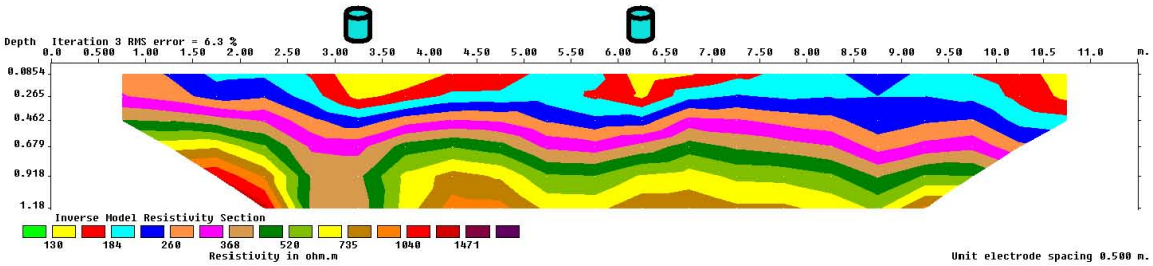

Figure 21 (g) Infiltration Survey 7
Δt = 5:26 - 7:25, Infiltr. A: 0 gal, Infiltr. B: 0 gal
Southampton infiltration measurements

****

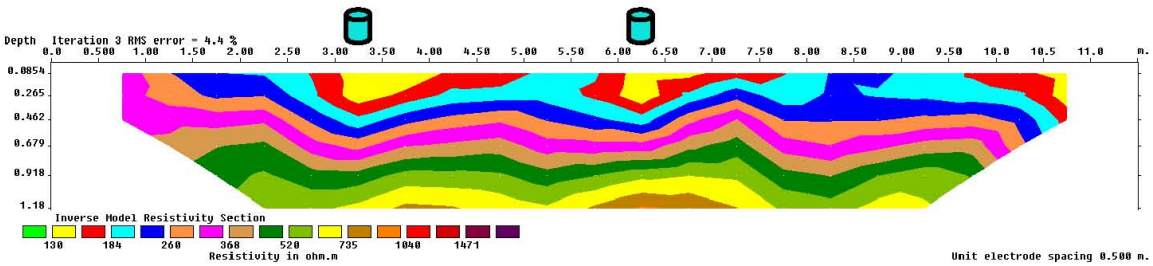

Figure 21 (h) Infiltration Survey 8
Δt = 7:26 - 8:25, Infiltr. A: 3 gal, Infiltr. B: 3 gal
Southampton infiltration measurements

****

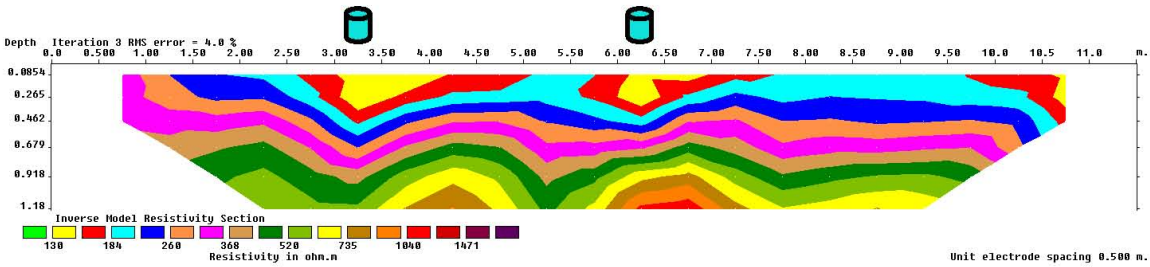

Figure 21 (i) Infiltration Survey 9
Δt = 8:26 - 9:25, Infiltr. A: 0 gal, Infiltr. B: 0 gal
Southampton infiltration measurements

****

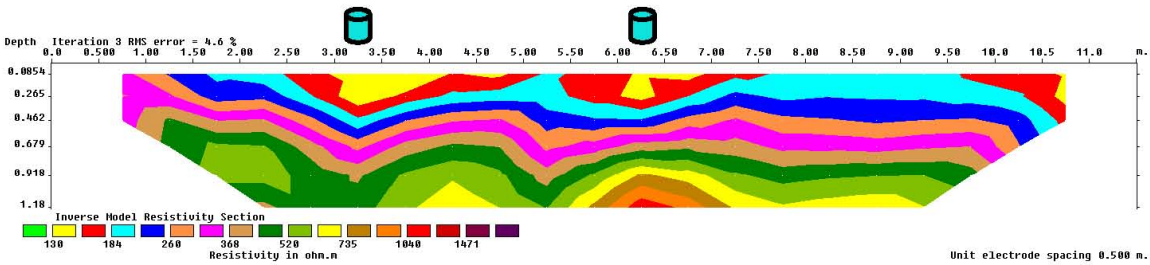

Figure 21 (j) Infiltration Survey 10
Δt = 9:26 – 10:25, Infiltr. A: 0 gal, Infiltr. B: 0 gal
Southampton infiltration measurements

****

7.10 Fourth Site: Middleburgh, Schoharie County, New York

The fourth site is located at 1248 Guinea Road Middleburgh, New York 12122. (Coordinates: N 42° 31' 5.3'', W 74° 23' 27.8''). Location information (detail from Breakabeen US Topographic Quadrangle map) and elevation information (elevation profiles in North-South and West-East directions) for the Middleburgh site were previously presented in Figures 2 and 3 respectively. The baseline measurements for the Middleburgh site (Figure 22 [a] and [b]), demonstrate a heterogeneous subsurface environment. Contrary to Long Island agricultural sites, in which resistivity values

increased with depth, at the Middleburgh site resistivity values decrease with depth. Most likely this effect demonstrates a shallow water table.

Further discussion on the Middleburgh baselines follows in a subsequent section of this dissertation. The baseline data collection program at the Middleburgh site was significantly more extensive than each of the three Long Island agricultural sites. More specifically, the Middleburgh baseline measurements exceeded in volume the amount of all the baseline data obtained from the three Long Island sites combined. The detailed subsurface characterization of the Middleburgh site through ERI measurements, a tracer experiment, and excavation aimed at a better understanding of the geophysical response of the tree roots.

7.11 Middleburgh baseline measurements

One representative dipole-dipole baseline measurement and one representative Wenner baseline measurement is presented in Figure 22. Cross sections of inverted resistivity data for the remaining baselines will be presented in Appendix 1. Chargeability (i.e., induced polarization) values ranged from 1.94 to 6.86 mV/V.

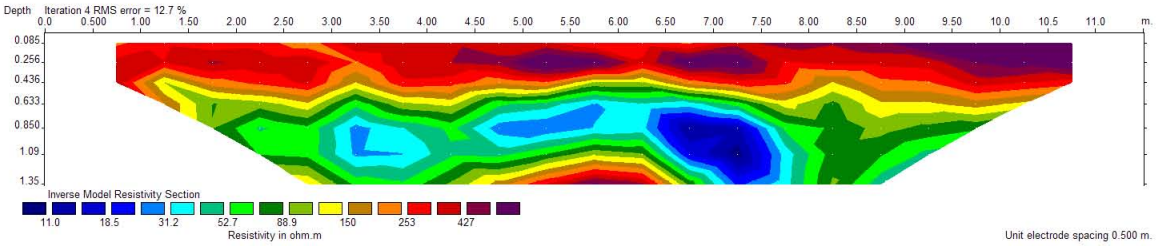

Figure 22 (a) Dipole – dipole
Middleburgh baseline measurements

****

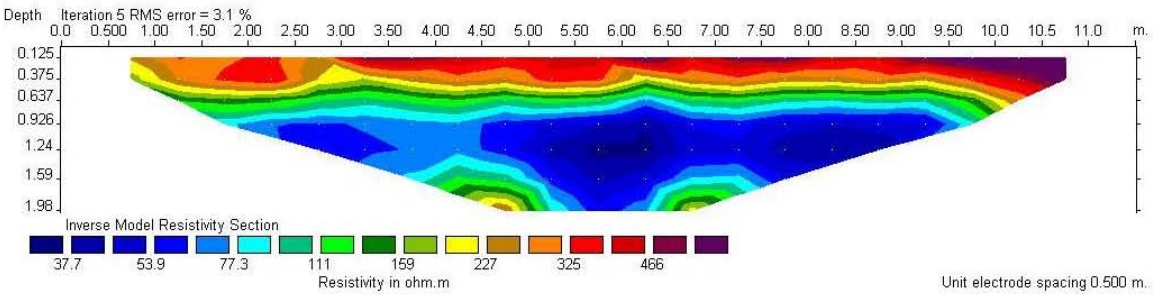

Figure 22 (b) Wenner
Middleburgh baseline measurements

****

7.12 Middleburgh infiltration measurements

A summary of the infiltration surveys conducted at the Middleburgh study site is presented in table 13, followed by the respective resistivity sections for the same site (Figure 23). Infiltration was carried out for approximately a one-hour period to achieve a steady state flow regime. Sixteen gallons of water were infiltrated through either infiltrometer during this time. Another fifteen gallons of 15 mg/L Lithium Chloride tracer was then injected during the experiment through each infiltrometer.

Table 13. Summary of Middleburgh Infiltration Surveys

		Infiltrometer A	Infiltrometer B
Survey #	Δt Hours : minutes	Amt. Water (gallons)	Amt. Water (gallons)
1	0:00 - 0:50	0	0
2	0:51 - 1:50	16	16
3	1:51 - 2:50	10 (LiCl)	10 (LiCl)
4	2:51 – 3:20	5 (LiCl)	5 (LiCl)
5	4:16 - 4:35	0	0
	Total Amt. Water	31	31

Unfortunately, equipment malfunction during infiltration has resulted in gaps between measurements. In addition, the cross sections that are available tend to display high RMS errors in the inverted sections. For these reasons conclusions based on these data are less reliable than those for the other sites.

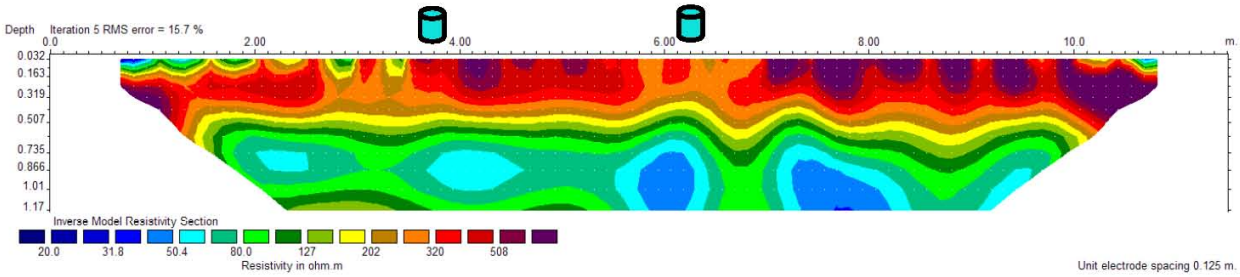

Figure 23 (a) Infiltration Survey 1
Δt = 0:00 - 0:50, Infiltr. A: 0 gal, Infiltr. B: 0 gal
Middleburgh infiltration measurements

****

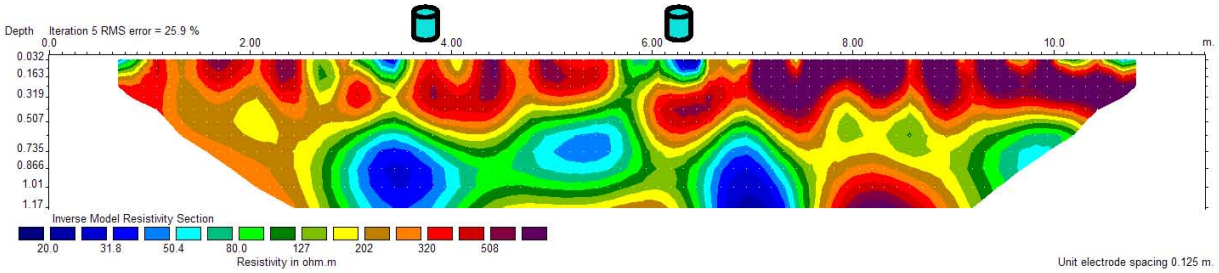

Figure 23 (b) Infiltration Survey 2
Δt = 0:51 - 1:50, Infiltr. A: 16 gal, Infiltr. B: 16 gal
Middleburgh infiltration measurements

****

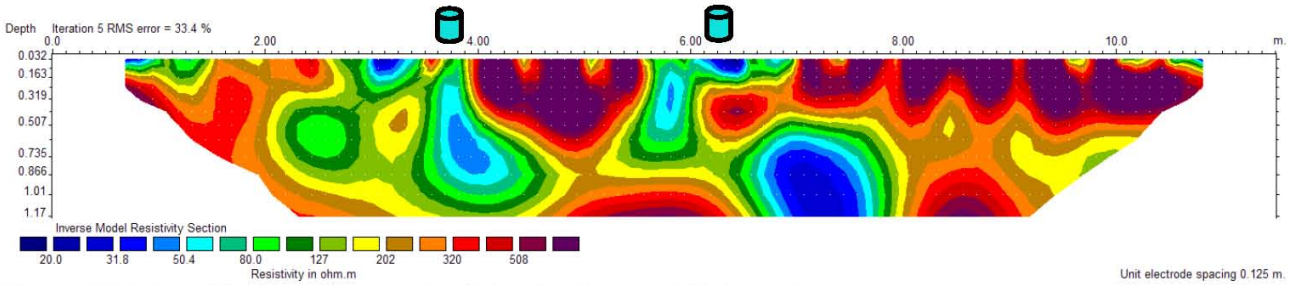

Figure 23 (c) Infiltration Survey 3 – Introduction of Lithium Tracer
Δt = 1:51 - 2:50, Infiltr. A: 10 gal, Infiltr. B: 10 gal
Middleburgh infiltration measurements

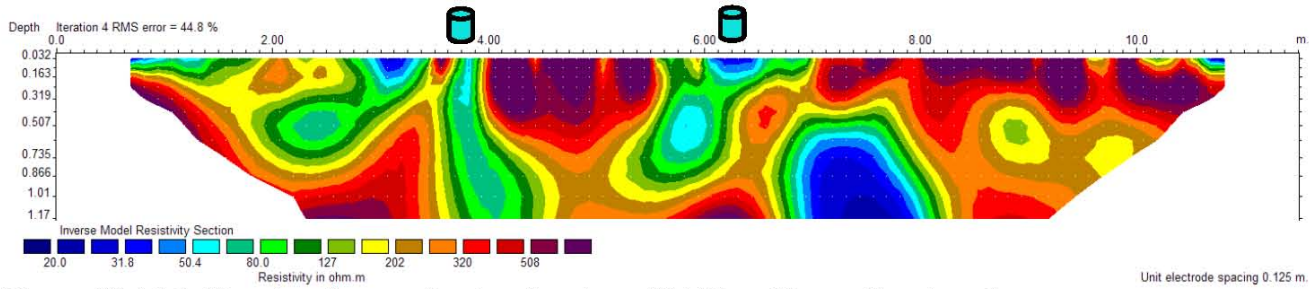

Figure 23 (d) Infiltration Survey 4 – Application of Lithium Tracer Continued
Δt = 2:51 – 3:20, Infiltr. A: 5 gal, Infiltr. B: 5 gal
Middleburgh infiltration measurements

****

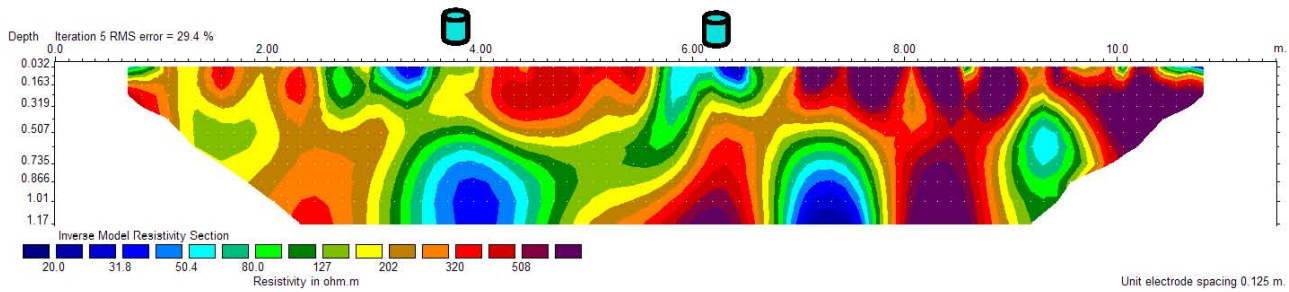

Figure 23 (e) Infiltration Survey 5
Δt = 4:16 - 4:35, Infiltr. A: 0 gal, Infiltr. B: 0 gal
Middleburgh infiltration measurements

****

CHAPTER 8. DISCUSSION

The RES2DINV software was employed for the processing of the geophysical data, and the results were presented in the previous section. Based on the RES2DINV contouring for the measurements during infiltration, a general reduction in the resistivity values can be seen reflecting infiltration in the vicinity of the two infiltrometers. This visual demonstration of the results through the resistivity software is successful in the evaluation of changes for a particular site. It is limited, however, as a comparison tool between sites due to the large resistivity variations between sites, which makes it difficult to produce universal contouring for all the sites. In order to proceed with the analysis and to effectively answer the first research question - whether the effect of infiltration can be detected in soils typical of the north-eastern United States – the original geophysical data were transferred to GIS software (ESRI- ArcGIS, 2008).

First, the inverted sections for the dipole-dipole array were extracted in coordinate form using the "Save data in XYZ format" command in the file menu of the display window of RES2DINV. Before plotting cross sections in GIS a statistical analysis was performed on the geophysical data. Since the position of the electrodes remained fixed before and during infiltration for every site, it follows that for any subsurface point in the inverted section the available resistivity data for that point includes four baseline values before infiltration, as well as additional values, which correspond to the measurements during infiltration. Using the four baseline values, average baseline resistivities and standard deviations were computed for the pre-infiltration stage. (As discussed previously, additional baseline measurements were obtained, including the reciprocal

dipole-dipole measurement, and two Wenner measurements in both the induced polarization mode and the standard mode. These were not used in this analysis. The reason for using only four out of the seven available baselines for the statistical analysis is consistency between the pre-infiltration and infiltration stages with regard to electrode array type and measurement mode.) Finally, the difference between each infiltration measurement and its corresponding baseline average at that point was divided by the standard deviation of the baseline measurements at that point. As expected the standard deviations increased with depth.

The results of this analysis were plotted in GIS and contoured in five classes consistent with the following breaks: minimum value to -3, -3 to -1.01, -1 to 1, 1.01 to 3, and 3.01 to maximum value. From the analysis described above, it follows that negative values are correlated with a reduction of the resistivity values, as opposed to positive values which are correlated to an increase of the resistivity values. For instance, the green color in the GIS sections presented below represents the class of negative values ranging from the most negative value to –3 times the standard deviation of the pre-infiltration measurements. Following this procedure it is possible to carry out an analysis of the following images based on the deviations from the baseline data. Effectively, differences above three standard deviations are unequivocally real and can be compared with infiltration locations, as well as any other possible factors able to produce equally significant changes for a given site.

8.1 Riverhead infiltration surveys

Starting with the Riverhead site (Figure 24 [a] through [f]), the experiment demonstrates a systematic decrease in resistivity values near the two infiltration locations. The images show the initiation of water plumes at both infiltration locations, which gradually expand both laterally and in a downward direction. The areas of reduced resistivity highlighted in green color have a clear connection with the water source. There is no area of reduced resistivity in any of the referenced sections without an apparent connection to the water source. On the other hand, areas of increased resistivity highlighted in pink color are on the bottom right corner of the sections surrounding the reduced resistivity area associated with infiltration. Additional areas of increased resistivity are observed under the left infiltrometer, as well. These areas are smaller in size compared to the large area observed on the bottom right of the sections. In both cases, however, those areas of increased resistivity are near the edges of the sections. This observation is consistent with the literature related to this phenomenon.

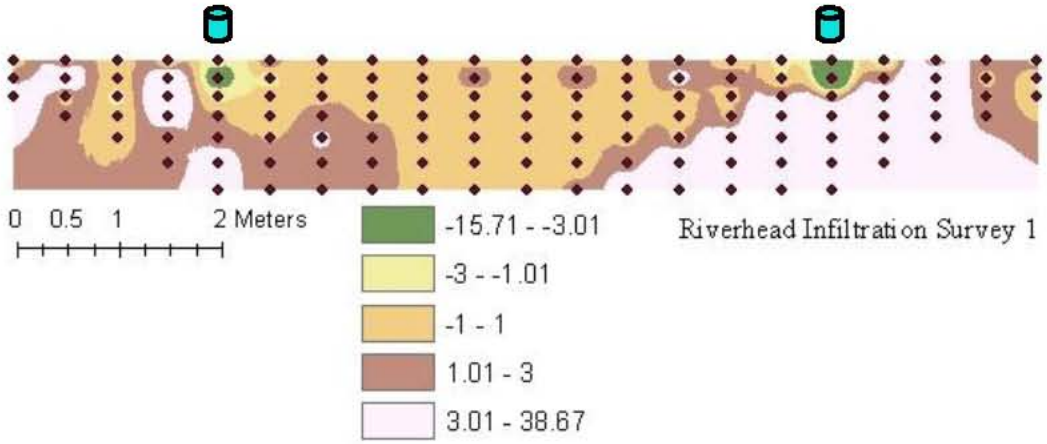

Figure 24 (a) $\Delta t = 00:51 - 01:35$, Infiltr. A: 8 gal, Infiltr. B: 12 gal Riverhead infiltration surveys

****

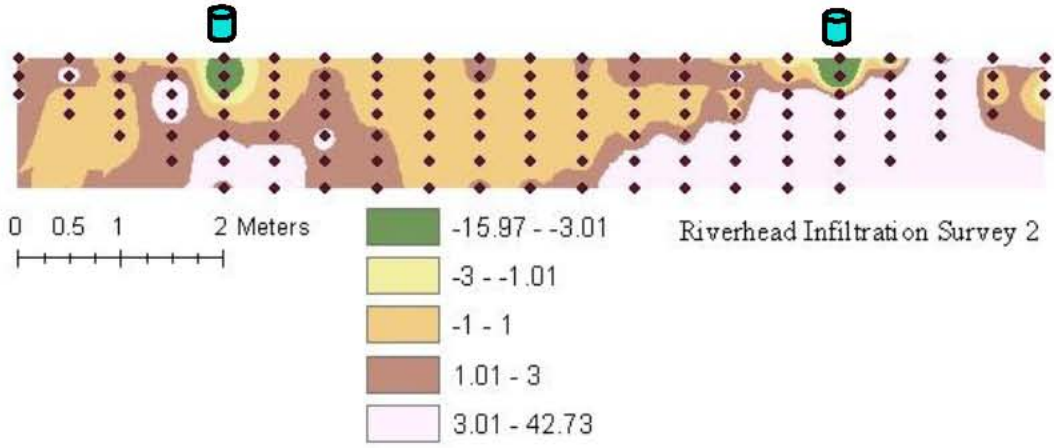

Figure 24 (b) Δt = 01:36 – 02:25, Infiltr. A: 4 gal, Infiltr. B: 4 gal
Riverhead infiltration surveys

****

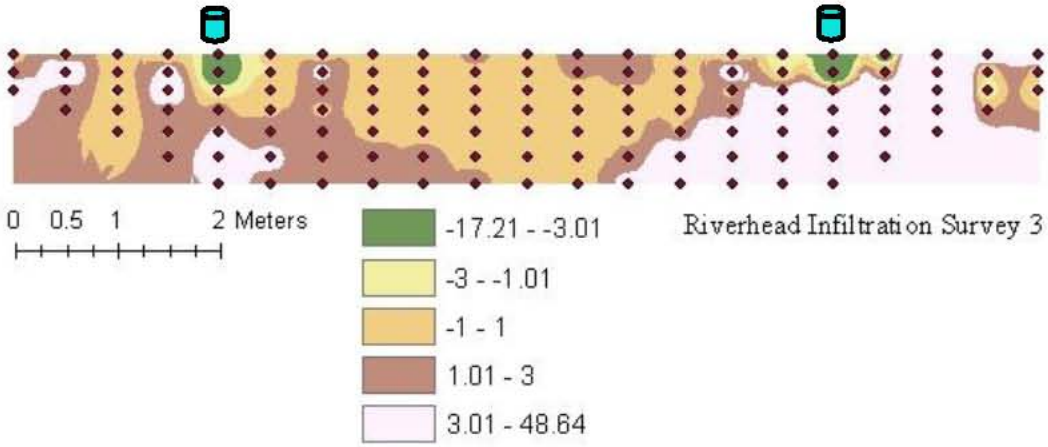

Figure 24 (c) Δt = 2:26 – 3:40, Infiltr. A: 4.5 gal, Infiltr. B: 7.5 gal
Riverhead infiltration surveys

****

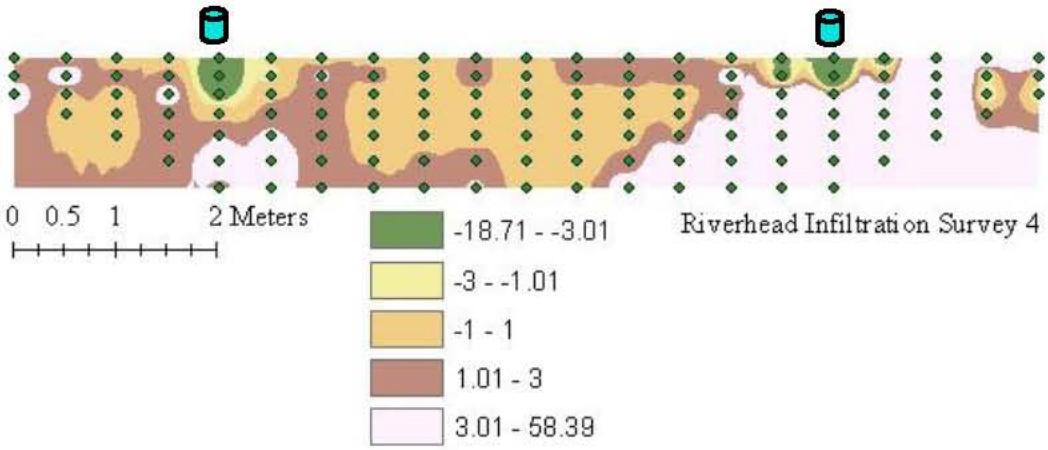

Figure 24 (d) Δt = 3:41 – 5:40, Infiltr. A: 4 gal, Infiltr. B: 9 gal
Riverhead infiltration surveys

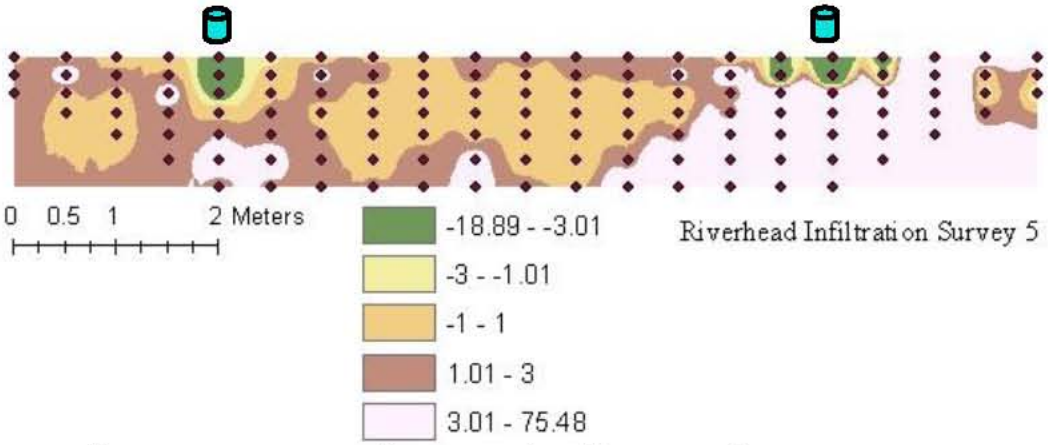

Figure 24 (e) Δt = 5:41 – 7:35 Infiltr. A: 4 gal, Infiltr. B: 4 gal
Riverhead infiltration surveys

****

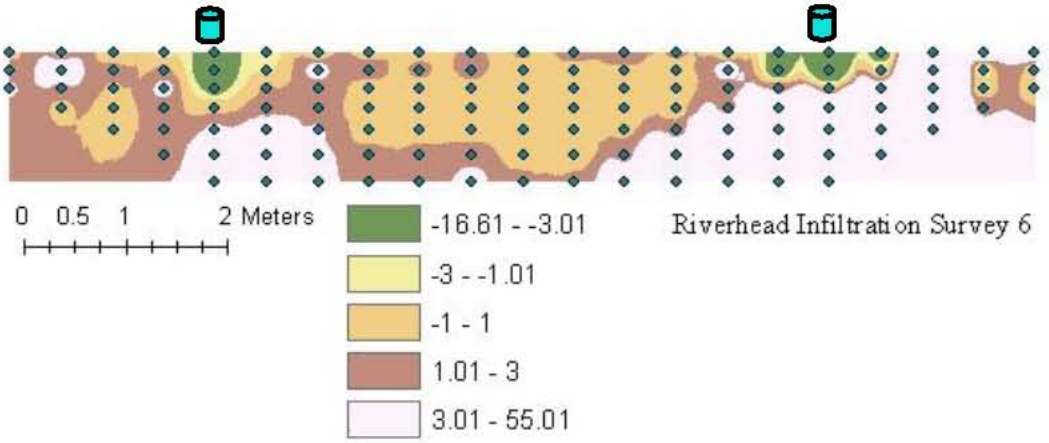

Figure 24 (f) Δt = 7:36 – 8:25, Infiltr. A: 0 gal, Infiltr. B: 0 gal
Riverhead infiltration surveys

****

First, Loke, who is the developer of the resistivity software RES2DINV that is employed in this dissertation, reported that due to an additive effect of all the mesh parameters associated with the model blocks located at or near the edges of the sections, unusually low or high resistivity values may be observed (Loke, 2004). This is an effect of the greater weights assigned to the model blocks at or near the edges of the section. Since the inverted model sections produced by the resistivity software RES2DINV and

their associated resistivity values are the basis for the current analysis in the GIS environment, it is expected that the effect of the side blocks will be systematically transferred to the GIS sections as well.

Second, Park (1998) also reported resistivity increases surrounding areas of decreased resistivity associated with infiltration and argued that they may be artifacts of the inversion process, thus a geological interpretation should not be attempted. He also hypothesized that resistivity increases at or near the surface may be attributed to moisture loss due to evaporation. One such isolated area of increased resistivity located near the surface is observed on the extreme right part of the Riverhead sections. Given the unusually high temperatures and dry weather conditions during the time that the Long Island experiments were conducted the evaporation argument is worth considering. However, specifically for the Riverhead site the fact that almost all areas of increased resistivity, including the near-surface area on the top right of the sections, are located near the edges of the sections makes the effect of the side blocks a more probable explanation.

In addition to the literature justification of the increased resistivity values, it is worth noting that in almost all sections there are several disparate points of increased resistivity. The fact that those points reappear in multiple sections in a systematic manner is indicative of a possible association to survey reading failures. Bad ground contact at certain electrodes may cause those failed readings, which do not represent a true resistivity reading. As mentioned above, there are no disparate points or other areas associated with lower resistivity anywhere within the Riverhead sections without having an apparent connection to infiltration. In this regard it may be important to note that,

although the electrodes were not moved, the baseline measurements were done a day before the infiltration measurements.

Finally, there is an agreement for the Riverhead site GIS sections presented here between the recorded infiltration rate and the magnitude of the resistivity change. The infiltration rate at the Riverhead site was the highest of the three Long Island sites. Based on the known geology for Riverhead, specifically the fact that sand is dominant in all soil layers, it is safe to assume that the amount of water that was injected was not enough to fully saturate the portion of the subsurface under evaluation. Nevertheless, the resistivity reduction at this site was also the largest of the three Long Island sites.

8.2 Mattituck infiltration surveys

The infiltration experiment conducted at the Mattituck site is unique in that it was combined with a real-time irrigation event. The irrigation lasted four hours and during this time approximately an estimated amount of 38 gallons of water was applied through a drip irrigation system uniformly along the survey line. This is in addition to 16 gallons injected through the left infiltrometer and 7 gallons of water injected through the right infiltrometer. The details of the irrigation event were outlined previously in the results section of this dissertation.

The experiment was conducted under record-high temperatures for the Long Island area following a prolonged period of unusually dry conditions. The soil compaction data obtained with the cone penetrometer at this site demonstrated that the soil was highly compacted even near the surface.

As observed in Figure 25 (a) through (f) areas of increased resistivity are observed near the surface, possibly due to the increased likelihood of significant evaporation expected during similar weather conditions. It is only after four hours in the infiltration experiment and apparently due to the additive effect of the irrigation that the areas of increased resistivity are gradually reduced and eventually replaced by decreased resistivity areas. The general pattern of the observed changes suggest a general downward movement of the water applied, although clear evidence of the infiltration effect (i.e. as established previously on the basis of equal or above three standard deviations from the baseline data) may be inferred for only the extreme top layer of the sections. One location of lower resistivity is observed at a location slightly to the right of the left infiltrometer. This suggests a lateral movement of the injected water originating from that infiltrometer. This lateral movement of the applied water is consistent with the high penetrometer readings, as in highly compacted soils lateral movement is more significant that vertical. The inferred areas of increased resistivity on the bottom left edges of the last two sections are likely associated with the effect of the side blocks discussed previously. It is interesting to note that there is an area of increased resistivity early on in the infiltration (i.e., near the left infiltrometer), which then dissipates as the infiltration progresses. This is not as strong in the other sites. It may be due to the fact that for this particular site the infiltration experiment was accompanied by irrigation along the survey line by means of a drip irrigation system.

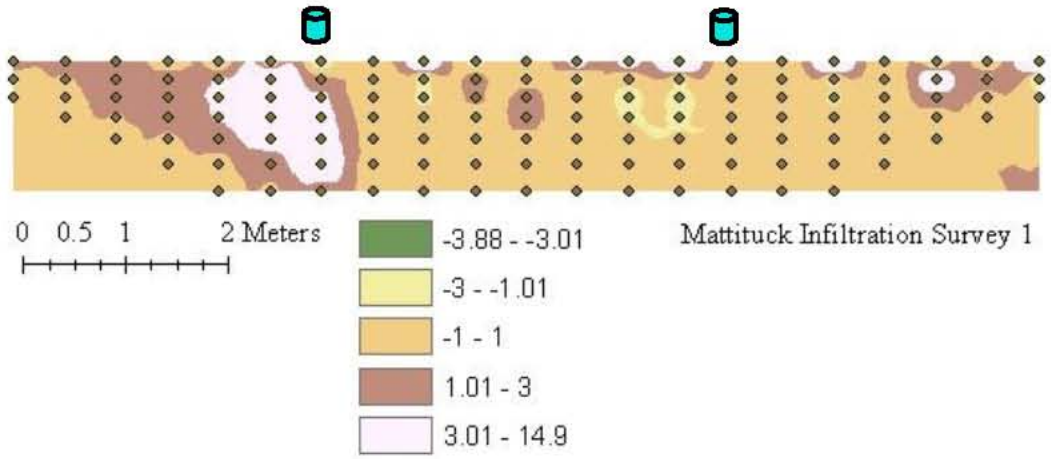

Figure 25 (a) Δt = 1:41 - 2:30, Infiltr. A: 4 gal, Infiltr. B: 4 gal
Mattituck infiltration surveys

****

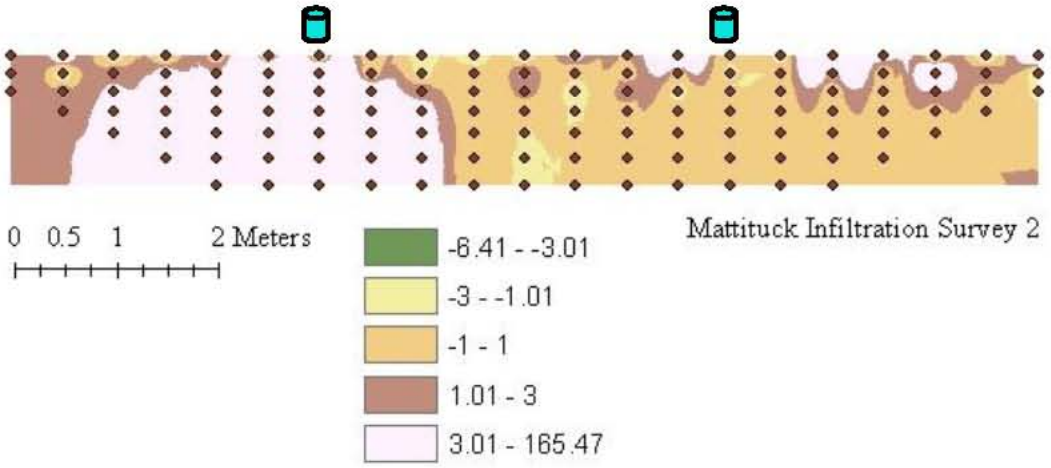

Figure 25 (b) Δt = 1:41 - 2:30, Infiltr. A: 4 gal, Infiltr. B: 4 gal
Mattituck infiltration surveys

****

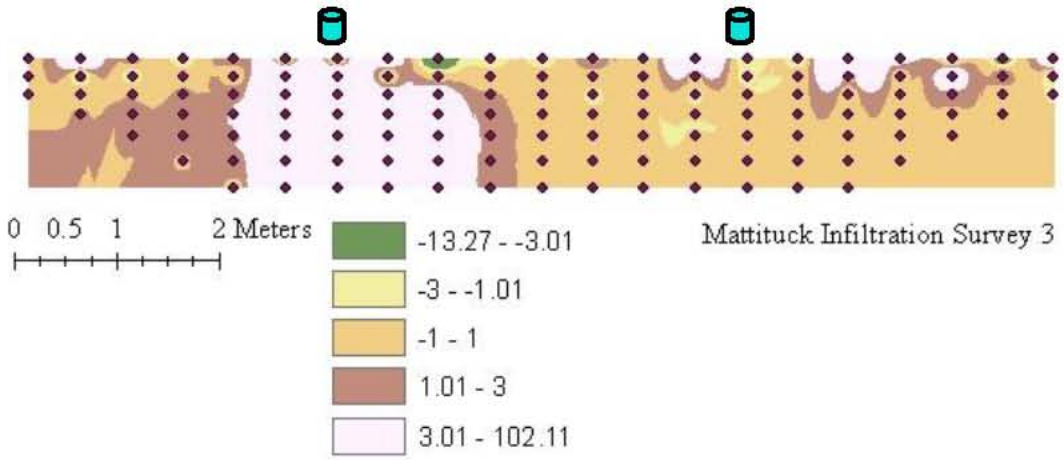

Figure 25 (c) Δt = 2:31 - 3:15, Infiltr. A: 2 gal, Infiltr. B: 1 gal
Mattituck infiltration surveys

****

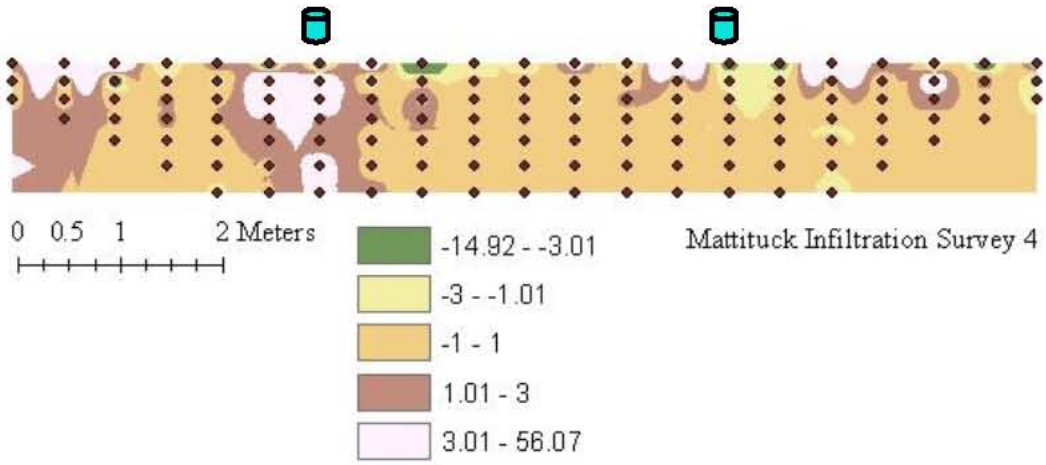

Figure 25 (d) Δt = 3:16 - 4:15, Infiltr. A: 0 gal, Infiltr. B: 0 gal
Mattituck infiltration surveys

****

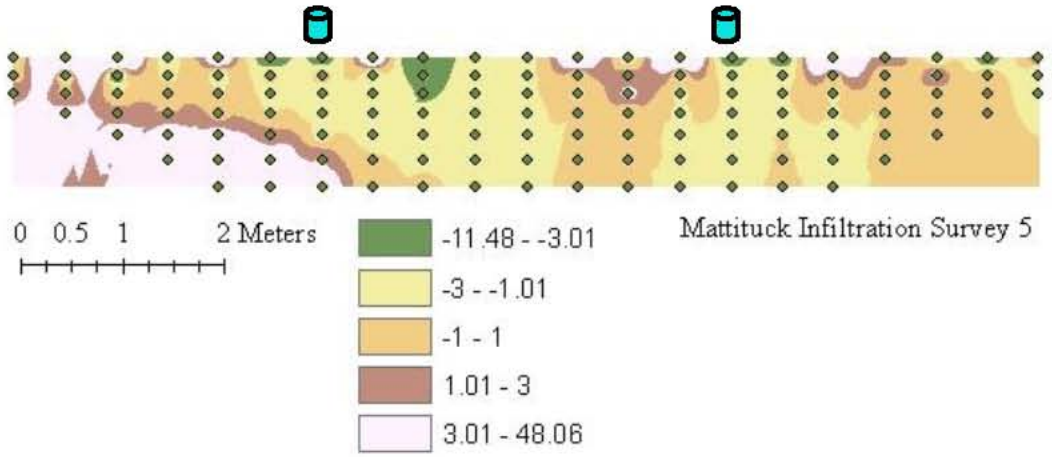

Figure 25 (e) Δt = 4:16 - 5:00, Infiltr. A: 0 gal, Infiltr. B: 0 gal
Mattituck infiltration surveys

****

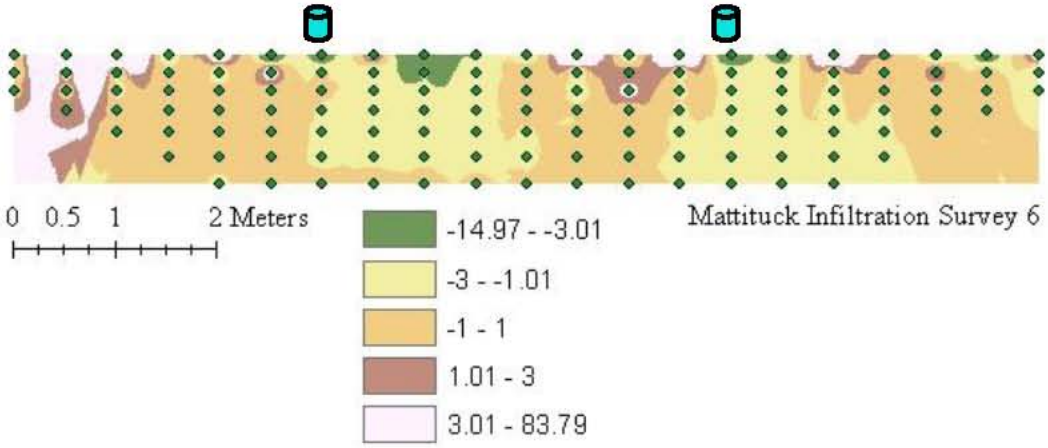

Figure 25 (f) Δt = 5:01 - 6:00, Infiltr. A: 3 gal, Infiltr. B: 2 gal
Mattituck infiltration surveys

****

8.3 Southampton infiltration surveys

The infiltration experiment conducted at the Southampton site produced less significant deviations from the baseline data, as can be inferred through the following sections. This is attributed to the lower overall apparent resistivity values observed at this particular site. In sections (d) through (h) of Figure 26 areas of lower resistivity began to develop under the infiltration locations, which fall within two standard deviations from the baseline data. Only on the last four infiltration sections are there isolated areas under the infiltration locations, exhibiting reduced resistivity areas of more than three standard deviations from the baseline data. This phenomenon is partially justified by the fact that this particular soil type, which is considered the most fertile across Suffolk County, has the highest available water capacity, as opposed to the Riverhead and Haven series, which both have a moderate available water capacity. It follows that the initial moisture levels were higher than the other two Long Island sites, therefore infiltration at this site produced a less prominent effect compared to the other experiments. This assumption is supported by the recorded infiltration rates for this site, which were the lowest from all the sites when irrigation is taken into account. More specifically, 15 gallons of water were injected through either infiltrometer over a period of 9 hours and 25 minutes.

Provided that those results were recorded in the absence of any significant sources of noise, it may be deduced that the method is limited in monitoring near surface infiltration in soils of low overall apparent resistivity, especially those which have a high available water capacity. On the other hand, the infiltration sections presented in the results section of this dissertation demonstrate a clear reduction in resistivity associated with infiltration. Although the subsequent analysis using GIS demonstrates that the

inferred resistivity reductions were not more than three standard deviations from the baselines, it is evident that an overall reduction associated with infiltration can be observed. It is noted that the area of lower resistivity observed at the right side of the infiltration sections processed with the RES2DINV software (Figure 21) does not show up in the analysis in the GIS environment, which means that is not statistically significant.

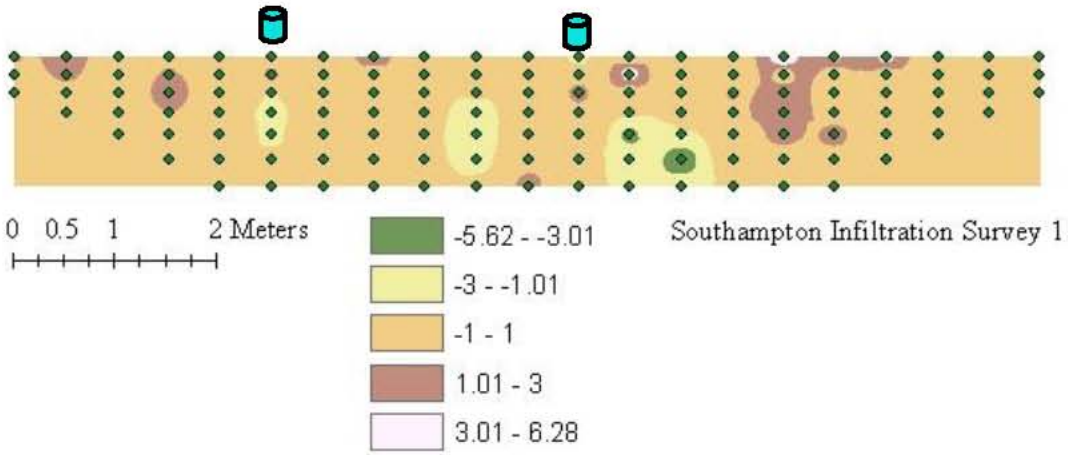

Figure 26 (a) Δt = 0:56 - 1:50, Infiltr. A: 4 gal, Infiltr. B: 4 gal
Southampton infiltration surveys

****

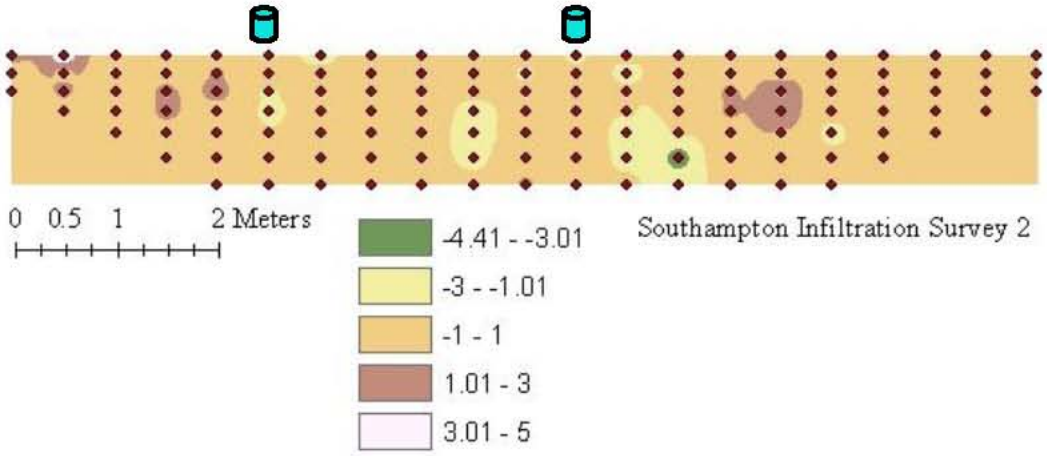

Figure 26 (b) Δt = 1:51 - 2:45, Infiltr. A: 0 gal, Infiltr. B: 0 gal
Southampton infiltration surveys

****

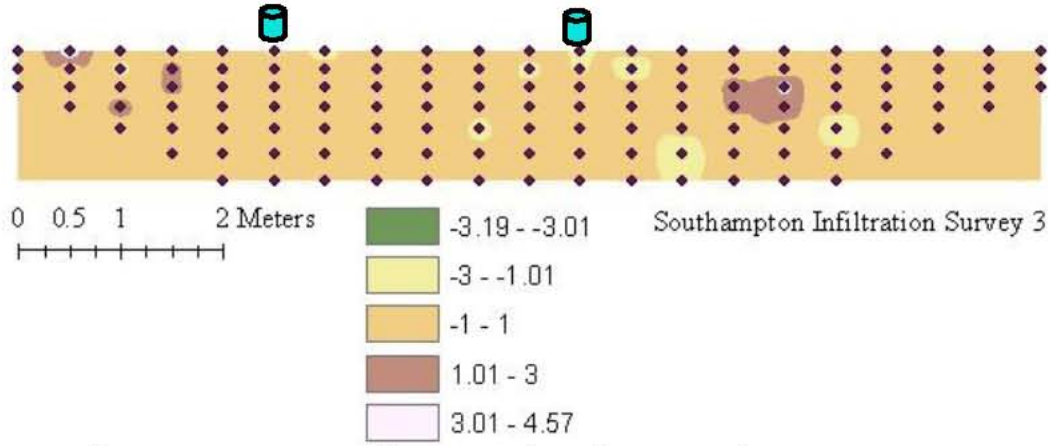

Figure 26 (c) Δt = 2:46 - 3:35, Infiltr. A: 4 gal, Infiltr. B: 4 gal
Southampton infiltration surveys

****

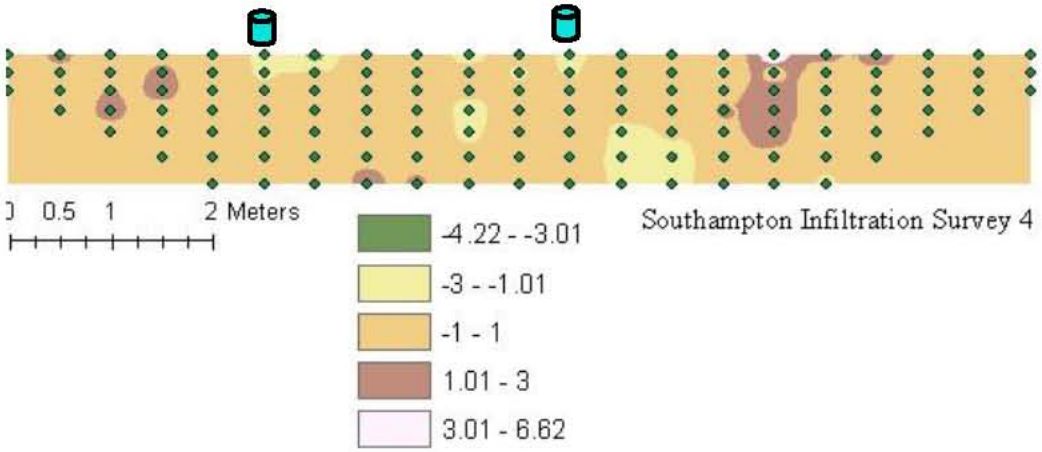

Figure 26 (d) Δt = 3:36 - 4:25, Infiltr. A: 5 gal, Infiltr. B: 0 gal
Southampton infiltration surveys

****

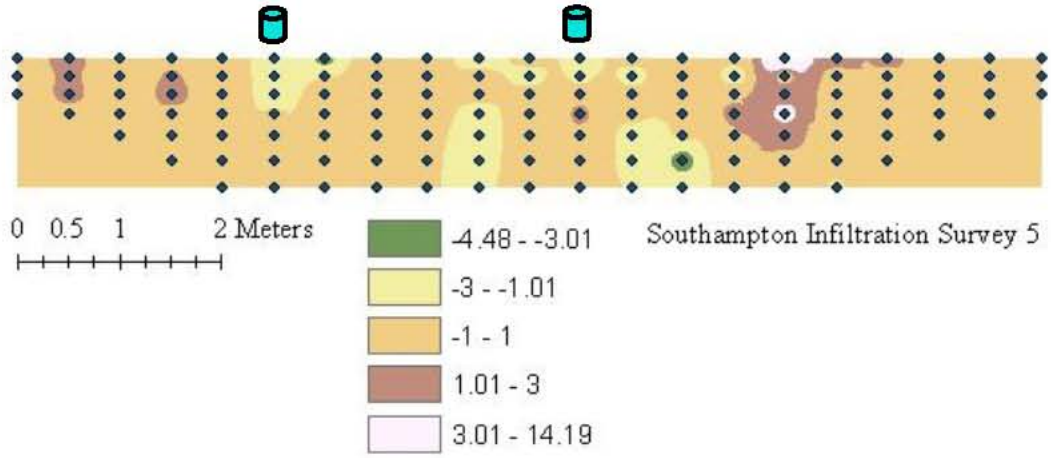

Figure 26 (e) Δt = 4:26 - 5:25, Infiltr. A: 0 gal, Infiltr. B: 4 gal
Southampton infiltration surveys

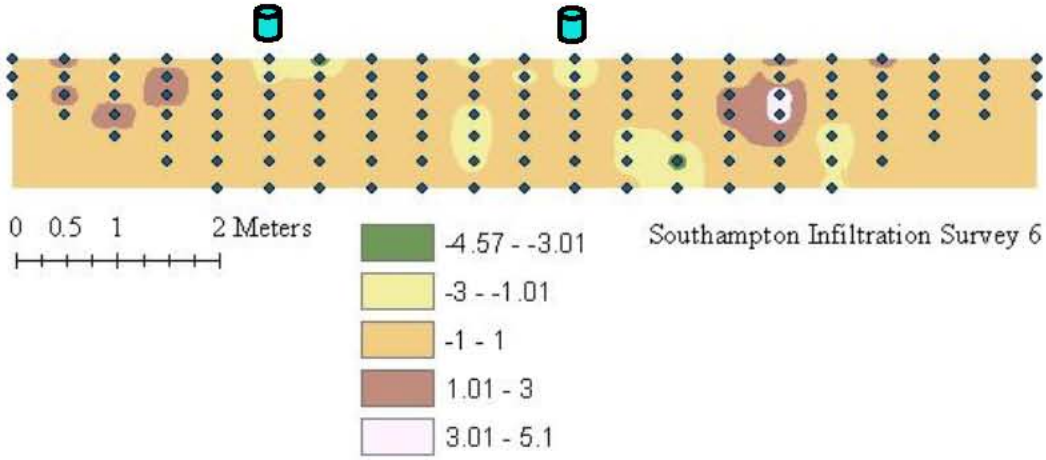

Figure 26 (f) Δt = 5:26 - 7:25, Infiltr. A: 0 gal, Infiltr. B: 0 gal
Southampton infiltration surveys

****

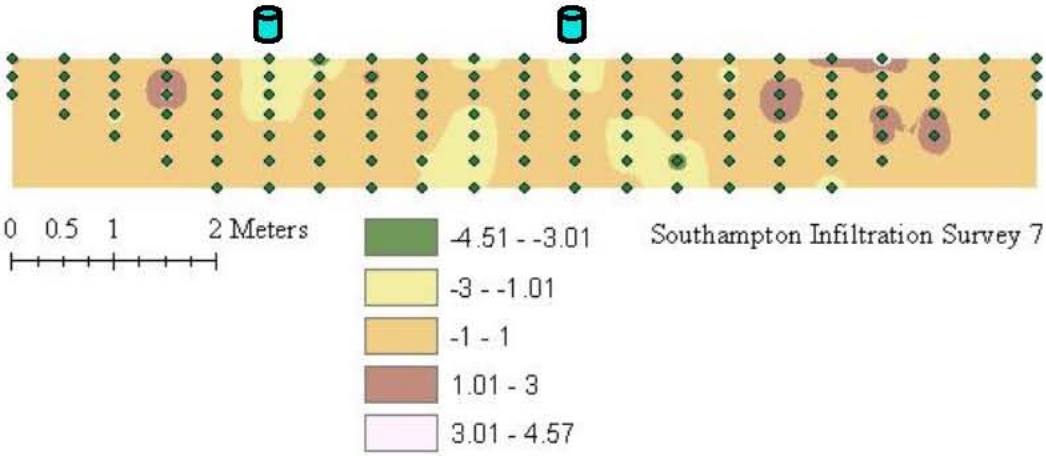

Figure 26 (g) Δt = 7:26 - 8:25, Infiltr. A: 3 gal, Infiltr. B: 3 gal
Southampton infiltration surveys

****

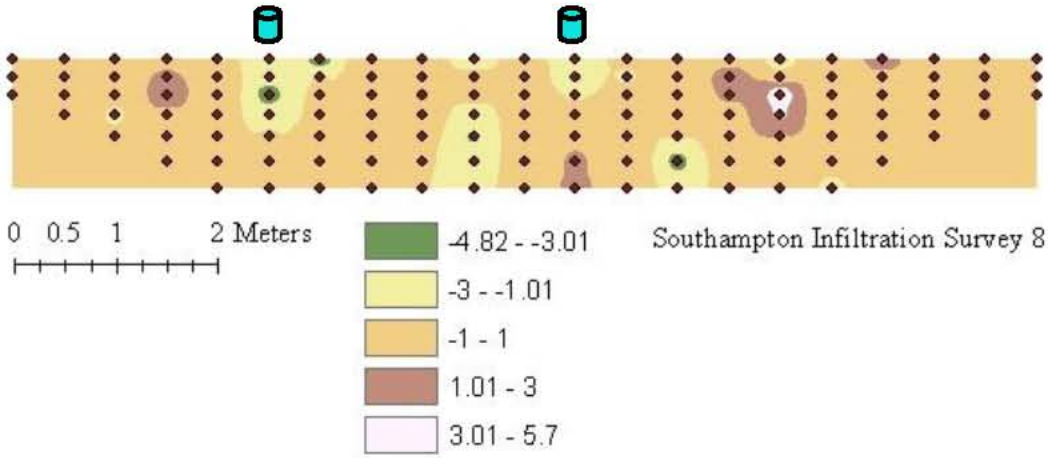

Figure 26 (h) Δt = 8:26 - 9:25, Infiltr. A: 0 gal, Infiltr. B: 0 gal
Southampton infiltration surveys

****

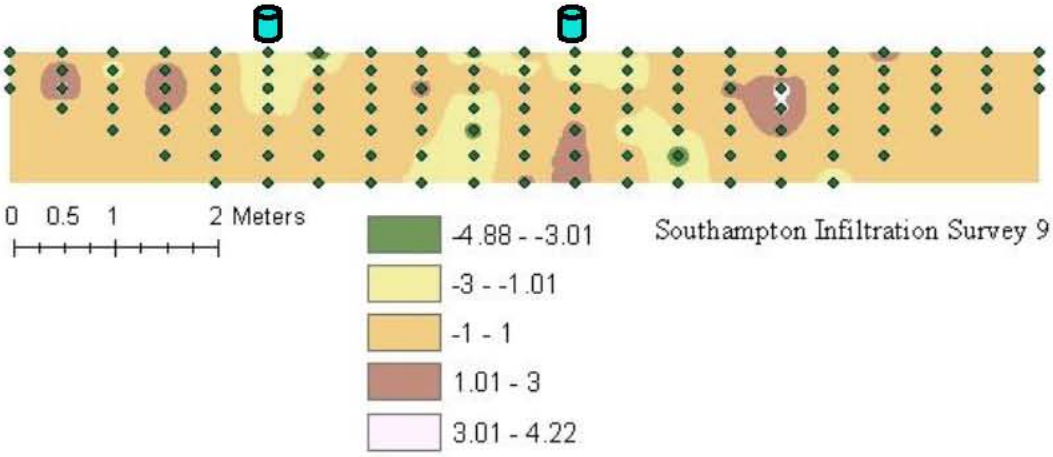

Figure 26 (i) Δt = 9:26 – 10:25, Infiltr. A: 0 gal, Infiltr. B: 0 gal
Southampton infiltration surveys

****

8.4 Middleburgh infiltration surveys

Infiltration in Middleburgh was carried out for approximately one-hour period to achieve a steady state flow regime. Sixteen gallons of water were infiltrated through either infiltrometer during this time. Another fifteen gallons of 15 mg/L Lithium Chloride tracer was injected during the experiment through each infiltrometer. Increased RMS errors were recorded during the infiltration surveys at Middleburgh, most likely associated with malfunctioning of the resistivity meter. Nethertheless, some conclusions can be drawn.

In sections b through e of Figure 27 areas of lower resistivity began to develop under the infiltration locations, which fall within three standard deviations from the baseline data. The general pattern of the changes suggest a downward movement of the water. This effect seems more prominent after the tracer application. Lower resistivities are observed at location adjacent to each infiltrometer, suggesting lateral movement of the water front. It is not clear what the inferred areas of increased resistivity demonstrate. Possibly, they are associated with signal deterioration due to equipment problems during the time of this experiment.

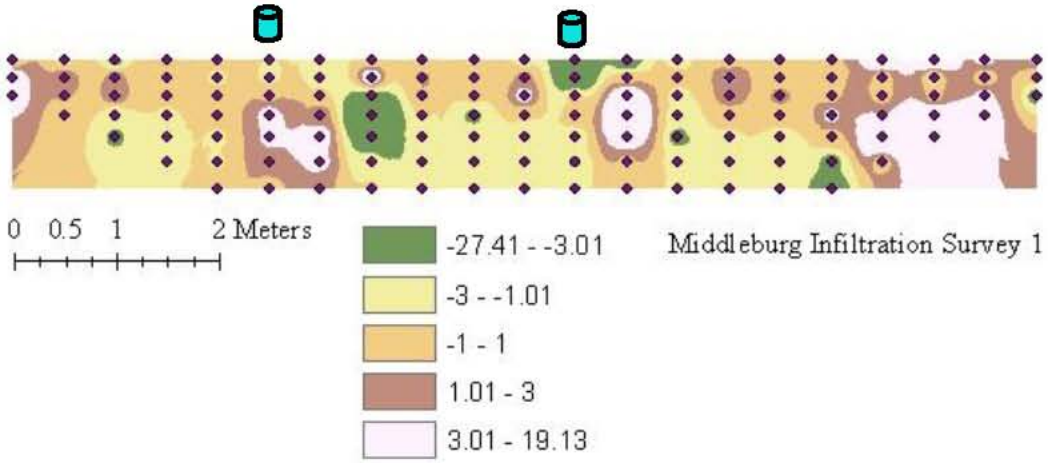

Figure 27 (a) Δt = 0:51 - 1:50, Infiltr. A: 16 gal, Infiltr. B: 16 gal
Middleburgh infiltration surveys

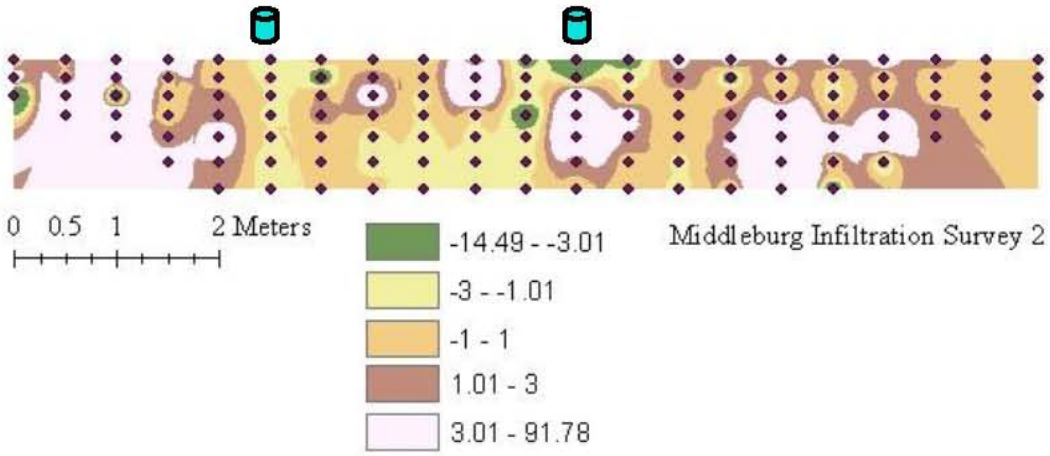

Figure 27 (b) Δt = 1:51 - 2:50, Infiltr. A: 10 gal, Infiltr. B: 10 gal
Middleburgh infiltration surveys

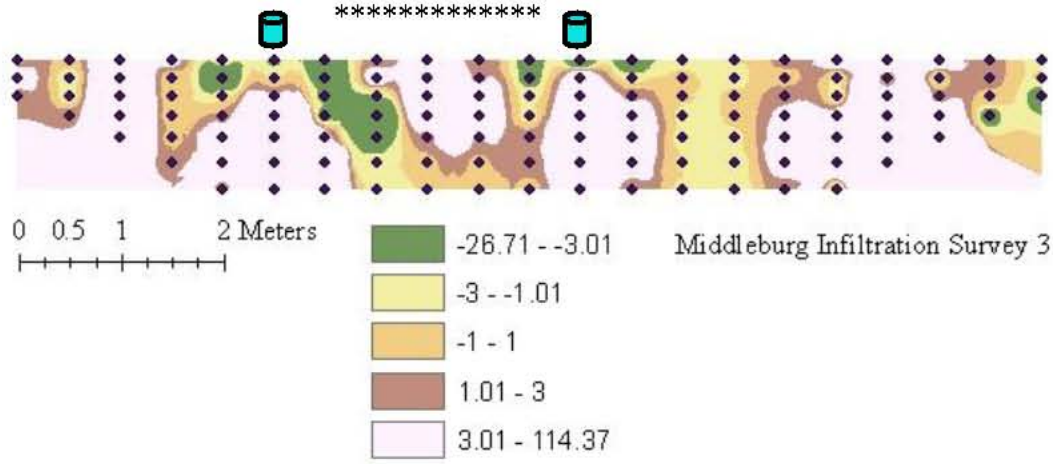

Figure 27 (c) Δt = 2:51 - 4:15, Infiltr. A: 5 gal, Infiltr. B: 5 gal
Middleburgh infiltration surveys

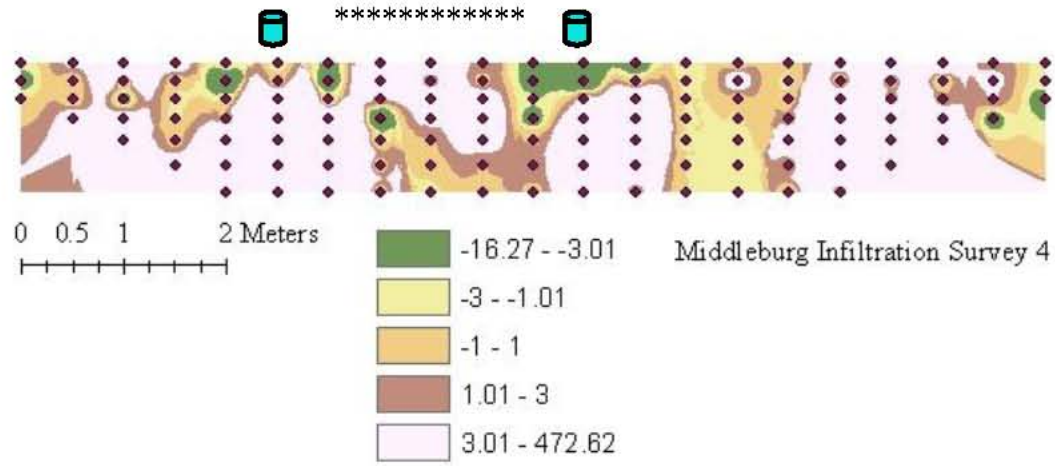

Figure 27 (d) Δt = 4:16 - 4:35, Infiltr. A: 0 gal, Infiltr. B: 0 gal
Middleburgh infiltration surveys

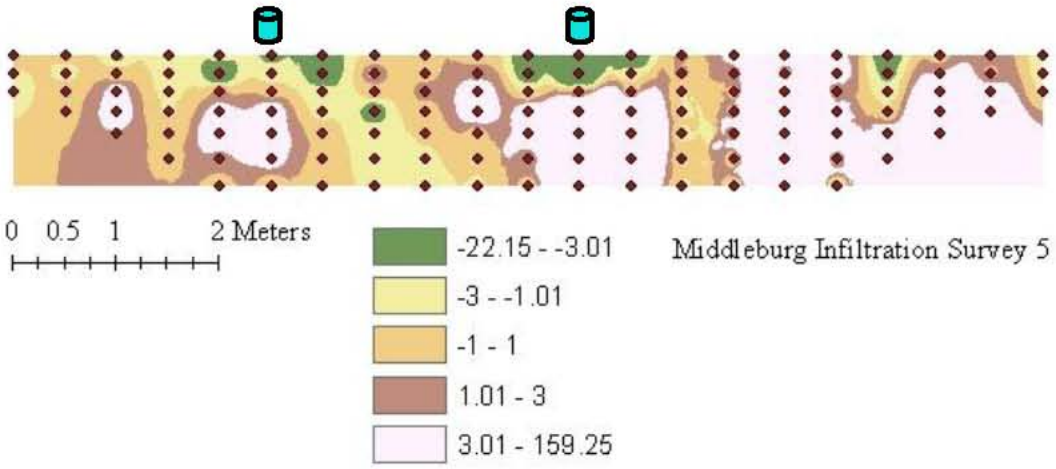

Figure 27 (e) Δt = 4:35 – 5:05, Infiltr. A: 0 gal, Infiltr. B: 0 gal
Middleburgh infiltration surveys

****

8.5 Baseline Measurements Analysis – Voronoi Maps

Based on the statistical analysis and the related discussion presented above, it follows that it is possible to clearly detect the effect of infiltration in the soils tested. Since the answer to the first research question was positive, and in an effort to evaluate the second research question -what geophysics demonstrates about the infiltration process in the soils sampled- summary statistics in GIS were produced. The potential practical applications of the ERI method in high-value agricultural fields on Long Island are also discussed.

The following four figures (Figures 28-31) include Voronoi maps for the three Long Island agricultural sites, as well as the non-agricultural site in Middleburgh. The Voronoi map tool is part of a number of exploratory spatial data analysis (ESDA) tools

available through the geostatistical analyst extension of the ArcGIS software. It makes possible a visual investigation of the baseline data.

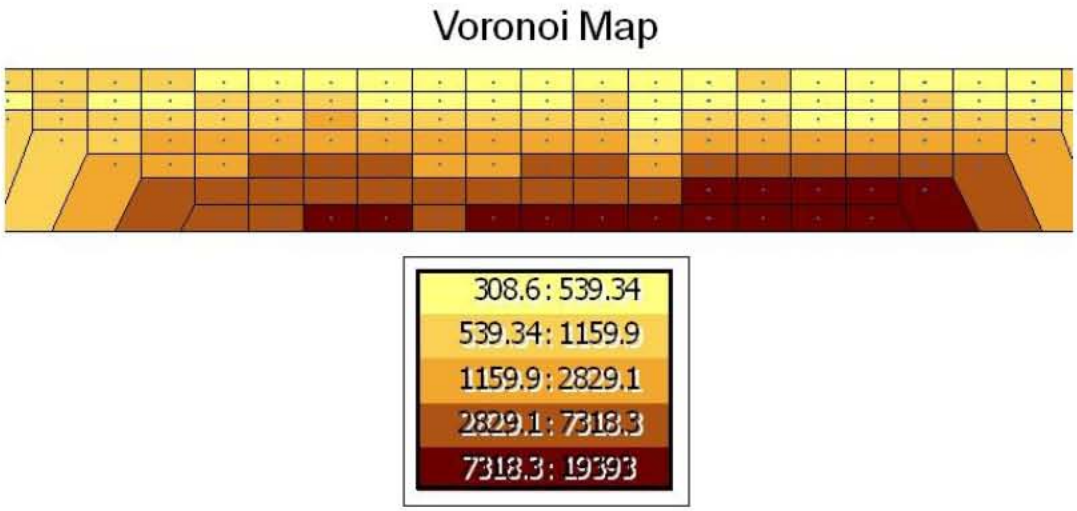

Figure 28. Voronoi map for the Riverhead Site
Baseline Geophysical Data – Summary Statistics
Riverhead (Soil Type: RdA Riverhead sandy loam)

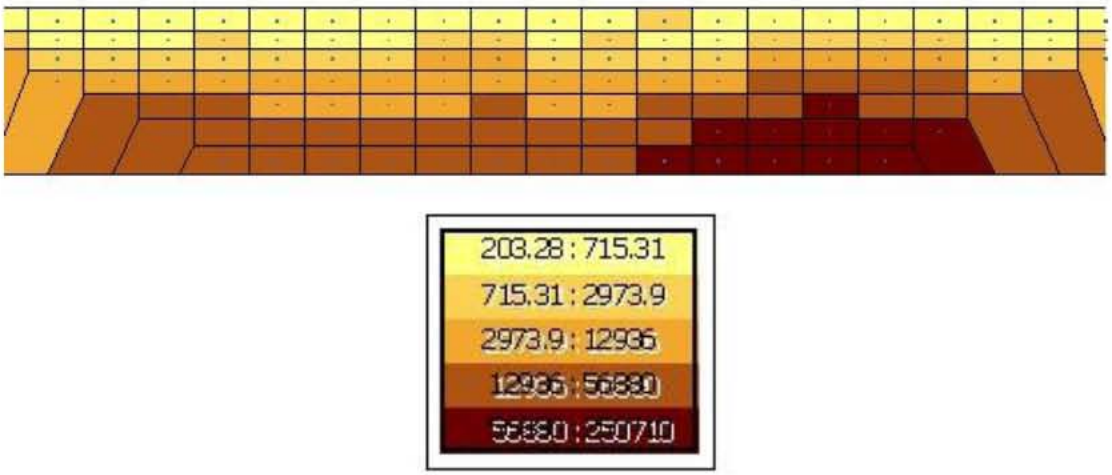

Figure 29. Voronoi map for the Mattituck Site
Baseline Geophysical Data – Summary Statistics
Mattituck (Soil Type: HaA, Haven loam)

****

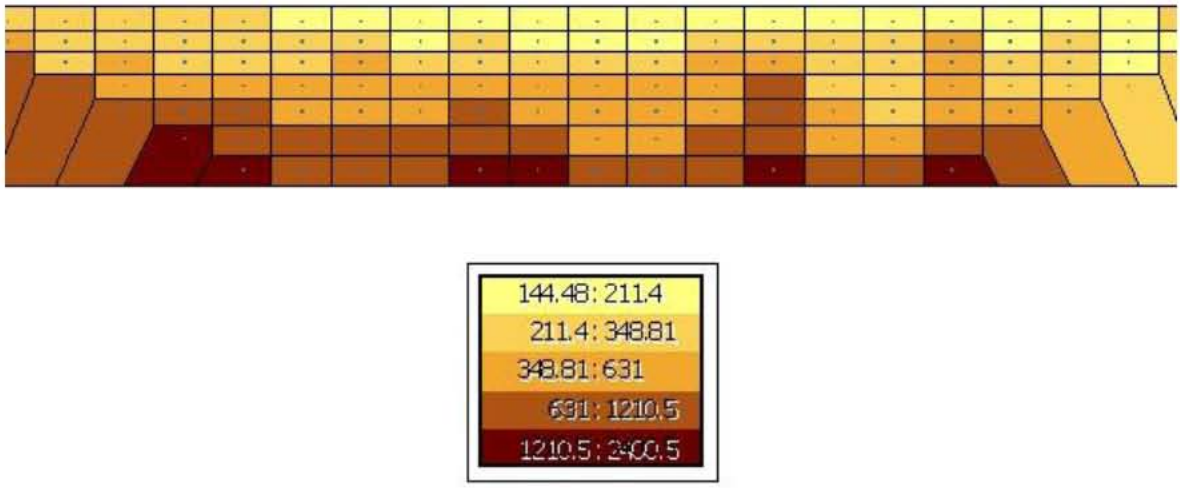

Figure 30. Voronoi map for the Southampton Site
Baseline Geophysical Data – Summary Statistics
Southampton (Soil Type: BgA, Bridgehampton silt loam)

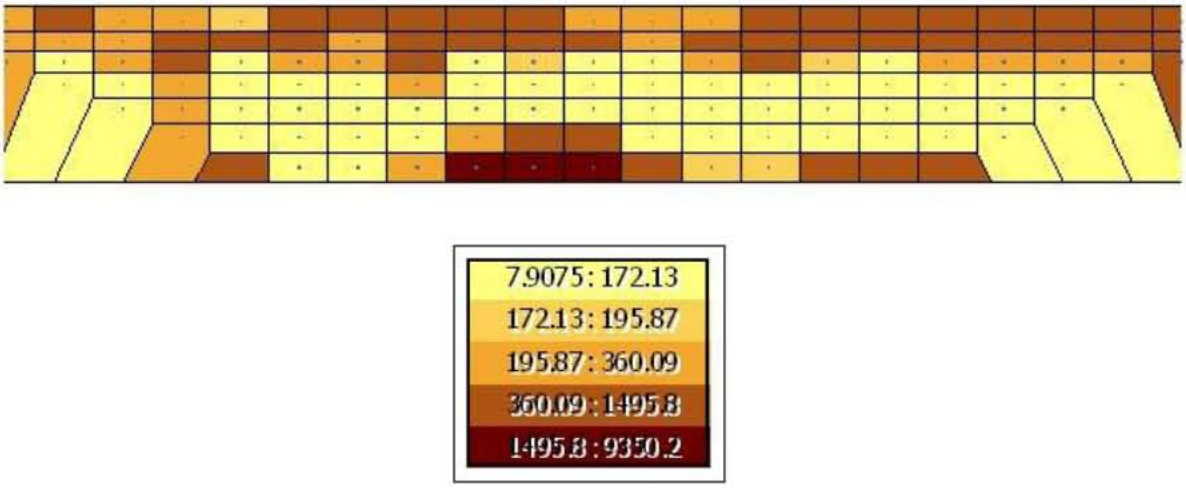

Figure 31. Voronoi map for the Middleburgh Site
Baseline Geophysical Data – Summary Statistics
Middleburgh (Soil Type: Schoharie Silty Clay Loam)

****

A Voronoi map displays the spatial variability of a dataset and is produced by combining a sequence of Voronoi polygons. In the case of geophysical data, such as those obtained for this dissertation, Voronoi polygons will be all –without exception- rectangular in shape. Each sample point will be located at the center of the rectangular cell. The area defined by each cell will be closer to the sample point in that cell than to any other sample point. Since four dipole-dipole baseline measurements are used for this analysis, it follows that four sample points exist at the same location. The mean of those four coincidental points was calculated and used in the construction of the Voronoi polygons (i.e., rectangular cells). All cells are then placed into five class intervals based on smart quantile classification (i.e., a data classification method that distributes a set of values into groups that contain an equal number of values).

There are several methods for assigning values to the Voronoi cells, including simple, mean, mode, cluster, entropy, median, standard deviation, and inter-quartile range. The mode method was selected as most appropriate for the analysis of the baseline geophysical data, as the values are estimated and assigned to each cell based on the most frequently occurring class of the cell and its neighbors. Neighbors of a sample point are the sample points whose cells share a border with the sample point in consideration.

Based on the histograms and Voronoi maps produced for each site, it is evident that the initial resistivity ranges for the Southampton and Middleburgh sites are much lower than those observed at the Riverhead and Mattituck sites. More specifically, the lowest resistivity values are observed at the Middleburgh site and the highest resistivity values are observed in Mattituck. As discussed in the previous section of this dissertation,

the results of the infiltration experiments are less clear when the initial resistivity values are lower.

The cells in Voronoi maps are classified into five classes. By comparing the four sites on a class by class basis, starting from the first class (i.e., near the surface) and proceeding to the fifth class (i.e., bottom of the sections), the following observations can be made: The lower value of the first class on Mattituck site's Voronoi map is lower than the one observed on the Riverhead site's Voronoi map. The higher value of the same class for Mattituck is higher than the one observed for Riverhead. In the remaining four classes for the Mattituck site we see consistently higher values than the four corresponding classes of the Riverhead Voronoi map, which are attributed to the soil compaction effect.

Dramatic resistivity increases between classes with increasing depth are observed in all the agricultural sites, except for the Southampton site. This phenomenon is particularly significant for the classes near the bottom of the sections, specifically the fourth and fifth class. The Voronoi map for the Southampton site reveals a more gradual progression of the resistivity values, which is attributed to the soil properties of the Bridgehampton soil series. It is a considered the most fertile soil in Suffolk County, based on its well-balanced proportions of sand, clay, and silt, as well as on its high available water capacity. The Voronoi map for Southampton verifies these attributes and, it further supports the assumption of a well-stratified soil profile.

The Voronoi map for the Middleburgh site (Figure 31), demonstrates a heterogeneous subsurface environment. Contrary to Long Island agricultural sites, in which resistivity values increased with depth, at the Middleburgh site resistivity values

decrease with depth. Most likely this effect demonstrates a shallow water table and the effect of the tree roots concentrated within the near-surface soil layer.

In summary, the exploratory spatial data analysis performed with the GIS software provided additional insights into the geophysical responses for the profiles of different soil types, as captured by the baseline surveying. The baseline results correspond well with the soil compaction data, available water capacity, and the anticipated (inferred) resistivity changes during the infiltration experiments. They do not agree with measurements of soluble salts. Based on those results, a number of practical applications of the ERI method in high-value agricultural fields on Long Island can be identified.

First, the ERI method can effectively substitute in part or entirely the use of the penetrometer instrument for the collection of soil compaction data in agriculture. The geophysical attributes that would enable the identification of soil compaction are the resistivity changes. Rapid increases of resistivity would indicate the presence of compacted layers near the surface. Gradual increases would indicate less compacted soils. The geophysical responses coupled with well-established sediment grain characteristics (e.g. USDA literature for soil texture for Long Island agricultural fields) can be a powerful tool in deciphering depths to hard-pan. The advantages of the ERI method over the use of the penetrometer instrument, include the fact that the latter is more user-dependent. The resistivity system is entirely automated, while the penetrometer user needs to manually apply continuous pressure to inject the rod inside the soil, while recording the values obtained in three-inch intervals.

Second, in accordance with the precision agriculture trend that finds an increasingly wider appeal, the ERI method is able to detect within-field variability. By browsing the field with ERI, those areas with significant soil compaction can be mapped. In this case, horizontal variations of resistivity would indicate localized areas of greater compaction (i.e. higher inferred resistivities) versus areas less affected by soil compaction (i.e. lower inferred resistivities). This fact can effectively guide the application of plowing within the field, as opposed to the common practice on Long Island of plowing the entire site based on the results of disparate penetrometer measurements. Depending on the method chosen for the resistivity measurements, this application may reduce fuel consumption and the labor associated with this agricultural practice. Similarly, and given the strong correlation between soil compaction levels and the behavior of fluids in the shallow subsurface, the ERI method may also guide irrigation application. More research in this area is needed, to narrow down the field situations (e.g. soil type and initial resistivity ranges), in which the ERI would be most applicable.

8.6 Baseline Measurements Analysis – Histograms

The histograms presented in Figures 32 through 35 illustrate frequency distributions of four dipole-dipole baseline measurements for each site. Summary statistics are also provided above the histograms for every site. The histogram tool is part of a number of exploratory spatial data analysis (ESDA) tools available through the geostatistical analyst extension of the ArcGIS software. It makes possible a visual exploration of the baseline data. Those data were extracted from the inverted resistivity sections.

In ArcGIS symbology the powers of ten included in the histograms are all positive. For instance, the first class of the histogram for the Riverhead site (Figure 32) includes resistivity values within the following range: 0.08 x 1000 = 80 Ohm-meter (lowest extreme) to 2.25 x 1000 = 2250 8 Ohm-meter (highest extreme). The count for all datasets is 508 points (i.e. 127 points per dipole-dipole baseline measurement x 4 available baselines = 508 points).

From the summary statistics, it is useful to note the median values for each dataset. The median is 2770.1 for the Riverhead site, 4612.6 for the Mattituck site, 324.3 for the Southampton site, and 240.45 for the Middleburgh site. Maximum values are typically inferred for the deeper layers near the bottom edges of the dipole-dipole cross sections (except for the Middleburgh site), and are typically associated with outliers. On the other hand, minimum values are observed mostly near the surface (except for the Middleburgh site), where the sensitivity of the instrument is significantly higher.

Count	: 508	Skewness	: 2.4131
Min	: 293.39	Kurtosis	: 9.4249
Max	: 21770	1-st Quartile	: 540.57
Mean	: 2770.1	Median	: 1055.6
Std. Dev.	: 3702.5	3-rd Quartile	: 3529.6

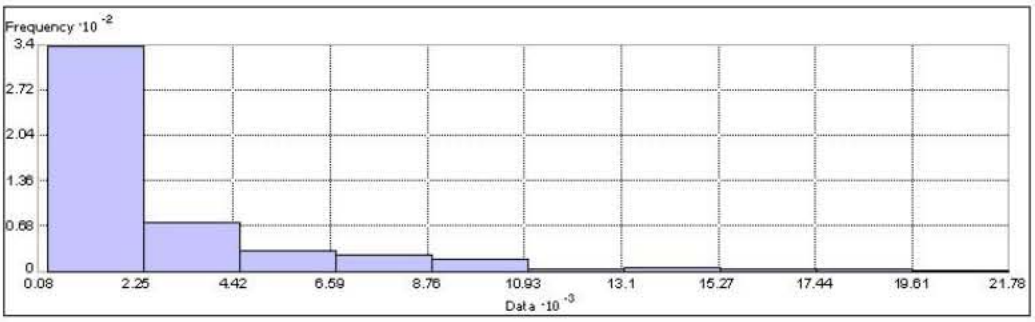

Figure 32. Histogram for the Riverhead Site
Baseline Geophysical Data – Summary Statistics
Riverhead (Soil Type: RdA Riverhead sandy loam)

****

Count	: 508	Skewness	: 5.5928
Min	: 197.12	Kurtosis	: 40.564
Max	: 473980	1-st Quartile	: 726.24
Mean	: 19571	Median	: 4612.6
Std. Dev.	: 49935	3-rd Quartile	: 15599

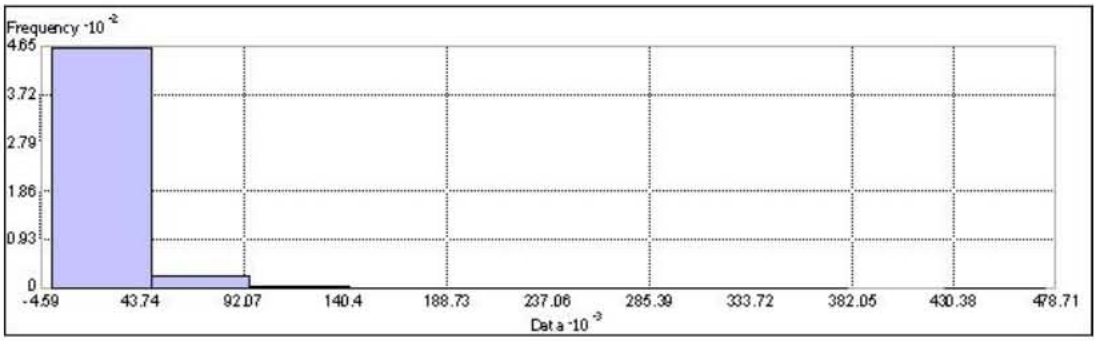

Figure 33. Histogram for the Mattituck Site
Baseline Geophysical Data – Summary Statistics
Mattituck (Soil Type: HaA, Haven loam)

****

Count	:508	Skewness	:5.7992
Min	:31.43	Kurtosis	:61.913
Max	:6974.1	1-st Quartile	:213.35
Mean	:478.46	Median	:324.3
Std. Dev.	:505.72	3-rd Quartile	:562.11

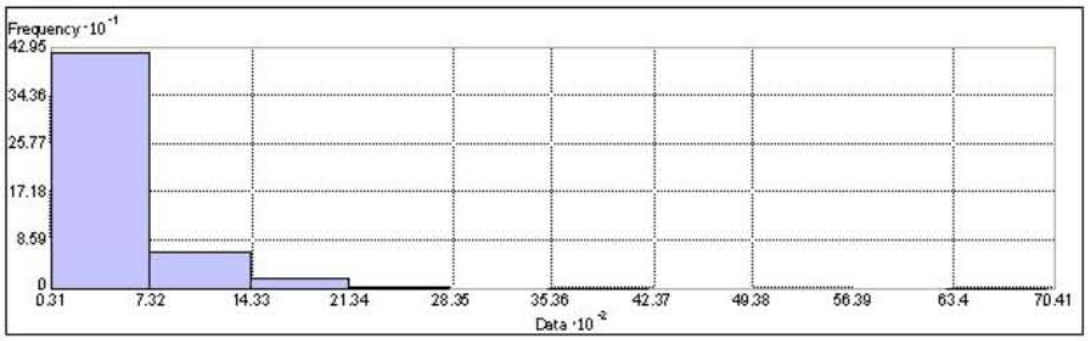

Figure 34. Histogram for the Southampton Site
Baseline Geophysical Data – Summary Statistics
Southampton (Soil Type: BgA, Bridgehampton silt loam)

****

Count	:508	Skewness	:10.25
Min	:5.27	Kurtosis	:122.93
Max	:14139	1-st Quartile	:90.35
Mean	:397.78	Median	:240.45
Std. Dev.	:1056.9	3-rd Quartile	:439.46

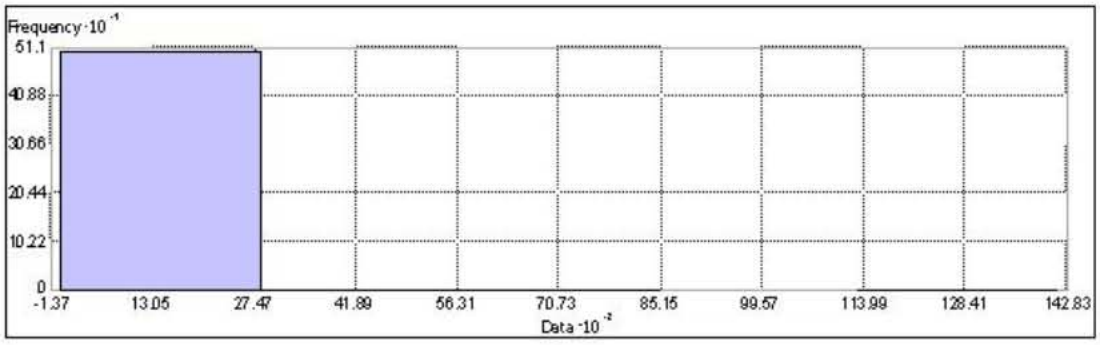

Figure 35. Histogram for the Middleburgh Site
Baseline Geophysical Data – Summary Statistics
Middleburgh (Soil Type: Schoharie Silty Clay Loam)

****

8.7 Baseline measurements analysis, Middleburgh Site, on the effects of tree roots

During the data collection program of this dissertation, a series of baseline measurements were obtained in an effort to evaluate both the measurement error and the differences between different soils, as observed through the resistivity cross sections. For all the sites the baseline surveys obtained during the pre-infiltration stage, included repeatability tests, the reciprocal measurement, two different electrode arrays, and two different measurement modes, as discussed previously. For the three Long Island sites, the baseline surveys were conducted along the exact same transect as the final infiltration survey line, except for the Riverhead site, in which additional baselines were obtained along a transect parallel to the line of the infiltration experiment. The observed differences between the Long Island sites were discussed earlier in this discussion section based on overall apparent resistivity values, differences in resistivity ranges from site to site, relation to soil compaction levels, relation to available water capacity, and other site-specific factors.

On the other hand, the data collection campaign at the Middleburgh site specifically during the pre-infiltration stage was different in that it was significantly more extensive. The baseline measurements exceeded in volume the amount of baseline data obtained from the three Long Island sites combined. One reason for the increased interest in the detailed subsurface characterization of the Middleburgh site was the owner's approval to excavate, as well as to use a Lithium tracer during the infiltration experiment. These provisions are virtually impossible to obtain in most agricultural sites, especially in high-value crops such as the three Long Island vineyards under evaluation. Therefore,

indirectly the Middleburgh site provided for an opportunity through the excavation results to further evaluate the validity of the resistivity signatures obtained through this geophysical method and through the specific equipment that was used for this dissertation.

Another reason for the increased interest in the Middleburgh site was to obtain data from a non-disturbed and non-agricultural site, as opposed to the rest of the sites under evaluation, which all had a long history of agricultural practice. Among the differences that are expected between an agricultural and a natural (i.e., undisturbed) site are the effect of fertilizer and pesticide application and the development of a hard pan by agricultural machinery traffic. Root growth in natural sites has an advantage over the agricultural sites not only in the absence of compacted soil layers, but also due to the additional available conduits created by earth-worms and decayed roots. Marshall et al., (1996) reported that soil compaction readings in natural sites are limited in the evaluation of root growth, as the penetrometer instrument cannot diverge from the straight line that is being injected along, in case it encounters a resistant feature. In contrast, for a tree root system there is a plethora of alternative paths through which roots may advance.

The process of evaluating the validity of the geophysical response in Middleburgh through extensive surveying and excavation proved particularly useful in obtaining new insights on the influence of tree roots on the resistivity sections. By extension, this research at the undisturbed and naturally forested site in Middleburgh may provide a better understanding on the effect of agricultural plants' roots on the geophysical response, as well.

Several authors have attempted to link geophysical results to the distribution of roots of various plant species. Nadezhdina and Cermak (2003) reported that the total volume of soil carrying roots can be determined by ground penetrating radar. Hagrey et al., (2004), explored the potential of surface geophysics to monitor water uptake by roots, as part of a larger water flow study through the vadose zone, and presented results from surveys carried out at a number of European sites. Hagrey (2007) reviewed applications of seismic, radar, and electrical methods for monitoring water migration patterns within roots, tree trunks, and soils.

In this dissertation a grid of dense dipole-dipole and Wenner measurements was carried out at the Middleburgh site and the relative position of four large trees to the survey lines was recorded. Figure 36 shows the distribution of the survey lines and the relative position of the trees. Survey lines a, b, and c are parallel to each other, separated by a distance of 1 meter. Survey line d intersects perpendicularly with lines a, b, and c. The unit electrode spacing for all the survey lines was 0.5 meters, as in the rest of the surveying in this dissertation, producing a transect of 11.5 meters in length (i.e. as the first electrode for each survey line marks point zero for measuring horizontal distance, it follows that the total length of the survey line is 11.5 meters). The first electrode for lines a, b, and c, as they are presented on Figure 36 is located on the left end of the line, and the twenty-fourth electrode on the right end of the line. During this surveying, the electrodes' position were carefully marked and the same holes were used for the crossing survey line d. Effectively, the location of electrodes number 11, 13, and 15 of survey line d coincide with the location of electrode number 10 for each of the survey lines a, b, and c. The first electrode for line d is located at the top end of the line, as presented in Figure

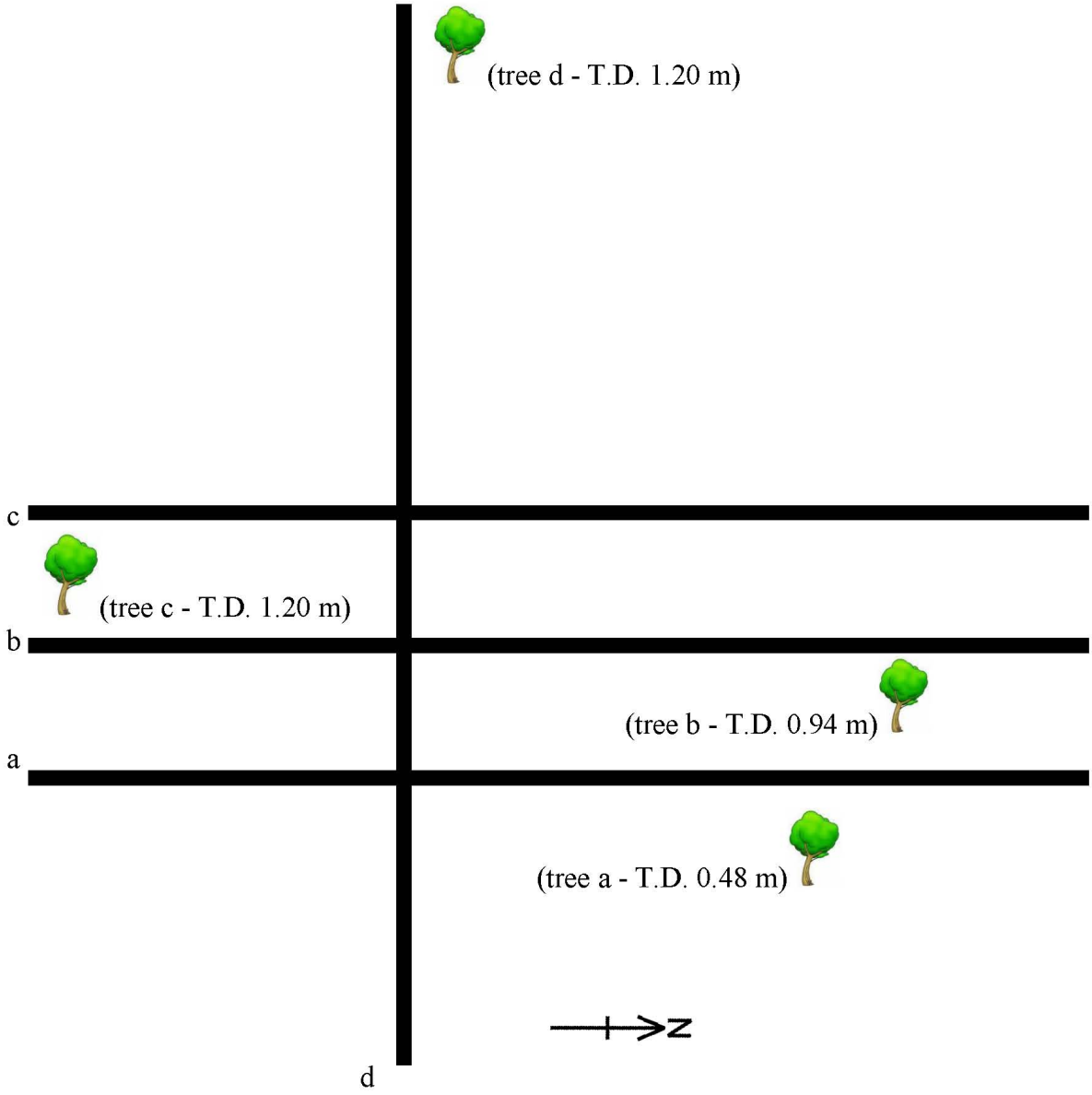

Figure 36. Middleburgh, Schematic diagram (not to scale) of distribution of survey lines and relative position of the trees.

Symbology			T.D.
Explanation	Tree location	Survey Line	trunk diameter

36 and the twenty-fourth electrode at the bottom end of the line. Line d was the final line along which the infiltration experiment took place and, subsuquently, the excavation.

The four trees are located adjacent to either one or two of the survey lines, as shown in Figure 36 (labeled as tree a, tree b, tree c, and tree d). Therefore, it is possible that roots of the same tree affected the resistivity values on more than one survey lines. For instance, the root effect onto the resistivity sections of tree b it is captured by lines a, b and c, and tree c by both survey lines b, c and d. On the other hand, tree a is adjacent only to survey line a and tree d is adjacent only to survey line d. More specifically, tree a is located between electrodes 16-17 of line a, tree b is located between electrodes 20-21 for both lines a and b, the center of the trunk of tree c is located directly across electrode 3 for both lines b and c, and the center of the trunk of tree d is located between electrodes 2-3 of line d. All four trees have varying trunk diameter ranges. The trunk diameter - measured one meter above ground- is 0.48 meters for tree a, 0.94 meters for tree b, and 1.20 meters for both trees c and d.

The root system provide nutrients, water, and anchorage. The root growth decreases as soil compaction increases. The excavation along survey line d revealed that tree roots were spead over a significant extent laterally further away from the expected radius around trees' trunks, suggesting both a compacted layer near the surface and a shallow water table. The roots of tree d, which was one of the largest, were exposed after excavation to reveal that vertical penetration was limited to less than one meter from the surface.

The inverted model resistivity sections (Figures 37-40), for the four survey lines presented in conjuction with Figure 36 demonstrate that tree roots correspond to areas of higher resistivity, intercepted by a low resistivity area located directly under the tree. For instance, in Figure 37 higher resistivities -in relation to the rest of the section- are observed at the top right part of the section. This corresponds to the effect of roots originating from trees a and b, which are located on either side of survey line a, as it shown in Figure 36. Those higher resistivities observed in the vicinity of large trees are attributed to the presence of long, thick and dry roots. Furthermore, the expected moisture contrast developed by water absorption from the roots is also responsible for the observed higher resistivity areas located in the subsurface area in the vicinity of the trees. In the absence of tree roots, moisture levels are higher at the rest of the section, thus resistivity levels are lower. Localized areas of slightly lower resistivity directly underneath the trees are attributed to the fact that most of the water absorption is taking place at the roots' tips located within roughly concentric circles that extend outwards from the trunk.

The resistivity sections (lines a, b, c, and d in Figure 36, and Appendix 1) reflect the surface topography and the corresponding orientation of a shallow water table. Line d runs horizontally along the strike of the water table. Lines a, b, and c, reflect the fact that the water table dips toward a north direction.

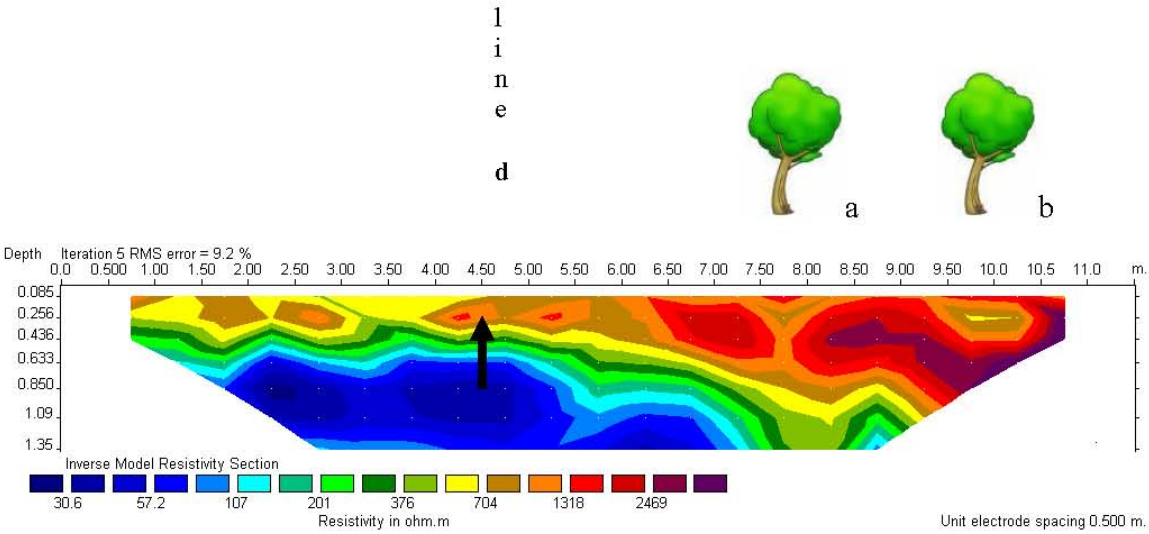

Figure 37. Middleburgh, Survey Line a – Dipole-Dipole Baseline Measurement
Line a - (tree a - T.D. 0.48 m) Located between electrodes 16-17 of line a
(tree b - T.D. 0.94 m) Located between electrodes 20-21 of lines a + b

****

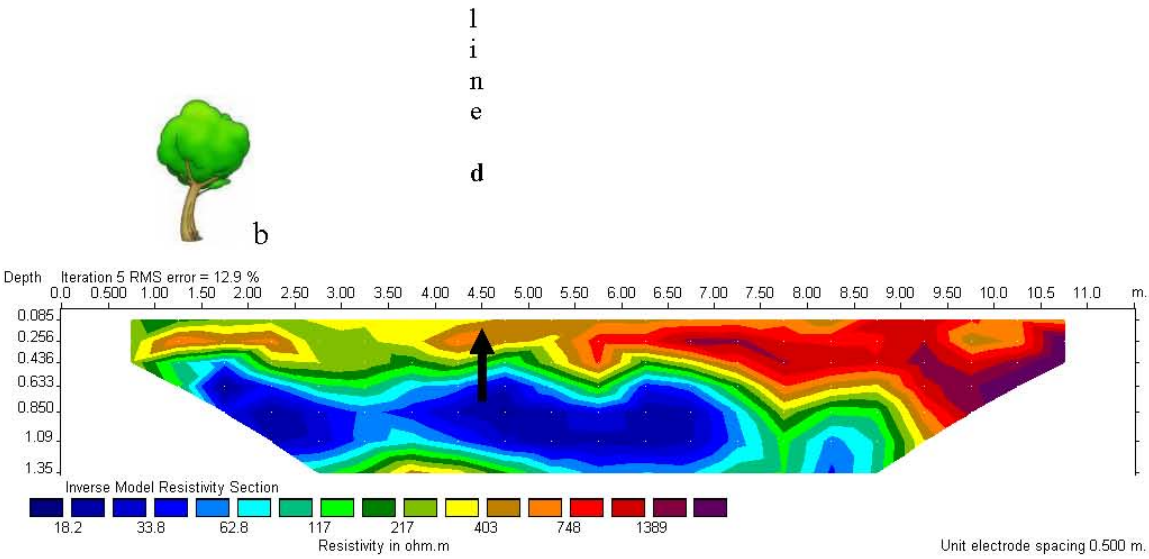

Figure 38 Middleburgh, Survey Line b – Dipole-Dipole Baseline Measurement
Line b - (tree b - T.D. 0.94 m)
Located between electrodes 20-21 of lines a + b

****

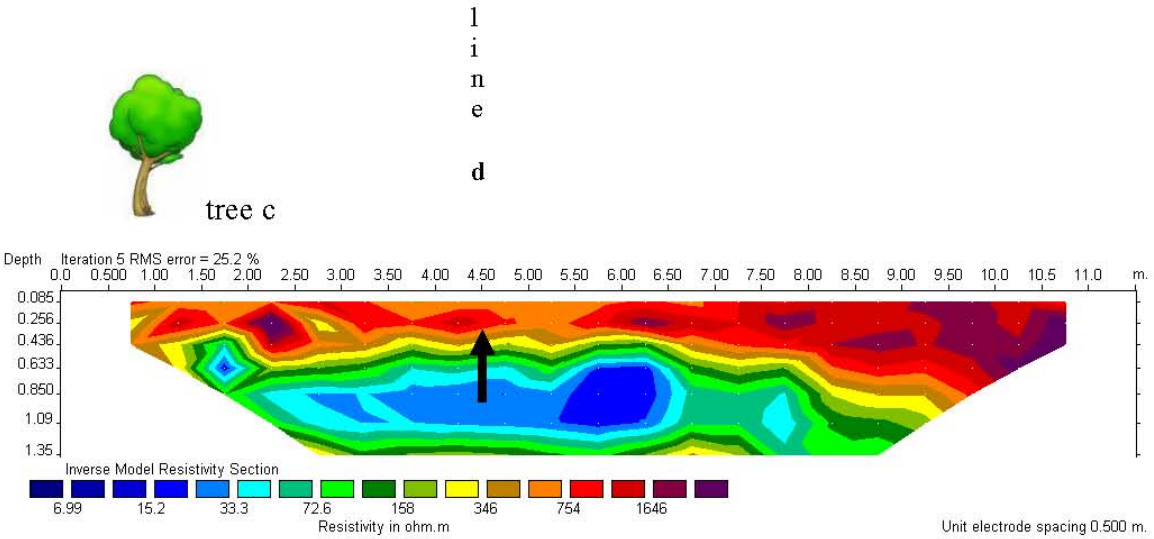

Figure 39 Middleburgh, Survey Line c – Dipole-Dipole Baseline Measurement
Line c - (tree c - T.D. 1.20 m)
Center of trunk located over electrode 3 of lines b + c

****

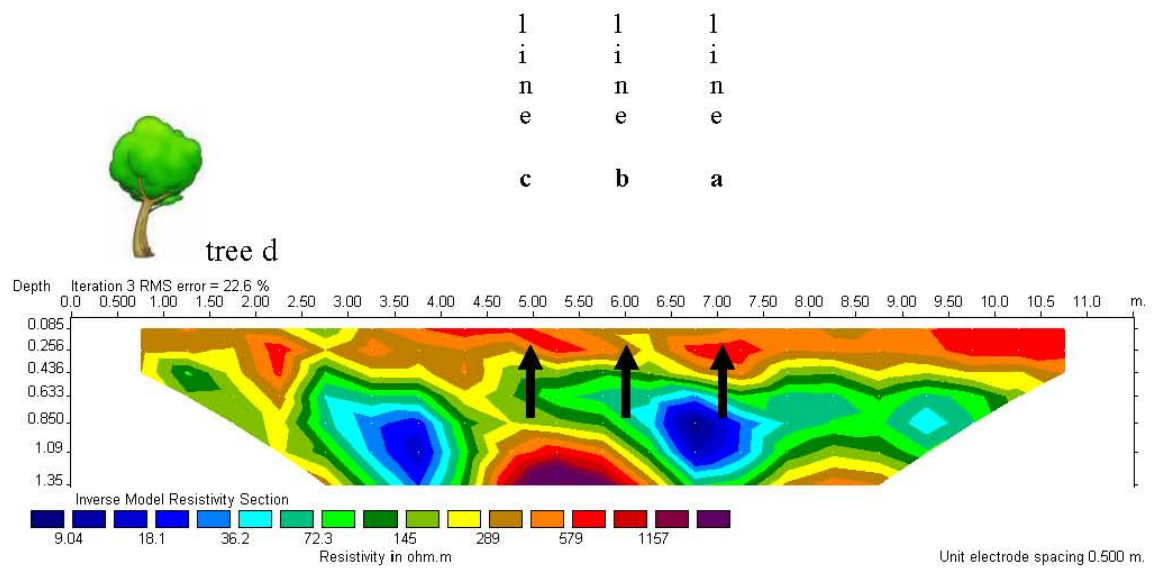

Figure 40 Middleburgh, Survey Line d – Dipole-Dipole Baseline Measurement
Line d (tree d - T.D. 1.20 m)
Center of trunk located over the middle point between electrodes 2-3 of line d

****

CHAPTER 9. CONCLUSIONS

Based on the statistical analysis of the inverted resistivity datasets, it is concluded that resistivity differences can unequivocally detect infiltration in soils typical of the north-eastern United States. Generally, the sensitivity is higher in soils that demonstrate high overall apparent resistivity values and low available water capacity (usually, these will be soils with high sand content). Thus, inferences based on baseline geophysical measurements can be applicable on agricultural sites exhibiting high overall resistivity values (e.g., sandy soils).

The geophysical results during infiltration correlate well with soil compaction data. It follows that the ERI method can be used as a proxy for compaction in agricultural applications. Temporal variations in the upper 1.5 meters (relevant to agriculture) of the subsurface can be monitored successfully with ERI. The major advantage of the ERI method over traditional soil compaction tester (i.e., penetrometer) is that it can effectively and non-destructively map within-field variability and guide agricultural practices. The ERI method can constitute a supplementary valuable tool for vertical profiling of the hydrological dynamics in the unsaturated zone.

The geophysical results also correlate with the literature data for available water capacity levels. The infiltration experiment at the Southampton site (Bridgehampton soil series), which has the highest available water capacity, produced a less prominent geophysical effect compared to the other experiments at Riverhead (Riverhead soil series) and Mattituck (Haven loam series). It follows that the ERI method is limited in monitoring near surface infiltration in soils that have high available water capacity. On the other hand, the infiltration sections presented for the Southampton site demonstrated a

clear reduction in resistivity associated with infiltration. Although the subsequent analysis using GIS demonstrated that the inferred resistivity reductions were not more than three standard deviations from the baselines, it was evident that an overall reduction associated with infiltration can be observed.

Soluble salts (Table 5) in the soil do not correlate with the resistivity values measured in the field. For instance, high salinity levels were observed for both Riverhead (high overall apparent resistivity values) and Southampton (low overall apparent resistivity values). On the other hand, low salinity levels were observed for both Mattituck (highest overall apparent resistivity values) and Middleburgh (lowest overall apparent resistivity values). It appears that in these soils it is porosity, compaction, and water content that affect the resistivity results more than anything else. Also the Lithium Chloride did not produce a major enhancement of the resistivity effect of infiltration at the one site at which it was tried.

Chargeability (i.e., induced polarization) values for the Wenner array are low in the agricultural sites, as expected from the low prevalence of clay. The values in Middleburgh were somewhat higher and decreased with increasing depth, which is in agreement with the soil sampling data that show more clay in the shallower layer.

In the absence of agricultural practices, the subsurface geology is more complex. Specifically for a naturally forested site, the infiltration process is complicated due to the additional flow paths created by the action of earth worms and the presence of dead roots. Under conditions of increased soil heterogeneity, instead of the formation of a continuous water plume as occurred in the homogeneous agricultural soils, the location of the

infiltrated water seems to be highly influenced by the soil heterogeneity, and the water front is scattered into discontinuous layers and travels in additional directions.

The ERI method successfully maps the tree root zone of mature trees. Geophysical measurements in combination with the excavation results demonstrated a correlation between near-surface high-resistivity areas adjacent to mature trees and the spatial extent of the root zone. Localized areas of lower resistivity areas were inferred directly underneath the trees. They are attributed to the fact that most of the water absorption is taking place at the roots' tips located within roughly concentric circles that extend outwards from the trunk.

APPENDIX 1

ELECTRICAL RESISTIVITY CROSS SECTIONS BASELINE MEASUREMENTS (SOFTWARE RES2DINV)

Seven data sets were collected for each site in the pre-infiltration stage. Out of these seven data sets, five were obtained using the dipole-dipole array and two using the Wenner array. There was one measurement from each array type in the induced polarization (IP) mode. The remaining measurements were all conducted in standard mode. One of the five dipole-dipole array measurements was a reciprocal measurement, in which the current and potential electrode pairs are interchanged. The electrical resistivity baseline cross sections for the Riverhead site were presented in chapter 7.2. Appendix 1 includes the remaining electrical resistivity baseline cross sections for Mattituck, Southampton, and Middleburgh. Seven baseline data sets were collected for each of the Middleburgh lines (lines a, c, and d), except for line b, at which only one dipole-dipole measurement and one Wenner measurement was obtained. From the three types of sections and pseudosections described in the methods section of this dissertation (measured apparent resisitivity, calculated apparent resisitivity, and inverse model resistivity) only the inverted sections will be presented.

1.1 Mattituck, inverted resistivity baseline cross sections (Dipole-Dipole)

Resistivity contour values were set by means of a logarithmic contour interval. The factor to increase contour values was set to 1.41 (doubles every 2 contours). The minimum value entered was 200.

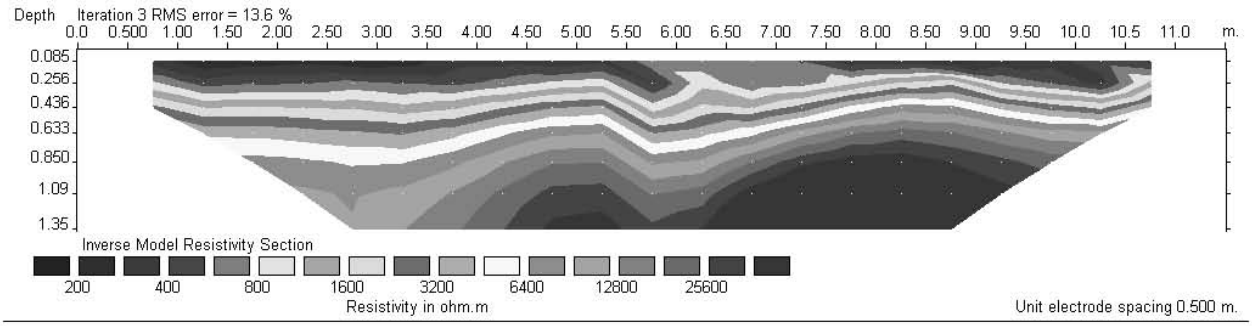

Dipole – dipole 1, Mattituck baseline measurements

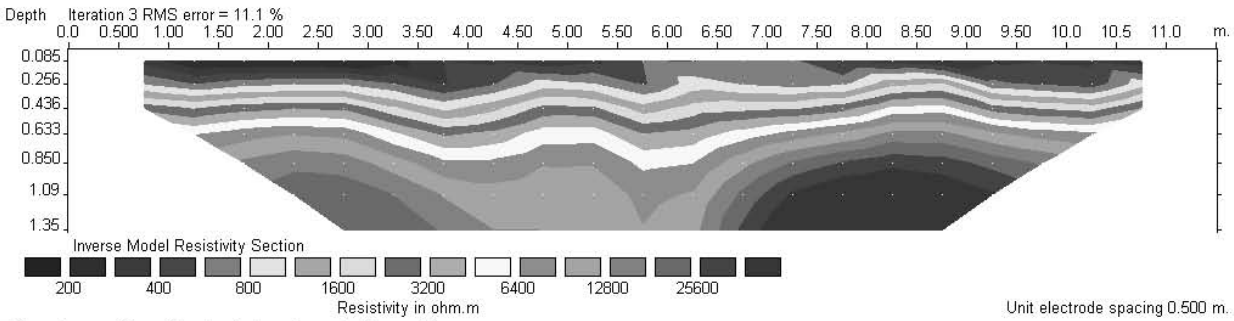

Dipole – dipole 2, Mattituck baseline measurements

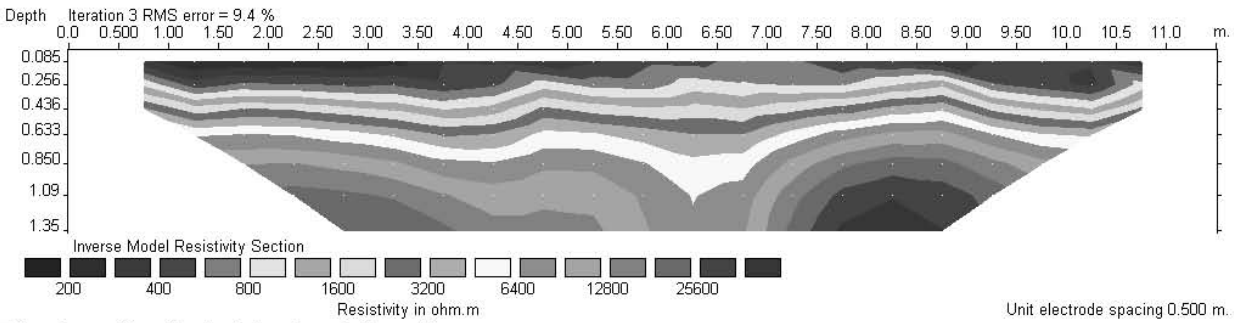

Dipole – dipole 3, Mattituck baseline measurements

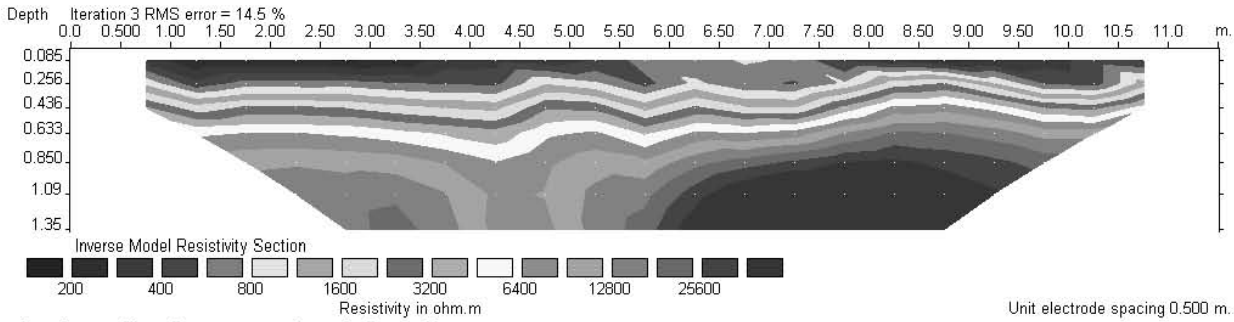

Dipole – dipole 4, Mattituck baseline measurements

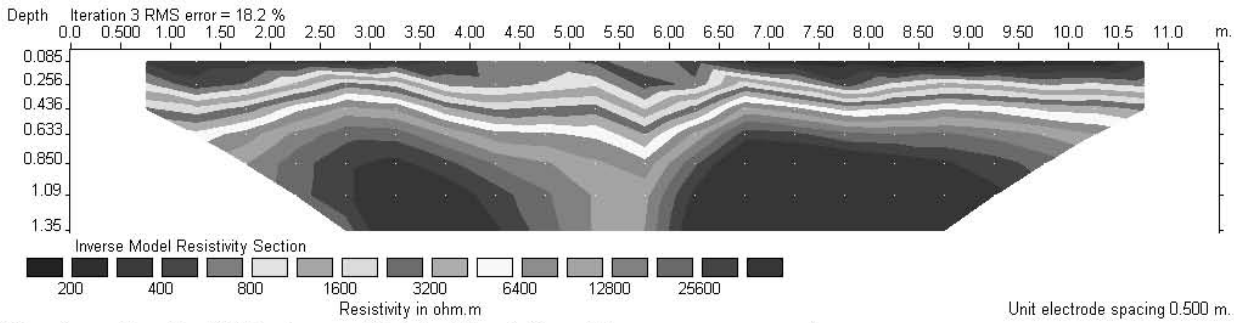

Dipole – dipole 5 (Reciprocal), Mattituck baseline measurements

1.2 Mattituck, inverted resistivity baseline sections (Wenner profiling)

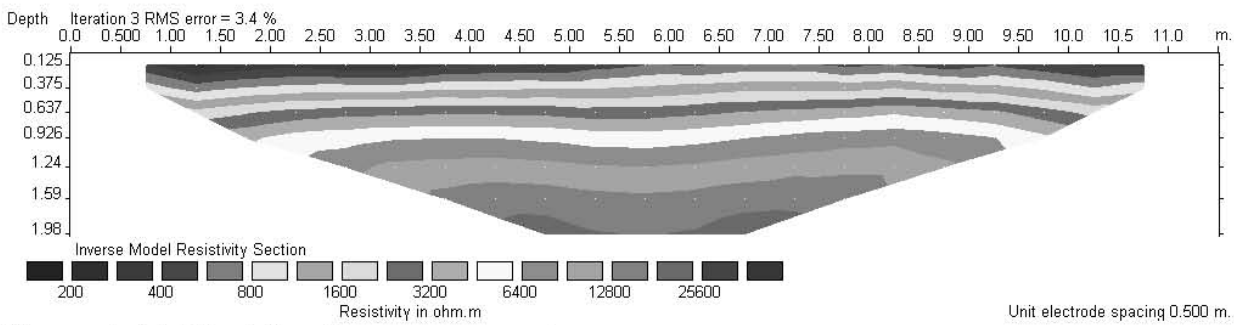

Wenner 1, Mattituck baseline measurements

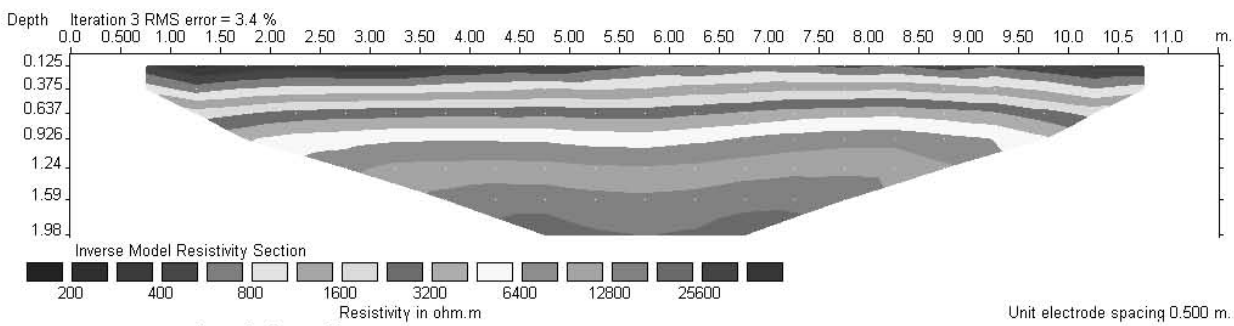

Wenner 2, Mattituck baseline measurements

1.3 Southampton, inverted resistivity baseline cross sections (Dipole-Dipole)

Resistivity contour values were set by means of a logarithmic contour interval. The factor to increase contour values was set to 1.19 (doubles every 4 contours). The minimum value entered was 140.

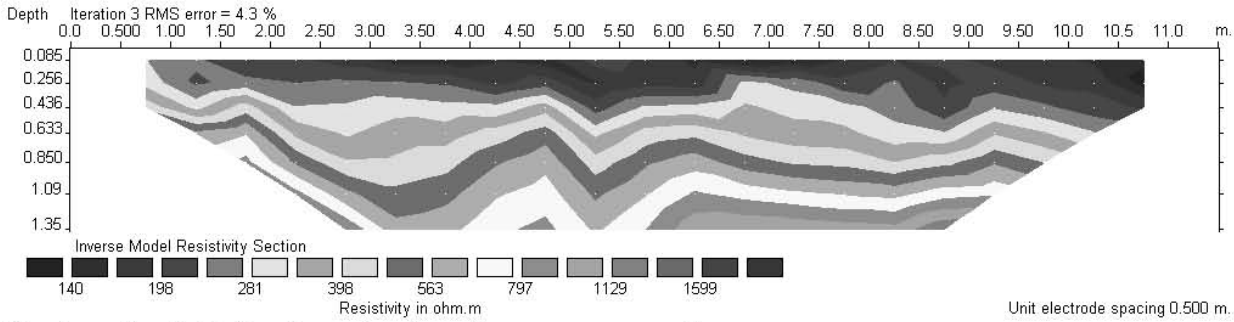

Dipole – dipole 2, Southampton baseline measurements

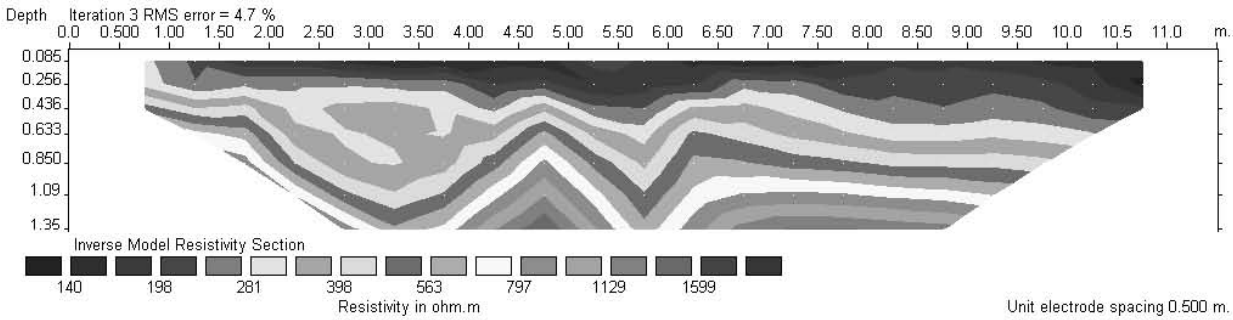

Dipole – dipole 3, Southampton baseline measurements

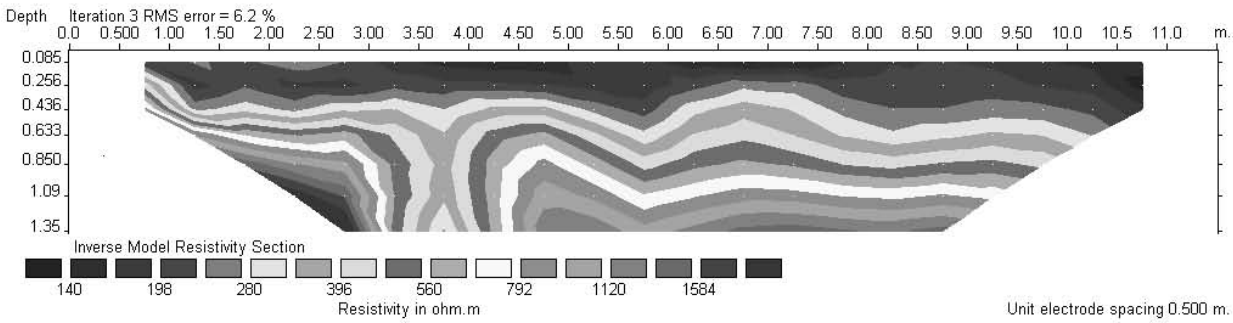

Dipole – dipole 4, Southampton baseline measurements

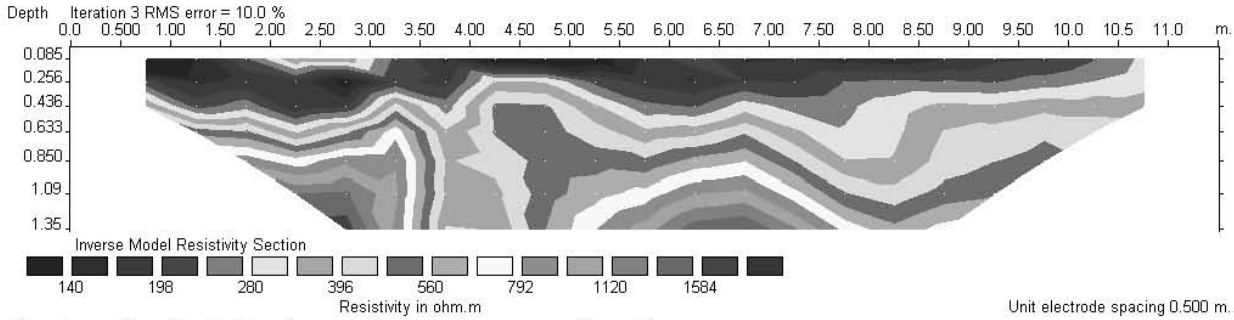

Dipole – dipole 5 (Reciprocal), Southampton baseline measurements

1.4 Southampton, inverted resistivity baseline sections (Wenner profiling)

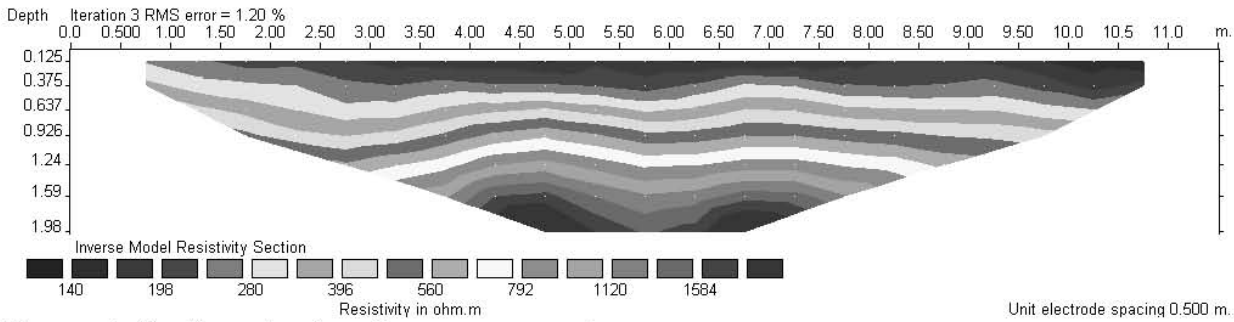

Wenner 1, Southampton baseline measurements

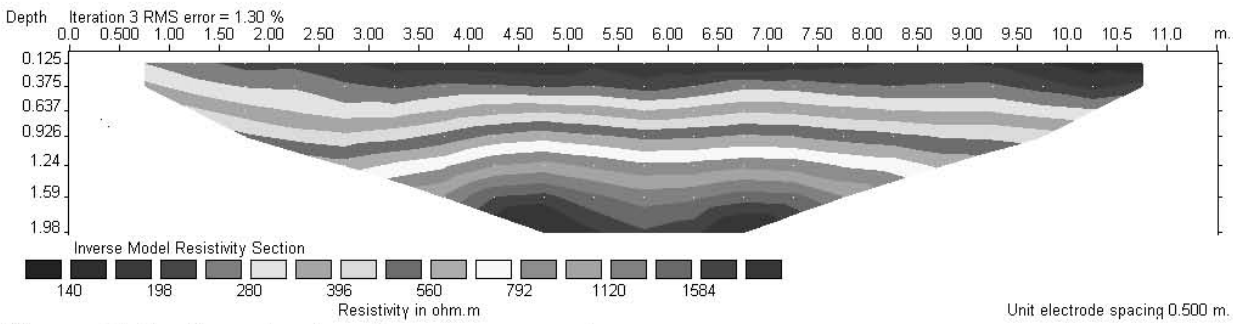

Wenner 2, Southampton baseline measurements

1.5 Middleburgh, line a, inverted resistivity baseline cross sections (Dipole-Dipole)

Resistivity contour values were set by means of a logarithmic contour interval. The factor to increase contour values was set to 1.41 (doubles every 2 contours). The minimum value entered was 15.

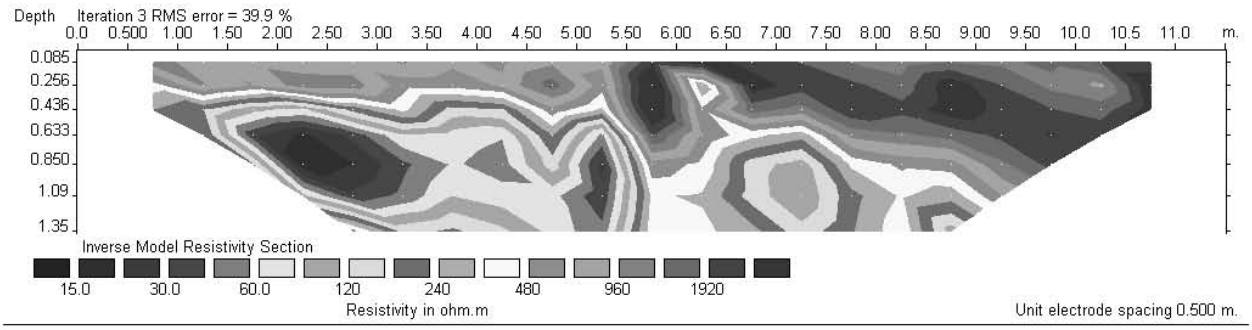

Dipole – dipole 1, Line a, Middleburgh baseline measurements

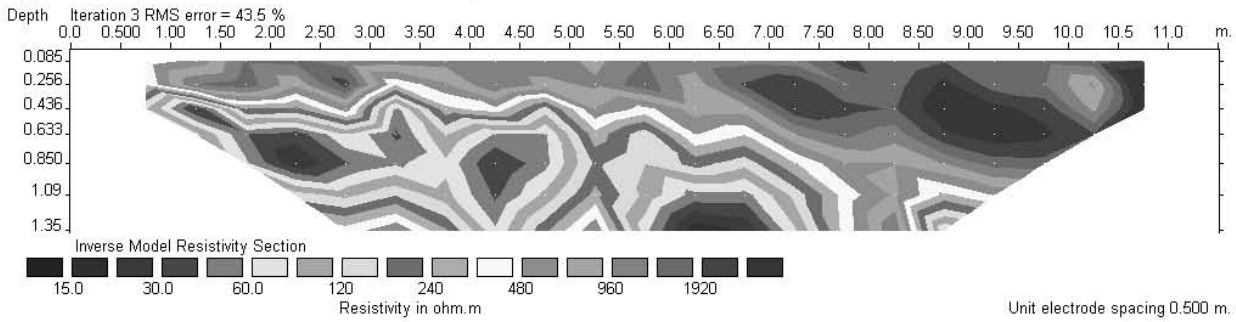

Dipole – dipole 2, Line a, Middleburgh baseline measurements

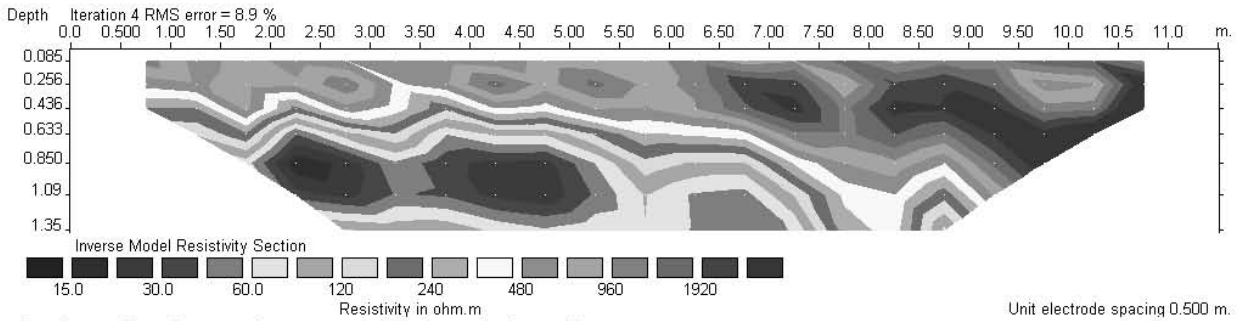

Dipole – dipole 3, Line a, Middleburgh baseline measurements

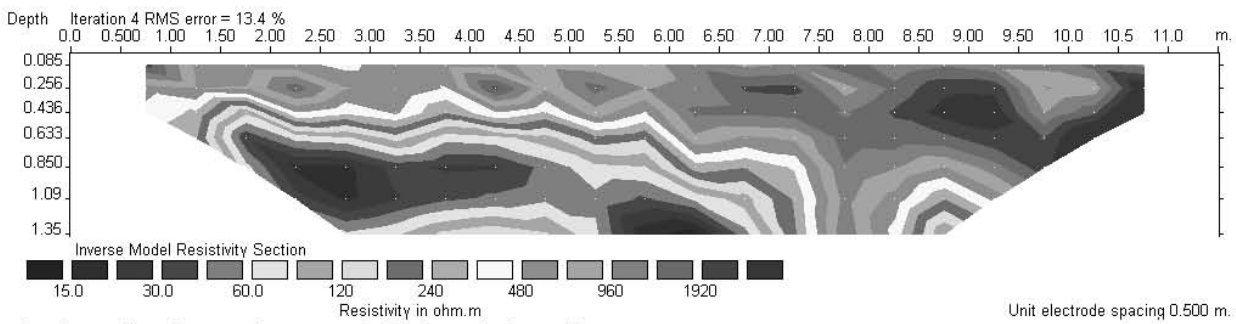

Dipole – dipole 4, Line a, Middleburgh baseline measurements

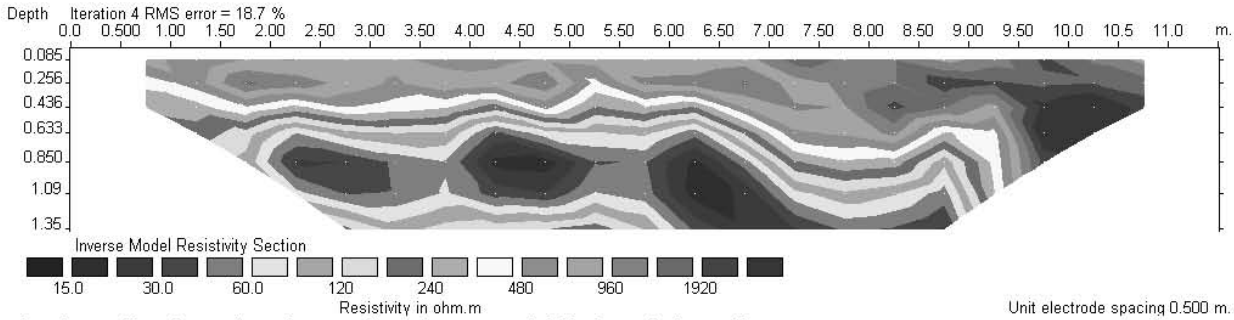

Dipole – dipole 5 (Reciprocal), Line a, Middleburgh baseline measurements

1.6 Middleburgh, line a, inverted resistivity baseline sections (Wenner profiling)

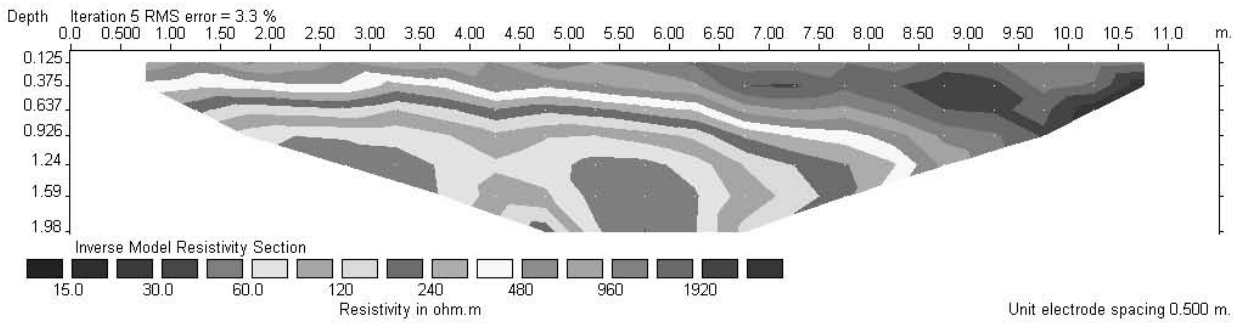

Wenner 1, Line a, Middleburgh baseline measurements

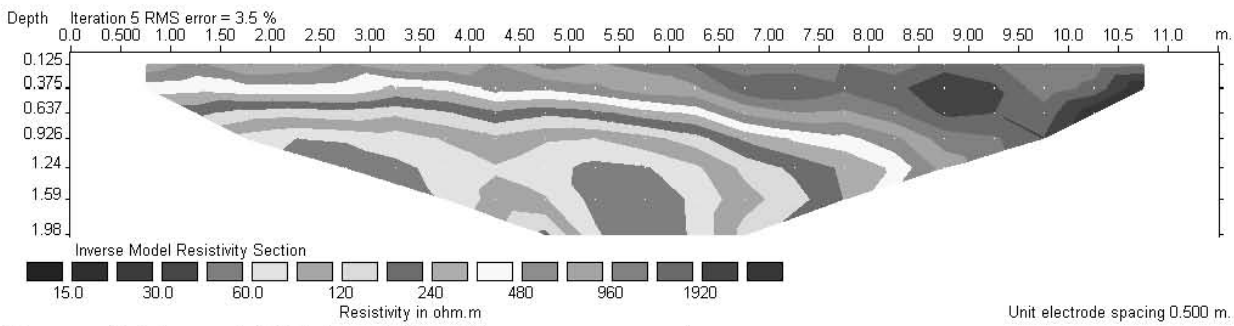

Wenner 2, Line a, Middleburgh baseline measurements

1.7 Middleburgh, line b, inverted resistivity baseline cross sections (Dipole-Dipole)

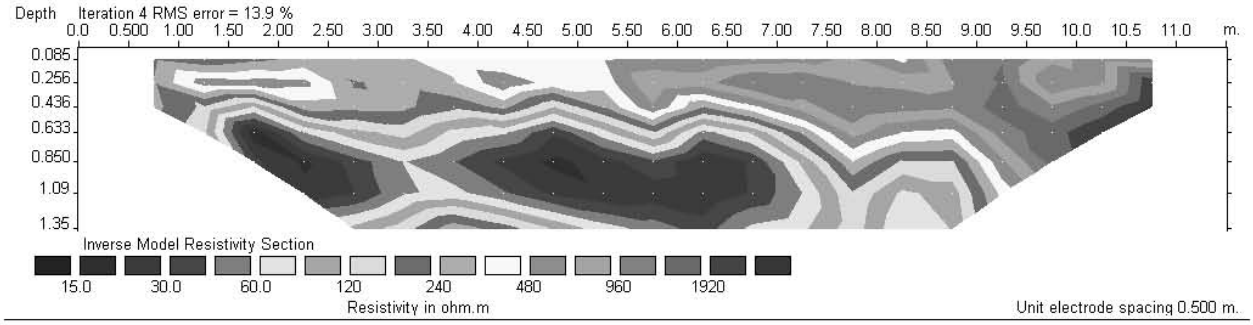

Dipole – dipole 1, Line b, Middleburgh baseline measurements

1.8 Middleburgh, line b, inverted resistivity baseline sections (Wenner profiling)

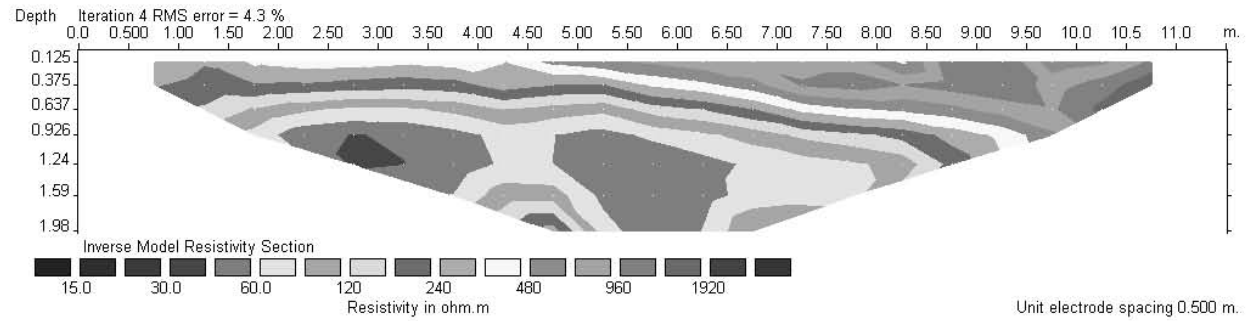

Wenner 1, Line b, Middleburgh baseline measurements

1.9 Middleburgh, line c, inverted resistivity baseline cross sections (Dipole-Dipole)

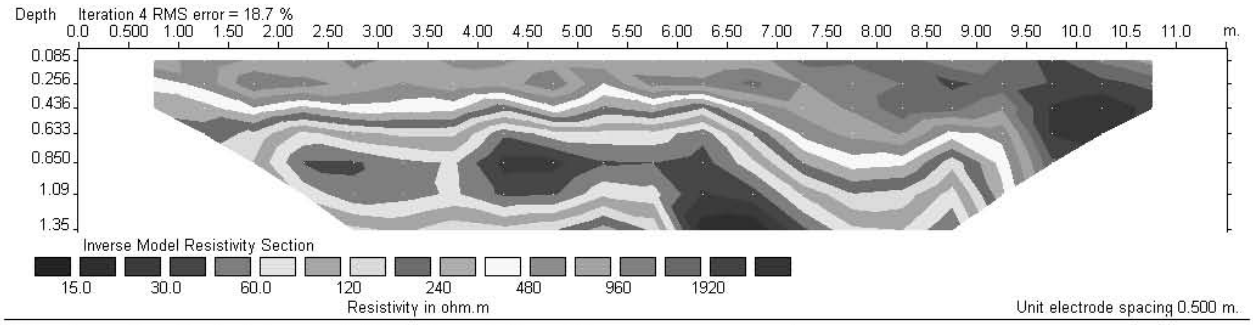

Dipole – dipole 1, Line c, Middleburgh baseline measurements

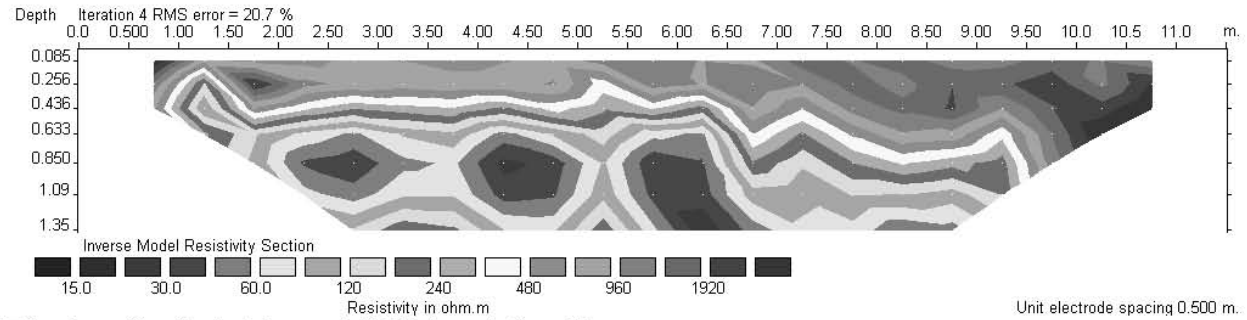

Dipole – dipole 2, Line c, Middleburgh baseline measurements

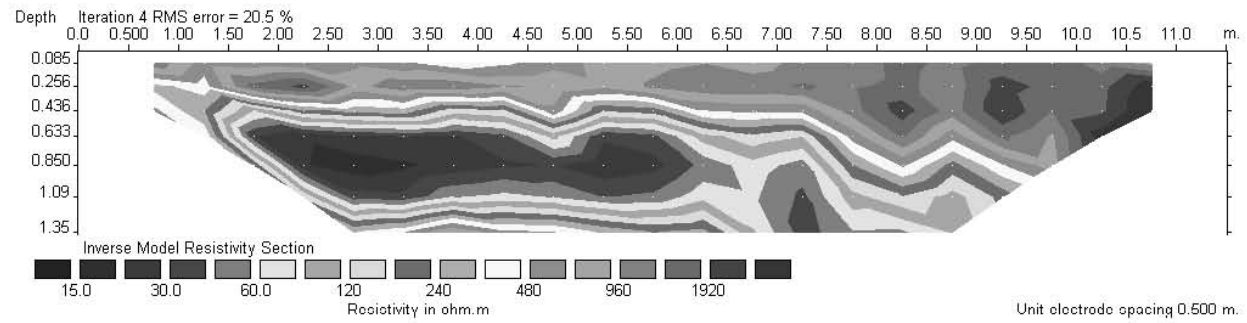

Dipole – dipole 3, Line c, Middleburgh baseline measurements

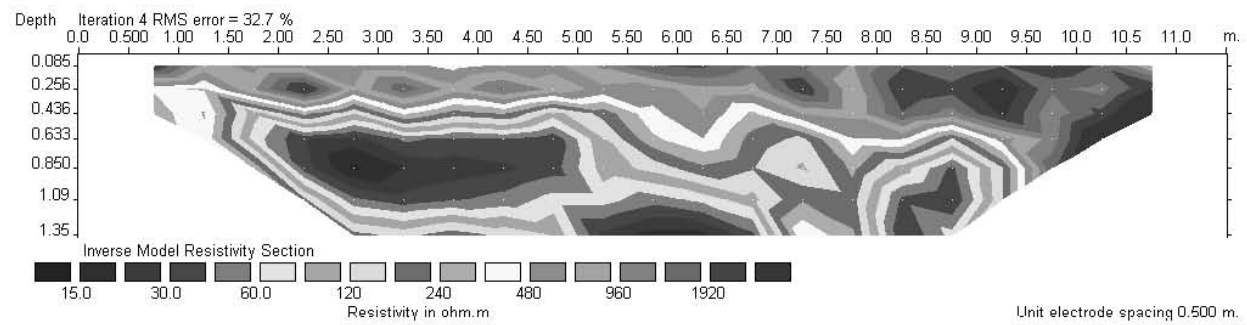

Dipole – dipole 4, Line c, Middleburgh baseline measurements

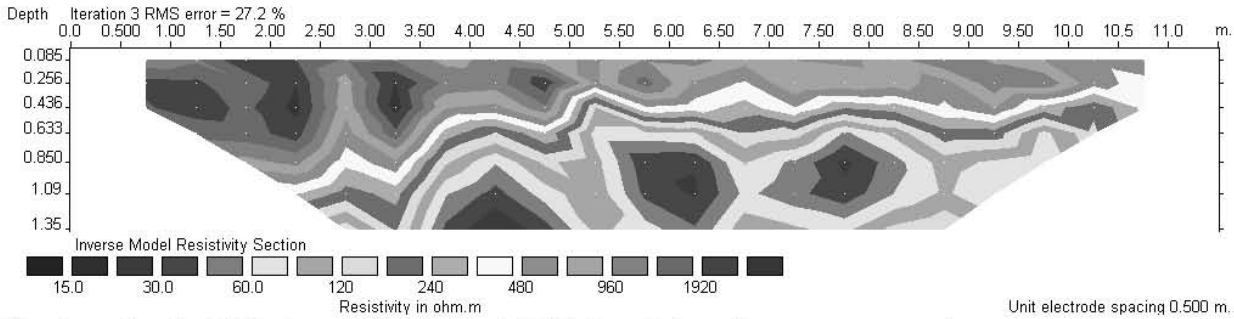

Dipole – dipole 5 (Reciprocal), Line c, Middleburgh baseline measurements

1.10 Middleburgh, line c, inverted resistivity baseline sections (Wenner profiling)

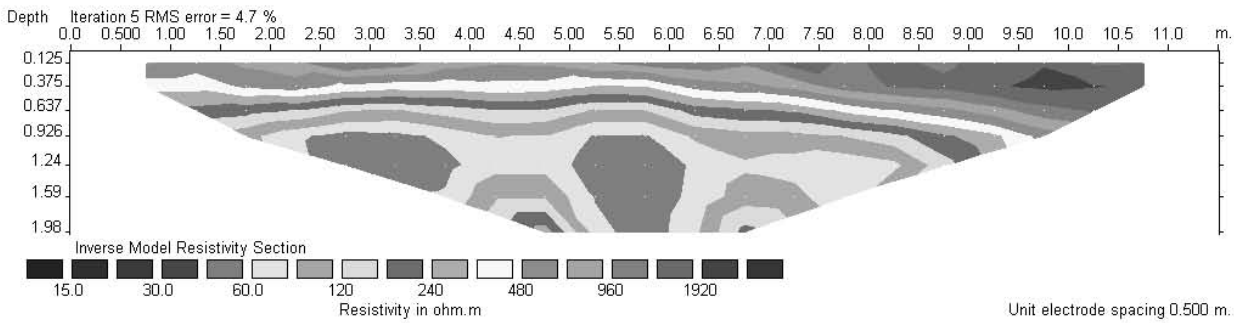

Wenner 1, Line c, Middleburgh baseline measurements

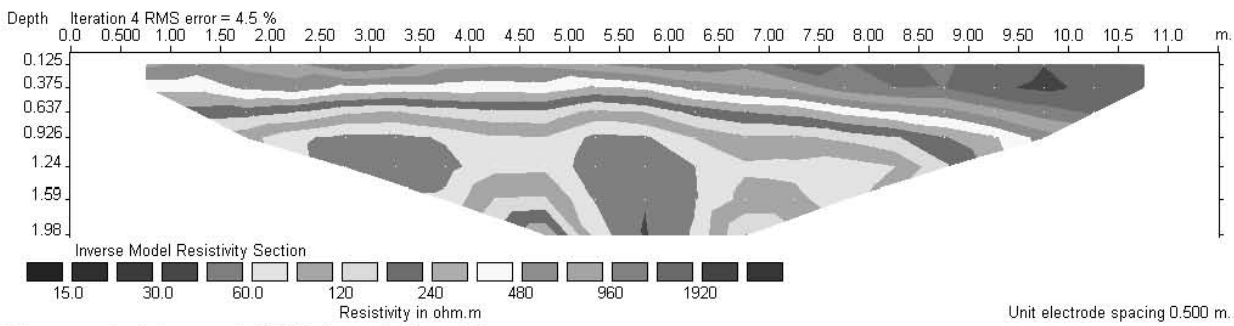

Wenner 2, Line c, Middleburgh baseline measurements

1.11 Middleburgh, line d, inverted resistivity baseline cross sections (Dipole-Dipole)

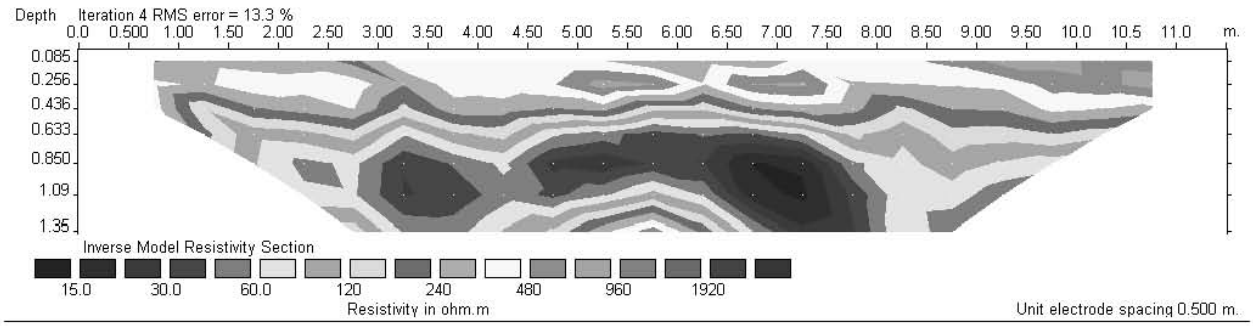

Dipole – dipole 1, Line d, Middleburgh baseline measurements

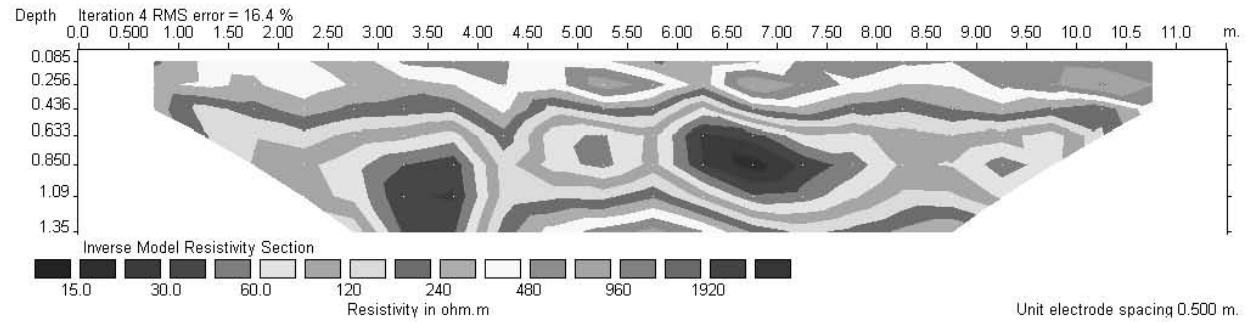

Dipole – dipole 2, Line d, Middleburgh baseline measurements

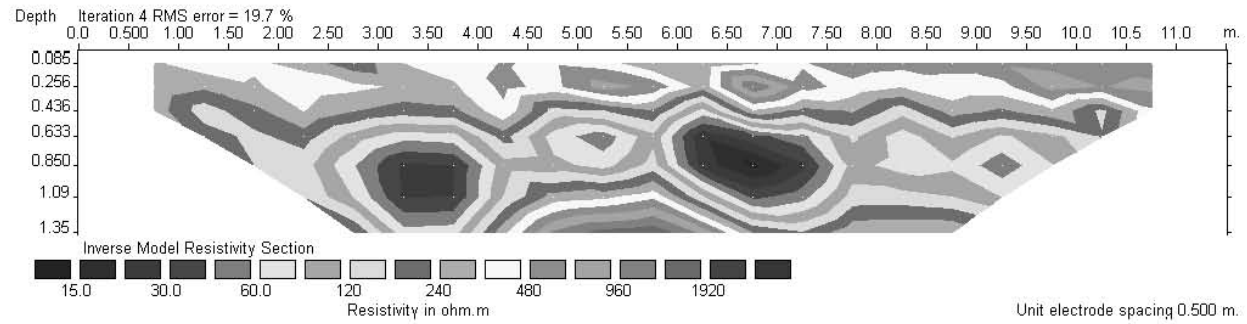

Dipole – dipole 3, Line d, Middleburgh baseline measurements

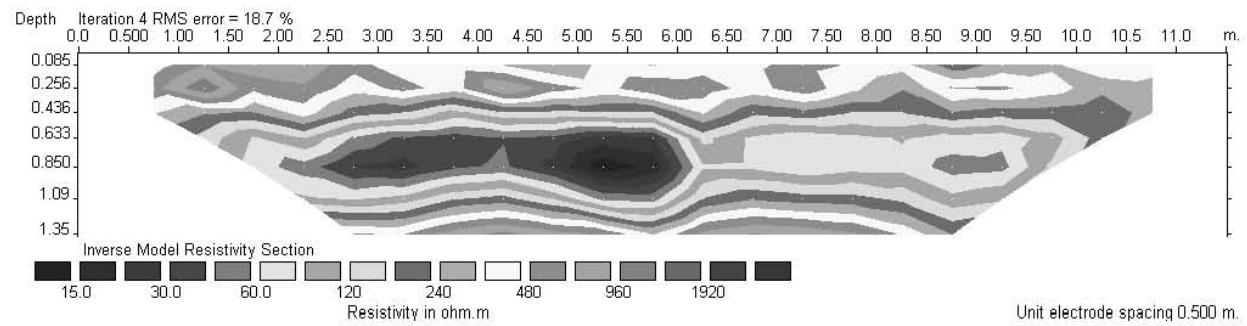

Dipole – dipole 4, Line d, Middleburgh baseline measurements

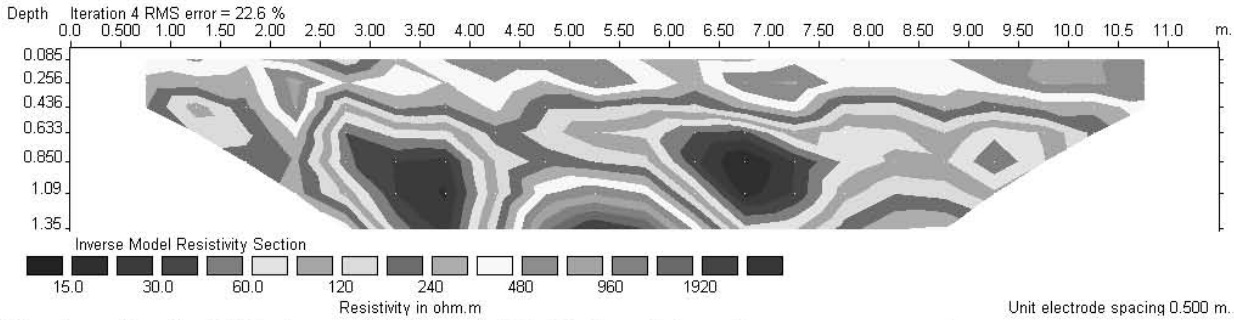

Dipole – dipole 5 (Reciprocal), Line d, Middleburgh baseline measurements

1.12 Middleburgh, line d, inverted resistivity baseline sections (Wenner profiling)

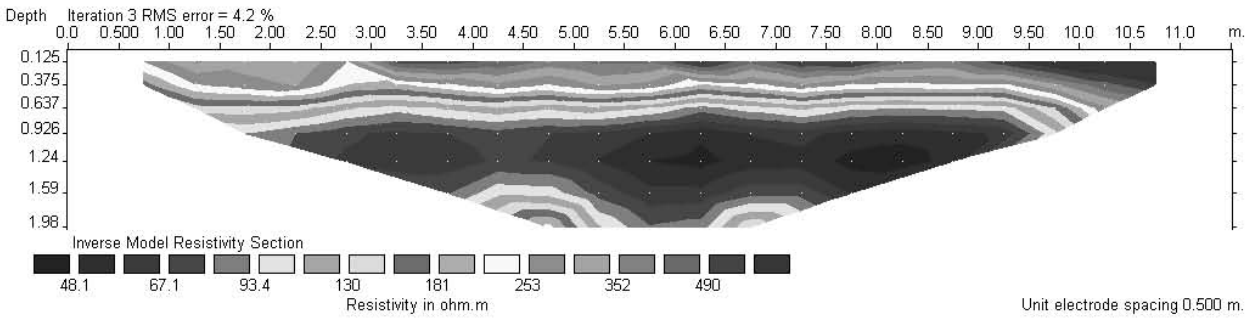

Wenner 1, Line d, Middleburgh baseline measurements

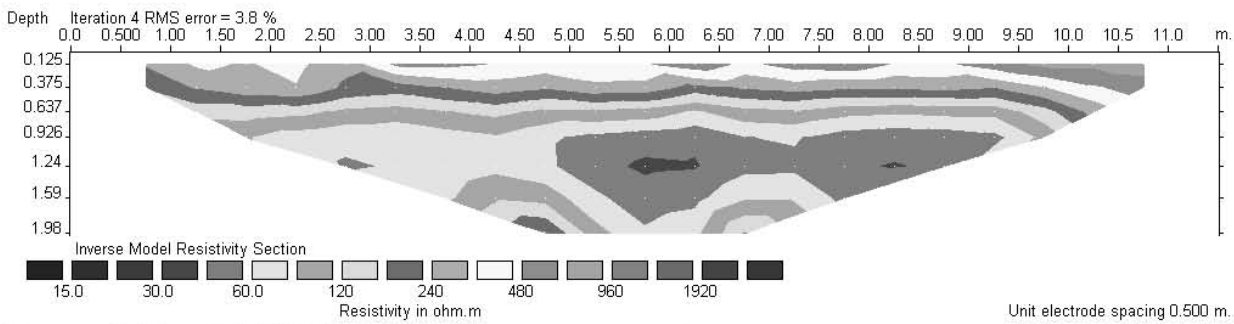

Wenner 2, Line d, Middleburgh baseline measurements

APPENDIX 2

RAW RESISTIVITY DATA

BASELINE & INFILTRATION MEASUREMENTS

The data collection program was divided into a pre-infiltration stage and an infiltration stage. Seven data sets were collected for each site in the pre-infiltration stage. Out of these seven data sets, five were obtained using the dipole-dipole array and two using the Wenner array. There was one measurement from each array type in the induced polarization (IP) mode. The remaining measurements were all conducted in standard mode. One of the five dipole-dipole array measurements was a reciprocal measurement, in which the current and potential electrode pairs are interchanged. During the infiltration stage, data were collected during different time intervals. Only the dipole-dipole array was used during infiltration. Appendix 2 includes all the resistivity data taken for this dissertation. The data are presented in tabular form, starting with the pre-infiltration dipole-dipole and Wenner array data. Finally, the infiltration dipole-dipole array data are also presented in tabular form.

RAW DATA TABLES SYMBOLOGY
(EXCERPTS FROM SYSCAL KID SWITCH-24 OPERATING MANUAL)

Dipole- Dipole

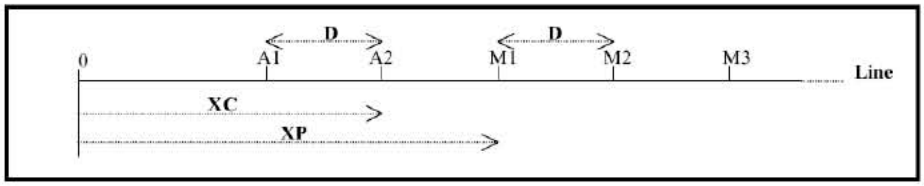

A1, A2: Current electrodes
M1, M2: Potential Electrodes
XC: abscissa of the nearest current electrode from the M1M2 dipole
XP: abscissa of the nearest potential electrode from the A1A2 dipole
D: length of dipoles (current and potential): 0.5 meters

Wenner PRF (Wenner profiling)

Wenner profiling is a restriction of the Sclumberger* profiling: PP=CC/3

- X: abscissa of the centre of P1P2 (Mid) (the direction being C1C2)
- CC/3: a third of the distance between the current electrodes

*Sclumberger PRF (Sclumberger profiling)

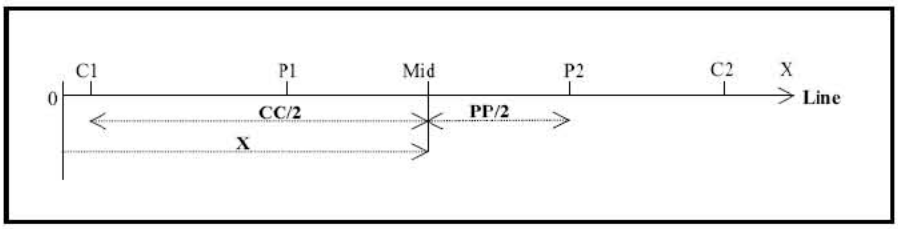

Riverhead	Baselines		Survey 1		Survey 2	Survey 3	Survey 4	Survey 5
Dipole Dipole				Chargeability			Reciprocal	
Data point #	XC	XP	Rho	M	Rho	Rho	Rho	Rho
1	0.50	1.00	567.53	2.38	571.24	575.05	500.23	579.16
2	0.50	1.50	651.67	1.97	652.52	658.37	587.36	657.81
3	0.50	2.00	812.88	2.64	802.81	1000.43	791.36	836.03
4	0.50	2.50	1012.1	3.04	997.56	1085.86	1085.12	988.51
5	0.50	3.00	1019.29	2.49	1009.55	1014.21	1215.97	978.66
6	0.50	3.50	1444.15	3.56	1415.1	1421.71	1389.9	1413.39
7	0.50	4.00	1553.3	1.42	1514.38	1505.47	1740.69	1591.21
8	0.50	4.50	1672.94	2.51	1638.29	1524.02	1693.29	1654.2
9	0.50	5.00	1558.42	3.44	1527.24	1327.74	1966.52	1563.02
10	1.00	1.50	596.26	2.15	592.41	593.52	492.76	594.37
11	1.00	2.00	674.83	2.02	674.29	677.17	631.99	682.52
12	1.00	2.50	882.61	2.33	875.52	881.19	898.73	876.07
13	1.00	3.00	917.8	2.09	913.05	928.66	1012.86	918.99
14	1.00	3.50	1270.85	2.44	1248.37	1286.16	1238.04	1277.37
15	1.00	4.00	1415.39	0.41	1429.53	1456.16	1533.12	1452.42
16	1.00	4.50	1531.68	0.96	1496.65	1533.05	1545.76	1557.3
17	1.00	5.00	1433.54	1.43	1371.81	1350.12	1830.17	1413.22
18	1.00	5.50	1906.26	2.17	1770.99	1658.92	2090.88	1806.08
19	1.50	2.00	595.47	2.72	591.52	594.06	506.08	607.57
20	1.50	2.50	711.22	2.72	710.77	715.86	698.67	720.41
21	1.50	3.00	752.56	1.82	725.61	731.77	817.07	754.71
22	1.50	3.50	1076.26	2.87	1075.81	1093.2	995.08	1093.4
23	1.50	4.00	1259.01	2.47	1250.05	1291.98	1327.33	1282.4
24	1.50	4.50	1357.29	1.39	1365.49	1390.01	1351.12	1364.09
25	1.50	5.00	1276.59	3.33	1252.2	1260.46	1617.46	1300.23
26	1.50	5.50	1629.83	0.62	1638.4	1607.84	2008.51	1613.65
27	1.50	6.00	1630.01	1.56	1757.29	1667.9	1879.83	1672.14
28	2.00	2.50	570.23	3.72	574.75	574.51	536.13	576.12
29	2.00	3.00	595.2	2.32	597.96	601.06	528.29	602.76
30	2.00	3.50	915.08	2.92	901.48	906.5	677.12	917.49
31	2.00	4.00	1115.04	1.65	1122.65	1148.28	923.87	1156.94
32	2.00	4.50	1226.99	1.76	1256.93	1244.9	994.35	1261.4

33	2.00	5.00	1178.05	2.8	1211.12	1199.52	1184.72	1175.83
34	2.00	5.50	1543.44	3.45	1549.53	1535.67	1516.14	1515.83
35	2.00	6.00	1525.99	2.23	1707.86	1662.49	1492.48	1551.46
36	2.00	6.50	1579.59	-0.08	1756.33	1622.44	1864.87	1561.11
37	2.50	3.00	556.9	3.23	568.26	569.23	435.78	568.38
38	2.50	3.50	786.6	2.45	795.56	799.76	497.31	803.75
39	2.50	4.00	1054.06	1.7	1129.3	1125.61	726.03	1073.09
40	2.50	4.50	1217.89	1.18	1498.52	1257.26	819.98	1206.49
41	2.50	5.00	1167.03	2.23	1193.28	1201.22	1016.93	1170.78
42	2.50	5.50	1508.87	0.25	1530.74	1515.54	1322.29	1509
43	2.50	6.00	1572.04	0.75	1640.87	1585.93	1287.44	1610.11
44	2.50	6.50	1646.7	3.83	1750.29	1707.66	1663.48	1624.16
45	2.50	7.00	2001.04	4.02	2155.14	2043.68	1905.17	2016.58
46	3.00	3.50	620.67	3.08	626.86	627.96	432.64	621.9
47	3.00	4.00	819.18	1.48	826.1	834.52	547.58	837.77
48	3.00	4.50	1011.18	1.4	1201.58	1059.35	622.1	1011.31
49	3.00	5.00	1008.55	1.47	1189.92	1019.31	864.08	1017.36
50	3.00	5.50	1335.83	1.36	1417.25	1385.18	1115.21	1342.11
51	3.00	6.00	1429.61	2	1494.74	1447.32	1144.95	1432.08
52	3.00	6.50	1608.26	0.28	1552.92	1519.15	1527.58	1443.91
53	3.00	7.00	1874.17	4.9	1920.54	1931.52	1762.46	1768.63
54	3.00	7.50	2011.78	2.11	2177.62	2063.19	2123.8	1932.73
55	3.50	4.00	496.98	2.04	504.22	506.86	428.95	510.28
56	3.50	4.50	637.3	1.66	642.99	643.83	481.85	646.12
57	3.50	5.00	684.44	2.04	894.46	665.88	647.45	686.7
58	3.50	5.50	931.72	1.98	958.52	941.13	900.61	953.59
59	3.50	6.00	1052.77	2.16	1057.22	1045.69	942.33	1034.34
60	3.50	6.50	1134.2	3.16	1191.36	1146.28	1273.11	1118.64
61	3.50	7.00	1388.58	5.51	1290.63	1376.23	1527.69	1349.51
62	3.50	7.50	1536.82	2.2	1693.28	1523.69	1842.81	1475.47
63	3.50	8.00	1668.19	3.01	1707.18	1648.01	1691.74	1636.96
64	4.00	4.50	568.34	2.13	569.05	569.44	410.04	573.17
65	4.00	5.00	633.19	2.17	634.72	633.87	534.51	636.11
66	4.00	5.50	939.01	2.67	1070.93	960.63	745.24	921.81
67	4.00	6.00	1086.93	2.29	1123.04	1081.96	817.49	1084.92

68	4.00	6.50	1225.73	2.45	1251.08	1211.88	1130.51	1185.57
69	4.00	7.00	1499.31	1.51	1510.45	1470.36	1334.17	1438.1
70	4.00	7.50	1661.51	2.32	1660.14	1635.68	1659.77	1612.28
71	4.00	8.00	1814.63	1.98	1847.92	1833.73	1570.59	1800.65
72	4.00	8.50	2123.83	1.46	2175.45	2131.6	2065.14	2088.93
73	4.50	5.00	453.78	2.29	459.87	460.86	463.76	461.54
74	4.50	5.50	645.94	1.35	653.49	650.96	649.74	666.15
75	4.50	6.00	792.09	1.9	970.84	800.21	718.86	814.11
76	4.50	6.50	921.1	1.12	1161.69	936.61	1000.67	937.72
77	4.50	7.00	1147.72	2.38	1338.75	1166.46	1195.77	1165.37
78	4.50	7.50	1269.22	1.89	1307.84	1309.44	1479.72	1357.68
79	4.50	8.00	1449.75	2.53	1495.41	1464.23	1426.23	1460.92
80	4.50	8.50	1709.34	2.68	1814.58	1749.76	1882.67	1744.3
81	4.50	9.00	1922.54	1.68	1957.18	1888.61	2095.97	1855.17
82	5.00	5.50	536.5	1.69	537.63	537.4	501.74	546.02
83	5.00	6.00	618.18	1.96	630.1	619.98	533.47	623.93
84	5.00	6.50	770.88	1.65	925.72	778.4	783.36	773.94
85	5.00	7.00	981.96	2.02	1205.52	980.36	954.04	981.19
86	5.00	7.50	1103.07	2.07	1366.19	1127.13	1198.18	1089.97
87	5.00	8.00	1250.78	2.19	1456.87	1278.56	1163.12	1270.71
88	5.00	8.50	1500.72	2.35	1685.4	1559.89	1538.09	1530.34
89	5.00	9.00	1673.5	2.29	1838.19	1656.8	1757.92	1653.49
90	5.00	9.50	1839.37	1.3	1954.97	1855.9	1687.97	1905.68
91	5.50	6.00	429.99	2.31	428.23	428.63	431.16	434.72
92	5.50	6.50	528.66	1.57	520.82	533.9	616.55	533.26
93	5.50	7.00	700.46	2.31	843.63	703.54	816.62	708.44
94	5.50	7.50	816.35	1.62	1006.64	824.8	1074.62	817.53
95	5.50	8.00	935.37	1.83	995.32	924.17	1062.25	948.26
96	5.50	8.50	1138.71	0.88	1245.85	1152.65	1450.51	1183.22
97	5.50	9.00	1297.2	1.57	1342.83	1277.48	1647.54	1286.12
98	5.50	9.50	1481.3	1.32	1576.48	1469.88	1661.54	1467.15
99	5.50	10.00	1943.31	0.67	2038.55	1881.66	1808.38	1935.37
100	6.00	6.50	494.95	2.4	494.51	498.25	539.62	498.53
101	6.00	7.00	640.08	2.48	642.54	644.76	660.14	648.02
102	6.00	7.50	775.04	1.75	902.09	774.66	931.54	765.95

103	6.00	8.00	892	1.79	1069.93	908.8	1004.2	895.19
104	6.00	8.50	1114.03	1.79	1252.94	1171.24	1343.9	1139.04
105	6.00	9.00	1275.9	1.65	1468.69	1357.88	1566.25	1295.21
106	6.00	9.50	1505.39	1.11	1727.21	1536.32	1548.56	1485.78
107	6.00	10.00	1946.22	1.15	2241.35	2021.26	1607.27	1968.2
108	6.00	10.50	2090.07	1.57	2572.55	2101.85	1840.47	2114.72
109	6.50	7.00	457.29	3.07	460.83	462.9	465.14	463.84
110	6.50	7.50	531.34	2.08	537.27	535.95	628.14	535.98
111	6.50	8.00	647.56	1.87	757.82	632.24	667.84	646.63
112	6.50	8.50	853.5	2.39	745.09	850.93	1039.88	856.35
113	6.50	9.00	1010.19	1.91	1007.03	1022.92	1180.55	1021.12
114	6.50	9.50	1164.3	1.33	1166.03	1201.72	1171.31	1202.54
115	6.50	10.00	1593.73	2.49	1728.33	1620.29	1264.85	1648.11
116	6.50	10.50	1770.4	2.61	1875.12	1754.04	1440.17	1777.02
117	6.50	11.00	2003.92	1.23	1944.45	1865.76	1460.82	1901.76
118	7.00	7.50	420.47	2.46	419.46	421.36	566.31	420.38
119	7.00	8.00	474.74	1.92	478.04	478.68	646.2	479.82
120	7.00	8.50	645.61	1.54	878.19	622.61	1016.89	644.36
121	7.00	9.00	803.68	1.81	863.12	815.39	1227.38	807.28
122	7.00	9.50	982.97	1.22	1014.52	1021.03	1244.94	986.02
123	7.00	10.00	1366.83	1.81	1398.89	1362.02	1353.57	1396.62
124	7.00	10.50	1507.45	1.15	1610.49	1526.36	1504.64	1579.58
125	7.00	11.00	1707.23	1.96	1709.75	1710.52	1600.45	1674.06
126	7.50	8.00	424.44	2.6	423.86	430.76	510.6	432.36
127	7.50	8.50	546.54	1.33	549.89	551.51	834.3	554.16
128	7.50	9.00	709.22	1.53	791.93	720.03	1084.37	715.57
129	7.50	9.50	941.91	1.02	927.94	933.29	1141.88	936.01
130	7.50	10.00	1323.17	2.05	1363.02	1317.04	1254.93	1350.14
131	7.50	10.50	1529.96	1.04	1549.53	1481.9	1432.07	1539.23
132	7.50	11.00	1699.33	0.86	1826.04	1680.52	1560.4	1750.72
133	8.00	8.50	426.04	1.77	429.75	432.7	627.95	433.07
134	8.00	9.00	489.63	1.85	496.38	495.09	795.94	499
135	8.00	9.50	675.3	1.21	729.38	674.26	912.81	658.81
136	8.00	10.00	1011.2	1.93	1004.37	995.67	1088.58	1007.73
137	8.00	10.50	1192.93	1.83	1230.73	1220.06	1275.24	1209

138	8.00	11.00	1385.89	1.15	1441.02	1402.5	1404.39	1406.07
139	8.50	9.00	434.8	2.82	432.65	434.96	561.97	438.28
140	8.50	9.50	522.31	1.27	526.65	528.99	597.62	529.07
141	8.50	10.00	810.21	1.69	827.37	801.6	756.77	815
142	8.50	10.50	986.85	1.62	1009.51	1006.63	909.81	1019.54
143	8.50	11.00	1185.94	1.19	1214.05	1206.13	990.87	1225.49
144	9.00	9.50	527.84	1.42	530.67	537.64	572.5	537.98
145	9.00	10.00	696.67	1.94	698.24	696.9	714.58	699.81
146	9.00	10.50	889.95	1.11	903.13	898.28	882.8	908.1
147	9.00	11.00	1089.91	0.89	1118.34	1099.41	988.56	1105.74
148	9.50	10.00	501.05	2.36	502.65	504.31	598.03	511.58
149	9.50	10.50	630.21	1.49	626.09	629.22	682.01	635.92
150	9.50	11.00	807.75	1.02	841.7	804.54	808.36	803.82
151	10.00	10.50	483.57	1.98	491.38	492.37	593.83	497.44
152	10.00	11.00	579.28	1.22	583.83	585.9	658.81	586.87
153	10.50	11.00	495.23	1.38	499.5	497.71	582.19	502.65

Riverhead			Survey 6		Survey 7
Wenner PRF				Chargeability	
Data point #	X	CC/3	Rho	M	Rho
1	0.75	0.5	704.09	2.51	701.43
2	1.5	1	1071.87	2.28	1066.99
3	2.25	1.5	1636.09	3.03	1610.78
4	3	2	2064.29	2.65	2070.48
5	3.75	2.5	2486.52	3.29	2444.16
6	4.5	3	2819.89	3.21	2807.43
7	5.25	3.5	3191.99	3.67	3170.2
8	1.25	0.5	719.44	2.53	716.95
9	2	1	1166.46	2.51	1162.77
10	2.75	1.5	1550.42	3.21	1544.44
11	3.5	2	2022.73	3	2026.68
12	4.25	2.5	2333.34	3.06	2355.91
13	5	3	2817.32	3.32	2841.68
14	5.75	3.5	3106.06	3.52	3095.08
15	1.75	0.5	714.08	2.57	724.3
16	2.5	1	1220.5	2.48	1203.77
17	3.25	1.5	1612.31	3.06	1579.1
18	4	2	2008.1	2.99	2003.13
19	4.75	2.5	2423.41	3.05	2426.5
20	5.5	3	2714.59	3.37	2716.54
21	6.25	3.5	3066.33	3.51	3087.56
22	2.25	0.5	749.61	2.48	756.13
23	3	1	1110.52	2.38	1105.17
24	3.75	1.5	1543.87	3.16	1543.12
25	4.5	2	1971.77	2.85	1952.92
26	5.25	2.5	2372.48	2.95	2371.85
27	6	3	2727.15	3.25	2664.59
28	2.75	0.5	771.65	2.62	776.98
29	3.5	1	1077.03	2.31	1081.29
30	4.25	1.5	1601.38	3.11	1594.6
31	5	2	1946.59	2.74	1950.98
32	5.75	2.5	2297.06	2.99	2295.18
33	6.5	3	2689.55	3.13	2666
34	3.25	0.5	664.61	2.46	665.52
35	4	1	1198.16	2.57	1192.88
36	4.75	1.5	1537.09	2.87	1545.76

37	5.5	2	1938.99	2.67	1901.51
38	6.25	2.5	2333.66	2.99	2334.78
39	7	3	2726.98	3.28	2772.09
40	3.75	0.5	765.1	2.52	767.33
41	4.5	1	1167.15	2.25	1166.94
42	5.25	1.5	1526.28	2.72	1514.52
43	6	2	1877.73	2.72	1849.88
44	6.75	2.5	2370.28	2.93	2379.88
45	4.25	0.5	687.67	2.49	685.03
46	5	1	1044.18	2.06	1041.85
47	5.75	1.5	1458.16	3.02	1450.23
48	6.5	2	1949.59	2.71	1938.41
49	7.25	2.5	2349.34	2.99	2310.5
50	4.75	0.5	704.77	2.03	706.73
51	5.5	1	1050.87	2.16	1053.04
52	6.25	1.5	1483.23	2.87	1486.12
53	7	2	1939.8	2.81	1958.34
54	7.75	2.5	2399.5	3.01	2370.13
55	5.25	0.5	589.37	2.16	598.04
56	6	1	1043.43	2.32	1053.23
57	6.75	1.5	1487.44	3.01	1465.62
58	7.5	2	1953.07	2.7	1958.66
59	5.75	0.5	681.5	2.02	684.35
60	6.5	1	998.38	1.99	1002.55
61	7.25	1.5	1498.4	2.95	1508.36
62	8	2	1999.24	2.71	1980.2
63	6.25	0.5	604.66	2.33	602.24
64	7	1	1002.09	2.14	1009.26
65	7.75	1.5	1519.42	2.91	1510.9
66	8.5	2	1974.27	2.67	1960.06
67	6.75	0.5	591.22	2.06	591.9
68	7.5	1	1041.39	2.18	1052.08
69	8.25	1.5	1528.4	2.94	1535.59
70	7.25	0.5	615.68	2.28	615.65
71	8	1	1012.94	2.32	997.86
72	8.75	1.5	1531.04	2.69	1524.67
73	7.75	0.5	578.58	2.25	581.09
74	8.5	1	1061.48	2.04	1051.1
75	9.25	1.5	1481.81	3.27	1486.72
76	8.25	0.5	578.83	2.1	587.65
77	9	1	1055.78	2.12	1056.92
78	8.75	0.5	648.3	2.07	651.3
79	9.5	1	1016.7	1.9	1012.05
80	9.25	0.5	620.82	1.96	624.75
81	10	1	1077.86	2.13	1062.28
82	9.75	0.5	642.23	1.95	645.79
83	10.25	0.5	690.11	2.25	680.59
84	10.75	0.5	645.27	2.24	646.03

Riverhead	Infiltration		Survey 1	Survey 2	Survey 3	Survey 4
Dipole Dipole						
Data point #	XC	XP	Rho	Rho	Rho	Rho
1	0.50	1.00	595.78	604.18	602.66	602.6
2	0.50	1.50	696.39	700.91	697.18	711.02
3	0.50	2.00	857.17	870.96	899.42	897
4	0.50	2.50	1087.69	991	878.09	854.69
5	0.50	3.00	1073.96	1130.29	1101.36	1092.41
6	0.50	3.50	1525.27	1557.28	1547.05	1552.05
7	0.50	4.00	1729.93	1730.53	1687.81	1689.07
8	0.50	4.50	2068.75	1997	1772.78	1777.31
9	0.50	5.00	1522.68	1614.63	1679.06	1728.61
10	1.00	1.50	602.25	605.52	614.71	614.5
11	1.00	2.00	701.57	722.5	741.57	743.41
12	1.00	2.50	936.15	853.5	768.83	748.61
13	1.00	3.00	947.67	973.42	943.72	929.28
14	1.00	3.50	1310.79	1336.74	1350.05	1365.81
15	1.00	4.00	1518.84	1501.54	1556.5	1557.08
16	1.00	4.50	1834.53	1585.43	1621.32	1640.38
17	1.00	5.00	1429.98	1504.65	1512.65	1520.09
18	1.00	5.50	1630.96	1889.04	1844.48	1900.18
19	1.50	2.00	608.36	624.02	638.55	631.18
20	1.50	2.50	759.57	683.55	626.49	601.52
21	1.50	3.00	777.98	797.82	785.56	746.97
22	1.50	3.50	1142.31	1139.16	1171.59	1175.44
23	1.50	4.00	1335.92	1338.7	1362.01	1362.21
24	1.50	4.50	1446.59	1470.21	1493.9	1453.01
25	1.50	5.00	1349.32	1333.12	1341.51	1349.1
26	1.50	5.50	1692.25	1647.69	1644.19	1719.97
27	1.50	6.00	1611.31	1778.97	1669.3	1777.55
28	2.00	2.50	602.08	553.35	507.09	490.44
29	2.00	3.00	624.23	636.5	622.63	615.48
30	2.00	3.50	948.84	995.62	994.43	1008.18
31	2.00	4.00	1178.31	1215.47	1238.71	1232.49
32	2.00	4.50	1331.36	1368.74	1394.97	1362.62

33	2.00	5.00	1239.11	1247.48	1271.16	1292.85
34	2.00	5.50	1535.88	1380.43	1633.7	1413.64
35	2.00	6.00	1614.72	1595.86	1669.48	1609.69
36	2.00	6.50	1609.23	1661.89	1751.28	1615.24
37	2.50	3.00	568.22	549.76	527.93	508.52
38	2.50	3.50	824.68	855.55	850.92	845.97
39	2.50	4.00	1117.92	1152.56	1146.81	1122.2
40	2.50	4.50	1282.15	1300.87	1309.88	1351.93
41	2.50	5.00	1159.9	1276.62	1262.61	1263.91
42	2.50	5.50	1364.78	1614.19	1580.71	1615.88
43	2.50	6.00	1531.83	1741.66	1708.6	1729.75
44	2.50	6.50	1592.05	1799.77	1787.6	1757.34
45	2.50	7.00	1953.27	2201.16	2330.85	2137.35
46	3.00	3.50	653.14	533.31	520.48	503.14
47	3.00	4.00	876.37	716.03	687.18	672.42
48	3.00	4.50	1104.23	880.69	862.5	821.25
49	3.00	5.00	1050.13	887.64	839.21	814.47
50	3.00	5.50	1241.58	1142.31	1083.33	1076.97
51	3.00	6.00	1393.13	1251.41	1178.85	1157.94
52	3.00	6.50	1551.22	1313.34	1243.18	1214.54
53	3.00	7.00	1933.89	1560.99	1532.67	1431.9
54	3.00	7.50	2074.38	1795.42	1705	1670.46
55	3.50	4.00	515.23	536.4	539.89	542.5
56	3.50	4.50	664.44	708.92	712.88	720.74
57	3.50	5.00	725.47	771.16	769.95	750.05
58	3.50	5.50	969.41	1025.37	1030.34	1009.65
59	3.50	6.00	1086.07	1184.92	1155.17	1136.4
60	3.50	6.50	1208.58	1229.63	1228.02	1200.39
61	3.50	7.00	1406.16	1479.79	1497.31	1442.04
62	3.50	7.50	1556.9	1709.73	1688.83	1653.28
63	3.50	8.00	1690.89	1823.57	1787.34	1668.15
64	4.00	4.50	580.73	586.33	590.23	594.64
65	4.00	5.00	665.34	676.81	676.6	681.24
66	4.00	5.50	965.08	972.66	980.1	979.08
67	4.00	6.00	1137.08	1145.24	1151.44	1166.28

68	4.00	6.50	1246.54	1256.81	1278.86	1296.49
69	4.00	7.00	1514.22	1570.1	1547.01	1570
70	4.00	7.50	1701.92	1764.46	1814.35	1770.41
71	4.00	8.00	1845.46	1860.58	1872.87	1899.04
72	4.00	8.50	2138.31	1667.86	1683.26	1587.96
73	4.50	5.00	479.93	479.49	482.77	486.09
74	4.50	5.50	668.63	673.09	675.42	682.5
75	4.50	6.00	836.18	844.16	841.38	848.65
76	4.50	6.50	941.4	980.75	996.96	964.32
77	4.50	7.00	1209.35	1208.2	1218.72	1226.2
78	4.50	7.50	1330.32	1404.26	1421.62	1453.74
79	4.50	8.00	1504.09	1558.97	1575.86	1523.89
80	4.50	8.50	1806.14	1384.45	1306.98	1271.31
81	4.50	9.00	1964.75	1942.11	1956.6	1835.63
82	5.00	5.50	546.37	548.43	554.58	549.93
83	5.00	6.00	657.91	661.46	667.19	672.14
84	5.00	6.50	793.7	811.52	815.72	816.08
85	5.00	7.00	1023.02	1058.95	1027.71	1009.96
86	5.00	7.50	1160.26	1200.81	1187.99	1208.25
87	5.00	8.00	1296.21	1326.06	1342.58	1298
88	5.00	8.50	1563.63	1139.3	1158.47	1102.28
89	5.00	9.00	1724.91	1696.5	1733.04	1616.8
90	5.00	9.50	1950.28	2042.55	2069.41	2201.46
91	5.50	6.00	450.46	453.81	454.21	457.55
92	5.50	6.50	558.83	559.92	565.51	565.7
93	5.50	7.00	738.08	738.5	740.03	741.64
94	5.50	7.50	857.85	897.07	889.3	901.89
95	5.50	8.00	965.38	1018.39	1008.51	978.64
96	5.50	8.50	1199.18	928.38	922.05	835.41
97	5.50	9.00	1346.1	1361.66	1342.07	1257.02
98	5.50	9.50	1545.37	1642.31	1658.96	1568.13
99	5.50	10.00	2048.78	2131.44	2196.98	2038.87
100	6.00	6.50	495.83	506.23	505.71	506.65
101	6.00	7.00	653.4	665.75	668.29	661.77
102	6.00	7.50	789.27	821.64	824.21	801.05

103	6.00	8.00	905.02	973.62	942.54	929.65
104	6.00	8.50	1142.69	887	856.72	834.39
105	6.00	9.00	1322.02	1316.68	1348.19	1238.85
106	6.00	9.50	1517.67	1586.35	1680.08	1627.49
107	6.00	10.00	2062.28	2142.84	2246.05	2116.52
108	6.00	10.50	2241.14	2256.12	2423.88	2297.9
109	6.50	7.00	475.86	470.96	477.22	481.58
110	6.50	7.50	561.15	576.31	584.03	588.54
111	6.50	8.00	689.61	712.67	708.08	706.31
112	6.50	8.50	896.45	689.84	666.67	651.8
113	6.50	9.00	1071.52	1062.2	1045.97	997.05
114	6.50	9.50	1241.11	1331.68	1330.37	1349.95
115	6.50	10.00	1727.99	1778.59	1751.24	1790.12
116	6.50	10.50	1904.25	1915.09	1950.87	1962.34
117	6.50	11.00	2022.42	2076.65	2119.11	2149.75
118	7.00	7.50	426.18	445.72	435.96	433.05
119	7.00	8.00	498.05	511.05	514.09	514.82
120	7.00	8.50	679.99	527.69	496.68	494.08
121	7.00	9.00	845.86	834.74	825.88	782.23
122	7.00	9.50	1025.19	1081.9	1097.96	1111.57
123	7.00	10.00	1393.6	1491.36	1516.24	1518.59
124	7.00	10.50	1613.65	1646.85	1667.85	1686.29
125	7.00	11.00	1772.83	1764.64	1830.67	1849.94
126	7.50	8.00	436.08	444.08	440.29	443.17
127	7.50	8.50	570.37	440.46	430.71	410.9
128	7.50	9.00	746.77	739.93	725.57	686.95
129	7.50	9.50	958.98	1006	1018.83	1044.82
130	7.50	10.00	1391.61	1437.12	1439.08	1452.55
131	7.50	10.50	1581.89	1611.54	1652.28	1667.61
132	7.50	11.00	1783.41	1836.18	1829.89	1861.42
133	8.00	8.50	450.62	347.38	336.57	323.45
134	8.00	9.00	517.87	535.19	524.4	496.16
135	8.00	9.50	697.75	773.86	779.71	797.76
136	8.00	10.00	1037.58	1141.17	1151.21	1174.3
137	8.00	10.50	1263.69	1376.34	1424.67	1415.74

138	8.00	11.00	1446.79	1567.78	1552.21	1600.02
139	8.50	9.00	456.42	367.77	353.65	328.16
140	8.50	9.50	550.2	543.91	536.64	536.79
141	8.50	10.00	869.18	822.29	827.39	820.14
142	8.50	10.50	1066.43	1083.72	1062.4	1040.44
143	8.50	11.00	1277.28	1252.14	1208.31	1213.87
144	9.00	9.50	548.62	419.68	405.39	385.22
145	9.00	10.00	729.56	568.92	552.79	528.7
146	9.00	10.50	958.83	726.68	705.78	676.75
147	9.00	11.00	1144.88	890.57	856.59	836.56
148	9.50	10.00	528.28	541.25	546.12	540.77
149	9.50	10.50	663.2	681.77	681.68	660.94
150	9.50	11.00	840.46	866.43	863.72	839.84
151	10.00	10.50	508.38	512.86	515.76	527.4
152	10.00	11.00	605.63	619.2	621.59	636.05
153	10.50	11.00	523.19	513.66	526.68	532.6

Riverhead	nfiltration		Survey 5	Survey 6	Survey 7	Survey 8
Dipole Dipole						
Data point #	XC	XP	Rho	Rho	Rho	Rho
1	0.50	1.00	605.49	608.44	603.49	600.58
2	0.50	1.50	713.5	716.23	719.49	725.28
3	0.50	2.00	895.86	894.03	859.9	882.41
4	0.50	2.50	839.01	831.43	821.7	872.54
5	0.50	3.00	1075.79	1051.17	1038.16	1022.26
6	0.50	3.50	1590.33	1581.95	1612.81	1630.89
7	0.50	4.00	1700.43	1698.31	1667.4	1770.33
8	0.50	4.50	1775.91	1740.26	1795.34	1843.24
9	0.50	5.00	1636.66	1631.74	1667.4	1735.56
10	1.00	1.50	622.99	622.55	626.28	620.21
11	1.00	2.00	742.03	742.59	756.5	728.85
12	1.00	2.50	730.8	722.45	708.63	763.62
13	1.00	3.00	901.48	900	889.19	871.58
14	1.00	3.50	1383.48	1379.11	1385.5	1411.42
15	1.00	4.00	1534.38	1536.48	1543.01	1590.56
16	1.00	4.50	1608.9	1601.89	1650.24	1650.98
17	1.00	5.00	1537.09	1522.68	1536.11	1591.47
18	1.00	5.50	1851.25	1881.07	1915.62	1988.52
19	1.50	2.00	640.85	638.91	626.91	619.98
20	1.50	2.50	593.14	591.17	599.49	609.46
21	1.50	3.00	746.84	742.18	740.66	718.9
22	1.50	3.50	1204.5	1200.16	1181.48	1227.63
23	1.50	4.00	1363.83	1365.01	1393.13	1406.31
24	1.50	4.50	1446.67	1461.6	1473.98	1478.27
25	1.50	5.00	1365.72	1369.82	1416.68	1389.35
26	1.50	5.50	1709.15	1737.15	1750.26	1785.16
27	1.50	6.00	1739.75	1783.97	1958.21	1943.43
28	2.00	2.50	478.79	481.28	470.82	492.96
29	2.00	3.00	596.38	595.55	582.68	573.1
30	2.00	3.50	1017.57	1012.76	1027.05	1044.63
31	2.00	4.00	1220.09	1243.98	1270.92	1265.17
32	2.00	4.50	1357.42	1363.86	1366.38	1369.53

33	2.00	5.00	1293.59	1305.29	1228.48	1330.37
34	2.00	5.50	1629.25	1638.27	1649.51	1698.1
35	2.00	6.00	1698.48	1784.74	1748.45	1763.46
36	2.00	6.50	1740.84	1769.89	1842.86	1836.63
37	2.50	3.00	486.34	470.36	456.24	450.27
38	2.50	3.50	833.75	822.85	805.96	798.65
39	2.50	4.00	1107.55	1077.47	1082.9	1082.58
40	2.50	4.50	1240.91	1262.27	1243.8	1216.84
41	2.50	5.00	1236.91	1237.74	1219.86	1202.57
42	2.50	5.50	1566.85	1591.99	1562.28	1554.3
43	2.50	6.00	1718.48	1657.14	1675.32	1608.47
44	2.50	6.50	1771.02	1699.24	1759.36	1720.17
45	2.50	7.00	2083.79	2128.95	2079.08	2114.63
46	3.00	3.50	496.58	503.75	490.75	526.18
47	3.00	4.00	668	670.37	667.73	707.26
48	3.00	4.50	809.87	811.82	807.64	854.14
49	3.00	5.00	816.48	822.26	808.17	874.62
50	3.00	5.50	1050.36	1037.42	1062.87	1126.95
51	3.00	6.00	1149.4	1137.87	1158.65	1252.01
52	3.00	6.50	1218.55	1189.16	1238.36	1304.71
53	3.00	7.00	1417.36	1449.11	1459.22	1634.15
54	3.00	7.50	1633.31	1651.03	1676.25	1674.05
55	3.50	4.00	533.38	534.92	528.18	520.55
56	3.50	4.50	704.04	699.17	675.16	670.09
57	3.50	5.00	766.89	753.17	735.9	725.92
58	3.50	5.50	1009.32	1015.69	993.41	974.4
59	3.50	6.00	1132.36	1104.69	1108.69	1087.5
60	3.50	6.50	1175.71	1205.35	1210.58	1126.34
61	3.50	7.00	1487.02	1450.28	1453.65	1400.56
62	3.50	7.50	1709.42	1689.45	1731.91	1601.44
63	3.50	8.00	1660.07	1593.63	1636.8	1505.33
64	4.00	4.50	597.83	606.9	593.21	600.15
65	4.00	5.00	685.41	691.77	696.79	703.06
66	4.00	5.50	982.31	988.36	994.65	1012.05
67	4.00	6.00	1180.44	1176.14	1184.24	1188.9

68	4.00	6.50	1297.98	1312.6	1309.01	1332.7
69	4.00	7.00	1583.12	1609.92	1611.53	1624.98
70	4.00	7.50	1807	1846.97	1885.11	1897.2
71	4.00	8.00	1895.48	1786.5	1822.48	1850.3
72	4.00	8.50	1558.66	1581.69	1635.72	1687.29
73	4.50	5.00	489.17	485.84	489.49	492.44
74	4.50	5.50	681.48	685.27	691	699.39
75	4.50	6.00	849.68	856.72	854.59	870.1
76	4.50	6.50	991.66	1000.64	1008.09	1020.61
77	4.50	7.00	1231.41	1250.73	1247.86	1294.12
78	4.50	7.50	1458.12	1431.18	1493.23	1498.68
79	4.50	8.00	1500.6	1476.87	1461.78	1434.68
80	4.50	8.50	1245.27	1305.65	1281.18	1321.81
81	4.50	9.00	1784.89	1801.09	1703.96	1776.63
82	5.00	5.50	559.73	568.83	559.47	561.49
83	5.00	6.00	674.4	670.3	665.9	664.69
84	5.00	6.50	819.81	817.42	825.83	830.56
85	5.00	7.00	1038.47	1054.49	1043.81	1019.81
86	5.00	7.50	1223.1	1240.61	1215	1244.47
87	5.00	8.00	1284.95	1276.32	1205.42	1238.46
88	5.00	8.50	1053.89	1188.71	1070.32	1189.06
89	5.00	9.00	1643.31	1580.5	1620.48	1487.37
90	5.00	9.50	2093.62	2163.79	2157.37	2235.9
91	5.50	6.00	454.14	464.23	457.04	456.51
92	5.50	6.50	576.47	577.32	576.81	570.75
93	5.50	7.00	750.02	750.7	753.65	790.24
94	5.50	7.50	898.01	900.54	906.94	918.06
95	5.50	8.00	961.12	947.64	916.32	932.91
96	5.50	8.50	832.23	852.39	887.38	879.68
97	5.50	9.00	1233.56	1195.77	1175.82	1217.28
98	5.50	9.50	1670.92	1664.11	1661.68	1694.17
99	5.50	10.00	2130.48	2153.4	2094.4	2142.29
100	6.00	6.50	518.25	514.04	511.64	514.33
101	6.00	7.00	668.09	667.96	674.93	675.86
102	6.00	7.50	824.48	835.63	836.28	844.84

103	6.00	8.00	916.25	905.62	876.36	871.36
104	6.00	8.50	799.69	803.38	840.09	869.96
105	6.00	9.00	1190.53	1180.3	1146.1	1182.71
106	6.00	9.50	1632.64	1639.01	1676.5	1704.7
107	6.00	10.00	2099	2160.39	2170.05	2211.85
108	6.00	10.50	2285.54	2304.97	2325.53	2331.9
109	6.50	7.00	480.64	478.1	476.52	479.77
110	6.50	7.50	593.68	588.7	587.16	591.42
111	6.50	8.00	685.37	676.41	661.96	661.47
112	6.50	8.50	627.99	620.44	654.32	679.67
113	6.50	9.00	962.08	940.34	930.06	920.93
114	6.50	9.50	1371.61	1397.39	1371.54	1392.25
115	6.50	10.00	1820.82	1828.64	1851.53	1870.33
116	6.50	10.50	1976.63	1970.87	1970.5	2017.81
117	6.50	11.00	2153.99	2128.02	2183.67	2167.54
118	7.00	7.50	442.14	444.41	443.77	441.05
119	7.00	8.00	498.72	498	485.13	477.56
120	7.00	8.50	482.35	467.5	499.07	514.31
121	7.00	9.00	768.27	748.74	736.87	727.22
122	7.00	9.50	1115.7	1145.5	1127.84	1143.99
123	7.00	10.00	1516.07	1554.22	1572.31	1523.59
124	7.00	10.50	1719.39	1687.99	1723.67	1732.73
125	7.00	11.00	1839.7	1851.56	1895.4	1891.22
126	7.50	8.00	439.48	437.35	429.13	427.02
127	7.50	8.50	402.59	393.23	424.15	437.57
128	7.50	9.00	667.38	659.9	645.88	653.04
129	7.50	9.50	1039.64	1055.93	1056.96	1071.84
130	7.50	10.00	1468.45	1489.62	1499.54	1508.77
131	7.50	10.50	1709.12	1737.02	1706.71	1729.23
132	7.50	11.00	1905.16	1897.06	1900.74	1915.8
133	8.00	8.50	309.01	304.99	320.62	332.81
134	8.00	9.00	478.91	469.91	455.39	456.2
135	8.00	9.50	810.58	808.23	797	806.97
136	8.00	10.00	1191.57	1195.05	1183.56	1195.3
137	8.00	10.50	1428.31	1437.14	1441.4	1433.43

138	8.00	11.00	1644.04	1643.38	1629.32	1631.5
139	8.50	9.00	306.8	295.69	303.36	304.74
140	8.50	9.50	507.83	485.98	492.25	496.11
141	8.50	10.00	784.59	767.94	752.8	756.11
142	8.50	10.50	987.93	970.11	953.02	949.28
143	8.50	11.00	1181.47	1154.63	1121.47	1105.98
144	9.00	9.50	374.77	365.85	390.3	398.09
145	9.00	10.00	514.49	504.21	539.75	553.17
146	9.00	10.50	662.55	647.29	686.73	712.1
147	9.00	11.00	798.34	781.33	843.88	863.02
148	9.50	10.00	531.94	526.49	513.43	499.86
149	9.50	10.50	652.66	643.43	627.74	620.26
150	9.50	11.00	823.06	816.04	793.7	778.08
151	10.00	10.50	527.74	532.66	526.38	535.95
152	10.00	11.00	637.85	647.07	646.89	652.5
153	10.50	11.00	533.56	539.87	532.38	532.24

Mattituck	Baselines		Survey 1		Survey 2	Survey 3	Survey 4	Survey 5
Dipole Dipole				Chargeability				Reciprocal
Data point #	XC	XP	Rho	M	Rho	Rho	Rho	Rho
1	0.50	1.00	356.08	0.91	332.92	336.88	334.94	506.79
2	0.50	1.50	723.38	0.95	693.22	686.3	690.25	762.71
3	0.50	2.00	1047.66	-4.99	989.95	1108.77	1084.25	1211.35
4	0.50	2.50	1224.86	3.09	1479.4	1448.14	1428.84	2079.51
5	0.50	3.00	1252.76	-1.39	2042.15	2038.06	2059.79	3086.76
6	0.50	3.50	1867.09	1.43	2223.04	3097.17	3200.72	2831.84
7	0.50	4.00	2280.88	3.08	2207.48	2262.2	2304.11	3032.6
8	0.50	4.50	2154.56	3.91	2310.25	2255.56	2285.7	3211.22
9	0.50	5.00	3051.51	15.32	2855.7	2750.48	2782.5	3122.11
10	1.00	1.50	427.13	1.29	437.57	440.27	441.46	448.48
11	1.00	2.00	678.96	1.83	676.68	680.82	684.27	668.92
12	1.00	2.50	833.33	1.39	916.36	898.02	903.29	1113.49
13	1.00	3.00	1030.17	0.71	1506.94	1077.32	1089.93	2052.59
14	1.00	3.50	1388.74	1.64	1541.2	1469.08	1505.92	2410.32
15	1.00	4.00	1734.91	0.33	1894.89	1790.08	1858.68	3071.72
16	1.00	4.50	1893.77	0.68	2046.28	2024.89	2012.53	3436.72
17	1.00	5.00	2298.44	1.21	2499.38	2375.11	2417.93	2991.96
18	1.00	5.50	2797.41	1.9	2964.24	3013.82	3010.23	3638.82
19	1.50	2.00	343.04	2.49	325.04	329.99	334.23	475.06
20	1.50	2.50	494.51	2.35	496.57	497.9	498.07	681.39
21	1.50	3.00	634.54	0.24	802.95	633.24	632.34	1218.86
22	1.50	3.50	879.97	1.04	926.34	899.21	908.72	1855.79
23	1.50	4.00	1101.93	0.49	1149.35	1136.8	1120.83	2831.97
24	1.50	4.50	1257.41	-0.06	1311.29	1272.32	1253.26	2303.07
25	1.50	5.00	1594.8	-5.62	1499.22	1503.46	1593.28	2195.86
26	1.50	5.50	1920.72	1.2	1788.45	1975.47	1924.96	2605.26
27	1.50	6.00	1964.81	0.59	2145.67	2031.32	2025.83	2356.11
28	2.00	2.50	362.75	1.14	375.53	373.04	371.65	491.08
29	2.00	3.00	509.67	-0.2	490	508.96	515.78	958.75
30	2.00	3.50	769.24	1	877.21	806.43	792.66	1233.12
31	2.00	4.00	1034.37	0.34	1101.24	1066.7	1087.53	2095.62
32	2.00	4.50	1231.6	0.14	1259.29	1245.53	1263.21	3054.55

33	2.00	5.00	1507.43	14.77	1582.03	1594.7	1619.57	3551.23
34	2.00	5.50	1952.96	-0.72	2091.54	2081.22	2140.88	3287.89
35	2.00	6.00	2084.37	0.17	2279.63	2176.72	2223	2503.94
36	2.00	6.50	2562.09	0.83	2648.84	2597.87	2630.94	2591.58
37	2.50	3.00	413.65	0.13	391.36	398.04	402.12	810.83
38	2.50	3.50	633.38	1.64	621.83	631.2	637.14	1095.91
39	2.50	4.00	953.47	1.47	970.11	888.08	875.96	1689.7
40	2.50	4.50	1247.82	2.15	1134.28	1119.62	1154.23	2520.75
41	2.50	5.00	1451.39	-7.35	1452.68	1460.57	1472.39	2975.19
42	2.50	5.50	1725.11	-2.89	1785.91	1868.43	1988.01	3762.47
43	2.50	6.00	2501.16	2.5	2070.79	2069.96	2077.64	3249.01
44	2.50	6.50	2327.07	14.3	2603.33	2451.56	2614.53	3234.56
45	2.50	7.00	2687.93	-15.62	2812.33	2703.52	2824.53	4398.54
46	3.00	3.50	449.02	1.82	447.27	450.97	457.99	620.96
47	3.00	4.00	590.55	0.23	580.52	592.39	590.46	1036.84
48	3.00	4.50	803.57	1.18	843.17	812.56	828.93	1391.48
49	3.00	5.00	1109.94	6.1	1110.95	1114.24	1116.85	1901.23
50	3.00	5.50	1453.21	-1.07	1387.8	1472.31	1500.24	2653.54
51	3.00	6.00	2080.4	3.49	1640.4	1581.87	1612.55	2510.41
52	3.00	6.50	1966.19	3.63	2065.58	2038.3	2074.38	2835.42
53	3.00	7.00	2014.21	-4.59	2232.36	2165.23	2266.09	3589.13
54	3.00	7.50	2290.15	-29.12	2216.46	2111.9	2212.56	3322.2
55	3.50	4.00	395.74	0.07	396.49	397.71	396.75	731.21
56	3.50	4.50	615.56	2.37	612.3	612.67	618.84	1161.76
57	3.50	5.00	892.19	2.2	879.79	907.82	923.54	1509.68
58	3.50	5.50	1258.8	-0.98	1252.05	1221.39	1282.93	1870.09
59	3.50	6.00	1624.29	2.36	1412.66	1384.15	1410.96	2713.6
60	3.50	6.50	1886.57	1.64	1799.76	1741.92	1807.66	2695.05
61	3.50	7.00	2075.26	1.82	1984.33	1900.03	2002.17	3472.12
62	3.50	7.50	2015.36	3.71	1919.32	1896.25	1951.12	3892.17
63	3.50	8.00	2817.86	1.09	2527.36	2517.81	2567.7	3835.1
64	4.00	4.50	467.32	2.3	456.37	455.8	460.68	682.11
65	4.00	5.00	782.42	4.25	788.52	796.55	799.02	966.58
66	4.00	5.50	1214.95	-1.12	1198.76	1203.29	1207.12	1269.45
67	4.00	6.00	1750.95	2.4	1542.99	1453.1	1773.51	1661.08

68	4.00	6.50	2057.02	3.84	1809.35	1811.43	2202.14	1945.7
69	4.00	7.00	2856.96	4.83	2144.35	2135.55	2221.73	2560.08
70	4.00	7.50	2834.35	4.78	2068.37	2065.86	2113.91	2336.9
71	4.00	8.00	3061.17	1.48	2852.02	2710.58	2852.45	2023.8
72	4.00	8.50	2876.84	1.09	2712.78	2619.26	2799.78	2313.6
73	4.50	5.00	602.87	2.02	607.37	605.77	613.85	760
74	4.50	5.50	953.4	-0.87	944.3	952.73	945.61	1093.09
75	4.50	6.00	1231.36	1.56	1241.87	1246.53	1241.48	1277.71
76	4.50	6.50	1685.57	1	1704.77	1711.55	2061.08	1744.5
77	4.50	7.00	1884.14	1.45	1937.92	1963.55	2211.61	2360.02
78	4.50	7.50	2449.31	4.52	1920.15	1910.03	1565.95	2757.24
79	4.50	8.00	3550.19	4.7	2660.56	2618.95	2607.45	2762.1
80	4.50	8.50	3630.69	4.78	2534.4	2531.97	2522.47	2881.23
81	4.50	9.00	3411.28	3.11	3041.7	2970.83	3068.96	4143.61
82	5.00	5.50	569.13	-3.22	555.78	554.62	558.67	850.13
83	5.00	6.00	819.91	1.77	813.87	782.82	817.8	1059.75
84	5.00	6.50	1247.55	0.56	1303.87	1231.6	1372.48	1392.71
85	5.00	7.00	1548.02	1.55	1655.59	1482.96	1615.15	2013.33
86	5.00	7.50	1853.25	2.77	1653.2	1568.64	1874.48	2230.77
87	5.00	8.00	2703.05	2.48	2396.17	2226.19	2691.1	2400.78
88	5.00	8.50	2803.62	2.87	2484.97	2138.3	2777.7	2730.98
89	5.00	9.00	3552.71	3.01	2911.92	2709.76	3452.84	3545.25
90	5.00	9.50	3630.05	3.75	2797.23	2734.42	3100.45	3335.09
91	5.50	6.00	555.37	2.46	556.28	569.66	580.25	585.82
92	5.50	6.50	999.21	3.1	1014.69	1033.73	1031.7	817.45
93	5.50	7.00	1228.46	1.72	1407.64	1410.16	1360.48	1307.75
94	5.50	7.50	1604.23	2.66	1308.23	1469.28	1635.38	1758.28
95	5.50	8.00	2300.53	2.39	2226.15	2138.99	2365.48	1781.65
96	5.50	8.50	2437.88	2.88	2118.88	2167.59	2530.23	2109.88
97	5.50	9.00	3204.75	3.66	2870.33	2593.91	3032.3	2142.55
98	5.50	9.50	3192.29	3.71	2836.51	2480.13	3322.85	2203.8
99	5.50	10.00	3450.44	3.72	2724.71	2262.98	3474.24	2078.93
100	6.00	6.50	828.49	2.09	831.11	829.52	838.17	552.37
101	6.00	7.00	1090.01	1.69	1082.92	1087.39	1113.27	942.74
102	6.00	7.50	1227.28	0.73	1238.77	1241.68	1254.29	1216.78

103	6.00	8.00	1949.34	0.99	2034.07	1862.52	2038.81	1479.96
104	6.00	8.50	2375.89	3.54	2156.68	2092.83	2332.08	1830.82
105	6.00	9.00	2827.41	3.53	2487.87	2673.35	3000.82	2289.44
106	6.00	9.50	2389.17	-1.09	2750.79	2344.53	3244.12	2373.39
107	6.00	10.00	2408.35	0.47	2567.38	2613.32	3388.41	2613.77
108	6.00	10.50	2972.86	-0.07	2757.06	2557.67	3961.67	4068.41
109	6.50	7.00	758.64	1.08	752.33	750.72	758.19	610.95
110	6.50	7.50	953.36	0.23	950.05	953.94	959.57	810.32
111	6.50	8.00	1492.89	0.17	1488.53	1483.21	1505.08	1003.91
112	6.50	8.50	1951.85	3.08	1969.15	1837.46	1820.13	1464.21
113	6.50	9.00	2265.08	1	2212.28	2276.39	2298.61	2127.27
114	6.50	9.50	2918.63	4.95	3272.93	2241.03	2623.42	2732.79
115	6.50	10.00	3603.72	5.46	3885.76	2107.75	3735.34	3189.5
116	6.50	10.50	4609.24	6.61	2726.71	2415.38	4789.9	4426.31
117	6.50	11.00	6153.08	7.04	3212.95	3108.13	6778.8	5015.72
118	7.00	7.50	661.35	0.79	664.24	666.98	674.33	459.34
119	7.00	8.00	1178.73	0.87	1157.59	1158.98	1164.47	619.25
120	7.00	8.50	1439.48	2	1435.08	1427.05	1467.58	970.18
121	7.00	9.00	2034.38	1.01	2022.76	2024.53	2041.29	1416.67
122	7.00	9.50	2629.61	4.37	2658.63	2515.21	2399.54	1846.91
123	7.00	10.00	3076.89	4.1	3051.56	2478.06	3198.59	2267.47
124	7.00	10.50	4030.97	6.04	3586.39	2706.72	4118.03	3329.14
125	7.00	11.00	5456.5	5.7	4760.96	3514.55	5680.01	4207.27
126	7.50	8.00	761.1	1.51	740.81	759.74	751.87	394.18
127	7.50	8.50	1022.75	1.65	1022.9	1028.71	1032.05	589.84
128	7.50	9.00	1675.8	1.58	1678.92	1673.14	1690.39	1046.13
129	7.50	9.50	1743.69	0.33	1807.02	1885.59	1790.72	1497.59
130	7.50	10.00	2458.34	3.12	2264.24	2230.62	3109.04	1696.26
131	7.50	10.50	3148.08	3.86	3138.16	2608.12	3259.28	1954.04
132	7.50	11.00	4608.17	4.54	3403.5	3826.15	4584.1	2303.81
133	8.00	8.50	600.29	2.19	606.31	610.28	619.72	460.66
134	8.00	9.00	1058.47	1.68	1076.91	1082.31	1096.4	648.21
135	8.00	9.50	1148.37	0.23	1174.97	1192.79	1206.84	1021.94
136	8.00	10.00	1648.76	2.72	1627.68	1490.2	1846.17	1063.66
137	8.00	10.50	2246.91	4.06	1895.12	1692.97	2447.66	1516.96

138	8.00	11.00	3496.13	4.04	2345.03	2349.79	3654.04	1882.42
139	8.50	9.00	816.8	1.44	810.74	816.26	810.57	405.72
140	8.50	9.50	931.6	0.88	936.22	938.81	955.76	516.26
141	8.50	10.00	1228.92	1.26	1200.93	1218.9	1315.35	826.7
142	8.50	10.50	1899.52	3.13	1928.29	1725.32	2042.68	1389.23
143	8.50	11.00	2973.79	3.32	2587.45	2337.6	3160.33	2031.36
144	9.00	9.50	478.3	1.48	479.37	487.48	495	368.95
145	9.00	10.00	680.35	1.06	678.96	683.36	682.31	483.03
146	9.00	10.50	1032.45	1.9	979.58	981.91	1176.17	1084.25
147	9.00	11.00	1692.9	2.12	1652.18	1590.44	1831.93	1622.47
148	9.50	10.00	489.45	1.3	487.7	478.5	477.47	332
149	9.50	10.50	667.39	0.7	667.74	669.03	671.08	689.28
150	9.50	11.00	1337.77	1.38	1297.79	1209.6	1286.64	1015.05
151	10.00	10.50	433.47	1.77	436.38	443.79	448.42	441.83
152	10.00	11.00	755.05	1.47	753.92	761.77	756.51	706.78
153	10.50	11.00	496.95	2.01	495.66	498.17	499.94	335.96

Mattituck			Survey 6		Survey 7
Wenner PRF				Chargeability	
Data point #	X	CC/3	Rho	M	Rho
1	0.75	0.5	726.04	0.92	728.51
2	1.5	1	1059.78	1.77	1056.98
3	2.25	1.5	1780.6	2.25	1799.4
4	3	2	2346.56	2.14	2337.1
5	3.75	2.5	2814.08	2.16	2810.54
6	4.5	3	3436.84	2.6	3397.2
7	5.25	3.5	4118.97	2.72	4168.49
8	1.25	0.5	509.97	1.6	508.66
9	2	1	1243.34	1.85	1252.3
10	2.75	1.5	1773.42	2.35	1798.76
11	3.5	2	2418.05	2.01	2395.85
12	4.25	2.5	2904.88	2.45	2933.05
13	5	3	3537.55	2.56	3525.56
14	5.75	3.5	4355.29	2.98	4349.54
15	1.75	0.5	616.62	1.48	618.23
16	2.5	1	1234.47	1.95	1242.34
17	3.25	1.5	1830.39	2.31	1843.73
18	4	2	2419	1.88	2440.27
19	4.75	2.5	3083.34	2.39	3123.71
20	5.5	3	3723.22	2.68	3696.9
21	6.25	3.5	4390.67	3.01	4447.64
22	2.25	0.5	623.86	1.79	626.11
23	3	1	1144.65	1.4	1140.38
24	3.75	1.5	1859.35	2.71	1904.81
25	4.5	2	2488.97	2.52	2477.53
26	5.25	2.5	3086.51	2.36	3066.46
27	6	3	3812.06	2.82	3864.89
28	2.75	0.5	608.25	1.56	610.24
29	3.5	1	1261.68	1.47	1249.06
30	4.25	1.5	1942.6	2.33	1947.91
31	5	2	2583.83	2.09	2590.3
32	5.75	2.5	3210.2	2.32	3210.05
33	6.5	3	3915.21	2.74	3966.19
34	3.25	0.5	593.09	0.71	599.01
35	4	1	1399.77	1.67	1390.09
36	4.75	1.5	1969.59	2.42	1967.09

37	5.5	2	2614.18	2.08	2660.93
38	6.25	2.5	3373.79	2.87	3385.2
39	7	3	4083.49	2.79	4012.23
40	3.75	0.5	705.25	1.78	708.27
41	4.5	1	1338.07	1.46	1328.18
42	5.25	1.5	2048.28	2.24	2065.89
43	6	2	2813.05	2.26	2793.45
44	6.75	2.5	3399.05	2.39	3421.41
45	4.25	0.5	742.06	1.49	749.1
46	5	1	1400.33	2.7	1386.26
47	5.75	1.5	2160.25	2.42	2145.5
48	6.5	2	2860.69	2.11	2856.38
49	7.25	2.5	3495.42	2.59	3491.93
50	4.75	0.5	722.54	1.08	724.87
51	5.5	1	1554.1	1.93	1540.13
52	6.25	1.5	2276.57	2.66	2269.55
53	7	2	2838.28	2.4	2840.83
54	7.75	2.5	3502.95	2.6	3518.74
55	5.25	0.5	849.97	2.86	846
56	6	1	1592.66	1.16	1616.38
57	6.75	1.5	2363.19	2.62	2363.74
58	7.5	2	3007.72	2.36	2972.62
59	5.75	0.5	954.04	0.59	957.45
60	6.5	1	1682.44	1.75	1702.2
61	7.25	1.5	2360.87	2.47	2360.81
62	8	2	2920.87	2.24	2928.56
63	6.25	0.5	928.99	1.7	901.61
64	7	1	1770.42	2.6	1744.54
65	7.75	1.5	2318.34	2.42	2337.64
66	8.5	2	2852.27	2.15	2815.33
67	6.75	0.5	1054.93	1.91	1052.84
68	7.5	1	1700.34	1.95	1710.09
69	8.25	1.5	2290.21	2.34	2293.53
70	7.25	0.5	1036.34	2.19	1033.23
71	8	1	1671.76	1.37	1685.68
72	8.75	1.5	2367.62	2.31	2325.09
73	7.75	0.5	926.62	1.15	934.49
74	8.5	1	1651.57	1.91	1642.37
75	9.25	1.5	2228.83	2.38	2240.91
76	8.25	0.5	1053.86	1.45	1051.59
77	9	1	1615.86	1.78	1629.04
78	8.75	0.5	840.03	1.91	829.16
79	9.5	1	1634.38	1.5	1618.42
80	9.25	0.5	933.99	1.41	931.39
81	10	1	1400.61	1.45	1399.28
82	9.75	0.5	766.44	1.39	767.8
83	10.25	0.5	699.65	2.37	695.24
84	10.75	0.5	696	1.94	696.65

Mattituck	Infiltration		Survey 1	Survey 2	Survey 3	Survey 4	Survey 5	Survey 6	Survey 7
Dipole Dipole									
Data point #	XC	XP	Rho	Rho	Rho	Rho	Rho	Rho	Rho
1	0.50	1.00	346.59	354.17	342.72	338.48	347.47	359.51	372.87
2	0.50	1.50	714.64	722.41	660.72	647.44	656.91	669.73	704.54
3	0.50	2.00	1049.26	1083.9	1162.22	1069.1	967.34	969.42	986.28
4	0.50	2.50	1227.11	1574.86	1780.33	1486.19	1652.48	1797.85	1871.93
5	0.50	3.00	1426.14	1845.21	2067.92	1994.55	1177.78	1348.06	1351.07
6	0.50	3.50	1860.05	1896.56	2551.69	2622.87	2005.16	2978.63	2786.17
7	0.50	4.00	2179.07	2315.35	4434.54	4810.78	5283.69	5393.44	3975.67
8	0.50	4.50	2569.59	2520.02	4033.17	2621.56	5106.4	5143.56	2709.85
9	0.50	5.00	2812.86	2963.85	3062.1	3418.78	6905.83	7278.16	3863.11
10	1.00	1.50	471.73	457.63	374.61	312.8	263.18	230.62	207.02
11	1.00	2.00	743.57	724.02	644.68	544.23	451.27	368.88	310.64
12	1.00	2.50	973.72	935.63	892.5	865.74	784.29	918.81	671.89
13	1.00	3.00	1153.07	1605.29	1345.46	806.59	735.13	699.68	518.52
14	1.00	3.50	1574.87	1646.74	1204.83	890.58	821.1	762.62	878.17
15	1.00	4.00	1888.47	1993.72	2011.65	2082.3	1939.2	1753.78	1537.41
16	1.00	4.50	2181.21	2226.38	2216.32	1648.22	1409.96	1280.91	1153.97
17	1.00	5.00	2527.82	2492.32	2379.39	2497.9	2072.23	1881.01	1679.25
18	1.00	5.50	3064.33	3078.69	2684.36	2311.65	1986.38	1915.11	1783.95
19	1.50	2.00	360.52	339.61	292.11	254.28	223.84	207.38	193.75
20	1.50	2.50	541.17	501.85	492.25	504.82	496.35	496.91	487.43
21	1.50	3.00	653.94	867.61	618.31	499.16	486.86	436.88	418.68
22	1.50	3.50	941.71	870.42	623.12	618.4	614.53	608.45	650.2
23	1.50	4.00	1160.08	1205.81	1320.41	1462.59	1582.89	1530.08	1415.5
24	1.50	4.50	1347.53	1407.97	1503.01	1208.51	1178.43	1136.46	1093.91
25	1.50	5.00	1622.7	1580.38	1686.73	1870.46	1764.29	1679.58	1601.3
26	1.50	5.50	2048.5	2019.69	1865.3	1816.37	1812.34	1781.91	1762.11
27	1.50	6.00	2006.51	2489.01	2642.92	2995.35	3484.31	3817.1	4042.38
28	2.00	2.50	393.67	385.96	373.77	369.74	354.82	342.48	349.99
29	2.00	3.00	528.42	529.96	466.95	380.77	335.68	318.07	314.9
30	2.00	3.50	840.52	958.49	554.03	509.07	484.49	484.08	596.04
31	2.00	4.00	1100.96	1255.21	1216.85	1345.49	1341.97	1308.69	1262.57
32	2.00	4.50	1315.54	1415.72	1438.5	1138.89	1073.78	1030.19	1070.96

33	2.00	5.00	1690.11	1625.77	1694.5	1897.44	1709.85	1611.8	1616.02
34	2.00	5.50	2212.54	2266.71	1922.37	1890.73	1794.96	1736.21	1824.35
35	2.00	6.00	2284.56	3336.92	2726.57	3046.61	3556.08	3885.94	4086.22
36	2.00	6.50	2547.33	2846.07	2461.45	2049.49	1721.38	1567.07	1852.05
37	2.50	3.00	414.27	406.82	321.18	238.81	194.88	173.62	163.38
38	2.50	3.50	685.57	562.79	389.08	328.87	300.4	271.95	272.25
39	2.50	4.00	946.2	1165.04	933.07	955.89	897.68	819	738.02
40	2.50	4.50	1222.03	1293.55	1167.71	881.07	772.15	678.61	685.18
41	2.50	5.00	1606.43	1452.63	1452.86	1462.13	1307.83	1170.16	1133.3
42	2.50	5.50	2094.13	1968.86	1688.87	1484.26	1382.9	1321.8	1262.25
43	2.50	6.00	2188.1	2342.92	2479.06	2636.06	2875.08	3035.19	2543.42
44	2.50	6.50	2664.24	2761.08	2286.2	1727.54	1362.17	1266.63	1340.33
45	2.50	7.00	2468.81	3325.58	3713.04	4047.3	4255.17	3360.02	4191.56
46	3.00	3.50	479.29	367.81	266.8	262.51	243.16	223.83	214.92
47	3.00	4.00	623.37	616.56	662.04	767.61	766.06	716.19	638.5
48	3.00	4.50	876.4	949.52	901.13	787.71	714.9	661.31	844.71
49	3.00	5.00	1365.27	1116.09	1228.39	1437.51	1366.73	1263.12	1187.88
50	3.00	5.50	1585.82	1527.02	1490.4	1573.16	1561.78	1632.01	1557.39
51	3.00	6.00	1743.28	2306.18	2325.36	2892.63	3365.22	3993.96	3775.89
52	3.00	6.50	2186.33	2165.33	1938.46	1584.15	1469.39	1476.86	2078.42
53	3.00	7.00	2442.88	2710.78	3501.2	4252.21	4831.77	5265.91	5322.44
54	3.00	7.50	2566.71	2101.35	1925.38	1839.53	1846.67	2020.69	1836.39
55	3.50	4.00	433.68	407.01	350.27	325.51	283.76	251.38	226.18
56	3.50	4.50	687.2	679.67	559.1	378.72	305.84	268.26	261.76
57	3.50	5.00	979.08	903.71	860.86	783	631.04	555.78	518.97
58	3.50	5.50	1487	1378.95	1092.75	899.14	775.97	718.67	699.03
59	3.50	6.00	1507.37	2095.51	1836.43	1748.91	1749.25	1846.36	1877.79
60	3.50	6.50	1956.36	2199.96	1541.28	1064.32	861.44	802.85	821.64
61	3.50	7.00	2136.35	2638.67	2798.14	2736.21	2770.39	2732.92	2636.43
62	3.50	7.50	2322.8	1876.29	1513.97	1235.39	1017.95	912.01	752.55
63	3.50	8.00	2799.56	2737.01	1995.05	1541.27	1186.09	1007.72	1090.64
64	4.00	4.50	522.37	379.2	244.89	162.73	142.28	130.06	128.44
65	4.00	5.00	865.97	606.21	477.58	440.27	385.16	344.89	333.72
66	4.00	5.50	1320.83	1005.73	684.48	570.02	544.17	526.34	519.17
67	4.00	6.00	1493.77	1577.61	1199.87	1211.11	1364.98	1475.31	1537.95

68	4.00	6.50	1956.96	1524.63	1062.85	796.15	651.79	586.02	589.05
69	4.00	7.00	2286.62	2045.59	1966.35	2023.23	2254.29	2397.16	2326.05
70	4.00	7.50	3129.24	1518.28	1028.51	943.17	890.22	850.69	746.19
71	4.00	8.00	3167.31	2237.13	1407.15	1187.64	1047.92	955.54	1085.81
72	4.00	8.50	3062.88	2776.72	2637.5	2527.34	2603.29	2564.39	2478.21
73	4.50	5.00	638.04	498.55	503.39	522.61	432.53	364.53	335.65
74	4.50	5.50	997.71	959.87	835.07	835.26	766.53	684.63	618
75	4.50	6.00	1309.63	1383.17	1639.19	2028.35	2212.07	2219.8	2087.23
76	4.50	6.50	1772.46	1733.03	1462.05	1305.89	1089.08	948.38	896.55
77	4.50	7.00	2060.65	2395.29	3009.86	3781.5	4031.84	3978.06	3547.01
78	4.50	7.50	2641.44	1750.11	1590.32	1689.77	1623.39	1479.99	1160.25
79	4.50	8.00	3533.46	2638.28	2198.8	2236.68	1950.06	1721.25	1782.58
80	4.50	8.50	2731.55	3453.74	4342.38	4857.26	4892.39	4667.42	4193.21
81	4.50	9.00	3321.26	3131.17	3563	4036.41	4113.04	4005.9	3933.7
82	5.00	5.50	621.19	731.18	475.37	324.99	257.02	221.95	221.19
83	5.00	6.00	897.69	1044.87	1045.89	921.09	898.75	872.87	865.03
84	5.00	6.50	1399.89	1521.19	1038.58	671.27	518.64	440.58	438.93
85	5.00	7.00	1566.5	2265.69	2170.9	1969.27	1955	1877.18	1829.98
86	5.00	7.50	2076.31	1553.74	1168.98	934.76	821.81	739.48	659.67
87	5.00	8.00	2806.11	2405.69	1693.45	1293.29	1059.6	903.32	1016.24
88	5.00	8.50	3026.79	3624	3339.36	2869.92	2674.54	2496.34	2448.26
89	5.00	9.00	3075.62	2856.74	2713.45	2412.42	2205.02	2203.83	2257.47
90	5.00	9.50	3645.13	2681.49	1960.79	1589.94	1480.18	1336.64	1260.85
91	5.50	6.00	600.44	630.94	739.31	705.47	633.11	574.83	564.06
92	5.50	6.50	1091.19	1009.11	803.57	575.76	423.89	355.03	357.52
93	5.50	7.00	1341.8	1579.37	1770.87	1918.92	1831.06	1692.31	1605.94
94	5.50	7.50	1756.51	1123.63	962.49	913.5	807.18	684.09	622.62
95	5.50	8.00	2416.47	2053.84	1444.8	1339.87	1078.63	913	1025.16
96	5.50	8.50	2468.64	2970.8	3001.23	3091.45	2848.11	2649.94	2571.03
97	5.50	9.00	2874.71	2284.35	2480.32	2617.23	2444.07	2404.31	2463.72
98	5.50	9.50	2896.6	2132.9	1790.47	1663.78	1677.14	1422.71	1382.2
99	5.50	10.00	2728.73	3382.75	2359.53	2144.38	1918	1711.79	1650.86
100	6.00	6.50	912.63	725.77	592.43	464.32	342.26	276.63	232.97
101	6.00	7.00	1189.31	1223.51	1227.4	1215.4	1144.58	1084.61	1030.03
102	6.00	7.50	1378.92	1034.42	694.82	594.27	529.36	484.75	444.5

103	6.00	8.00	2169.08	1816.35	1106.51	909.96	748.52	662.19	799.01
104	6.00	8.50	2092.29	2855.76	2400.64	2250.97	2148.72	2084.45	2075.05
105	6.00	9.00	2708.37	2351.14	2044.81	1962.44	1956.12	1955.52	2216.52
106	6.00	9.50	2547.11	2118.45	1518.44	1345.89	1273.98	1101.68	1216
107	6.00	10.00	2481.77	3784.36	1959.85	1624.61	1446.31	1334.07	1513.26
108	6.00	10.50	2790.62	4382.5	2517.81	2403.49	2223.13	2053.47	2041.33
109	6.50	7.00	803.09	989.59	1173.49	1318.05	1371.54	1341.89	1288.7
110	6.50	7.50	1070.27	782.2	688.68	704.09	702.51	687.88	630.01
111	6.50	8.00	1601.96	1440.81	1212.92	1192.43	1129.42	1175.8	1264.6
112	6.50	8.50	1886.22	2474.5	3027.35	3185.25	3547.57	3690.02	3626.54
113	6.50	9.00	2933.9	2176.13	2722	2960.74	3321.25	3590.89	3804.5
114	6.50	9.50	3174.75	2092.25	3130.46	2077.51	2250.75	3108.23	2306.15
115	6.50	10.00	3703.48	3474.95	3518.97	2606.69	2643.94	4071.41	2835.07
116	6.50	10.50	2924.89	4785.65	4244.1	3950.03	4176.32	6042.37	5612.37
117	6.50	11.00	5359.4	5938.99	3371.47	4029.54	4601.08	7672.06	5455.99
118	7.00	7.50	739.11	467.88	308.62	214.43	160.28	133.1	130.57
119	7.00	8.00	1246.15	971.66	654.89	465.64	337.16	352.43	332.86
120	7.00	8.50	1528.51	1902.46	1761.09	1448.21	1226.56	1118.42	1136.88
121	7.00	9.00	2273.84	1947.74	1983.02	1331.28	1222.14	1163.34	1346.52
122	7.00	9.50	2794.59	1842.48	1714.97	1017.68	884.59	1416.07	863.55
123	7.00	10.00	3195.47	1696.34	2560.27	1334.7	1083.19	1074.33	1077.74
124	7.00	10.50	3765.48	4173.29	3510.42	2042.47	1756.5	1582.77	2745.23
125	7.00	11.00	4539.04	4638.55	2882.39	2163.91	1945.53	1986.68	2247.93
126	7.50	8.00	813.43	717.45	637.5	567.69	480.16	424.33	457.85
127	7.50	8.50	1130.98	1737.94	2126.69	2244.73	2276.13	2161.41	1965.74
128	7.50	9.00	1826.34	1835.09	2190.06	2384.34	2530.88	2634.38	2548.63
129	7.50	9.50	1971.59	1974.85	1974.09	1940.19	2041.17	1833.59	1861.06
130	7.50	10.00	2616.32	3032.78	2855.78	2669.46	2473.79	2483.68	2457.02
131	7.50	10.50	2902.48	3760.33	3990.9	4349.36	4337.8	4317.36	4056.61
132	7.50	11.00	4132.74	5029.52	4160.19	4571.1	4816.18	5035.04	5376.57
133	8.00	8.50	690.74	947.34	856.55	707.24	555.93	453.87	358.4
134	8.00	9.00	1210.49	820.94	785.05	737.21	665.42	613.39	531.8
135	8.00	9.50	1360.83	990.4	796.18	682.67	603.44	489.63	440.37
136	8.00	10.00	1842.36	1662.89	1155.68	973.74	845.52	826.56	631.93
137	8.00	10.50	2491.72	2403.69	1692.83	1636.31	1456.55	1492.52	1273.28

138	8.00	11.00	3329.68	1886.67	1768.62	1762.85	1688.32	1966.74	1764.87
139	8.50	9.00	878.31	474.13	351.89	304.19	269.72	250.06	301.72
140	8.50	9.50	1021.71	671.82	449.03	385.62	326.64	286.52	328.24
141	8.50	10.00	1263.74	1139.92	798.92	641.64	521.08	481.81	539.21
142	8.50	10.50	2038.46	1677.58	1288.79	1188.34	995.02	1031.31	1116.92
143	8.50	11.00	3103.48	1822.92	1457.18	1348.92	1227.96	1434.64	1630.46
144	9.00	9.50	535.08	591.99	510.83	456.29	398.34	322.03	311.53
145	9.00	10.00	719.24	920.61	962.21	825.56	722.37	667.24	646.8
146	9.00	10.50	1174.14	1480.74	1663.84	1671.08	1545.61	1408.37	1288.88
147	9.00	11.00	1961.92	1805.18	1988.24	2067.12	2085.71	2088.86	1982.01
148	9.50	10.00	518.7	662.43	741.68	597.81	472.3	419.31	392.38
149	9.50	10.50	718.4	829.39	980.87	1027.4	940.16	875.98	803.27
150	9.50	11.00	1251.34	1121.45	1207.16	1288.33	1346.27	1413.58	1364.05
151	10.00	10.50	474.9	439.76	365.79	345.12	291.19	238.4	249.81
152	10.00	11.00	808	565.41	437.56	446.65	439.82	425.87	429.79
153	10.50	11.00	531.91	342.83	289.53	254.98	243.08	238.92	256.89

Southampton	Baselines		Survey 2	Survey 3	Survey 4	Survey 5
Dipole Dipole						Reciprocal
Data point #	XC	XP	Rho	Rho	Rho	Rho
1	0.50	1.00	287.88	283.58	282	146.66
2	0.50	1.50	296.5	329.94	316.44	190.58
3	0.50	2.00	501.94	521.15	523.43	421.9
4	0.50	2.50	422.57	439.19	680.36	261.87
5	0.50	3.00	434.92	448.65	950.27	866.42
6	0.50	3.50	462.34	427.83	555.12	542.52
7	0.50	4.00	520.11	493.22	611.37	429.06
8	0.50	4.50	584.04	565.66	665.77	321.75
9	0.50	5.00	587.41	731.42	786.79	304.34
10	1.00	1.50	275.57	278.17	273.41	170.67
11	1.00	2.00	347.13	344.27	345.73	207.39
12	1.00	2.50	372.76	377.03	374.08	234.84
13	1.00	3.00	388.84	395.78	389.11	276.47
14	1.00	3.50	423.62	425.86	422.68	248.75
15	1.00	4.00	461.01	463.35	461.33	298.78
16	1.00	4.50	500.11	549.28	507.31	288.86
17	1.00	5.00	595.49	798.27	585.69	322.95
18	1.00	5.50	602.83	656.62	556.12	375.61
19	1.50	2.00	249.55	246.18	245.4	196.84
20	1.50	2.50	273.13	281.48	280.43	227.4
21	1.50	3.00	323.87	314.24	314.08	266.17
22	1.50	3.50	355.32	355.53	346.85	271.1
23	1.50	4.00	395.45	387.92	381.14	317.66
24	1.50	4.50	382.2	395.28	384.48	383.65
25	1.50	5.00	486.3	502.9	488.99	452.87
26	1.50	5.50	501.1	485.84	447.81	502.56
27	1.50	6.00	504.54	540.73	498.73	530.23
28	2.00	2.50	220.14	217.46	214.69	201.56
29	2.00	3.00	253.6	255.02	250.87	232.71
30	2.00	3.50	287.33	299.87	304.38	281.11
31	2.00	4.00	341.65	335.2	326.92	333.2
32	2.00	4.50	344.4	334.89	337.27	354.83

33	2.00	5.00	425.55	429.74	422.85	390.81
34	2.00	5.50	423.3	378.35	396.48	450.5
35	2.00	6.00	427.92	421.19	421.87	473.16
36	2.00	6.50	496.92	509.72	466.08	492.35
37	2.50	3.00	210.39	208.03	207	205.13
38	2.50	3.50	256.52	255.74	254.87	227.89
39	2.50	4.00	305.86	314.59	318.72	311.99
40	2.50	4.50	325.73	329.17	320.94	340.33
41	2.50	5.00	385.19	381.75	381.89	372.73
42	2.50	5.50	378.44	367.46	373.02	416.24
43	2.50	6.00	380.82	382.07	392.39	457.17
44	2.50	6.50	425.26	440.31	425.58	500.49
45	2.50	7.00	437.22	458.13	498.17	561.33
46	3.00	3.50	210.18	208.11	206.87	197.83
47	3.00	4.00	245.99	245.1	243.98	252.3
48	3.00	4.50	293.43	290.74	289.91	325.98
49	3.00	5.00	346.94	356.22	353.53	363.54
50	3.00	5.50	333.49	334.34	333.34	387.52
51	3.00	6.00	353.03	354.4	356.63	415.69
52	3.00	6.50	403.7	410.88	406.46	427.9
53	3.00	7.00	445.88	459.54	464.9	497.13
54	3.00	7.50	470.4	492.62	484.81	517.03
55	3.50	4.00	200.69	198.51	195.8	198.4
56	3.50	4.50	222.04	219.54	218.91	256.17
57	3.50	5.00	301.38	316.01	313.55	317.85
58	3.50	5.50	295.69	299.33	295.96	344.73
59	3.50	6.00	305.15	306.03	299.56	371.94
60	3.50	6.50	337.83	362.09	377.29	385.88
61	3.50	7.00	408.49	404.26	408.23	434.03
62	3.50	7.50	421.07	423.49	434.94	460.43
63	3.50	8.00	499.91	503.15	470.57	466.11
64	4.00	4.50	184.98	183.18	181.78	201.72
65	4.00	5.00	261.19	261.07	259.64	256.76
66	4.00	5.50	282.47	283.12	282.92	305.29
67	4.00	6.00	299.84	303.54	298.52	341.25

68	4.00	6.50	353.47	350.26	347.83	352.68
69	4.00	7.00	396.37	402.46	390.57	386.42
70	4.00	7.50	422.8	419.51	406.14	376.64
71	4.00	8.00	458.39	494.81	458.28	435.37
72	4.00	8.50	466.08	528.74	524.88	491.12
73	4.50	5.00	211.9	211.02	208.16	208.66
74	4.50	5.50	229.32	227.57	225.4	257.26
75	4.50	6.00	271.76	273.85	272.42	318.23
76	4.50	6.50	333.6	337.55	335.29	311.75
77	4.50	7.00	378.98	384.75	376.5	367.09
78	4.50	7.50	393.83	404.92	399.86	391.46
79	4.50	8.00	458.89	454.3	483.12	386.1
80	4.50	8.50	451.21	505.15	547.56	441.33
81	4.50	9.00	524.53	560.63	588.02	450.99
82	5.00	5.50	171.52	170.19	168.44	184.21
83	5.00	6.00	215.98	216.83	214.47	252.93
84	5.00	6.50	274.8	283.34	281.46	278.69
85	5.00	7.00	325.04	329.94	337.06	331.46
86	5.00	7.50	347.74	352.5	373.96	346.91
87	5.00	8.00	401.11	425.23	414.6	348.54
88	5.00	8.50	393.46	462.67	428.38	399.63
89	5.00	9.00	499.77	503.48	541.14	461.37
90	5.00	9.50	494.42	512.94	568.58	473.03
91	5.50	6.00	185.69	184.63	183.69	180.93
92	5.50	6.50	255.37	254.33	253.87	213.28
93	5.50	7.00	315.92	320.1	319.25	269.56
94	5.50	7.50	342.59	342.27	343.48	293.43
95	5.50	8.00	375.86	388.43	392	300.7
96	5.50	8.50	412.74	436.47	422.02	338.37
97	5.50	9.00	450.19	454.84	499.39	392.65
98	5.50	9.50	484.19	485.16	531.56	401.2
99	5.50	10.00	527.53	479.19	556.84	491.68
100	6.00	6.50	189.3	188.39	186.41	167.6
101	6.00	7.00	259.38	258.44	257.77	225.92
102	6.00	7.50	291.55	313.82	309.53	276.86

103	6.00	8.00	378.33	356.68	352.85	279.48
104	6.00	8.50	347.04	353.65	363.98	319.66
105	6.00	9.00	531.07	440.39	402.78	398.69
106	6.00	9.50	476.49	465.49	426.2	443.72
107	6.00	10.00	511.52	522.62	481.62	551.6
108	6.00	10.50	520.09	506.6	493.23	641.11
109	6.50	7.00	214.29	211.89	210.14	206.21
110	6.50	7.50	261.51	259.15	258.44	257.57
111	6.50	8.00	317.79	317.14	314.53	308.19
112	6.50	8.50	328.38	329.26	330	346.06
113	6.50	9.00	351.83	392.29	390.07	409.08
114	6.50	9.50	444.71	405.53	418.1	427.65
115	6.50	10.00	438.16	433.05	452.38	489.43
116	6.50	10.50	368.57	452.52	483.1	588.73
117	6.50	11.00	494.19	484.74	495.3	705.69
118	7.00	7.50	206.41	204.04	203.17	181.86
119	7.00	8.00	259.37	259.46	256.67	218.23
120	7.00	8.50	289.66	293.56	295.2	290.34
121	7.00	9.00	315.24	340.15	339.26	324.51
122	7.00	9.50	370.47	365	377.16	342.79
123	7.00	10.00	401.67	408.03	412.84	390.95
124	7.00	10.50	399.81	412.73	420.96	452.43
125	7.00	11.00	452.85	523.22	491.14	508.04
126	7.50	8.00	204.41	201.61	200.49	194.26
127	7.50	8.50	256.3	256.02	254.21	242.69
128	7.50	9.00	283.03	294.65	305.56	306.93
129	7.50	9.50	333.85	338.75	325.34	324.07
130	7.50	10.00	354.02	350.77	351.94	357.54
131	7.50	10.50	354.26	365.13	349.32	408.47
132	7.50	11.00	406.61	426.13	402.89	400.44
133	8.00	8.50	200.07	198.83	198.43	205.71
134	8.00	9.00	227.92	228.18	227.87	254.23
135	8.00	9.50	281.05	263.86	254.84	306.31
136	8.00	10.00	304.32	307.15	309.87	334.55
137	8.00	10.50	299.57	290.99	306.19	382.23

138	8.00	11.00	339.33	361.77	331.74	375.85
139	8.50	9.00	207	206.97	206.56	206.51
140	8.50	9.50	235.38	234.37	238.96	250.78
141	8.50	10.00	292.39	290.52	289.5	325.75
142	8.50	10.50	290.35	292	283.5	372.84
143	8.50	11.00	328.57	312.24	318.23	372.41
144	9.00	9.50	203.1	202.2	202.1	211.82
145	9.00	10.00	229.82	227.52	227.66	278.99
146	9.00	10.50	246.79	250.33	248.53	374.11
147	9.00	11.00	288.81	277.69	283.96	369.39
148	9.50	10.00	197.64	196.11	194.8	244.63
149	9.50	10.50	205.91	207.69	209.45	339.02
150	9.50	11.00	249.32	248.79	247.2	374.07
151	10.00	10.50	172.22	170.93	169.93	270.26
152	10.00	11.00	192.22	190.62	186.91	309.3
153	10.50	11.00	149.49	149.37	147.72	283.85

Southampton			Survey 6		Survey 7
Wenner PRF				Chargeability	
Data point #	X	CC/3	Rho	M	Rho
1	0.75	0.5	315.08	2.28	317.54
2	1.5	1	373.03	0.81	374.12
3	2.25	1.5	454.77	2.88	452.75
4	3	2	543.65	2.11	549.78
5	3.75	2.5	639.1	1.67	646
6	4.5	3	741.04	1.99	739.68
7	5.25	3.5	846.47	1.77	851.43
8	1.25	0.5	298.39	0.79	298.28
9	2	1	369.03	1.29	368.84
10	2.75	1.5	450.54	2.33	448.88
11	3.5	2	542.6	1.7	543.59
12	4.25	2.5	650.06	1.31	651.75
13	5	3	740.65	1.3	744.21
14	5.75	3.5	855.7	2.19	851.31
15	1.75	0.5	274.08	1.67	273.83
16	2.5	1	371.33	1.66	371.07
17	3.25	1.5	442.05	2.32	436.91
18	4	2	545.34	1.15	543.54
19	4.75	2.5	647.01	1.7	649.68
20	5.5	3	746.99	1.89	741.61
21	6.25	3.5	855.29	2	855.99
22	2.25	0.5	270.4	1.67	270.14
23	3	1	342.72	1.17	343.89
24	3.75	1.5	441.51	2.13	441.47
25	4.5	2	558.59	1.42	557.18
26	5.25	2.5	638.29	1.28	642.46
27	6	3	741.51	1.74	740.86
28	2.75	0.5	249.32	1.44	249.38
29	3.5	1	341.71	0.87	341.11
30	4.25	1.5	447.4	2.46	446.03
31	5	2	545.78	1.53	545.21
32	5.75	2.5	631.33	1.37	632.04
33	6.5	3	743.4	1.92	745.17
34	3.25	0.5	235.98	1.13	235.49
35	4	1	341.43	1.1	341.4
36	4.75	1.5	455.07	2.46	454.07

37	5.5	2	535.41	1.29	533.88
38	6.25	2.5	633.45	1.44	635.17
39	7	3	742.6	2.16	741.53
40	3.75	0.5	236.12	1.28	236.49
41	4.5	1	333.41	1.39	334.02
42	5.25	1.5	438	2.43	437.41
43	6	2	531.04	1.52	531.94
44	6.75	2.5	617.03	1.29	618.28
45	4.25	0.5	238.7	1.69	237.17
46	5	1	343.21	1.19	341.68
47	5.75	1.5	435.83	2.24	435.84
48	6.5	2	514.14	1.43	515.56
49	7.25	2.5	630.36	1.72	629.78
50	4.75	0.5	214.14	1.42	216.02
51	5.5	1	345.47	1.32	346.55
52	6.25	1.5	422.79	2.48	419.46
53	7	2	515.02	1.09	518.76
54	7.75	2.5	646.57	1.48	644.9
55	5.25	0.5	239.65	1.24	239.3
56	6	1	330.34	1.13	331.14
57	6.75	1.5	429.06	2.3	427.83
58	7.5	2	529.22	1.3	529.22
59	5.75	0.5	218.47	1.56	218.05
60	6.5	1	332.89	1.34	332.43
61	7.25	1.5	428.52	2.17	428.56
62	8	2	539.93	1.37	536.26
63	6.25	0.5	230.87	0.94	230.25
64	7	1	342.37	1.2	345.34
65	7.75	1.5	438.23	2.07	435.99
66	8.5	2	543.31	1.42	542.77
67	6.75	0.5	235.42	1.85	235.55
68	7.5	1	338.13	0.99	336.68
69	8.25	1.5	428.81	1.97	428.77
70	7.25	0.5	242.72	1.11	244.12
71	8	1	336.56	1.15	335.08
72	8.75	1.5	435.93	2.13	436.72
73	7.75	0.5	236.1	1.36	236.34
74	8.5	1	335	1.39	334.81
75	9.25	1.5	422.65	2.7	424.01
76	8.25	0.5	238.22	1.54	240.08
77	9	1	328.19	1.46	327.79
78	8.75	0.5	234.6	1.16	235.29
79	9.5	1	308.58	1.39	309.02
80	9.25	0.5	232.69	1.54	233.04
81	10	1	291.55	1.16	291.79
82	9.75	0.5	214.51	1.36	213.76
83	10.25	0.5	201.29	1.93	202.14
84	10.75	0.5	187.09	2.1	187.32

Southampton	Infiltration		Survey 1	Survey 2	Survey 3	Survey 4	Survey 5
Dipole Dipole							
Data point #	XC	XP	Rho	Rho	Rho	Rho	Rho
1	0.50	1.00	301.13	299.48	299.58	303.42	297.17
2	0.50	1.50	326.54	320.16	334.76	315	321.04
3	0.50	2.00	369.67	364.66	397.01	582.64	561.51
4	0.50	2.50	354.4	374.28	397.53	517.95	469.65
5	0.50	3.00	351.52	320.02	328.07	381.09	349.8
6	0.50	3.50	377.55	377.97	391.65	465.91	443.14
7	0.50	4.00	420.07	429.92	414.84	509.18	510.99
8	0.50	4.50	442.82	424.47	423.8	556.92	599.2
9	0.50	5.00	555.61	521.38	506.95	748.36	802.17
10	1.00	1.50	287.92	286.8	285.7	284.28	283.33
11	1.00	2.00	348.59	351.82	350.5	351.4	352.37
12	1.00	2.50	360.01	369.22	399.42	410.94	410.16
13	1.00	3.00	369.19	313.17	319.91	340.4	325.64
14	1.00	3.50	386.92	383.17	409.69	460.44	374.72
15	1.00	4.00	417.46	437.94	462.49	501.94	447.51
16	1.00	4.50	459.99	459.37	487.26	541.49	527.93
17	1.00	5.00	542.73	528.67	613.24	640.86	630.01
18	1.00	5.50	567.34	479.98	532.93	671.81	708.2
19	1.50	2.00	260.66	262.13	260.24	259.76	258.81
20	1.50	2.50	291.05	296.83	300.31	301.43	302.45
21	1.50	3.00	309.22	268.46	285.62	279.01	282.66
22	1.50	3.50	332.97	337.59	357.05	374.66	325.09
23	1.50	4.00	357.09	379.47	391.69	412.9	411.24
24	1.50	4.50	372.89	379.25	419.5	456.55	425.62
25	1.50	5.00	438.67	464.68	440.12	530.39	546.58
26	1.50	5.50	412.33	434.79	457.65	578.91	535.91
27	1.50	6.00	463.59	444.37	503.36	524.71	505.73
28	2.00	2.50	224.11	228.45	230.2	229.97	231.36
29	2.00	3.00	261.1	226.88	216.53	212.08	207.29
30	2.00	3.50	290.56	280	307.68	309.86	274.47
31	2.00	4.00	319.04	325.05	346.46	348.68	350.33
32	2.00	4.50	336.61	349.23	341.98	382.6	370.61

33	2.00	5.00	396.54	388.38	421.32	421.65	412.35
34	2.00	5.50	375.79	387.05	444.48	375.97	434.07
35	2.00	6.00	417.73	384.07	425.54	325.46	386.24
36	2.00	6.50	482.33	457.78	486.8	473.47	509.6
37	2.50	3.00	219.09	192.19	182.64	177.6	171.58
38	2.50	3.50	261.56	268.77	262.82	259.32	224.24
39	2.50	4.00	300.02	305.23	324.64	319.6	326.24
40	2.50	4.50	314.68	326.23	342.22	348.75	355.76
41	2.50	5.00	375.36	379.49	429.21	402.16	415.42
42	2.50	5.50	350.65	376.63	369.59	360.54	379.31
43	2.50	6.00	374.7	353.94	351.71	339.4	325.1
44	2.50	6.50	463.1	424.55	480.32	429.53	400.14
45	2.50	7.00	512.75	487.55	527.66	418.1	479.06
46	3.00	3.50	212.23	217.44	212.42	203.68	163.27
47	3.00	4.00	246.62	265.07	266.37	258.07	248.26
48	3.00	4.50	267.61	272.02	294.03	299.87	294.73
49	3.00	5.00	320.56	340.34	353.05	350.2	361.48
50	3.00	5.50	337.47	302.21	339.29	339.1	308.51
51	3.00	6.00	342.69	299.03	302.08	283.44	322.53
52	3.00	6.50	407.75	352.87	366.41	364.07	406.24
53	3.00	7.00	461.63	385.7	469.98	494.23	448.53
54	3.00	7.50	496.73	358.18	487.6	477.24	420.64
55	3.50	4.00	207.4	169.92	166.13	164.59	158.42
56	3.50	4.50	228.68	192.51	188.5	188.4	186.74
57	3.50	5.00	294.15	252.99	261.6	258.24	248.23
58	3.50	5.50	273.64	243.6	242.42	235.72	258.38
59	3.50	6.00	272	223.28	216.02	223.78	211.29
60	3.50	6.50	353.69	318.21	282.27	275.4	288.6
61	3.50	7.00	395.99	348.86	317.14	310.93	338.13
62	3.50	7.50	414.94	327.66	307.45	307.66	357.96
63	3.50	8.00	474.23	385.49	306.77	332.55	398.51
64	4.00	4.50	191.5	190.56	191.11	192.28	172.05
65	4.00	5.00	265.35	270.57	272.57	272.21	255.61
66	4.00	5.50	267.08	291.31	290.12	292.98	275.03
67	4.00	6.00	293.8	263.24	259.07	254.83	246.68

68	4.00	6.50	346.49	351.48	340.96	347.58	328.71
69	4.00	7.00	390.43	430.72	403.43	400.79	396.86
70	4.00	7.50	416.18	425.01	409.77	403.38	397.07
71	4.00	8.00	476.46	457.06	510.21	459.65	451.79
72	4.00	8.50	534.8	543	502.09	477.55	497.41
73	4.50	5.00	217.8	217.06	216.71	216.56	208.82
74	4.50	5.50	235.22	241.15	241.66	243.14	248.22
75	4.50	6.00	275.16	248.71	242.67	236.08	239.23
76	4.50	6.50	333.54	329.7	329.6	326.72	329.58
77	4.50	7.00	382.2	387.27	393.86	395.95	403.44
78	4.50	7.50	406.69	397.15	404.2	403.23	413.99
79	4.50	8.00	462.8	388.54	450.5	456.91	482.03
80	4.50	8.50	504.15	534.69	509.85	488.11	501.39
81	4.50	9.00	555.65	617.74	519.27	508.58	539.96
82	5.00	5.50	176.89	180.27	180.35	180.96	182.01
83	5.00	6.00	221.62	203.33	196.15	190.9	187.6
84	5.00	6.50	280.67	278.93	277.67	272.69	275.49
85	5.00	7.00	328.4	340.67	339.19	338.48	340.35
86	5.00	7.50	346.18	351.8	351	351.92	356.68
87	5.00	8.00	401.81	400.85	395.64	396.24	397.67
88	5.00	8.50	425.27	429.52	423.16	426.26	439.53
89	5.00	9.00	472.41	436.94	483.48	449.13	458.49
90	5.00	9.50	510.92	453.49	478.08	453.18	452.58
91	5.50	6.00	190.67	171.63	164.44	158.67	153.82
92	5.50	6.50	259.47	258.93	253.54	245.52	241.54
93	5.50	7.00	317.14	335.14	336.24	326.7	325.2
94	5.50	7.50	339.8	351.09	351.13	344.11	341.95
95	5.50	8.00	382.13	390.56	391.96	385.33	378.65
96	5.50	8.50	406.87	419.13	422.55	413.03	400.77
97	5.50	9.00	442.08	449.36	451.94	433.14	440.15
98	5.50	9.50	462.19	439.67	452.18	435.75	445.86
99	5.50	10.00	479.38	445.53	467.71	452.49	457.61
100	6.00	6.50	194.21	193.6	192.93	189.88	183.3
101	6.00	7.00	263.88	282	279.03	278.89	273.59
102	6.00	7.50	304.6	314.35	326.89	327.81	335.55

103	6.00	8.00	338.9	353.25	354.73	348.58	351.44
104	6.00	8.50	352.78	377.34	392.03	383.88	365.9
105	6.00	9.00	374.87	366.7	403.83	399.82	396.42
106	6.00	9.50	394.97	388.39	417.89	418.46	424.54
107	6.00	10.00	412.02	463.46	448.35	455.68	479.4
108	6.00	10.50	402.41	526.76	436.83	423.22	427.62
109	6.50	7.00	221.47	199.45	192.4	187.77	186.54
110	6.50	7.50	267.45	239.54	233.4	227.77	227.5
111	6.50	8.00	307.16	289.45	281.17	276.91	277
112	6.50	8.50	311.92	314.7	285.81	292	293.34
113	6.50	9.00	323.77	317.8	293.24	293.64	313.18
114	6.50	9.50	322.34	309.13	304.1	312.58	330.28
115	6.50	10.00	314.31	318.35	336.3	360.11	365.36
116	6.50	10.50	250.24	278.07	357.54	367.67	335
117	6.50	11.00	350.68	314.64	432.14	433.89	279.43
118	7.00	7.50	215.44	213.13	212.66	213.02	211.2
119	7.00	8.00	268.79	268.35	267.66	268.27	267.17
120	7.00	8.50	300.47	299.89	303.34	302.71	301.52
121	7.00	9.00	329.31	336.87	324.91	334.06	330.64
122	7.00	9.50	314.11	351.38	348.41	345.78	344.57
123	7.00	10.00	332.06	337.78	369.1	364.3	377.19
124	7.00	10.50	277.55	335.61	365.03	357.31	377.42
125	7.00	11.00	429.89	380	395.82	448.29	426.43
126	7.50	8.00	209.4	213.43	212.28	211.99	211.78
127	7.50	8.50	264.19	265.59	266.29	265.72	265.4
128	7.50	9.00	302.41	294.12	293.71	303.57	303.52
129	7.50	9.50	316.66	338.41	346.52	326.3	334.58
130	7.50	10.00	311.12	364	356.23	355.56	358.59
131	7.50	10.50	274.54	349.13	349.29	346.01	347.35
132	7.50	11.00	274.69	391.31	401.71	402.96	403.24
133	8.00	8.50	209.22	208.12	207.84	208.07	207.23
134	8.00	9.00	236.89	237.48	236.91	236.09	236.63
135	8.00	9.50	278.79	276.83	281.58	283.7	285.24
136	8.00	10.00	302.17	296.37	309.07	307.33	319.32
137	8.00	10.50	294.76	275.54	311.51	302.93	305.65

138	8.00	11.00	318.54	342.06	341.94	345.38	345.58
139	8.50	9.00	219.5	216.19	215.94	216.24	218.23
140	8.50	9.50	241.08	240.96	238.81	237.82	236.79
141	8.50	10.00	291.54	282.09	278.14	263.29	260.71
142	8.50	10.50	286.44	282.18	276.43	268.01	265.18
143	8.50	11.00	322.11	323.38	308.35	314.05	322.67
144	9.00	9.50	214.34	212.85	210.89	210.93	209.68
145	9.00	10.00	235.33	234.81	234.1	235.04	233.44
146	9.00	10.50	261.51	254.64	251.87	253.63	252.71
147	9.00	11.00	294.68	291.51	288.85	291.91	291.26
148	9.50	10.00	206.88	206.37	205.63	204.55	203.88
149	9.50	10.50	213.05	215.86	215.43	215.09	217.44
150	9.50	11.00	247.63	257.32	257.35	258.38	257.16
151	10.00	10.50	179.17	178.21	177.03	176.78	175.7
152	10.00	11.00	188.83	189.56	188.26	189.25	187.64
153	10.50	11.00	155.36	154.48	153.78	152.48	153.03

Southampton	Infiltration		Survey 6	Survey 7	Survey 8	Survey 9	Survey 10
Dipole Dipole							
Data point #	XC	XP	Rho	Rho	Rho	Rho	Rho
1	0.50	1.00	298.87	299.28	298.69	297.62	297.72
2	0.50	1.50	335.78	324.65	319.88	322.05	335.14
3	0.50	2.00	398.8	580.22	373.57	370.71	384.35
4	0.50	2.50	398.46	465.61	359.08	359.98	367.08
5	0.50	3.00	307.86	392.77	289.07	295.96	289.46
6	0.50	3.50	335.88	386.46	319.48	320.85	299.8
7	0.50	4.00	426.31	471.61	435.15	434.49	388.38
8	0.50	4.50	446.64	497	461.28	495.12	365
9	0.50	5.00	514.66	674.94	571.45	558.53	487.44
10	1.00	1.50	282.78	282.66	282.51	282.2	281.26
11	1.00	2.00	353.54	356.98	355.3	353.03	353.79
12	1.00	2.50	396.56	396.7	360.68	359.42	360.32
13	1.00	3.00	307.86	337.52	301.1	304.67	327.19
14	1.00	3.50	359.25	375.14	349.55	331.17	337.21
15	1.00	4.00	465.07	511.2	440.54	442.1	435.84
16	1.00	4.50	463.11	473.97	464.9	475.5	460.72
17	1.00	5.00	551.82	678.12	562.38	568.94	516.89
18	1.00	5.50	566.28	674.18	551.54	518.55	465.14
19	1.50	2.00	259.11	259.19	260.46	254.82	255.97
20	1.50	2.50	300.08	297.99	292.11	288.23	286.75
21	1.50	3.00	280.81	274.6	254.03	254.43	276.93
22	1.50	3.50	316.49	317.77	285.49	276.93	300.47
23	1.50	4.00	411.87	413.42	371.98	369.09	389.64
24	1.50	4.50	418.83	435.94	385.94	387.64	420.57
25	1.50	5.00	484.78	507.88	459.64	457.55	466.26
26	1.50	5.50	445.59	492.86	450.12	427.3	418.24
27	1.50	6.00	501.87	543.17	405.47	406.12	493.8
28	2.00	2.50	229.09	224.75	223.45	220.76	218.4
29	2.00	3.00	205.34	207.84	211.55	214.66	214.67
30	2.00	3.50	263.32	259.26	248.23	242.19	257.46
31	2.00	4.00	343.68	342.75	333	332.28	325.41
32	2.00	4.50	376.47	359.11	354.01	354.22	336.45

33	2.00	5.00	409.22	412	422.2	425.25	398.61
34	2.00	5.50	386.18	373.22	391.19	395.61	356.32
35	2.00	6.00	376.12	341.83	363.52	354.05	380.42
36	2.00	6.50	490.06	476.05	469.86	466.23	449.56
37	2.50	3.00	172.08	172.49	174.66	175.54	176.98
38	2.50	3.50	224.5	224.29	220.85	218.89	218.4
39	2.50	4.00	327.39	323.93	313.49	318.34	322.31
40	2.50	4.50	338.12	377.11	339.4	341.16	333.55
41	2.50	5.00	405.4	408.95	411.94	416.82	397.75
42	2.50	5.50	361.87	379.85	385.58	383.25	373.61
43	2.50	6.00	338.58	300.83	352.77	341.28	351.32
44	2.50	6.50	422.15	387.24	458.91	436.72	419.41
45	2.50	7.00	447.07	455.68	581.85	548.19	531.83
46	3.00	3.50	156.3	152.93	145.14	139.48	136.8
47	3.00	4.00	241.96	238.2	231.12	224.46	220.39
48	3.00	4.50	280.71	275.63	264.12	254.15	258.5
49	3.00	5.00	342.51	343.77	332.83	317.13	301.14
50	3.00	5.50	337.78	317.03	322.37	304.63	290.41
51	3.00	6.00	303.74	284.13	263.13	269.24	285.36
52	3.00	6.50	376.73	356.43	348.83	336.19	331.9
53	3.00	7.00	413.32	418.03	463.72	490.41	419.88
54	3.00	7.50	417.93	388.65	444.99	425.32	439.68
55	3.50	4.00	158.5	159.21	160.35	161.06	162.12
56	3.50	4.50	188.22	189.75	193.34	195.02	196.67
57	3.50	5.00	255.89	254.79	247.94	263.49	269.4
58	3.50	5.50	255.43	246.48	246.03	242.19	245.54
59	3.50	6.00	212.78	218.93	219.02	223.75	234.53
60	3.50	6.50	286.48	291.08	290.62	279.16	279.92
61	3.50	7.00	342.15	358.58	356.72	357.72	367.58
62	3.50	7.50	361.59	372.43	368.12	355.82	374.97
63	3.50	8.00	417.33	409.95	421.17	391.99	423.91
64	4.00	4.50	170.69	170.67	168.09	164.76	163.52
65	4.00	5.00	252.14	248.27	245.15	241.32	240.62
66	4.00	5.50	270.25	268.48	265.23	260.53	244.51
67	4.00	6.00	237.11	233.58	214.06	223.55	237.24

68	4.00	6.50	316.72	310.36	272.46	282.66	282.58
69	4.00	7.00	381.26	383.26	353.01	363.95	370.33
70	4.00	7.50	393.49	386.26	350.26	367.83	371.79
71	4.00	8.00	435.23	453.41	408.43	423.27	433.07
72	4.00	8.50	474.99	487.47	450.68	463.44	457.61
73	4.50	5.00	209.41	209.34	212.6	211.95	212.41
74	4.50	5.50	247.19	247.8	246.83	242.97	239.73
75	4.50	6.00	238.3	240.13	232.55	238.53	248.2
76	4.50	6.50	320.61	321.59	301.99	301.74	305.51
77	4.50	7.00	402.69	399.9	392.1	395.73	403.13
78	4.50	7.50	414.19	427.84	394.86	410.3	418.26
79	4.50	8.00	456.86	455.96	436.87	456.38	455.85
80	4.50	8.50	474.08	469	471.11	491.92	503.12
81	4.50	9.00	527.25	491.38	506.21	527.73	534.91
82	5.00	5.50	180.19	179.79	178.09	176.56	173.17
83	5.00	6.00	188.48	186.94	182.92	188.08	191.84
84	5.00	6.50	274.99	267.38	252.41	248.09	249.92
85	5.00	7.00	340.73	343.36	344.42	339.2	339.53
86	5.00	7.50	349.13	353.42	348.72	351.6	353.94
87	5.00	8.00	395.75	400.06	401.8	392.43	397.79
88	5.00	8.50	435.33	424.82	392.76	419.21	422.42
89	5.00	9.00	398.52	414.19	470.07	444.42	446.71
90	5.00	9.50	438.73	463.15	473.53	456.39	439.74
91	5.50	6.00	151.65	153.87	153.01	157.48	159.32
92	5.50	6.50	237.7	235.29	229.51	223.5	223.86
93	5.50	7.00	324.69	327.35	327.27	332.45	326.5
94	5.50	7.50	341.47	343.47	343.81	349.62	344.64
95	5.50	8.00	389.5	382.37	380.91	383.99	384
96	5.50	8.50	401.8	405.96	410.57	412.94	411.86
97	5.50	9.00	437.47	429.36	444.82	456.55	442.74
98	5.50	9.50	426.39	440.87	447.74	474.25	445.75
99	5.50	10.00	426.06	458.76	474.94	480.1	453.61
100	6.00	6.50	174.45	168.04	150.07	144.41	143.52
101	6.00	7.00	270.62	264.62	254.47	245.68	245.21
102	6.00	7.50	316.54	311.72	291.95	282.86	287.43

103	6.00	8.00	341.7	336.55	319.29	319.08	315.6
104	6.00	8.50	359.74	359.38	344.5	358.95	348.96
105	6.00	9.00	385.76	385.41	383.21	407.38	396.37
106	6.00	9.50	420.44	405.83	409.48	414.29	426.99
107	6.00	10.00	450.91	467.79	453.44	477.66	468.62
108	6.00	10.50	423.75	455.39	441.99	464.07	468.22
109	6.50	7.00	184.91	184.07	181.77	183.76	187.75
110	6.50	7.50	224.67	225.15	220.65	226	231.35
111	6.50	8.00	272.17	273.27	264.3	270.54	280.55
112	6.50	8.50	291.67	289.64	281.31	285.92	299.46
113	6.50	9.00	310.49	315.05	298.8	316.48	325.1
114	6.50	9.50	336.25	328.12	332.48	334.94	356.99
115	6.50	10.00	309.68	325.98	334.89	368.2	378.18
116	6.50	10.50	281.53	241.84	253.63	327.75	323.89
117	6.50	11.00	390.51	368.8	280.1	297.84	299.6
118	7.00	7.50	212.56	211.17	208.28	204.17	201.56
119	7.00	8.00	265.14	265.16	262.74	257.03	253.82
120	7.00	8.50	297.3	297.29	293.3	290.31	285.62
121	7.00	9.00	341.82	335.56	331.78	319.16	316.06
122	7.00	9.50	351	355.34	331.26	333.67	329.15
123	7.00	10.00	364.61	363.09	338.27	358.87	333.86
124	7.00	10.50	340.04	346.9	317.59	319.99	308.67
125	7.00	11.00	397.48	403.87	333.95	356.44	350.58
126	7.50	8.00	212.13	211.64	212.67	213.52	213.49
127	7.50	8.50	266.28	265.47	268.86	268.34	271.32
128	7.50	9.00	299.72	321.03	313.83	320.09	319.74
129	7.50	9.50	337.07	333.79	339.76	330.72	330.27
130	7.50	10.00	356.41	288.62	358.67	346.31	345.02
131	7.50	10.50	349.14	341.78	345.19	319.3	323.58
132	7.50	11.00	384.55	394.23	373.14	353.75	358.61
133	8.00	8.50	206.92	207.16	205.99	205.27	205.1
134	8.00	9.00	236.87	236.57	237.22	236.32	236.43
135	8.00	9.50	284.26	286.62	266.92	278.05	274.68
136	8.00	10.00	312.8	311.31	281.2	302.29	304.95
137	8.00	10.50	304.2	303.25	263.66	289.66	289.23

138	8.00	11.00	345.97	349	275.7	332.18	324.71
139	8.50	9.00	216.19	216.51	215.46	215.73	215.24
140	8.50	9.50	236	236.72	236.96	239.76	240.36
141	8.50	10.00	280.23	261.73	285.25	276.07	273.86
142	8.50	10.50	279.6	260.31	284.57	273.09	273.43
143	8.50	11.00	324.49	297.16	330.8	313.61	312.92
144	9.00	9.50	208.75	208.77	208.53	207.92	208.63
145	9.00	10.00	233.17	231.02	232.72	233.81	231.07
146	9.00	10.50	256.81	253.51	259.52	248.41	248.06
147	9.00	11.00	295.55	291.74	292.61	284.12	282.18
148	9.50	10.00	204.61	204.25	204.68	203.59	204.04
149	9.50	10.50	213.72	213.28	214.34	213.37	212.26
150	9.50	11.00	261.74	265.85	258.9	252.56	254.04
151	10.00	10.50	176.21	176.17	176.66	176.52	175.53
152	10.00	11.00	190.5	187.65	194.67	195.92	192.29
153	10.50	11.00	152.34	151.97	153.36	154.46	155.63

Line a

Middleburgh	Baselines		Survey 1		Survey 2	Survey 3	Survey 4	Survey 5
Dipole Dipole				Chargeability				Reciprocal
Data point #	XC	XP	Rho	M	Rho	Rho	Rho	Rho
1	0.50	1.00	396.83	0.69	394.51	421.42	416.02	2090.21
2	0.50	1.50	273.29	0.51	263	310.54	315.8	1516.18
3	0.50	2.00	124.06	-2.09	87.68	158.67	157.97	2362.88
4	0.50	2.50	72.41	-4.81	146.89	98.12	97.06	2712.72
5	0.50	3.00	96.96	-10.13	487.12	86.54	83.95	1659.3
6	0.50	3.50	709.94	21.65	118.64	74.81	59.35	1251.33
7	0.50	4.00	1884.41	15.05	169.42	76.03	81.6	713.29
8	0.50	4.50	60.57	125.26	226	90.47	95.75	490.88
9	0.50	5.00	1237.18	12.92	235.42	92.75	95.52	327.95
10	1.00	1.50	774.96	1.14	771.5	691.88	711.09	1135.73
11	1.00	2.00	322.96	0.32	323.45	363.81	363.25	1547.71
12	1.00	2.50	161.2	-0.9	165.96	189.58	189.93	2054.65
13	1.00	3.00	95.37	-1.76	105.6	130.38	130.59	1398.33
14	1.00	3.50	64.11	-2.87	68.41	91.4	92.02	1148.08
15	1.00	4.00	80.45	-1.28	71.35	82.85	77.41	685.89
16	1.00	4.50	107.07	56.6	61.94	77.42	97.59	594.67
17	1.00	5.00	123.72	-35.1	83.92	98.39	202.49	294.97
18	1.00	5.50	143.49	10.38	100.99	82.03	136.96	104.03
19	1.50	2.00	461.29	0.24	459.69	476.52	464.11	1100.69
20	1.50	2.50	268.21	-0.27	267.11	292.22	295.82	1435.3
21	1.50	3.00	114.66	-2.97	128.38	191.9	197.84	1128
22	1.50	3.50	43.43	-2.9	59.37	96.08	85.44	998.04
23	1.50	4.00	76.69	-8.48	20.93	65.84	67.68	628.07
24	1.50	4.50	66.86	29.05	53.69	71.53	79.16	568.75
25	1.50	5.00	96.38	1.73	105.76	51.47	79.66	285.42
26	1.50	5.50	139.15	-0.81	925.52	82.84	78.09	98.17
27	1.50	6.00	261.29	19.81	1395.36	106.15	58.48	104.32
28	2.00	2.50	634.33	-0.5	636.44	527.27	533.44	1447.63
29	2.00	3.00	363.37	0.89	387.76	416.81	414.5	1381.09
30	2.00	3.50	131.26	-1.5	136.26	195.43	194.1	1311.81
31	2.00	4.00	62.89	-6.52	118.8	110.96	114.21	858.42

32	2.00	4.50	73.84	-39.32	119.98	95.35	102.27	573.87
33	2.00	5.00	351.78	2.47	287.19	88.23	89.59	413.52
34	2.00	5.50	116.82	-0.4	578.07	94.43	23.39	164.24
35	2.00	6.00	213.76	12.1	756.05	113.68	94.65	111.59
36	2.00	6.50	311.5	7.43	571.78	122.05	38.29	99.96
37	2.50	3.00	652.1	2.02	657.45	651.46	642.13	1460.71
38	2.50	3.50	282.04	1.2	286.97	355.15	352.05	1694.03
39	2.50	4.00	134.92	0.2	132.47	186.76	184.69	1247.26
40	2.50	4.50	127.98	-0.38	109.21	143.91	135.41	1027.84
41	2.50	5.00	117.78	3.53	110.49	95.56	114.79	676.82
42	2.50	5.50	150.42	5.52	143.82	86.87	86.97	263.86
43	2.50	6.00	75.96	-5.2	87.52	94.18	72.81	173.34
44	2.50	6.50	94.15	-2.78	177.42	41.91	68.14	130.05
45	2.50	7.00	89.96	20.48	64.76	64.38	48.02	89.21
46	3.00	3.50	412.75	1.25	420.24	436.64	439.77	1595.35
47	3.00	4.00	217.29	1.55	180.47	256.63	267.03	1498.62
48	3.00	4.50	129.58	-3.94	82.78	185.71	182.84	1465.78
49	3.00	5.00	177.6	6.03	181.86	101.35	90.94	1002.86
50	3.00	5.50	751.86	15.63	607.36	81.25	76.94	423.42
51	3.00	6.00	71.17	-23.67	132.91	77.01	48.35	228.43
52	3.00	6.50	59.48	-35.29	196.01	72.86	54.46	145.44
53	3.00	7.00	47.93	-60.01	316.11	97.96	54.16	88.38
54	3.00	7.50	183.98	-2.86	240.16	119.86	85.47	104.97
55	3.50	4.00	498.87	1.51	496.78	460.07	462.75	880.06
56	3.50	4.50	329.98	0.33	312.91	394.4	392.94	1146.1
57	3.50	5.00	148.75	3.37	134.17	193.43	187.54	887.41
58	3.50	5.50	96.99	0.21	109.14	123.13	122.85	396.1
59	3.50	6.00	68.1	19.42	365.17	99.89	99.46	222.53
60	3.50	6.50	54.52	-9.63	63.28	84.99	69.72	136.46
61	3.50	7.00	54.04	-6.27	102.11	97.86	89.68	83.99
62	3.50	7.50	73.47	-5.38	937.64	114.06	108.8	80.49
63	3.50	8.00	48.88	43.52	1476.33	113.5	106.22	139.02
64	4.00	4.50	753.69	1.76	749.7	774.29	758.6	1360.92
65	4.00	5.00	354.03	0.81	354.94	427.5	427.35	1378.96
66	4.00	5.50	200.97	0.97	204.59	255.52	249.68	660.47

67	4.00	6.00	120.39	9.15	116.87	159.78	149.58	381.91
68	4.00	6.50	86.29	3.42	142.38	98.72	83.9	218.54
69	4.00	7.00	109.39	6.97	5.21	99.83	84.5	117.36
70	4.00	7.50	98.12	-4.47	75.03	66.69	86.3	92.88
71	4.00	8.00	78.25	-58.4	71.18	91.4	74.08	106.02
72	4.00	8.50	104.5	-8.5	18.19	102.02	88.15	82.04
73	4.50	5.00	597.21	-0.85	602.82	567.64	571.13	1460.42
74	4.50	5.50	433.38	1.05	451.02	441.53	433.22	827.95
75	4.50	6.00	225.47	-0.41	220.69	277.69	270.51	517.71
76	4.50	6.50	116.54	1.41	93.59	131.53	150.38	291.83
77	4.50	7.00	94.99	0.2	106.25	130.54	123.87	130.32
78	4.50	7.50	109.11	-4.13	74.8	114.33	114.43	99.77
79	4.50	8.00	74.83	7.65	71.24	75.68	81.23	95.36
80	4.50	8.50	110.72	-31.59	85.45	117.67	108.45	102.06
81	4.50	9.00	90.63	-52.64	57.7	75.52	81.69	104.63
82	5.00	5.50	953.33	1.4	942.14	845.47	835.94	750.51
83	5.00	6.00	613.41	0.85	615.85	633.09	664.95	593.95
84	5.00	6.50	299.82	2.41	310.28	364.41	368.08	367.16
85	5.00	7.00	216.37	1.52	182.38	287.54	293.39	154.33
86	5.00	7.50	178.77	0.28	166.85	221.16	207.44	102.7
87	5.00	8.00	146.88	5.59	131.53	136	130.08	83.4
88	5.00	8.50	199.04	-22.08	470.36	150.87	127.11	94.51
89	5.00	9.00	165.1	-9.14	752.23	114.67	129.17	109.32
90	5.00	9.50	166.19	38.19	222.55	78.97	34.09	98.76
91	5.50	6.00	892.94	1.01	899.01	854.23	863.56	834.76
92	5.50	6.50	527.92	2.53	509.12	589.68	590.96	637.08
93	5.50	7.00	374.03	2.42	379.46	519.68	514.98	271.95
94	5.50	7.50	337.75	1.7	1	379.32	382.45	158.02
95	5.50	8.00	149.15	-8.61	287.21	218.89	220.19	95.72
96	5.50	8.50	153.69	2.56	654.3	239.53	247.43	84.33
97	5.50	9.00	90.1	-55.66	1019.12	175.52	149.47	124.84
98	5.50	9.50	55.31	104.74	1623.43	116.56	82.36	106.13
99	5.50	10.00	23.17	5.84	2298.42	104.88	65.42	115.11
100	6.00	6.50	868.4	2.86	877.04	752.03	756.67	815.94
101	6.00	7.00	770.76	2.05	757.28	846.64	835.61	432.16

102	6.00	7.50	643.84	1.42	597.91	648.17	668.73	246.94
103	6.00	8.00	374.82	0.4	327.7	394.49	394.39	95.16
104	6.00	8.50	388.9	4.13	348.83	420.55	416.74	75.48
105	6.00	9.00	270.92	-10.09	232.67	265.88	271.96	88.53
106	6.00	9.50	189.33	1.71	186.88	153.07	171.26	81.61
107	6.00	10.00	170.14	7.52	160.57	120.46	131.42	85.28
108	6.00	10.50	194.15	32.83	173.53	123.94	165.41	117.14
109	6.50	7.00	1449.78	3.89	1493.55	1500.05	1493.67	572.07
110	6.50	7.50	1413.62	1.68	1434.51	1431.02	1413.36	421.84
111	6.50	8.00	829.4	1.97	796.97	899.79	904.49	200.96
112	6.50	8.50	881.86	1.06	782.3	1013.96	1012.86	105.84
113	6.50	9.00	512.11	3.92	199.34	688.94	678.44	93.18
114	6.50	9.50	251.89	1.1	449.3	361.03	403.81	70.3
115	6.50	10.00	104.04	0.91	1041.55	278.81	290.98	66.91
116	6.50	10.50	70.26	10.44	2054.44	287.5	346.69	107.91
117	6.50	11.00	33.12	135.27	2245.69	266.53	295.89	102.65
118	7.00	7.50	1668.6	2.56	1642.12	1377.55	1374.03	758.19
119	7.00	8.00	1170.87	1.74	1152.04	1098.67	1112.36	397.67
120	7.00	8.50	1452.63	2.11	1449.98	1423.29	1423.07	190.05
121	7.00	9.00	972.23	1.11	1032.44	1029.81	1007.25	137.5
122	7.00	9.50	612.36	-0.26	626.26	643.93	642.59	93.74
123	7.00	10.00	417.86	3.51	415.26	456.64	459.51	72.05
124	7.00	10.50	421.92	-4.11	412.83	467.37	476.48	97.08
125	7.00	11.00	393.57	-6.23	326.25	451.89	454.52	87.81
126	7.50	8.00	932.42	2.75	899	857.15	868.26	470.39
127	7.50	8.50	1602.08	2.42	1608.44	1485.17	1487.24	254.21
128	7.50	9.00	1241.27	2.67	1244.84	1252.44	1260.04	182.63
129	7.50	9.50	862.53	5.31	853.67	853.38	855.79	108.92
130	7.50	10.00	592.71	6.87	595.12	629.51	639.23	64.2
131	7.50	10.50	586.87	9.68	603.84	669.25	676.95	73.54
132	7.50	11.00	491.73	-0.25	552.34	679.19	695.48	68.72
133	8.00	8.50	1927.89	3.86	1960.35	1670.5	1639.95	437.22
134	8.00	9.00	1879.9	2.64	1892.79	1749.36	1724.71	349.2
135	8.00	9.50	1449.35	4.75	1461.47	1341.26	1328.19	193.81
136	8.00	10.00	1027.13	6.63	1053.94	1020.69	998.6	92.36

137	8.00	10.50	1099.93	3.11	1108.53	1142.71	1128.26		93.13
138	8.00	11.00	1074.83	-0.61	1088.66	1235.7	1230.34		81.37
139	8.50	9.00	1635.74	2.76	1657.14	1492.58	1492.88		637.39
140	8.50	9.50	1562.4	4.03	1558.2	1389.47	1392.13		415.2
141	8.50	10.00	1190.72	6.39	1208.76	1142.67	1141.82		192.35
142	8.50	10.50	1389.26	2.6	1365.9	1380.71	1385.9		132.25
143	8.50	11.00	1504.85	-1.06	1462.38	1635.72	1636.52		82.35
144	9.00	9.50	1751.79	7.67	1764.34	1508.09	1481.01		538.19
145	9.00	10.00	1629.78	8.76	1658.21	1466.5	1460.33		296.38
146	9.00	10.50	2189.34	4.27	2197.11	2064.17	2043.08		193.59
147	9.00	11.00	2731.44	0.84	2681.27	2737.28	2747.74		107.35
148	9.50	10.00	1381.47	12.84	1438.09	1131.37	1125.98		471.4
149	9.50	10.50	1722.08	9.34	1747.46	1579.37	1569.4		362.78
150	9.50	11.00	2359.21	4.03	2370.81	2357.3	2334.71		156.5
151	10.00	10.50	1288.55	13.56	1293.25	1150.9	1139.68		716.93
152	10.00	11.00	1691.4	9.78	1708.37	1524.84	1531.32		311.16
153	10.50	11.00	2531.94	6.83	2496.99	2123.91	2118.92		411.29

Line a

Middleburgh			Survey 6		Survey 7
Wenner PRF				Chargeability	
Data point #	X	CC/3	Rho	M	Rho
1	0.75	0.5	510.96	1.86	510.16
2	1.5	1	216.91	1.13	218.37
3	2.25	1.5	136.47	7.66	135.73
4	3	2	121.3	1.29	119.98
5	3.75	2.5	129.04	1.48	128.47
6	4.5	3	139.04	2.1	140.94
7	5.25	3.5	174.69	1.35	174.09
8	1.25	0.5	368.19	1.1	369.2
9	2	1	209.86	0.6	210.34
10	2.75	1.5	126.3	1.69	126.04
11	3.5	2	113.95	1.27	115.03
12	4.25	2.5	130.84	1.66	133.76
13	5	3	151.7	2.05	154.66
14	5.75	3.5	190.11	0.77	188.84
15	1.75	0.5	503.3	1.81	504.87
16	2.5	1	198.32	0.05	198.75
17	3.25	1.5	134.9	1.68	135.14
18	4	2	131.76	1.55	132.73
19	4.75	2.5	145.01	1.12	146.61
20	5.5	3	173.99	1.64	170.04
21	6.25	3.5	210.08	0.82	210.79
22	2.25	0.5	450.59	1.66	457.73
23	3	1	209.15	0.84	210.34
24	3.75	1.5	136.01	10.93	138.69
25	4.5	2	140.62	0.82	140.68
26	5.25	2.5	168.29	1.3	169.6
27	6	3	204.64	1.19	206.31
28	2.75	0.5	392.81	1.16	394.4
29	3.5	1	239.55	0.41	240.84
30	4.25	1.5	156.59	2.5	160.21
31	5	2	155.99	0.59	156.42
32	5.75	2.5	191.94	2.19	192.05
33	6.5	3	248.15	0.71	246.94
34	3.25	0.5	461.27	1.77	462.29
35	4	1	234	0.54	234.35
36	4.75	1.5	191.7	2.3	190.36

37	5.5	2	232.73	1.26	231.6
38	6.25	2.5	220.17	1.8	220.84
39	7	3	262.68	0.29	264.22
40	3.75	0.5	491.45	2	484.3
41	4.5	1	270.83	0.53	268.75
42	5.25	1.5	226	3.21	225.16
43	6	2	255.24	1.97	256.15
44	6.75	2.5	294.52	1.32	315.8
45	4.25	0.5	430.65	0.87	427.92
46	5	1	315.48	1.48	318.91
47	5.75	1.5	303.38	4	303.23
48	6.5	2	272.6	2.94	272.84
49	7.25	2.5	354.03	0.34	356.47
50	4.75	0.5	657.45	1.99	654.5
51	5.5	1	387.47	0.89	394.41
52	6.25	1.5	417.99	4.02	416.1
53	7	2	348.95	2.69	348.96
54	7.75	2.5	426.2	0.63	428.61
55	5.25	0.5	598.07	1.98	601.46
56	6	1	559.64	1.44	556.48
57	6.75	1.5	426.42	3.48	426.9
58	7.5	2	446.39	1.34	450.35
59	5.75	0.5	698.11	1.95	684.65
60	6.5	1	639.05	2.38	640.76
61	7.25	1.5	498.29	4.42	494.86
62	8	2	646.19	0.93	661.21
63	6.25	0.5	1021.59	2.58	1017.18
64	7	1	743.92	2.97	741.93
65	7.75	1.5	589.52	3.49	588.87
66	8.5	2	646.16	2.6	642.95
67	6.75	0.5	955.59	3.12	942.72
68	7.5	1	862.67	2.96	859.82
69	8.25	1.5	869.1	3.53	875.77
70	7.25	0.5	1080.11	2.95	1018.09
71	8	1	965.61	3.41	964.99
72	8.75	1.5	1039.67	4.43	1003.24
73	7.75	0.5	1381.73	3.67	1382.66
74	8.5	1	1184.81	4.16	1148.64
75	9.25	1.5	971.41	7.28	978.46
76	8.25	0.5	1111.74	3.18	1135.24
77	9	1	1417.35	5.07	1401.84
78	8.75	0.5	1495.74	5.78	1496.22
79	9.5	1	1324.8	6.26	1330.42
80	9.25	0.5	1352.77	6.44	1341.68
81	10	1	1328.25	7.17	1353.75
82	9.75	0.5	1280.24	9.88	1290.46
83	10.25	0.5	1570.18	9.24	1562.54
84	10.75	0.5	1573.16	8.6	1581.75

Line b

Middleburgh	Baselines		Survey	
Dipole Dipole				Chargeability
Data point #	XC	XP	Rho	M
1	0.50	1.00	193.75	4.65
2	0.50	1.50	209.45	4.57
3	0.50	2.00	134.19	2.98
4	0.50	2.50	92.26	2.13
5	0.50	3.00	70.31	1.26
6	0.50	3.50	83.47	2.09
7	0.50	4.00	92.1	5.13
8	0.50	4.50	86.62	1.68
9	0.50	5.00	91.39	4.48
10	1.00	1.50	316.24	7.2
11	1.00	2.00	211.95	5.49
12	1.00	2.50	132.21	4.11
13	1.00	3.00	92.98	3.48
14	1.00	3.50	81.86	3.06
15	1.00	4.00	77.23	8.31
16	1.00	4.50	75.01	6.96
17	1.00	5.00	43.37	7.14
18	1.00	5.50	92.92	5.6
19	1.50	2.00	277.77	5.4
20	1.50	2.50	178.44	3.89
21	1.50	3.00	117.99	3.81
22	1.50	3.50	90.75	3.84
23	1.50	4.00	65.33	2.89
24	1.50	4.50	33.48	12.33
25	1.50	5.00	63.44	1.13
26	1.50	5.50	81.11	4.96
27	1.50	6.00	50.51	2.34
28	2.00	2.50	271.48	3.08
29	2.00	3.00	195.95	3
30	2.00	3.50	144.54	3.39
31	2.00	4.00	99.6	3.84

32	2.00	4.50	78.5	3.7
33	2.00	5.00	39.23	9.61
34	2.00	5.50	75.58	4.48
35	2.00	6.00	37.88	-5.1
36	2.00	6.50	27.22	2.2
37	2.50	3.00	242.04	2.64
38	2.50	3.50	199.19	3.25
39	2.50	4.00	132.89	3.99
40	2.50	4.50	97.36	3.08
41	2.50	5.00	62.03	3.49
42	2.50	5.50	74.13	4.82
43	2.50	6.00	53.7	3.56
44	2.50	6.50	71.36	18.12
45	2.50	7.00	84.71	21.91
46	3.00	3.50	273.11	3.5
47	3.00	4.00	194.15	3.99
48	3.00	4.50	137.65	3.43
49	3.00	5.00	83.63	2.92
50	3.00	5.50	70.37	4.74
51	3.00	6.00	65.22	9.62
52	3.00	6.50	72.24	2.09
53	3.00	7.00	92.09	11.45
54	3.00	7.50	143.87	8.9
55	3.50	4.00	273.73	3.99
56	3.50	4.50	206.94	2.62
57	3.50	5.00	109.47	2.1
58	3.50	5.50	78.92	3.08
59	3.50	6.00	64.47	4.88
60	3.50	6.50	62.18	-9.38
61	3.50	7.00	87.15	8.99
62	3.50	7.50	225.5	3.94
63	3.50	8.00	79.71	7.3
64	4.00	4.50	374.43	1.36
65	4.00	5.00	199.66	2.86
66	4.00	5.50	123.92	3.06

67	4.00	6.00	85.87	3.59
68	4.00	6.50	75.34	-1.3
69	4.00	7.00	67.84	7.25
70	4.00	7.50	80.91	8.62
71	4.00	8.00	90.58	26.85
72	4.00	8.50	143.35	4.22
73	4.50	5.00	284.03	2.71
74	4.50	5.50	180.22	3.5
75	4.50	6.00	117.61	4.01
76	4.50	6.50	80.9	6.61
77	4.50	7.00	73.07	6.95
78	4.50	7.50	69.88	7.96
79	4.50	8.00	57.17	10.01
80	4.50	8.50	83.73	5.03
81	4.50	9.00	115.41	27.41
82	5.00	5.50	373.44	3.93
83	5.00	6.00	258.17	4.69
84	5.00	6.50	148.87	7.08
85	5.00	7.00	95.43	7.32
86	5.00	7.50	87.14	5.44
87	5.00	8.00	55.6	10.67
88	5.00	8.50	47.53	9.6
89	5.00	9.00	72.09	29.84
90	5.00	9.50	49.08	6.18
91	5.50	6.00	536.26	4.06
92	5.50	6.50	346.24	6.33
93	5.50	7.00	200.17	6.56
94	5.50	7.50	145.7	5.65
95	5.50	8.00	68.24	5.57
96	5.50	8.50	93.84	5.14
97	5.50	9.00	86.73	15.59
98	5.50	9.50	59.26	31.19
99	5.50	10.00	45.29	-25.79
100	6.00	6.50	568.15	6.03
101	6.00	7.00	406.65	5.71

102	6.00	7.50	308.43	4.3
103	6.00	8.00	144.29	5.84
104	6.00	8.50	163.24	7.41
105	6.00	9.00	125.78	5.68
106	6.00	9.50	61.59	16.04
107	6.00	10.00	96.13	14.76
108	6.00	10.50	82.84	34.9
109	6.50	7.00	628.09	5.26
110	6.50	7.50	571.28	3.08
111	6.50	8.00	273.87	5.38
112	6.50	8.50	322.17	6.1
113	6.50	9.00	215.87	13.47
114	6.50	9.50	83.45	-0.46
115	6.50	10.00	77.35	14.59
116	6.50	10.50	86.24	22.39
117	6.50	11.00	87.1	29.86
118	7.00	7.50	882.24	3.4
119	7.00	8.00	522.5	5.42
120	7.00	8.50	680.55	5.86
121	7.00	9.00	484.61	7.18
122	7.00	9.50	187.48	18.02
123	7.00	10.00	149.04	21.3
124	7.00	10.50	165.16	25.86
125	7.00	11.00	154.52	1.27
126	7.50	8.00	592.39	3.72
127	7.50	8.50	1013.48	4.73
128	7.50	9.00	809.9	6.71
129	7.50	9.50	328.08	12.81
130	7.50	10.00	260.25	17.1
131	7.50	10.50	276.96	10.47
132	7.50	11.00	271.69	13.85
133	8.00	8.50	1025.57	4.24
134	8.00	9.00	1093.35	4.96
135	8.00	9.50	483.13	12.59
136	8.00	10.00	404.89	12.26

137	8.00	10.50	449.26	10.34
138	8.00	11.00	421.14	13.28
139	8.50	9.00	602.64	5.12
140	8.50	9.50	370.67	10.68
141	8.50	10.00	358.63	11.46
142	8.50	10.50	444.31	9.23
143	8.50	11.00	452.26	7.58
144	9.00	9.50	807.91	11.18
145	9.00	10.00	842.83	10.78
146	9.00	10.50	1159.48	8.1
147	9.00	11.00	1307.52	6.29
148	9.50	10.00	842.34	12.34
149	9.50	10.50	1400.37	8.91
150	9.50	11.00	1817.56	7.84
151	10.00	10.50	670.83	3.17
152	10.00	11.00	1177.81	4.79
153	10.50	11.00	1129.89	4.91

Line b

Middleburgh			Survey	
Wenner PRF				Chargeability
Data point #	X	CC/3	Rho	M
1	0.75	0.5	236.65	6.11
2	1.5	1	139.15	3.03
3	2.25	1.5	115.77	3.18
4	3	2	105.29	1.96
5	3.75	2.5	109.57	2.43
6	4.5	3	120.21	2.9
7	5.25	3.5	136.64	2.71
8	1.25	0.5	204.19	4.51
9	2	1	150.27	3.41
10	2.75	1.5	107.24	2.82
11	3.5	2	99.37	2.25
12	4.25	2.5	105.24	1.63
13	5	3	117.44	2.81
14	5.75	3.5	140.08	3.04
15	1.75	0.5	249.33	4.26
16	2.5	1	145.38	3.12
17	3.25	1.5	102.74	4.82
18	4	2	96.85	2.48
19	4.75	2.5	111.65	2.84
20	5.5	3	123.07	3.69
21	6.25	3.5	141.44	3.16
22	2.25	0.5	226.45	3.97
23	3	1	135.56	2.83
24	3.75	1.5	96.88	10.16
25	4.5	2	99.2	2.8
26	5.25	2.5	110.72	2.88
27	6	3	133.73	3.71
28	2.75	0.5	229.8	3.07
29	3.5	1	135.36	3.07
30	4.25	1.5	103.09	10.55
31	5	2	102.43	2.97
32	5.75	2.5	113.01	4.04
33	6.5	3	146.06	5.96
34	3.25	0.5	222.59	3.06
35	4	1	133.97	3.18
36	4.75	1.5	111.52	11.71

37	5.5	2	121.18	3.5
38	6.25	2.5	128.96	4.48
39	7	3	131.31	4.05
40	3.75	0.5	268.37	3.25
41	4.5	1	145.41	3.86
42	5.25	1.5	127.55	11.05
43	6	2	136.23	4.93
44	6.75	2.5	154.5	5.1
45	4.25	0.5	236.09	3.42
46	5	1	170.12	4.16
47	5.75	1.5	132.14	6.87
48	6.5	2	133.5	5.56
49	7.25	2.5	147.97	5.67
50	4.75	0.5	311.21	3.58
51	5.5	1	192.26	3.99
52	6.25	1.5	198.24	7.76
53	7	2	162.33	6.58
54	7.75	2.5	168.13	6.27
55	5.25	0.5	334.63	3.99
56	6	1	230.87	3.97
57	6.75	1.5	222.64	15.45
58	7.5	2	173	6.58
59	5.75	0.5	388.98	4.48
60	6.5	1	272.38	4.34
61	7.25	1.5	202.95	10.87
62	8	2	253.8	7.17
63	6.25	0.5	478.2	4.2
64	7	1	421.43	5.85
65	7.75	1.5	209.98	8.17
66	8.5	2	264.82	8.6
67	6.75	0.5	604.33	4.47
68	7.5	1	448.2	6.45
69	8.25	1.5	373.99	10.23
70	7.25	0.5	577.39	4.87
71	8	1	334.84	6.77
72	8.75	1.5	495.93	9.16
73	7.75	0.5	826.87	4.66
74	8.5	1	521.82	7.97
75	9.25	1.5	429.13	12.3
76	8.25	0.5	505.98	5.59
77	9	1	888.78	7.34
78	8.75	0.5	866.45	6.61
79	9.5	1	784.35	7.92
80	9.25	0.5	816.94	7.62
81	10	1	531.82	8.6
82	9.75	0.5	688.11	9.28
83	10.25	0.5	881.85	7.19
84	10.75	0.5	1047.84	8.94

Line c

Middleburgh	Baselines		Survey 1		Survey 2	Survey 3	Survey 4	Survey 5
Dipole Dipole				Chargeability				Reciprocal
Data point #	XC	XP	Rho	M	Rho	Rho	Rho	Rho
1	0.50	1.00	353.47	-0.29	347.93	372.51	365	1702.88
2	0.50	1.50	339.25	1.5	330.4	339.43	336.95	2200.63
3	0.50	2.00	254.39	-3.59	258.35	255.26	254.16	1479.93
4	0.50	2.50	168.23	1.63	165.53	168.39	166.61	862.19
5	0.50	3.00	121.63	-0.82	118.2	114.46	118.23	590.59
6	0.50	3.50	102.68	2.63	91.89	222.07	97.66	312.92
7	0.50	4.00	135.99	10.74	116.88	118.21	109.44	101.61
8	0.50	4.50	118.9	9.13	143.8	144.27	950.48	146.9
9	0.50	5.00	136.57	-19.24	127.29	94.59	160.19	10.87
10	1.00	1.50	593.29	23.87	650.39	490.56	495.36	1695.9
11	1.00	2.00	432.86	2	448.91	393.7	393.78	1431.83
12	1.00	2.50	256.49	3.85	268.72	237.68	241.94	901.97
13	1.00	3.00	148.16	0.51	149.78	145.47	147.56	649.72
14	1.00	3.50	94.63	2.58	102.68	84.89	130.67	341.33
15	1.00	4.00	96.73	12.9	111.39	166.58	170.1	203.74
16	1.00	4.50	98.56	6.03	117.5	202.91	210.79	69.98
17	1.00	5.00	110.42	0.12	82.18	249.39	263.34	61.24
18	1.00	5.50	122.78	3.27	213.67	315.1	321.67	84.04
19	1.50	2.00	610.1	2.98	608.97	627.13	629.09	1402.65
20	1.50	2.50	418.62	4.75	415.14	425.22	428.49	1071.87
21	1.50	3.00	197.19	-0.28	186.02	197.81	201.17	854.9
22	1.50	3.50	109.56	6.42	107.03	98.72	86.54	481.1
23	1.50	4.00	90.66	2.73	89.05	112.62	173.87	285.68
24	1.50	4.50	81.91	1.13	88.22	75.22	80.02	138.07
25	1.50	5.00	71.94	30.5	84.18	69.78	148.04	59.95
26	1.50	5.50	98.94	-11.18	179.51	84.21	245.16	88.06
27	1.50	6.00	174.4	13.49	64.59	11.26	214.71	30.46
28	2.00	2.50	809.51	4.35	815.86	808.21	808.19	1477.65
29	2.00	3.00	420.74	-3.01	439.27	424.37	420.13	1489.61
30	2.00	3.50	198.8	-1.78	200.32	203.32	201.45	915.71
31	2.00	4.00	128.64	5.28	130.93	131.17	132.18	528.4

32	2.00	4.50	92.01	5.89	112.34	108.56	99.28	235
33	2.00	5.00	84.5	-22.33	102.82	86.08	94.39	128.53
34	2.00	5.50	84.54	31.46	112.21	130.96	97.7	79.52
35	2.00	6.00	5.75	194.05	111.44	148.98	85.66	74.96
36	2.00	6.50	100.33	30.23	98.23	101.57	178.16	90.4
37	2.50	3.00	516.83	-3.06	517.75	515.96	513.82	1379.86
38	2.50	3.50	293.66	-0.17	304.86	293.8	292.81	1136.8
39	2.50	4.00	182.62	-0.24	180.23	182.13	180.6	745.25
40	2.50	4.50	111.66	1.35	111.02	105.33	109.01	304
41	2.50	5.00	84.1	14.55	82.24	84.08	81.29	155.03
42	2.50	5.50	72.3	7.27	68.63	74.48	30.12	113.75
43	2.50	6.00	100.11	10.2	90.47	56.4	187.5	103.57
44	2.50	6.50	79.56	44.23	38.66	90.58	104.65	51.58
45	2.50	7.00	384.83	5.38	108.64	85.46	108.36	114.73
46	3.00	3.50	542.79	-0.08	545.46	545.5	550.93	1011.95
47	3.00	4.00	407.83	2.16	403.92	402.65	400.3	893.98
48	3.00	4.50	224.41	-0.4	225.22	222.05	220.26	402.5
49	3.00	5.00	120.04	-0.51	121.66	122.25	148.53	210.01
50	3.00	5.50	29.18	-2.85	91.36	82.05	93.66	125.53
51	3.00	6.00	102.43	-0.23	95.28	75.37	94.27	84.39
52	3.00	6.50	90.8	19.82	80.51	82.1	94.18	49.19
53	3.00	7.00	98.57	-0.69	88.55	92.3	78.47	75.35
54	3.00	7.50	113.88	-22.26	97.92	68.07	95.69	19.93
55	3.50	4.00	619.04	2.28	618.13	615.53	616.78	1274.58
56	3.50	4.50	411.58	-0.02	410.08	405.37	408.05	708.65
57	3.50	5.00	207.95	-1.57	207.42	207.17	208.3	433.47
58	3.50	5.50	105.48	-1.48	104.05	101.61	108.63	168.02
59	3.50	6.00	92.32	5.46	81.59	82.56	87.59	106.69
60	3.50	6.50	77.6	10.25	77.25	73.66	75.13	75.96
61	3.50	7.00	90.84	-2.92	95.17	96.02	90.56	91.92
62	3.50	7.50	91.11	-7.36	86.84	95.32	103.58	121.18
63	3.50	8.00	140.55	0.73	112.6	102.15	136.05	140.17
64	4.00	4.50	564.83	-0.29	564.78	563.3	561.81	758.02
65	4.00	5.00	351.47	0.29	348.26	346.45	347.52	588.57
66	4.00	5.50	159.99	-0.16	159.35	153.22	157.59	271.69

67	4.00	6.00	97.37	-2.36	92.85	96.44	95.55	109.83
68	4.00	6.50	44.74	14.15	67.25	62.32	70.33	71.14
69	4.00	7.00	74.49	-1.03	77.03	77	129.95	70.4
70	4.00	7.50	72.06	-1.39	66.32	67.73	72.29	39.94
71	4.00	8.00	80.6	-0.39	77.31	81.57	82.9	19.23
72	4.00	8.50	70.49	-5.89	64.22	48.19	46.9	90.93
73	4.50	5.00	554.63	2.06	559.08	559.39	560.23	1003.89
74	4.50	5.50	287.82	0.34	291.9	293.92	295.82	564.14
75	4.50	6.00	154.64	-0.35	151.65	150	152.83	228.86
76	4.50	6.50	94.63	-2.41	86.83	86.53	88.45	108.32
77	4.50	7.00	80.84	2.83	71.7	75.42	81.68	87.17
78	4.50	7.50	78.99	-0.2	57.15	67.88	66.92	80.62
79	4.50	8.00	82.29	-6.3	70.61	60.63	79.38	91.66
80	4.50	8.50	95.42	0.41	37.84	72.09	74.71	156.35
81	4.50	9.00	92.82	-74.98	23.64	24.51	100.5	87.39
82	5.00	5.50	501.84	1.55	502.24	499.5	502.31	691.54
83	5.00	6.00	293.28	-0.12	284.13	286.7	282.29	350.89
84	5.00	6.50	145.84	4.37	146.44	142.41	144.51	151.62
85	5.00	7.00	106.01	2.82	105.86	100.7	105.25	92.24
86	5.00	7.50	74.78	13.02	85.6	67.8	69.96	72.99
87	5.00	8.00	77.98	6.36	82.54	92.05	167.97	82.76
88	5.00	8.50	70.58	5.17	49.07	108.75	76.87	98.89
89	5.00	9.00	80.06	30.76	41.36	56.43	90.45	486.34
90	5.00	9.50	82.99	-42.66	127.66	82.92	91.55	97.85
91	5.50	6.00	620.67	-1.68	608.9	610.33	614.35	602.51
92	5.50	6.50	340.42	2.64	337.53	338.76	336.88	295.73
93	5.50	7.00	222.12	0.25	222.48	221.49	210.96	141.6
94	5.50	7.50	115.52	-1.32	112.99	109.46	112.86	107.47
95	5.50	8.00	94.82	4.82	95.74	94.7	94.26	76.54
96	5.50	8.50	72.26	3.21	68.74	66.68	72.52	60.01
97	5.50	9.00	78.69	2.65	53.38	72.58	76.28	72.76
98	5.50	9.50	98.24	-6.86	54.43	52.2	68.78	66.7
99	5.50	10.00	72	-0.98	77.38	90.7	70.34	18.14
100	6.00	6.50	671.59	5.13	675.56	683.96	680.09	511.93
101	6.00	7.00	550.55	1.16	562.38	556.7	560.25	304.47

102	6.00	7.50	266.51	0.58	261.96	267.85	268.43	164.14
103	6.00	8.00	188.81	2.16	196.2	197.61	190.03	108.68
104	6.00	8.50	103.11	-4.99	127.94	119.19	107.23	86.17
105	6.00	9.00	89.3	-14.43	84.22	96.64	105.84	72.06
106	6.00	9.50	77.26	7.3	56.33	71.38	90.62	70.32
107	6.00	10.00	44.52	-12.68	46.68	39.67	50.62	78.76
108	6.00	10.50	39.96	-136.96	37.74	43.82	63.62	78.45
109	6.50	7.00	1029.77	1.55	1010.19	1016.07	1018.9	539.17
110	6.50	7.50	596.71	0.95	588.79	592.15	579.99	352.3
111	6.50	8.00	434.34	3.05	431.28	422.05	427.07	210.83
112	6.50	8.50	237.9	0.96	215.8	212.74	225.6	138.34
113	6.50	9.00	186.47	2.09	186.3	166.58	182.71	82.97
114	6.50	9.50	139.16	-4.2	126.6	128.66	141.91	85.21
115	6.50	10.00	96.67	3.08	82.95	64.76	91.79	135.25
116	6.50	10.50	116.72	-21.92	68.28	87.9	85.07	111.67
117	6.50	11.00	147.85	0.35	11.16	88.63	137.91	129.14
118	7.00	7.50	760.2	2.53	744.75	753.94	754.66	576.89
119	7.00	8.00	713.78	3.37	714.47	716.03	711.84	417.97
120	7.00	8.50	396.07	2.01	391.64	396.87	397.74	229.18
121	7.00	9.00	306.3	2.89	301.16	305.49	303.7	116.99
122	7.00	9.50	211.14	1.82	217.44	208.81	202.25	89.11
123	7.00	10.00	104.02	1.69	112.37	112.48	108.41	79.74
124	7.00	10.50	80.74	1.9	84.58	94.56	80.66	91.22
125	7.00	11.00	86.53	1.87	108.66	102.19	93.86	119.07
126	7.50	8.00	1277.57	3.71	1286.46	1276.32	1268.73	615.86
127	7.50	8.50	878.06	2.1	884.11	880.96	886.63	398.27
128	7.50	9.00	833.95	0.84	755.84	767.02	757.62	181.37
129	7.50	9.50	526.9	-0.79	523.26	525	526.47	130.07
130	7.50	10.00	265.28	0.07	264.34	266.93	264.16	82.69
131	7.50	10.50	203.84	2.44	192.84	192.89	191.2	96.64
132	7.50	11.00	185.29	-1.53	203.99	204.57	190.88	114.63
133	8.00	8.50	1003.71	2.29	997.1	1010.95	1012.26	557.35
134	8.00	9.00	1190.64	1.98	1200.38	1166.92	1179.79	301.62
135	8.00	9.50	936.82	0.89	926.24	919.04	949.58	200.86
136	8.00	10.00	496.14	0.98	488.88	485.54	489.91	106.56

137	8.00	10.50	361.72	1.8	345.22	350.34	357.75	89.76
138	8.00	11.00	333.23	0.78	318.74	322.06	340.2	102.72
139	8.50	9.00	1467.71	3.4	1468.26	1434.15	1429.42	520.84
140	8.50	9.50	1475.29	1.27	1471.2	1461.59	1451.79	419.32
141	8.50	10.00	874.34	1.52	868.98	851.14	858.55	199.77
142	8.50	10.50	660.23	-0.01	666.27	652	653.35	104.13
143	8.50	11.00	617.6	1.47	623.35	616.85	611.02	107.26
144	9.00	9.50	1397.27	3.07	1418.77	1411.73	1424.45	825.83
145	9.00	10.00	1036.33	2.5	1045.39	1042.79	1048.37	427.91
146	9.00	10.50	869.04	-0.6	876.67	874.65	880.28	239.52
147	9.00	11.00	894.6	1.83	862.48	866.12	870.66	165.87
148	9.50	10.00	1386.6	4.4	1402.79	1390.46	1393	636.18
149	9.50	10.50	1432.92	1.78	1426.68	1433.04	1441.43	397.73
150	9.50	11.00	1520.24	3.59	1528.75	1527.02	1517.89	257.71
151	10.00	10.50	1706.73	2.28	1715.77	1698.35	1703.67	506.78
152	10.00	11.00	2268.68	4.18	2276.19	2261	2243.77	342.45
153	10.50	11.00	1744.32	6.84	1724.06	1721.41	1716.73	363.6

Line c

Middleburgh			Survey 6		Survey 7
Wenner PRF				Chargeability	
Data point #	X	CC/3	Rho	M	Rho
1	0.75	0.5	452.08	4.84	456.85
2	1.5	1	201.32	0.84	202.9
3	2.25	1.5	141.6	11.18	139.92
4	3	2	124.77	0.82	125.18
5	3.75	2.5	129.88	1.66	130.85
6	4.5	3	137.16	2.9	142.21
7	5.25	3.5	151.99	1.81	152.3
8	1.25	0.5	411.13	2.82	417.17
9	2	1	207.18	-0.49	210.49
10	2.75	1.5	148.68	6.12	148.4
11	3.5	2	123.87	1.17	123.44
12	4.25	2.5	126.09	1.16	124.66
13	5	3	142.54	1.82	140.17
14	5.75	3.5	157.92	1.54	159.83
15	1.75	0.5	528.93	4.25	531.94
16	2.5	1	241.9	1.02	241.08
17	3.25	1.5	136.2	9.94	137.04
18	4	2	116.18	1.15	117.77
19	4.75	2.5	125.59	1.54	127.3
20	5.5	3	138.24	1.68	140.05
21	6.25	3.5	155.19	1.28	156.14
22	2.25	0.5	472.35	2.45	470.22
23	3	1	246.24	1.58	246.96
24	3.75	1.5	124.28	16.25	122.95
25	4.5	2	111	1.78	110.49
26	5.25	2.5	128.32	1.26	128.67
27	6	3	142.61	1.97	141
28	2.75	0.5	549.21	2.42	550.21
29	3.5	1	220.71	0.29	219.95
30	4.25	1.5	117.83	1.96	121.74
31	5	2	118.14	1.6	118.12
32	5.75	2.5	127.37	1.47	127.04
33	6.5	3	149.18	4.16	146.69
34	3.25	0.5	473.34	1.25	478.26
35	4	1	184.13	1.38	183.75
36	4.75	1.5	124.5	6.61	126.21

37	5.5	2	123.97	1.08	123.05
38	6.25	2.5	133.4	1.17	133.27
39	7	3	148.59	1.72	148.97
40	3.75	0.5	457.28	1.04	449.84
41	4.5	1	198.67	0.72	199.84
42	5.25	1.5	135.62	9.54	137.94
43	6	2	132.03	1.08	132.03
44	6.75	2.5	145.11	0.56	144.57
45	4.25	0.5	477.4	2.35	473.12
46	5	1	217.65	0.45	217.98
47	5.75	1.5	161.53	8.56	161.77
48	6.5	2	153.92	0.91	153.99
49	7.25	2.5	164.42	1.25	164.34
50	4.75	0.5	449.05	0.88	439.49
51	5.5	1	250.8	0.91	252.13
52	6.25	1.5	161.82	1.45	161.81
53	7	2	159.83	0.45	160.05
54	7.75	2.5	157.83	1.48	158.27
55	5.25	0.5	470.46	1.46	472
56	6	1	260.4	0.96	259.08
57	6.75	1.5	216.38	4.37	217.31
58	7.5	2	192.17	1.01	186.91
59	5.75	0.5	488.3	2.03	493.14
60	6.5	1	291.17	1.22	291.94
61	7.25	1.5	249.56	1.74	251.17
62	8	2	217.94	1.76	215.44
63	6.25	0.5	645.32	1.02	645.06
64	7	1	379.52	0.71	375.06
65	7.75	1.5	277.2	3.78	278.21
66	8.5	2	222.86	2.38	226.44
67	6.75	0.5	591.43	2.1	603.36
68	7.5	1	509.53	0.95	508.06
69	8.25	1.5	326.78	5.88	318.62
70	7.25	0.5	940.77	2.15	946.62
71	8	1	598.39	1.35	596.39
72	8.75	1.5	428.95	5.96	427.71
73	7.75	0.5	805.25	1.32	820.09
74	8.5	1	583.54	2.34	587.19
75	9.25	1.5	450.03	5.43	454.59
76	8.25	0.5	1161.47	3.37	1134.6
77	9	1	775.96	2.37	761.18
78	8.75	0.5	1058.72	2.9	1072.91
79	9.5	1	1030.01	2.94	1009.06
80	9.25	0.5	1270.94	3.68	1252.16
81	10	1	940.94	3.27	930.47
82	9.75	0.5	1496.8	3.08	1462.84
83	10.25	0.5	1322.2	5.53	1344.06
84	10.75	0.5	1328.12	3.88	1352.73

Line d

Middleburgh	Baselines		Survey 1		Survey 2	Survey 3	Survey 4	Survey 5
Dipole Dipole				Chargeability			Reciprocal	
Data point #	XC	XP	Rho	M	Rho	Rho	Rho	Rho
1	0.50	1.00	303.43	6.54	305.19	305.92	563.25	307.59
2	0.50	1.50	229	5.45	232.02	244.47	366.96	229.78
3	0.50	2.00	188.21	4.69	186.54	230.45	200.66	232.42
4	0.50	2.50	128.9	3.59	126.7	162.24	103.24	151.37
5	0.50	3.00	141.05	2.71	137.17	171.69	102.77	163.05
6	0.50	3.50	109.99	3.52	116.45	131.74	92.34	163.66
7	0.50	4.00	114.76	8.07	136.36	181.45	196.97	155.69
8	0.50	4.50	117.46	3.29	128.73	192.16	171.5	171.89
9	0.50	5.00	155.07	5.72	161.72	227.53	470.07	309.19
10	1.00	1.50	253	6.92	259.14	262.01	548.27	259.06
11	1.00	2.00	217.41	5.08	218.03	218.28	320.42	217.5
12	1.00	2.50	137.37	5.23	137.55	166.94	140.88	165.88
13	1.00	3.00	122.23	4.46	129.65	159.75	87.3	147.51
14	1.00	3.50	98.82	3.53	90	115.17	62.85	113.07
15	1.00	4.00	87.05	6.85	88.74	130.6	109.27	145.48
16	1.00	4.50	84.24	5.13	83.85	123.06	119.57	146.6
17	1.00	5.00	104.99	5.68	96.84	163.58	120.68	142.08
18	1.00	5.50	93.34	5.59	76.15	236.78	108.25	133.41
19	1.50	2.00	301.45	6.73	304.16	306.46	459.53	305.53
20	1.50	2.50	218.88	5.2	221.16	221.28	239.9	227.8
21	1.50	3.00	199.81	5.32	201.06	229.47	126.56	229.22
22	1.50	3.50	123.6	4.03	122.14	140.84	118.52	156.15
23	1.50	4.00	100.75	3.72	101.97	131.95	181.53	123.19
24	1.50	4.50	90.06	3.24	87.37	113.29	130.48	124.05
25	1.50	5.00	85.33	3.5	94.88	120.65	115.02	128.6
26	1.50	5.50	72.69	12.04	92.87	164.21	111.28	83.68
27	1.50	6.00	121.62	1.4	121.47	172.31	351.71	138.31
28	2.00	2.50	258.7	5.99	260.11	259.11	366.11	263.32
29	2.00	3.00	275.83	6.35	277.15	276.43	236.19	280.96
30	2.00	3.50	156.94	4.48	157.82	196.46	156.87	191.61
31	2.00	4.00	113.25	3.66	112.05	146.43	97.54	134.45

32	2.00	4.50	79.28	2.93	82.44	108.31	67.03	97.82
33	2.00	5.00	80.01	2.75	92.59	110.19	99.24	123.7
34	2.00	5.50	64.66	-0.7	76.85	134.89	93.69	122.57
35	2.00	6.00	92.93	3.18	96.52	147.07	268.2	109.95
36	2.00	6.50	101.46	2.36	85.86	163.45	303.96	122.43
37	2.50	3.00	361.87	6.03	364.54	366.19	359.74	366.22
38	2.50	3.50	236.17	4.13	238.54	239.19	248.78	241.65
39	2.50	4.00	159.48	3.22	155.91	194.19	139.45	186.34
40	2.50	4.50	97.5	3	100.45	133.07	106.31	109.15
41	2.50	5.00	80.89	3.01	86.88	112.8	98.69	115.82
42	2.50	5.50	69.66	-1.03	79.56	154.14	88.5	125.33
43	2.50	6.00	95.48	0.35	94.38	133.55	164.13	136.16
44	2.50	6.50	82.53	0.98	82.78	119.59	264.11	107.72
45	2.50	7.00	94.06	11.89	103.83	98.77	368.09	185.72
46	3.00	3.50	190.24	3.99	190.31	189.41	330.91	190.98
47	3.00	4.00	155.1	3.02	156.08	162.29	198.37	158.78
48	3.00	4.50	91.68	3.6	92.12	126.42	123.94	95.88
49	3.00	5.00	71.57	3.83	72.16	82.93	75.12	79.08
50	3.00	5.50	58.17	2.44	59.26	66.18	67.61	59.85
51	3.00	6.00	62.51	0.39	62.17	60.36	79.84	52.06
52	3.00	6.50	52	1.12	41.03	46.59	130.88	34.68
53	3.00	7.00	59.08	11.13	60.41	63.5	180.76	13.57
54	3.00	7.50	65.6	4.09	57.4	86.92	196.98	12.69
55	3.50	4.00	308.36	1.9	306	306.67	307.44	306.75
56	3.50	4.50	204.14	2.47	202.99	202.9	196.65	203.31
57	3.50	5.00	143.55	3.21	140.18	172.35	116.09	139.53
58	3.50	5.50	98.7	1.39	101.45	94.69	65.57	90.68
59	3.50	6.00	85.8	2.43	79.24	88.38	87.47	89.3
60	3.50	6.50	73.55	-1.59	54.33	88.72	94.23	79.51
61	3.50	7.00	69.11	-7.21	88.37	62.36	126.25	67.11
62	3.50	7.50	46.25	-1.05	96.13	102.18	150.7	43.96
63	3.50	8.00	50.75	-9.89	109.23	99.4	225.82	43.02
64	4.00	4.50	335.93	3.06	339.72	341.57	380.26	342.33
65	4.00	5.00	254.09	2.33	255.45	255.47	248.75	256.52
66	4.00	5.50	153.29	1.13	173.23	152.68	140.45	153.63

67	4.00	6.00	110.01	2.36	124.84	109.28	111.48	103.23
68	4.00	6.50	63.79	-0.23	97.53	70.97	97.4	57.29
69	4.00	7.00	80.98	5.74	127.01	102.23	117.7	96.56
70	4.00	7.50	82.99	5.71	155.54	249.77	134.58	147.15
71	4.00	8.00	76.26	-6.38	141.58	141.17	164.84	137.59
72	4.00	8.50	97.92	-6.39	170.42	199.58	188.64	166.82
73	4.50	5.00	370.56	3.07	369.56	372.27	416.74	374.82
74	4.50	5.50	256.78	2.07	272.85	271.16	241.82	272.54
75	4.50	6.00	169.36	2.6	184.91	182.03	183.74	187.51
76	4.50	6.50	87.15	1.09	118.06	118.17	112.4	115.71
77	4.50	7.00	89.85	2.76	145.77	152.91	111.73	160.39
78	4.50	7.50	88.72	-0.17	174.77	218.86	112.58	200.8
79	4.50	8.00	74.11	2.86	212.7	262.39	120.81	209.22
80	4.50	8.50	90.72	-1.05	311.37	316.55	141.42	324.98
81	4.50	9.00	101.13	2.64	363.52	453.22	184.9	358.8
82	5.00	5.50	344.26	2.51	348.38	349.13	212.01	349.93
83	5.00	6.00	251.81	2.94	265.24	302.98	194.09	268.49
84	5.00	6.50	112.9	1.16	136.54	132.57	118.46	131.51
85	5.00	7.00	102.1	3.73	145.99	149.97	84.24	149.38
86	5.00	7.50	74.64	1.45	133.2	140.64	61.8	142.52
87	5.00	8.00	64.48	1.54	120.42	144.74	80.43	152.71
88	5.00	8.50	60.32	0.79	138.66	177.92	52.97	207.51
89	5.00	9.00	71.83	-4.2	187.62	210.1	91.78	267.25
90	5.00	9.50	73.83	4.22	179.76	281.2	96.37	271.16
91	5.50	6.00	380.55	3.61	380.12	379.15	382.75	383.09
92	5.50	6.50	188.99	1.59	196.58	200.87	252.93	196.33
93	5.50	7.00	168.03	5.38	189.19	189.47	175.87	188.58
94	5.50	7.50	95.86	2.01	137.81	135.68	111.2	135.91
95	5.50	8.00	65.44	3.56	127.81	144.62	90.01	129.28
96	5.50	8.50	65.65	0.37	160.68	177.45	65.25	152.03
97	5.50	9.00	77.77	-7.13	190.95	214.66	90.81	201.64
98	5.50	9.50	83.35	-0.53	247.67	306.76	97.55	222.32
99	5.50	10.00	87.19	6.91	310.52	317.83	111.95	405.34
100	6.00	6.50	212.5	2.17	212.4	213.22	349.68	214.27
101	6.00	7.00	239.82	6.27	239.27	242.92	259.94	243.07

102	6.00	7.50	124.23	3.25	156.41	165.12	157.09	158.77
103	6.00	8.00	70.66	4.34	88.69	105	111.72	99.35
104	6.00	8.50	55.62	1.76	107.78	110.23	108.4	105.28
105	6.00	9.00	50.23	8.24	134.46	81.15	111.46	68.34
106	6.00	9.50	54.78	1.03	130.74	163.15	176.01	118.39
107	6.00	10.00	47.04	3.02	140.28	141.77	238.6	109.72
108	6.00	10.50	69.6	4.78	194.12	254.16	265.03	161.77
109	6.50	7.00	419.2	3.81	419.3	419.17	377.05	418.63
110	6.50	7.50	246.8	3.6	247.98	247.98	261.53	247.47
111	6.50	8.00	118.11	4.75	117.59	133.99	158.8	132.4
112	6.50	8.50	87.42	1.66	72.42	84.8	105.03	74.43
113	6.50	9.00	84.35	1.38	71.82	74.6	168.48	63.73
114	6.50	9.50	55.46	-1.82	50.52	62.93	188.88	65.74
115	6.50	10.00	29.03	-0.31	47.73	41.24	258.9	43.53
116	6.50	10.50	20.57	50.04	41.44	34.33	272.62	49.98
117	6.50	11.00	48.76	-6.02	192.11	193.47	386.64	188.76
118	7.00	7.50	372	3.61	377.74	377.66	340.17	376.57
119	7.00	8.00	191.89	5.95	192.04	192.97	215.12	193.26
120	7.00	8.50	105.94	1.99	117.45	118.66	117.61	117.32
121	7.00	9.00	81.04	0.32	92.62	92.15	156.24	93.6
122	7.00	9.50	65.65	-0.61	74.84	70.98	159.57	70.94
123	7.00	10.00	38.59	-13.89	109.16	108.4	174.96	121.57
124	7.00	10.50	39.09	-12.67	128.07	146.05	205.08	126.11
125	7.00	11.00	19.06	-43.24	154.21	154.59	183.48	127.24
126	7.50	8.00	308.71	6.95	308.03	309.96	306.34	309.2
127	7.50	8.50	197.44	3.3	202.4	201.07	167.29	201.37
128	7.50	9.00	135.05	2.99	152.85	146.52	189.96	153.6
129	7.50	9.50	94.17	2.55	130.37	121.1	163.39	135.26
130	7.50	10.00	79.31	-2.43	136.32	123.92	176.2	140.82
131	7.50	10.50	68.87	-0.02	88	153.91	181.6	180.04
132	7.50	11.00	63.62	-0.92	209.37	240.63	265.71	215.2
133	8.00	8.50	327.41	3.11	330.13	332.01	190.44	332.8
134	8.00	9.00	246.03	3.63	258.78	262.06	257.89	261.28
135	8.00	9.50	155.85	4.04	199.64	192.44	191.32	185.3
136	8.00	10.00	105.98	3.03	162.73	153.67	160.52	158.92

137	8.00	10.50	75.69	1.3	160.02	155.03	151.75	168.47
138	8.00	11.00	69.43	3.55	188.83	197.61	181.02	161.23
139	8.50	9.00	353.49	4.85	355.74	353.93	365.58	361.28
140	8.50	9.50	241.51	4.97	265.14	263.12	280.79	262.22
141	8.50	10.00	147.04	4.11	182.39	178.79	218.85	179.11
142	8.50	10.50	98.47	2.89	143.77	143.32	127.17	139.34
143	8.50	11.00	70.76	2.13	128.69	134.5	148.06	133.44
144	9.00	9.50	365.86	5.95	367.75	368.89	261.99	369.34
145	9.00	10.00	240.2	5.11	260.88	258.55	223.21	254.35
146	9.00	10.50	154.26	3.82	186.89	179.07	142.43	169.93
147	9.00	11.00	94.92	3.18	125.98	142.11	128.37	125.33
148	9.50	10.00	457.7	5.67	460.47	464.9	307.37	463.12
149	9.50	10.50	320.82	4.45	330.06	329.57	217.2	325.44
150	9.50	11.00	181.89	3.36	211.78	224.57	198.3	215.54
151	10.00	10.50	545.84	4.76	551.94	552.43	262.74	554.7
152	10.00	11.00	368.77	4.36	358.23	361.62	227.55	369.54
153	10.50	11.00	562.72	5.01	563.53	562.31	308.56	563.35

Line d

Middleburgh			Survey 6		Survey 7
Wenner PRF				Chargeability	
Data point #	X	CC/3	Rho	M	Rho
1	0.75	0.5	180.97	6.11	183.56
2	1.5	1	163.81	4.98	163.23
3	2.25	1.5	106.45	3.23	105.95
4	3	2	112.5	2.68	111.71
5	3.75	2.5	112.88	2.19	113.46
6	4.5	3	124.19	2.26	124.57
7	5.25	3.5	129.92	2.25	129.62
8	1.25	0.5	260.58	6.04	264.56
9	2	1	167.69	3.95	168.64
10	2.75	1.5	118.76	3.16	118.37
11	3.5	2	110.41	2.32	110.68
12	4.25	2.5	118.64	1.94	115.22
13	5	3	124.23	2.2	123.82
14	5.75	3.5	130.73	2.52	129.09
15	1.75	0.5	238.05	5.51	240.7
16	2.5	1	142.57	3.05	142.32
17	3.25	1.5	115.56	5.7	115.02
18	4	2	112.17	2.45	112.5
19	4.75	2.5	110.16	2.17	110.6
20	5.5	3	116.82	2.25	119.98
21	6.25	3.5	128.03	2.3	127.5
22	2.25	0.5	288.07	5.37	294.48
23	3	1	150.97	3.8	150.61
24	3.75	1.5	127.49	4.89	126.93
25	4.5	2	106.46	2.19	106.48
26	5.25	2.5	110.81	2.65	110.92
27	6	3	115.74	2.56	115.72
28	2.75	0.5	199.68	4.82	203.43
29	3.5	1	178.32	4.02	179.11
30	4.25	1.5	110.63	3.7	110.24
31	5	2	99.4	2.5	99.54
32	5.75	2.5	106.41	2.01	106.24
33	6.5	3	117.04	2.43	116.74
34	3.25	0.5	288.94	3.75	292.18
35	4	1	170.41	3.51	170.66
36	4.75	1.5	113.73	3.36	112.84

37	5.5	2	98.15	2.1	97.55
38	6.25	2.5	106.29	2.16	104.87
39	7	3	113.93	2.69	112.51
40	3.75	0.5	241.05	3	243.13
41	4.5	1	144.65	2.8	144.44
42	5.25	1.5	93.46	3.68	92.85
43	6	2	93.97	2.38	92.98
44	6.75	2.5	101.86	2.16	101.66
45	4.25	0.5	284.08	2.49	288.28
46	5	1	137.92	2.55	138.04
47	5.75	1.5	97.75	3.38	96.78
48	6.5	2	95.16	2.47	94.07
49	7.25	2.5	101.09	2.01	101.81
50	4.75	0.5	285.32	2.48	289.04
51	5.5	1	156.89	3.92	158.69
52	6.25	1.5	98.61	4.79	98.41
53	7	2	97.69	2.01	97.19
54	7.75	2.5	98.57	2.18	99.47
55	5.25	0.5	312.45	3.01	316.43
56	6	1	158.66	3	159.21
57	6.75	1.5	104.93	3.69	103.67
58	7.5	2	94.21	1.97	92.27
59	5.75	0.5	246.61	2.99	251.69
60	6.5	1	145.79	3.13	144.63
61	7.25	1.5	101.52	3.08	100.12
62	8	2	92.79	2.51	91.85
63	6.25	0.5	325.07	3.06	330.91
64	7	1	136.98	3.25	136.14
65	7.75	1.5	106.51	3.55	105.7
66	8.5	2	95.11	2.84	94.25
67	6.75	0.5	244.6	3.56	252.14
68	7.5	1	159.15	3.43	159.52
69	8.25	1.5	97.48	3.56	97.33
70	7.25	0.5	299.07	4.12	305.14
71	8	1	155.16	4.84	154.82
72	8.75	1.5	99.25	5	99.52
73	7.75	0.5	296.3	4.17	305.86
74	8.5	1	141.74	3.9	141.03
75	9.25	1.5	119.96	6.86	118.66
76	8.25	0.5	278.4	5.17	284.62
77	9	1	162.36	4.07	161.07
78	8.75	0.5	284.08	4.61	297.46
79	9.5	1	195.9	4.01	196.71
80	9.25	0.5	340.52	5.12	348.79
81	10	1	233.17	4.97	230.26
82	9.75	0.5	385.6	5.07	398.58
83	10.25	0.5	433.38	5.47	430.62
84	10.75	0.5	514.36	6.1	529.28

Middleburgh	Infiltration		Survey 1	Survey 2	Survey 3	Survey 4	Survey 5
Dipole Dipole							
Data point #	XC	XP	Rho	Rho	Rho	Rho	Rho
1	0.50	1.00	307.59	316.19	315.07	293.08	291.82
2	0.50	1.50	229.78	232.2	230.18	207.19	277.13
3	0.50	2.00	232.42	184.19	179.22	392.66	347.1
4	0.50	2.50	151.37	134.87	118.72	126.96	116.45
5	0.50	3.00	163.05	104.37	125.2	53.34	43.37
6	0.50	3.50	163.66	146.87	116.92	1157.9	850.82
7	0.50	4.00	155.69	143.57	133.83	1720.02	152.5
8	0.50	4.50	171.89	141.08	0.69	1214.35	1191.89
9	0.50	5.00	309.19	157.25	150.69	739.39	674.19
10	1.00	1.50	259.06	266.42	261.74	218.21	221.89
11	1.00	2.00	217.5	221.28	208.22	201.85	195.71
12	1.00	2.50	165.88	143.2	125.18	131.72	117.47
13	1.00	3.00	147.51	104.04	109.63	66.75	53.86
14	1.00	3.50	113.07	96.83	96.6	424.77	183.5
15	1.00	4.00	145.48	96.5	100.02	418.49	315.1
16	1.00	4.50	146.6	79.12	100.17	417.7	247.77
17	1.00	5.00	142.08	98.15	99.49	386.4	216.53
18	1.00	5.50	133.41	88.07	83.91	12.67	90.98
19	1.50	2.00	305.53	317.51	280.56	222.92	224.29
20	1.50	2.50	227.8	234.7	207.89	180.13	181.08
21	1.50	3.00	229.22	159.3	124.74	78.54	74.58
22	1.50	3.50	156.15	132.36	153.34	287.58	240.94
23	1.50	4.00	123.19	119.78	133.29	288.59	209.97
24	1.50	4.50	124.05	90.51	105.04	229.67	218.49
25	1.50	5.00	128.6	100.91	113.57	157.9	153.13
26	1.50	5.50	83.68	129.55	93.46	103.66	9.87
27	1.50	6.00	138.31	81.1	300.48	182.75	111.68
28	2.00	2.50	263.32	271.69	232.55	176.44	176.94
29	2.00	3.00	280.96	216.1	140.11	87.35	84.23
30	2.00	3.50	191.61	173.38	212.46	212.65	173.65
31	2.00	4.00	134.45	136.67	165.56	263.51	161.12

32	2.00	4.50	97.82	85.5	106.75	203.19	243.3
33	2.00	5.00	123.7	96.56	102.4	148.79	349.25
34	2.00	5.50	122.57	84.2	76.28	32.9	59.86
35	2.00	6.00	109.95	81.41	104.42	137.2	278.08
36	2.00	6.50	122.43	93.99	452.85	462.06	531.5
37	2.50	3.00	366.22	285.36	161.55	92.55	92.63
38	2.50	3.50	241.65	264.65	332.28	228.33	227.43
39	2.50	4.00	186.34	210.28	271.5	285.39	247.77
40	2.50	4.50	109.15	119.02	159.18	214.78	284.9
41	2.50	5.00	115.82	106.1	127.25	190.68	206.73
42	2.50	5.50	125.33	86.44	90.14	75.77	47.38
43	2.50	6.00	136.16	85.55	69.94	7.27	54.87
44	2.50	6.50	107.72	92.54	389.89	429.04	328.99
45	2.50	7.00	185.72	119.76	139.09	449.13	369.48
46	3.00	3.50	190.98	187.72	231.87	126.83	123.76
47	3.00	4.00	158.78	195.41	264.61	186.18	181.3
48	3.00	4.50	95.88	110.13	159.78	170.79	163.87
49	3.00	5.00	79.08	83.81	116.99	120.68	104.23
50	3.00	5.50	59.85	58.79	69.92	50.01	59.71
51	3.00	6.00	52.06	57.57	46.07	56.52	70.27
52	3.00	6.50	34.68	62.07	47.07	308.82	121.23
53	3.00	7.00	13.57	83.92	109.17	187.24	110.71
54	3.00	7.50	12.69	86.11	96.02	50.97	68.41
55	3.50	4.00	306.75	228.13	108.17	84.74	83.61
56	3.50	4.50	203.31	159.13	85.86	87.81	87.24
57	3.50	5.00	139.53	114.67	62.23	63.93	65.44
58	3.50	5.50	90.68	70.64	34.22	28.64	27.93
59	3.50	6.00	89.3	62.61	22.1	36.41	27.35
60	3.50	6.50	79.51	58	47.33	107.4	38.62
61	3.50	7.00	67.11	78.92	43.15	82.49	62.88
62	3.50	7.50	43.96	78.88	32.03	38.35	68.98
63	3.50	8.00	43.02	72.76	38.3	37.32	55.46
64	4.00	4.50	342.33	334.42	304.26	261.35	259.75
65	4.00	5.00	256.52	248.89	238.08	195.37	194.99
66	4.00	5.50	153.63	132.75	105.3	78.3	76.86

67	4.00	6.00	103.23	87.82	71.18	37.28	56.88
68	4.00	6.50	57.29	64.96	80.95	49.45	22.81
69	4.00	7.00	96.56	90.77	277.73	61.96	75.21
70	4.00	7.50	147.15	83.57	226.34	29.82	33.52
71	4.00	8.00	137.59	58.09	187.26	1.16	16.75
72	4.00	8.50	166.82	83.46	162.26	25.92	12.86
73	4.50	5.00	374.82	398.78	405.19	351.6	352.53
74	4.50	5.50	272.54	244.78	201.18	152.96	152.26
75	4.50	6.00	187.51	150.54	100.57	68.1	80.91
76	4.50	6.50	115.71	88.59	154.05	141.23	133.24
77	4.50	7.00	160.39	119.38	228.52	259.43	240.25
78	4.50	7.50	200.8	91.46	205.72	239.8	215.53
79	4.50	8.00	209.22	79.18	210.53	227.18	234.86
80	4.50	8.50	324.98	82.84	208.77	319.34	304.31
81	4.50	9.00	358.8	73	240.13	480.45	383.23
82	5.00	5.50	349.93	324.01	271.65	202.48	201.39
83	5.00	6.00	268.49	220.58	121.63	119.84	112.06
84	5.00	6.50	131.51	117.43	185.6	198.78	318.91
85	5.00	7.00	149.38	143.04	242.47	326.74	628.37
86	5.00	7.50	142.52	77.72	132.56	276.71	404.42
87	5.00	8.00	152.71	59.09	90.93	249.78	249.67
88	5.00	8.50	207.51	66.1	159.99	261.54	394.72
89	5.00	9.00	267.25	65.11	109.29	260.28	475.5
90	5.00	9.50	271.16	73.01	55.68	320.97	523.41
91	5.50	6.00	383.09	307.08	147.37	115.08	115.63
92	5.50	6.50	196.33	214.91	284.11	197.97	198.67
93	5.50	7.00	188.58	271.28	411.73	366.55	359.44
94	5.50	7.50	135.91	133.86	193.57	242.04	249.87
95	5.50	8.00	129.28	80.93	121.16	129.61	162.74
96	5.50	8.50	152.03	73.06	77.71	163.97	178.55
97	5.50	9.00	201.64	81.64	92.92	213.08	245.59
98	5.50	9.50	222.32	52.53	90.93	206.03	261.77
99	5.50	10.00	405.34	66.98	48.89	269.3	281.04
100	6.00	6.50	214.27	149.08	160.46	92.53	91.84
101	6.00	7.00	243.07	266.9	340.7	240.39	239.01

102	6.00	7.50	158.77	137.46	176.62	179.94	158.62
103	6.00	8.00	99.35	70.63	89.97	81.87	96.19
104	6.00	8.50	105.28	53.71	61.19	68.2	83.72
105	6.00	9.00	68.34	51.81	56.44	35.65	38
106	6.00	9.50	118.39	51.15	47.55	52.74	76.56
107	6.00	10.00	109.72	57.61	43.98	72.82	37.24
108	6.00	10.50	161.77	40.89	31.23	51.78	21.38
109	6.50	7.00	418.63	351.38	159.82	131.29	130.68
110	6.50	7.50	247.47	224.8	107.28	103.2	102.6
111	6.50	8.00	132.4	108.56	52.62	56.12	54.21
112	6.50	8.50	74.43	77.36	35.13	37.89	31.78
113	6.50	9.00	63.73	67.69	30.14	56.12	44.88
114	6.50	9.50	65.74	62.1	39.71	41.16	37.93
115	6.50	10.00	43.53	57.34	40.31	31.57	29.69
116	6.50	10.50	49.98	32.59	21.37	21.03	22.32
117	6.50	11.00	188.76	6.3	15.15	42.22	42.13
118	7.00	7.50	376.57	316	281	215.99	215.4
119	7.00	8.00	193.26	157.48	146.73	116.77	116.83
120	7.00	8.50	117.32	86.14	102.02	79.34	78.67
121	7.00	9.00	93.6	63.51	91.9	65.18	64.56
122	7.00	9.50	70.94	35.89	83.65	58.17	60.44
123	7.00	10.00	121.57	11.3	36.46	57.79	61.32
124	7.00	10.50	126.11	29.83	31.03	7.84	18.98
125	7.00	11.00	127.24	69.02	64.92	46.31	26.99
126	7.50	8.00	309.2	322.9	311.91	278.25	278.57
127	7.50	8.50	201.37	203.69	193.49	193.83	194.25
128	7.50	9.00	153.6	125.62	161.07	139.07	140.47
129	7.50	9.50	135.26	79.4	143.92	117.46	117.47
130	7.50	10.00	140.82	90.97	159.44	111.79	110.27
131	7.50	10.50	180.04	36.92	212.2	85.16	96.64
132	7.50	11.00	215.2	39.7	174.54	85.88	102.41
133	8.00	8.50	332.8	341.63	341.88	317.07	317.75
134	8.00	9.00	261.28	250.9	262.82	226.33	232.19
135	8.00	9.50	185.3	151.26	194.03	159.69	168.04
136	8.00	10.00	158.92	104.78	144.99	138.95	137.39

137	8.00	10.50	168.47	79	146.49	144.84	137.34
138	8.00	11.00	161.23	56.42	153.24	173.62	168.37
139	8.50	9.00	361.28	373.76	375.76	372.4	372.04
140	8.50	9.50	262.22	247.1	242.2	260.91	259.63
141	8.50	10.00	179.11	143.3	178.18	348	347.15
142	8.50	10.50	139.34	98.89	108.15	260.02	161.75
143	8.50	11.00	133.44	66.97	131.5	134.24	146.4
144	9.00	9.50	369.34	381.07	379.68	381.26	379.8
145	9.00	10.00	254.35	240.45	240.76	332.79	329.63
146	9.00	10.50	169.93	153.01	179.53	186.13	198.3
147	9.00	11.00	125.33	91.49	124.62	141.99	157.96
148	9.50	10.00	463.12	470.59	474.2	483.68	482.19
149	9.50	10.50	325.44	320.38	324	334.43	333.23
150	9.50	11.00	215.54	176.6	180.04	225.14	233.03
151	10.00	10.50	554.7	571.69	578.15	568.74	565.75
152	10.00	11.00	369.54	376.81	377.39	379.41	371.46
153	10.50	11.00	563.35	586.58	588.36	588.35	586.42

BIBLIOGRAPHY

Alumbaugh D., Chang P. Y., Paprocki L., Brainard R. J., Glass J. R., and Rautman A. C., Estimating moisture contents in the vadose zone using cross-borehole ground penetrating radar: A study of accuracy and repeatability, Water Resources Research, 2002, Vol. 38, No. 12, 1309, doi:10.1029/2001WR000754.

Allred B., Daniels J. J., Allred A., Ehsani M. R., Handbook of agricultural geophysics, Published by CRC Press, 2008, 432 pages.

Amidu S. A. and Dunbar J. A., Geoelectric studies of seasonal wetting and drying of a Texas vertisol, Vadose Zone Journal, 2007, Vol. 6, pp. 511-523

Aristodemou E., and Thomas-Batts A., DC resistivity and induced polarization investigation at a waste disposal site and its environments, Journal of Applied Geophysics, 2000, Vol. 44, pp. 275-302.

Binley A., Cassiani G., Middleton R., and Winship P., Vadose zone model flow model parameterization using cross-borehole radar and resistivity imaging, Journal of Hydrology, 2002, Vol. 267, pp. 147-159.

Binley A., Winship P., Middleton R., Pokar M., and West J., High-resolution characterization of vadose zone dynamics using cross-borehole radar, Water Resources Research, 2001, Vol., No. 11, pp. 2639-2652.

Buxton H. T., Smolensky D. A., and Shernoff P. K., Hydrogeologic correlations for selected wells on Long Island, New York-A data base and retrieval program: U.S. Geological Survey, Water-resources investigations report 86-4318, 107 pages.

Carothers, J., Imagery technology meets vineyard management, Practical Winery & Vineyard, May 2000, Vol. 21, No. 1, pp. 54– 62.

Claridge G. G. C., Campbell I. B., Balks M. R., Movement of salts in Antarctic soils: experiments using lithium chloride, Permafrost and Periglacial Processes, 1999, Vol.10, No. 3, pp. 223-233.

Clearbout, J. F., and Muir, F., Robust modeling with erratic data, Geophysics, 1973, Vol. 38, pp. 826-844.

Corwin D.L., and Lesch S.M., Applications of apparent soil electrical conductivity in precision agriculture, Computers and Electronics in Agriculture, 2005, Vol. 46, No. 1-3, pp. 11-43.

Corwin D. L., Lesch S. M., Oster J. D., and Kaffka S. R., Monitoring management-induced spatio-temporal changes in soil quality through soil sampling directed by apparent electrical conductivity, Geoderma, 2006, Vol. 131, No. 3-4, pp. 369-387.

Curtis B., and Kelly W.E., Resistivity-recharge relationships-field study, Journal of Hydrology, 1990, Vol. 118, pp. 39-53.

Da Costa J. P., Michelet F., Germain C, Lavialle O., and Grenier G, Delineation of vine parcels by segmentation of high resolution remote sensed images, Precision Agriculture, 2007, Vol. 8, pp. 95–110, DOI 10.1007/s11119-007-9031-3

Daily, W., Ramirez, A., LaBrecque, and D., Nitao, J., Electrical resistivity tomography of vadose water movement, Water Resources Research, 1992, Vol. 28, No. 5, pp. 1429-1442.

DeGroot-Hedlin, C., and Constable, S. C., Occam's inversion to generate smooth, two-dimensional models from magnetotelluric data, Geophysics, 1990, Vol. 55, pp. 1613–1624.

Delenne C, Rabatel G, and Deshayes M., An automatized frequency analysis for vine plot detection and delineation in remote sensing, IEEE Geoscience and remote sensing letters, July 2008, Vol. 5, No. 3.

DeLima O. A. L., and Niwas S., Estimation of hydraulic parameters of shaly sandstone aquifers from geoelectrical measurements. Journal of Hydrology, 2000, Vol. 235, pp. 12-26.

Dierberg F. E. and De Busk T. A., An evaluation of two tracers in surface-flow wetlands: rhodamine-WT and Lithium, Wetlands , 2005, Vol. 25, No. 1, pp. 8-25.

Doolittle J. A., and Collins M. E., Use of soil information to determine application of ground penetrating radar, Journal of Applied Geophysics, 1995, Vol. 33, No. 1-3, pp. 101-108.

Doolittle J. A., Minzenmayer F. E., Waltman S.W., Benham E.C., Tuttle J.W. and Peaslee S.D., Ground-penetrating radar soil suitability map of the conterminous United States, Geoderma, 2007, Vol.141, No. 3-4, pp. 416-421.

Edet A. E., and Okereke C. S., Assessment of hydrogeological conditions in basement aquifers of the Precambrian Oban massif, southeastern Nigeria, Journal of Applied Geophysics, 1997, Vol. 36, pp. 195-204.

Edwards L. S., A modified pseudosection for resistivity and induced polarization, Geophysics, 1977, Vol. 42, pp. 1020-1036.

Eppstein J. M., Dougherty E. D., Efficient three-dimensional data inversion: Soil characterization and moisture monitoring form cross-well ground-penetrating radar at a Vermont test site, Water Resources Research, 1998, Vol. 34, No. 8, pp. 1889-1900.

Ezzedine S., and Rubin Y., Bayesian integration of hydrogeological and geophysical data for site characterization: Theory and application to the LLNL superfund site, proceedings of the symposium: Bridging the gap between measurements and modeling in heterogeneous media, Berkeley, March 25-28, 2002.

Ferre, T. P. A., Hinnell, A. C., and Blainey, J. B., Inferring hydraulic properties using surface-based electrical resistivity during infiltration, The Leading Edge, 2006, Vol. 25, pp. 720-723.

Flury, M., and N. N. Wai, Dyes as tracers for vadose zone hydrology, Reviews of Geophysics, 2003, Vol. 41, No. 1, 1002, doi:10.1029/2001RG000109.

Frohlich R. K., Urish W. D., Fuller J., and O'Reilly M., Use of geoelectrical methods in groundwater pollution surveys in a coastal environment, Journal of Applied Geophysics, 1994, Vol. 32, pp. 139-154.

Griffiths D. H., and Turnbull J., A multi-electrode array for resistivity surveying. First Break, July 1985, Vol. 3, No. 7.

Griffiths D. H., Turnbull J., and Olayinca A. L., Two-dimensional resistivity mapping with a computer-controlled array. Journal of Applied Geophysics, 1990, Vol. 29, pp. 211-226.

Grote K., Hubbard S., and Rubin Y., Field- scale estimation of volumetric water content using ground-penetrating radar wave techniques, Water Resources Research, 2003, Vol. 39, No. 11, 1321.

Hagrey S. A. A., Geophysical imaging of root-zone, trunk, and moisture heterogeneity, Journal of Experimental Botany, 2007, Special Issue: Imaging Stress Responses in Plants, Vol. 58, pp. 839-854.

Hagrey S. A. A., Meissner R., Werban U., Rabbel W., and Ismaeil A., Hydro-, bio-geophysics, The Leading Edge, Special section: Near-surface problems and solutions, 2004, Vol. 23, No. 7, DOI:10.1190/1.1776739

Hall A., Louis J. P. and Lamb D. W., Low-resolution remotely sensed images of winegrape vineyards map spatial variability in planimetric canopy area instead of leaf area index, Australian Journal of Grape and Wine Research, 2008, Vol. 14, No. 1, pp. 9 – 17.

Hollenbeck K. J., and Jensen K.H., Maximum-likelihood estimation of unsaturated hydraulic parameters, Journal of Hydrology, 1998, Vol. 210, pp. 192-205.

Johnson C.K., Eskridge K.M., Corwin D.L., Apparent soil electrical conductivity: Applications for designing and evaluating field-scale experiments, Computers and Electronics in Agriculture, 2005, Vol. 6, No 1-3, pp. 181-202.

Kalinski R. J., Kelly W. E., Bogardi I., and Pesti G., Electrical resistivity measurements to estimate travel times through unsaturated ground water protective layers, Journal of Applied Geophysics, 1993, Vol. 30, pp. 161-173.

Kean W. K, Waller M. J., Layson H. R., Monitoring moisture migration in the vadose zone with resistivity, Ground Water, 1987, Vol. 25, No 5, pp. 562-571.

Kearey P., Brooks M., and Hill I., An Introduction to Geophysical Exploration, Blackwell Science; 3rd Edition, 2002.

Keller, G. V. and Frischknecht, F. C., Electrical methods in geophysical prospecting, Oxford: Pergamon Press, 1966.

Kowalsky B. M., Chen J., and Hubbard S. S., Joint inversion of geophysical and hydrological data for improved subsurface characterization, The Leading Edge, Special Section: Hydrogeophysics, June 2006, Vol. 25, No. 6 DOI:10.1190/1.2210057

Kowalsky B. M., Dietrich P., Teutsch, and Rubin Y., Forward modeling of ground-penetrating radar using outcrop images and multiple scenarios of water saturation, Water Resources Research, 2001, Vol. 37, No. 6, pp. 1615-1625.

Loke, M. H., Electrical imaging surveys for environmental and engineering studies – A practical guide to 2D and 3D surveys. Short training course lecture notes. University Sains Malaysia, Penang, Malaysia.

Loke, M. H., and Barker, R. D., Rapid least-squares inversion of apparent resistivity pseudosections using a quasi-Newton method, Geophysical Prospecting, 1996, Vol. 44, pp. 131-152.

Loke, M. H., and Barker, R. D., Practical techniques for 3D resistivity surveys and data inversion, Geophysical Prospecting, 1996, Vol. 44, pp. 499–523.

Loke M. H., and Dahlin T., A comparison of the Gauss-Newton and quasi-Newton methods in resistivity imaging inversion, Journal of Applied Geophysics, 2002, Vol. 49, pp. 149-162.

Lesch S.M., Corwin D.L., Robinson D.A., Apparent soil electrical conductivity mapping as an agricultural management tool in arid zone soils, Computers and Electronics in Agriculture, 2005, Vol. 46, No. 1-3, pp. 351-378.

Lund, K. and Young K.L., Contaminant transport in high arctic soils: a tracer experiment, Permafrost and Periglacial Processes, Vol. 16, pp.195–207.

Mazac O., Kelly W. E., and Landa I., A hydrogeological model for relations between electrical and hydraulic properties of aquifers, Journal of Hydrology, 1985, Vol. 79, pp. 1-19.

Mazac O., Cisleslerov M., and Vogel T., Application of geophysical methods in describing spatial variability of saturated hydraulic conductivity in the zone of aeration, Journal of Hydrology, 1988, Vol. 103, pp. 117-126.

Martin, T.D., Creed, J.T., and Brockhoff, C.A., Sample preparation procedure for spectrochemcial determination of total recoverable elements: U.S. Environmental Protection Agency Report, Revision 2.8, EMMC Version, 12 pages.

McClymonds N. E., and Franke O. L., Water-transmitting properties of aquifers on Long Island, New York, U.S. Geological Survey, Professional paper 627-E.

Meju M. A., Geoelectrical investigation of old/abandoned, covered landfill sites in urban areas: model development with a genetic diagnosis approach. Journal of Applied Geophysics, 2000, Vol. 44, pp. 115-150.

Michot, D., Y. Benderitter, A. Dorigny, B. Nicoullaud, D. King, and Tabbagh A., Spatial and temporal monitoring of soil water content with an irrigated corn crop cover using surface electrical resistivity tomography, Water Resourses Research, 2003, Vol. 39, No. 5, 1138, doi:10.1029/2002WR001581.

Mota, R., Monteiro dos Santos, F., 2D sections of porosity and water saturation percent from combined resistivity and seismic surveys for hydrogeologic studies, The Leading Edge, 2006, Vol. 25, pp. 735-737.

Mussett E. A., and Khan M. A., Looking into the earth, an introduction to geological geophysics, Published by Cambridge University Press, 2000, 470 pages.

Nadezhdina N., and Cermák J., Instrumental methods for studies of structure and function of root systems of large trees, Journal of Experimental Botany, 2003, Vol. 54, No. 387, pp. 1511-1521.

National Research Council, Precision Agriculture in the 21st century: Geospatial and information technologies in crop management, National Research Council (U.S.). Committee on assessing crop yield: Site-specific farming, information systems, and research opportunities, published by National Academies Press, 1997, 149 pages.

Niwas S., and Singhal D. C., Estimation of aquifer transmissivity from Dar-Zarouk parameters in porous media, Journal of Hydrology, 1981, Vol. 50, pp. 393-399.

Park, S.K., Fluid migration in the vadose zone from 3-D inversion of resistivity monitoring data. Geophysics, 1998, Vol. 63, No. 1, pp. 41-51.

Rhoades, J. D., Ingvalson, R. D., Determining salinity in field soils with soil resistance measurements, Soil Science Society of America Journal, 1971, Vol. 35, pp. 54-60.

Rhoades, J. D., Shouse, P. J., Alves, W. J., Manteghi, Nahid A., Lesch, S. M., Determining soil salinity from soil electrical conductivity using different models and estimates, Soil Science Society of America Journal, 1990, Vol. 54, pp. 46-54.

Robinson D. A., Binley A., Crook N., Day-Lewis F. D., Ferré T. P. A., Grauch V. J. S., Knight R., Knoll M., Lakshmi V., Miller R., Nyquist J., Pellerin L., Singha K., Slater L., Advancing process-based watershed hydrological research using near-surface geophysics: a vision for, and review of, electrical and magnetic geophysical methods, Hydrological Processes, 2008, Vol. 22 No. 18, pp. 3604 – 3635

Rockhold L. M., Simmons S. C., and Fayer J. M., An analytical solution technique for one-dimensional, steady vertical water flow in layered soils, Water Resources Research, 1997, Vol. 33, No. 4, pp. 897-902.

Rubin, Y., G. Mavko, and Harris J., Mapping permeability in heterogeneous aquifers using hydrological and seismic data, Water Resources Research, 28(1997), No. 7, 1192–1800.

Sasaki Y., Two-dimensional joint inversion of magnetotelluric and dipole-dipole resistivity data, Geophysics, 1989, Vol. 49, pp. 149-162.

Sasaki Y., Resolution of resistivity tomography inferred from numerical simulation. Geophysical prospecting, 1992, Vol. 40, pp. 453-464.

Sénéchal P., Perroud H., Kedziorek M., Bourg A., and Gloaguen E., Non destructive geophysical monitoring of water content and fluid conductivity anomalies in the near surface at the border of an agricultural field, Subsurface Sensing Technologies and Applications, 2005, Vol. 6, No. 2, pp. 167-192.

Simunek J., and van Genuchten M. T., Estimating unsaturated soil hydraulic properties form tension disc infiltrometer data by numerical inversion, Water Resources Research, 1996, Vol. 32, No. 9, 2683-2696.

Smolensky D. A., Buxton H. T., and Shernoff P.K., Hydrologic framework of Long Island, New York: U.S. Geological Survey, Hydrologic investigations atlas HA-709, 3 sheets, scale 1:250,000.

Stumm F, Lange A. D., and Candella J. L., Hydrogeology and extent of saltwater intrusion on Manhasset Neck, Nassau County, New York. U. S. Geological Survey, Water-resources investigations report 00-4193, Coram, New York.

Van, G. P., S.K. Park and P. Hamilton, Monitoring leaks from storage ponds using resistivity methods, Geophysics, 1991, Vol. 56, No. 8, pp. 1267-1270.

van Overmeeren, Sariowan S. V., and Gehrels J. C., Ground penetrating radar for determining volumetric soil water content; results of comparative measurements at two test sites, 1997, Journal of Hydrology, Vol. 197, pp. 316-338.

Vanderborght, J., A. Kemna, H. Hardelauf, and Vereecken H., Potential of electrical resistivity tomography to infer aquifer transport characteristics from tracer studies: A synthetic case study, Water Resources Research, 2005, Vol. 41, W06013, doi:10.1029/2004WR003774.

United States Department of Agriculture Soil Conservation Service, Soil Survey of Suffolk County, New York, April 1975.

United States Department of Agriculture, Natural Resources Conservation Service, National Cooperative Soil Survey, Suffolk County, New York. http://websoilsurvey.nrcs.usda.gov

Wempe W., and Mavko G., A new method for constraining total porosity: The new total porosity-electrical resistivity upper bound, The Leading Edge, 2006, Vol. 25, No. 6, DOI:10.1190/1.2210054

Yadav G. S., and Abolfazi H., Geoelectrical soundings and their relationship to hydraulic parameters in semiarid regions of Jalore, northwestern India. Journal of Applied Geophysics, 1998, Vol. 39, pp. 35-51.

Yeh J. T. C., Liu S., Glass R. J., Baker K., Brainard J. R., Alumbaugh D., and LaBrecque D., A geostatistically based inverse model for electrical resistivity surveys and its applications to vadose zone hydrology, Water Resources Research, 2002, Vol. 38, No. 12, 1278.

Zou Z. Y., Young M. H., and Wierenga P. J., Estimation of depth averaged unsaturated soil hydraulic properties from infiltration experiments, Journal of Hydrology, 2001, Vol. 242, pp. 26-42.